NTNU – Trondheim
Norwegian University of
Science and Technology

Jette Well Productivity and IOR Evaluations

Tonje Winther

Petroleum Geoscience and Engineering
Submission date: June 2014
Supervisor: Jon Kleppe, IPT

Norwegian University of Science and Technology
Department of Petroleum Engineering and Applied Geophysics

Abstract

In this thesis the productivity of well 25/8-D-1 AH T3 in the Jette field has been evaluated by estimating the productivity index. The productivity index has been estimated in two ways; with the use of a pseudo-steady state model and multi-rate tests. It was observed that the well suffers from a poor Productivity Index (PI), with a low and unstable production due to slugging. A sensitivity analysis was performed on several input parameters in order to investigate the reasons for the poor PI. The sensitivity analysis gave indications to what kind of well intervention measures which may be reasonable to implement in order to increase the productivity.

Six cases of well intervention measures were implemented and simulated with Schlumberger's simulation propriety ECLIPSE 100. The cases consist of infill drilling and acid squeeze. All six cases showed an increase in Recovery Factor (RF); 1-30% increase from the basecase. The new well paths were designed with the Petrel software to obtain an optimized connection factor, giving a smoother wellbore location in the grid blocks. Up to four completion options have been suggested for the cases, where the most optimal options have been considered to be a barefoot solution or a an openhole completion with standalone metal mesh screens, inflow control devices and swell packers (as well 25/8-D-1 AH T3). The Net Present Value (NPV) was calculated for all cases and completion options with the basis of the costs and revenue, and have been used to evaluate the sustainability of the well intervention measures.

The infill drilling measures consist of laterals towards north, east and west of Well D. It is observed, from the simulations, that the laterals towards east give highest increased oil RF compared to the basecase; 29.2%. Acid squeeze gives an increased oil RF of 9.8%. The costs of the drilling and completion operations were calculated using all inclusive day rates. Assessed risks and unforeseen time delays due to conditions like hole instability and cleaning, well control, stuck pipe, etc. were included in the probability distribution. Almost all cases were found to obtain a positive NPV, being profitable. Case 2 and Case 3, with laterals towards east, are found to be the most profitable cases.

Sammendrag

I denne avhandlingen er produktiviteten til brønn 25/8-D-1 AH T3 i Jettefeltet blitt evaluert ved å estimere produktivitetsindeksen. Produktivitetsindeksen har blitt estimert på to måter; ved bruken av en pseudo-stabil tilstandsmodell og ved bruk av flerratetester. Det ble funnet at at brønnen ikke produserer optimalt; en lav produktivitetsindeks. Det ble også observert at det er en lav og ustabil produksjon grunnet slugging. En sensitivitetsanalyse ble utført på flere av inputparameterene for å undersøke hva som fører til den lave produktivitetsindeksen. Sensitivitetsanalysen ga indikasjoner på hvilke typer brønnintervensjonstiltak som kan være mulig å innføre for å øke produktiviteten.

Seks tilfeller av brønnintervensjonstiltak ble iverksatt og simulert med Schlumbergers simuleringsprogram ECLIPSE 100. Tiltakene består av boring av flere brønnbaner og syrestimulering. Alle de seks tilfellene viste en økning i oljeutvinningsfaktor; 1-30% økning fra nåværende tilfelle. De nye brønnbanene ble utformet med programvaren Petrel for å oppnå en optimal forbindelsesfaktor, noe som gir en jevnere brønnbaneplassering i rutenettblokkene. Opp til fire kompletteringsalternativer har blitt foreslått for tiltakene, der de mest optimale alternativene har blitt anslått å være en barfot løsning og/eller en åpenhulls komplettering med metall sandskjermer, kontrollenheter for innstrømning og svellbare packere (slik som brønn 25/8-D-1 AH T3). Netto nåverdi har blitt beregnet for alle tiltakene og kompletteringsalternativene, på grunnlag av beregnede kostnader og inntekter, og har blitt brukt til å vurdere bærekraften i tiltakene.

Boretiltakene består av brønngrener mot nord, øst og vest for brønn 25/8-D-1 AH T3. Fra simuleringene er det observert at grenene mot øst gir høyest økt oljeutvinngsfaktor sammenlignet med nåværende tilfelle; 29.2%. Syrestimulering gir en økt oljeutvinngsfaktor på 9.8%. Kostnadene for bore- og kompletteringsoperasjonene ble beregnet ved hjelp av alt-inkluderende dagrater. Vurderte risikoer og uforutsette forsinkelser på grunn av forhold som hullustabilitet og renhold, brønnkontroll og fastsatt utstyr, osv. er inkludert i sannsynlighetsfordelingen. Nesten alle tiltakene ble anslått til å oppnå en positiv netto nåverdi, å være lønnsomme. Tiltak 2 og Tiltak 3, med grener mot øst, er anslått å være de mest lønnsomme tilfellene.

Acknowledgements

This thesis was carried out at the Department of Petroleum Engineering and Applied Geophysics, at the Norwegian University of Science and Technology (NTNU) during the spring of 2014. The thesis is prepared in cooperation with Weatherford Petroleum Consultants AS and Det Norske Oljeselskap ASA.

I would like to express my gratitude to Det Norske Oljeselskap ASA for providing me with data, and Weatherford Petroleum Consultants AS for providing material, office space and guidance. Special thanks are directed to my supervisor at Weatherford Petroleum Consultants AS, Erik Iversen Nakken, for his good ideas, constructive feedback, support during stressful times and the freedom I was provided while working on this thesis. I would also like to thank my supervisor at NTNU, professor Jon Kleppe, for his valuable guidance and support during my work with the master thesis. At last, I would like to thank Marte Stubsjøen, Jean-Christophe Barbier, Marit Kristin Krogstad, and the rest of the "Jette team" at Weatherford Petroleum Consultants AS, for including me in discussions and meetings. It has been a very rewarding process to be part of.

Trondheim, June 5, 2014

Tonje Winther

Contents

List of Figures

List of Tables

Glossaries

amalgamated	Mixed layers
barefoot	A well completion that has no casing or liner set across the reservoir formation, allowing the produced fluids to flow directly into the wellbore
bubble point	The pressure and temperature conditions at which the first bubble of gas comes out of solution in oil
Coiled Tubing	A long, continuous length of pipe wound on a spool
contingency	A future event or circumstances which is possible, but cannot be predicted with certainty
Darcy sand	Sand with high permeability, above 1 Darcy
drawdown	The difference between the average reservoir pressure and the flowing bottomhole pressure
drilling riser	A large-diameter pipe that connects the subsea Blowout Preventer (BOP) stack to a floating surface rig to take mud returns to the surface
Geosteering	The intentional directional control of a well based on the results of downhole geological logging measurements rather than three-dimensional targets in space, usually to keep a directional wellbore within a pay zone

P/T-gauge	A pressure/temperature gauge, used to measure and record downhole pressure and temperature. Installed as part of the completion
Recovery Factor	The recoverable amount of hydrocarbon initially in place, normally expressed as a percentage
Rotary Kelly Bushing	Reference datum; 40 m above sea level
saturated oil	The oil pressure is per definition lower than the bubble point pressure
technical limit	The ultimate limit in terms of performance
undersaturated oil	The oil pressure is per definition higher than the bubble point pressure
whipstock	A long steel casing that uses an inclined plane to cause the bit to deflect away from the original borehole at a slight angle
wireline	A general term used to describe well-intervention operations conducted using single-strand or multistrand wire or cable for intervention in oil or gas wells

Acronyms

AFE	Authorization For Expenditure
ALQ	Artificial Lift Quantity
AOF	Absolute Open Flow
BHP	Bottom Hole Pressue
BHT	Bottom Hole Temperature
BOP	Blow-Out Preventer
CAPEX	Capital Expenditure
CBP	Casing Bottom Pressure
CHP	Casing Head Pressure
CME	Constant Mass Expansion
CPI	Computer Processed Interpretation
CT	Coiled Tubing
CTD	Coiled Tubing Drilling
DC	Drilling and Completion
DLE	Differential Liberation Expansion
DLS	Dog Leg Severity
DP	Drill Pipe
ECD	Equivalent Circulation Density
EOR	Enhanced Oil Recovery
EOS	Equation of State
ESP	Electric Submersible Pumps
FGOR	Field Gas-Oil Ratio
FGPT	Field Gas Production Total
FOE	Field Oil Efficiency
FOPT	Field Oil Production Total
FPSO	Floating Production Storage and Offloading
FVF	Formation Volume Factor
FWPT	Field Water Production Total

GLV	Gas Lift Valve
GOC	Gas-Oil Contact
GOR	Gas Oil Ratio
HDT	High Density Turbidities
HWI	Heavy Well Intervention
ICD	Inflow Control Device
ID	Inner Diameter
IOR	Improved Oil Recovery
IPR	Inflow Performance Relationship
KPI	Key Performance Indicators
LDT	Low Density Turbidities
LPM	Liters Per Minute
LSOBM	Low-Solids, Oil-Based Mud
LWD	Logging While Drilling
LWI	Light Well Intervention
MD	Measured Depth
MDT	Modular formation Dynamics Tester
MEG	Methanol and Glycol
MPD	Managed Pressure Drilling
MPFM	Multi Phase Flow Meter
MSL	Mean Sea Level
MWD	Measurement While Drilling
MWI	Medium Well Intervention
NCS	Norwegian Continental Shelf
NPV	Net Present Value
OD	Outer Diameter
OPEX	Operational Expenditure
OWC	Oil-Water Contact
PCP	Progressing Cavity Pumping
PI	Productivity Index
PLEM	Pipeline End Manifold
PVT	Pressure Volume Temperature
RF	Recovery Factor

RKB	Rotary Kelly Bushing
RLWI	Riserless Light Well Intervention
RMS	Root Mean Square
SG	Specific Gravity
STOIIP	Stock Tank Oil Initially In Place
TD	Target Depth
THP	Tubing Head Pressure
TPR	Tubing Performance Relationship
TTDC	Through Tubing Drilling and Completion
TTRD	Through Tubing Rotary Drilling
TVD	True Vertical Depth
VFP	Vertical Flow Performance
WC	Water Cut
WGPT	Well Gas Production Total
WHP	Well Head Pressure
WOPT	Well Oil Production Total
WOR	Water Oil Ratio
WOW	Waiting on Weather
WWCT	Well Water Cut Total
WWPT	Well Water Production Total

Symbols

C_A	shape factor
C_i	cash flow
C_o	initial investment
L	well length
R_{sd}	solution gas oil ratio
S	skin factor
h	height
i	time of the cash flow in years
k_h	horizontal permeability
k_v	vertical permeability
kh	permeability thickness product
k	permeability
$mD * m$	unit for permeability thickness product
r_e	drainage radius
r	interest rate

1 Introduction

Oil and gas are life important energy resources where the industry is constantly being pushed beyond existing boundaries to supply the growing demand. It is unlikely that the industry will make sufficient new reserve discoveries, and/or develop existing resources fast enough to maintain production levels (as per 2013) for an extended period of time. This can be attributed to the increasing complexity of the remaining reserves, and escalating costs of developing these resources for production (Naterstad 2013). The trend of increasing consumption along with decreasing discoveries and dwindling producing resources has prompted the need for technological development and research. Recent years increase in oil prices have made deep water drilling and subsea field development technology economically viable, extending this window.

On the Norwegian Continental Shelf (NCS) the RF is high compared to the world average RF; it is estimated to 46% (as of April 2013) (Oljedirektoratet 2013). Even with a currently high RF important resources are left. Increasing average RF on the NCS by one per cent may yield more than 300 BNOK in additional revenues, provided current (as of 24.04.2014) oil prices (approximately 110 USD/BBL) (Labastidas Avila et al. 2013). Despite of the technological developments in the recent years with deep water drilling and subsea field development, it seems apparent that the most reasonable way of gaining this extra per cent is to recover the already available resources. This may be done by implementing Improved Oil Recovery (IOR) measures. IOR includes both well intervention and Enhanced Oil Recovery (EOR).

In order to decide on whether or not a field and its producing wells are candidates for IOR a thorough analysis of the production is necessary. The analysis may help to decide on which IOR measure(s) to implement. The productivity of a well is defined by the PI and is useful for describing its relative potential (Winther 2013). The PI, along with a sensitivity analysis, can give an indication of whether or not the well should be worked-over. Conversations with industry people has indicated that a good well has a productivity index of 30-60 $Sm^3/day/bar$ [1] (Winther 2013). Typical examples of work-over measures in wells with poor PI may include well stimulation, drilling of side-tracks or multi-laterals, perforating, or scale removal.

[1] Personal communication with Jean-Christophe Barbier. November 2013. Trondheim: Weatherford Petroleum Consultants AS

The Jette field is a subsea developed oil field in the Southern part of the North Sea, connected to the Jotun field. Jette's resources would not have been possible to produce without the already existing infrastructure in the area. It is developed with two horizontal producers, 25/8-E-1 H and 25/8-D-1 AH T3. Both the wells have gas lift. The field started its production the 19th of May 2013, and has experienced ample challenges during its producing life. One of the challenges is the low PI of the wells, particularly of well 25/8-D-1 AH T3. In *Productivity Index in Horizontal Wells* (Winther 2013) the PI of 25/8-E-1 H was estimated by the use of a model for horizontal wells in closed reservoir, multi-rate tests and build-up tests, and confirmed through inflow- and lift performance curves. It was found that the oil production in the well is highly dependent upon gas lift rate, and that the productivity index was most sensitive to formation height, well deviation and horizontal permeability. The objective in this thesis is to evaluate the additional well, well 25/8-D-1 AH T3, for well intervention measures.

The productivity index in this thesis will be calculated by the use of a pseudo-steady state model and multi-rate tests, and verified with a correlation between lift performance curves and inflow performance curves (Winther 2013). In order to determine which type of well intervention measure to implement, a thorough investigation of production history, log analysis, well path survey, production system, well test analysis and reservoir geometry, along with a sensitivity analysis, are needed. The data made available to produce the results in this report include log data, well tests, geometry of the production system, and production data from appraisal- and producing wells. The calculation of the parameters have to be made from empirical correlations or in software like WellFlo and PanSystem. With the use of the simulation propriety ECLIPSE 100 the future productivity and profitability of different well intervention measures may be evaluated, making it easier to decide on which measures to implement.

This thesis starts with a theoretical part in **Chapter 2-5**, which includes some definitions, an introduction to reservoir simulation and history matching, and a presentation of IOR and different measures within IOR and well intervention. As horizontal wells and their productivity indices are highly relevant in this thesis, theory about horizontal well technology, productivity index and well testing are described in **Appendix B**. The theory is taken from the project report *Productivity Index in Horizontal Wells* (Winther 2013). **Chapter 6** introduces the field and in **Chapter 7** the productivity of well 25/8-D-1 AH T3 is evaluated, and different IOR measures are considered. **Chapter 8** and **9** describes the simulation model, and the validation and history matching of the model. Well design, the simulation of well intervention measures and the results are presented in **Chapter 10** and **11**. Finally, an economic analysis, conclusions and ideas for future work are presented in **Chapter 12- 14**.

2 Previous Work

In September 2013 Det Norske Oljeselskap requested Weatherford Petroleum Consultants to carry out an in-depth study of the Jette wells 25/8-D-1 AH T3 and 25/8-E-1 H. The purpose of the study was to perform production performance diagnostics, identify measures to enhance the production, and evaluate well intervention opportunities. In addition to a study performed by Weatherford Petroleum Consultants, three students performed studies related to the Jette Field. The three student tasks consisted of a study of the productivity and future challenges of well 25/8-E-1 H, a theory study of well intervention measures in well 25/8-D-1 AH T3 and a simulation study of upscaling the existing simulation model.

The study performed by Weatherford Petroleum Consultants included the features below mentioned.

- Identification of root causes of production related problems in 25/8-D-1 AH T3.
- An evaluation of the effectiveness of clean-up, production and lift performance in 25/8-E-1 H to provide guidance for optimization/enhancements and potential future intervention measures.
- A proposal of a new well test program and analysis of the results with respect to inflow and lift performance, flow capacity and skin.
- A definition of alternative well intervention measures.

The study revealed ample challenges which initiated the need for several in-depth studies; it was observed that well 25/8-D-1 AH T3 had challenges with poor productivity and could possibly be a candidate for well work-over. The production system was suspected to have a poor design, and simulations of an improved design was recommended. Well 25/8-E-1 H was found to have an adequate production rate.

The findings in the study performed by Weatherford Petroleum Consultants decided the main topic of this master thesis; an in-depth evaluation of well 25/8-D-1 AH T3 in regards well intervention measures. Also, other studies have been initiated after the first study; Weatherford Petroleum Consultants was hired to conduct Phase 2 and Phase 3 of the study, and one student carries out a history matching study of the upscaled model. Some of the findings from the parallel projects are presented in **Section 6.6**. The development of knowledge and understanding of the field has been an ongoing process. When the project

was initiated, much of the information available was deemed inadequate or inaccurate. Thus, working on this project has been a matter of aiming for a moving target. The reader should take this into consideration.

3 Basic Definitions

Artificial Lift

Artificial lift is a method used to lower the producing Bottom Hole Pressure (BHP) to increase the drawdown in order to obtain a higher production rate from the well. Artificial lift can be used to generate flow from a well in which no fluids are being produced or to increase the flow rate from a producing well. Most oil wells require artificial lift at some point in the life of the field (Petrowiki 2014*a*). Artificial-lift systems use a range of operating principles, including rod pumping, gas lift and Electric Submersible Pumps (ESP). (Petrowiki 2014*a*)

Gas Lift

Gas lift is an artificial method in which gas is injected into the lower part of the production tubing. The bottomhole flowing pressure reduces when the injected gas mixes with producing fluids, decreasing the flowing pressure gradient in the production string. The production rate is increased by reducing wellbore flowing pressure. The injection gas is typically conveyed down the tubing-casing annulus and enters the production train through a series of gas-lift valves. (Golan & Whitson 2003)

Lift Curves

Modelled curves of a well and/or pipeline which calculates the pressure drop in the given well and/or pipeline.

Improved Oil Recovery

IOR is commonly used to describe any process, or combination of processes, that may be applied to economically increase the cumulative volume of oil that is recovered from a reservoir at an accelerated rate (Eoga 2014).

Enhanced Oil Recovery

An oil recovery enhancement method using sophisticated techniques that alters the original properties of the oil (Schlumberger 2014*c*). EOR increases reserves by mobilizing residual

oil trapped by capillary forces and oil that is too viscous to be effectively produced by for example water flooding. The key processes are chemical-, miscible-, and thermal flooding. (Hite et al. 2013)

Well Intervention

A well intervention, or well work, is any operation carried out on an oil or gas well during or at the end of its productive life, which alters the state of the well and/or well geometry, provides well diagnostics, or manages the production of the well. (Naterstad 2013)

Side-Track

A sidetrack is a secondary wellbore drilled away from the original wellbore. To sidetrack, a hole (called a window) is made in the casing above the obstruction. The well is then plugged with cement below the window. Special drill tools, such as a whipstock, bent housing, or bent sub are used to drill off at an angle from the main well. This new hole is completed in the same manner as any well after a liner is set. (OSHA 2014)

Multilateral Well

A well that has more than one branch radiating from the main borehole. Multilaterals can be relatively simple dual-opposing laterals, or complex multi-branched wells. With a multilateral well it is possible to produce from several reservoir zones simultaneously. (Schlumberger 2014*f*)

Milling

The use of a mill or similar downhole tool to cut and remove material from equipment or tools located in the wellbore. Successful milling operations require appropriate selection of milling tools, fluids and techniques. The mills, or similar cutting tools, must be compatible with the fish materials and wellbore conditions. The circulated fluids should be capable of removing the milled material from the wellbore. (Schlumberger 2014*e*)

Dog Leg

An abrupt turn, bend or change of direction in a survey line, a wellbore, or a piece of equipment. Dog-legs can be described in terms of their length and severity and quantified in degrees or degrees per unit of distance. (Schlumberger 2014*a*)

Drainage Shape

Drainage shape is the shape of the area that is drained by a well. The shape of the area is affected by total no-flow boundaries, representing a boundary along which no fluid enters the drainage area, for example faults and very tight sediments. Different geometries for

the drainage shape have been developed, also considering the location of the well inside. Shape factors are used to correlate the location of the well inside the drainage shapes. (Dake 2001)

Multiple Rate Test

Tests conducted at a series of different flow rates for the purpose of determining well deliverability, typically in gas wells where non-Darcy flow near the well results in a rate-dependent skin effect. Multiple-rate tests are sometimes required by regulatory bodies. (Winther 2013)

Pressure Buildup Test

The most popular transient well test. The test involves a well which has produced for a period of time. The analysis is easier if sufficient production time has occurred for the well to reach stabilization. After the production period, the well is shut-in. The bottomhole pressure during the shut-in period are monitored and recorded. A standard buildup test normally lasts tens of hours to several days. (Winther 2013)

Permeability

Permeability is a property of the porous medium and is a measure of the capacity of the medium to transmit fluids (Skjæveland & Kleppe 1992). Permeability is a tensor that in general is a function of pressure. In addition, permeability is dependent upon saturation history, wettability, temperature, viscous-, capillary- and gravitational forces and pore geometry (Winther 2013). The permeability often varies spatially by several magnitudes, and such heterogeneity may influence any IOR process.

Formation permeability may be determined or estimated on the basis of core analysis, well tests, production data, well log interpretations, or correlations based on rock parameters. (Skjæveland & Kleppe 1992)

Permeability Anisotropy

Anisotropy is defined as a predictable variation of a material with the direction in which it is measured, which can occur at all scales (Winther 2013). In rocks, the variation between permeability observed in vertical and horizontal permeability is anisotropy. This is often found where platy minerals, such as clays, align parallel to depositional bedding as sediments are compacted.

Skin Factor

The skin factor, S, is a dimensionless number representing the degree of formation damage caused by the positive pressure differential between the wellbore and formation

while drilling, which leads to an invasion of the latter by drilling mud whose solid particles are retained in the pores close to the wellbore thus reducing permeability in the restricted region (Dake 2001). It may also be caused by swelling of clay.

A positive skin value indicates some damage or influences that are impairing well productivity. A negative skin value indicates enhanced productivity, typically resulting from stimulation (Winther 2013). The value for the skin factor is highly dependent on the value of the permeability-thickness product, kh.

For simplicity, skin may be divided into mechanical skin and formation skin. Mechanical skin is the reduction in permeability in the near-wellbore area resulting from mechanical factors such as the displacement of debris that plugs the perforations or formation matrix (Winther 2013). Formation skin is due to the flow from the reservoir to the wellbore caused by pressure difference. The mechanical skin is often positive, while the formation skin is negative.

Pseudosteady-State Flow

In pseudosteady-state flow there is a no-flow outer boundary. Typically, no-flow boundaries result from the pressure of offset producing wells and/or geological barriers such as faults and pinchouts (Golan & Whitson 2003). The outer boundaries are influencing the pressure in the wellbore and this results in a stable rate of pressure decline throughout the system.

Steady-State Flow

Constant-pressure outer boundary, representing the boundary along which reservoir pressure is maintained at its initial value. The constant-pressure boundary condition is usually caused by either water influx from a very large aquifer, or by water or gas injection in offsetting wells, or any combination of the three. This is usually called steady-state flow. (Golan & Whitson 2003)

Bullheading

The most common method of a contingency well kill. Forcing fluids in the pipe into the formation at a pressure higher than the pore pressure and sometimes higher than the fracturing breakdown pressure. Used to displace a kick out of the pipe when wellbore and wellhead pressure limits permits. (Petrowiki 2014*b*)

4 Reservoir Simulation

Reservoir simulation has become an integral part of the oil and gas industry over the last 50 years (Samier 2011). Reservoir simulations may help to make large capital decisions, to estimate reserves, and to diagnose and improve the performance of producing reservoirs. Some of the incentives for undertaking reservoir simulation studies are listed in **Table 4.1**.

Table 4.1: Incentives for reservoir simulation, from Franchi (2006).

- Cash flow prediction
- Coordinate reservoir management activities
- Evaluate project performance - understand reservoir behavior
- Model sensitivity to estimated data - determine the need for additional data
- Estimate project life
- Predict recovery versus time
- Compare different recovery processes
- Plan development on operational changes
- Select and optimize project design
- Maximize economic recovery

Simulating may be defined as *assuming the appearance of without the reality* (Petrowiki 2014*c*). Simulation of petroleum reservoir performance refers to the construction and operation of a model whose behavoir assumes the appearance of actual reservoir behavoir. The model is a set of equations that, subject to certain assumptions, describes the physical processes active in the reservoir (Petrowiki 2014*c*). Although the model itself lacks the reality of the reservoir, the behavior of a valid model simulated, assumes the appearance of the actual reservoir.

The blocks in the horizontal direction in a simulation model are usually in the order of hundreds of meters due to the run time of the model. This implies that the reservoir model only has the capacity of showing the most significant properties of the actual reservoir and not at the desired one-metre scale. Petrophysical properties, pressure and saturations are assumed to be constant over a significant rock volume in the order of 100m x 100m x 10m.

There is a wide selection of available commercial reservoir simulators with different capabilities and solution techniques. In the following, the Schlumberger reservoir simulation software, ECLIPSE 100, will be described.

4.1 ECLIPSE 100

The ECLIPSE industry-reference simulator offers the industry's most complete and robust set of numerical solutions for fast and accurate prediction of dynamic behavior for all types of reservoirs and development schemes. The ECLIPSE simulator has been the benchmark for commercial reservoir simulation for more than 25 years due to its extensive capabilities, robustness, speed, parallel scalability, and unmatched platform coverage. (Schlumberger 2014*b*)

The name ECLIPSE was originally an acronym for "ECLs Implicit Program for Simulation Engineering" (Wikipedia 2013). ECLIPSE 100 is a fully implicit, three phase, three dimensional, general purpose black oil simulator with gas condensate option. The program can be used to simulate one, two or three phase systems (NTNU 2014). Some of the model features available in ECLIPSE 100 are listed in **Table 4.2**. In addition to the features listed in Table 4.2 ECLIPSE 100 contains multiple special extensions, for example Polymer, Multi Segment Well and Coal Bed Methane options. (Lorentzen 2013)

Table 4.2: Model features available in ECLIPSE 100, from Lorentzen (2013) page 3.

- Variety of grid geometry options such as corner point, block-centered and radial
- Able to model all recovery mechanisms
- Possibility of subdivision of reservoir into regions of different rock/fluid properties
- Local grid refinements
- Both dual porosity and dual permeability formulation option for fractured reservoirs
- Fault modeling with non-neighbouring connections
- Numerical and analytical aquifer modeling
- Miscible flood modeling for three components
- Non-Darcy flow
- Tracer, brine and API tracking
- Rock compaction
- Hysteresis

The ECLIPSE simulator is the most feature-rich and comprehensive reservoir simulator on the market, covering the entire spectrum of reservoir models, including black oil, compositional, thermal finite-volume and streamline simulation (Schlumberger 2012*a*). As ECLIPSE 100 provides a wide range of features and special extensions it is a natural choice for simulator of conducting simulations on.

4.2 A Reservoir Model

Reservoir simulations are built on reservoir models that include petrophysical characteristics required to understand the behavior of the fluids over time (Schlumberger 2014*k*). Reservoir models can be used to examine the flow of fluids within the reservoir

and from the reservoir, and are used for prediction and understanding of reservoir performance.

Reservoir models are created from static geological models containing up to tens of millions grid blocks. The model incorporates all the static geologic characteristics of the reservoir, which include the structural shape and thicknesses of the formations within the subsurface volume being modelled, their lithologies, the initial saturation and the porosity and permeability distribution. Porosity and permeability often vary from location to location, resulting in heterogeneity (Schlumberger 2014*j*). The more accurate model, the more grid blocks are needed.

4.3 History Matching

Once the objectives which will be incorporated in a reservoir model are defined, the development of the model proceeds in three stages; the history matching stage, the calibration stage and the prediction stage. The calibration stage provides a smooth transition between the history matching stage and the prediction stage. (Franchi 2006)

History matching is the act of adjusting a model of a reservoir until it closely reproduces the past behaviour of a reservoir (Schlumberger 2014*d*). If a coarse study is being performed, the quality of the match between observed and calculated parameters does not need to be as accurate as it would for a more detailed study. The tolerance of a coarse study is $\pm$ 10% drawdown, whilst for a study of greater reliability it should be reduced to $\pm$ 5%, or even less (Franchi 2006). The accuracy of the history matching depends on the quality of the reservoir model and the quality and quantity of pressure and production data (Schlumberger 2014*d*). A model may be considered reasonable if it does not violate any known physical constraints.

The important stages in history matching are data preparation, matching strategy, key history matching parameters, evaluation of the history match, deciding on a match and to test the reasonableness of the match. Among the data variables matched in a typical black oil or gas study are pressure, production rate, Water Oil Ratio (WOR), Gas Oil Ratio (GOR), and tracer data if it is available. More specialized studies, such as compositional or thermal studies, should also match data unique to the process, such as well stream composition or the temperature of produced fluids (Schlumberger 2014*d*). Production performance depends on input variables such as permeability distribution and fluid properties. The goal of the history match is to find a set of input variables that can reconstruct field performance. However, the uniqueness of a selected model is always a challenge in a successful history matching; there may exist several, very different solutions to the history match, not violating any known physical parameters. The uniqueness of history matching results in practice can be assessed only after individual and technical experience and/or by repeating history matching with different reservoir models (Rafiee 2011). The uniqueness problem arises from many factors. Most notable of these are unreliable or limited field data, interpretation errors, and numerical effects

(Schlumberger 2014*d*).

Once a model has been history matched, it can be used to simulate future reservoir behaviour with a higher degree of confidence, particularly if the adjustments are constrained by known geological properties in the reservoir. (Schlumberger 2014*d*)

5 Improved Oil Recovery

In today's society it is observed an increasing demand of petroleum as the consumption is increasing. The trend of a steady increase is illustrated in **Figure 5.1**. On the other hand, estimates of new discovered reserves have decreased steadily since 1970 (Labastidas Avila et al. 2013). The declined production, decreasing amount of new discovered reserves and high costs of green field developments prompt the need for an increase in the recovery factor at the already developed fields.

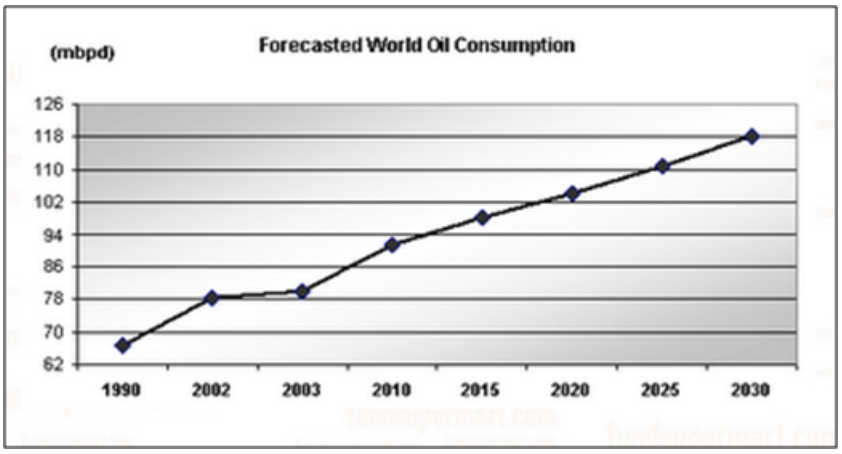

Figure 5.1: Forecasted world oil consumption, from Labastidas Avila et al. (2013), page 28.

The current, as of 2013, world average oil RF from oil fields is estimated to 30-35% (Eni 2014), whereas the recovery factor at the NCS is estimated to 46% (Oljedirektoratet 2013). This means that as much as 50-70% of the original oil in place is left when ending the production. Good reservoir properties have strongly contributed to the high RF on the NCS. In addition, extensive research, water and/or gas injection, 3D and 4D seismic data, systematic data collection for better reservoir understanding and drilling more wells than planned, technological development and close monitoring by the authorities have been important to increase the recovery (Oljedirektoratet 2011*b*). To this end, technological development and research are paramount (UiS 2014).

The primary measure of achieving increased recovery is by IOR. IOR recovers additional oil beyond fluid expansion, rock compressibility, gravitational drainage, pressure decline

and natural water- or gas drive. It may include chemical, mechanical, physical, or procedural processes, or a combination of the different methods. In this sense, IOR includes both EOR and well intervention. EOR consists of chemical and/or thermal processes, for example thermal flooding, surfactant injection and water-alternating-gas injection. Well intervention may for example include infill drilling, scale removal and hydraulic fracturing. EOR technologies are specifically designed to affect mostly the immobile oil that remains in the reservoir, while IOR strategies can be used to recover more of the remaining mobile oil and/or immobile oil. (Eoga 2014).

The potential for a later commitment to IOR is determined largely by the original development solution (Osmundsen 2011); either subsea development or topside development. Hence, it is important to carefully consider the choice of development with regards to later operations.

5.1 Subsea Operated Fields

Subsea production systems refer to production systems situated under water on the sea floor (Naterstad 2013). The complexity of subsea production systems can range from single satellite wells tied back to Floating Production Storage and Offloading (FPSO) units, to several wells in a subsea template. Small, deep and/or remote fields may be opened up for production with a subsea production system. A subsea facility can be a good solution where the distance to land or to existing platforms is short, and where a platform-based development would not be profitable. In recent years an increase of subsea wells are observed, leading to more production from subsea wells than from platform wells (Oljedirektoratet 2011*a*). See **Figure 5.2**.

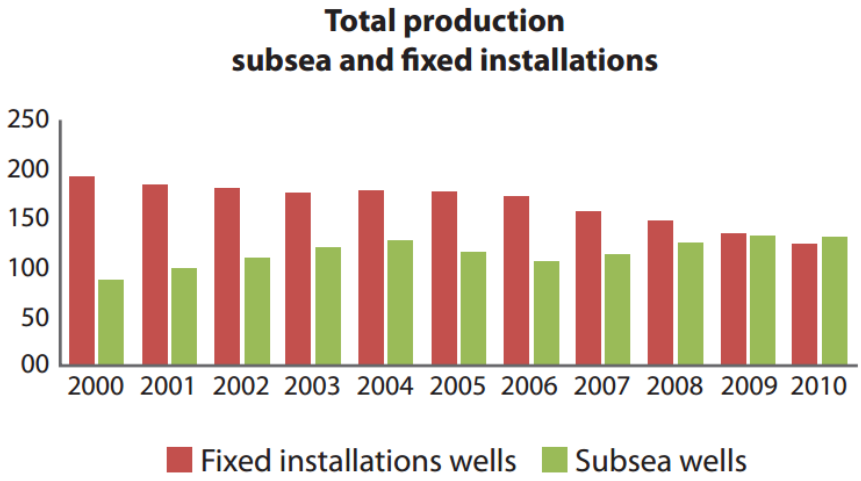

*Figure 5.2: Total production from subsea installations and fixed installations. There is observed a decrease in fixed installations and an increase in subsea installations. From Oljedirektoratet (2011*a*).*

When developing a subsea production system, the initial investment, Capital Expenditure (CAPEX), is lower than that of a topside operated field. The operating costs, Operational Expenditure (OPEX), remains higher throughout the service life of the field. This may make a subsea operated field more expensive to operate than a topside operated field. An important characteristic of subsea solutions is that they simplify a phased delineation and development of fields, and thereby normally provide an earlier start to production with the gathering of useful information. They usually involve pre-drilling, so that plateau production is reached quicker. Faster development and shorter time to plateau production almost always increase net present values. The recent years' high oil prices have made subsea field development technology economically viable. (Naterstad 2013)

Figure 5.3 shows the RF for both subsea operated fields and platform operated fields. Subsea wells normally underperform platform wells in RF with 15-20% (Iversen 2012).

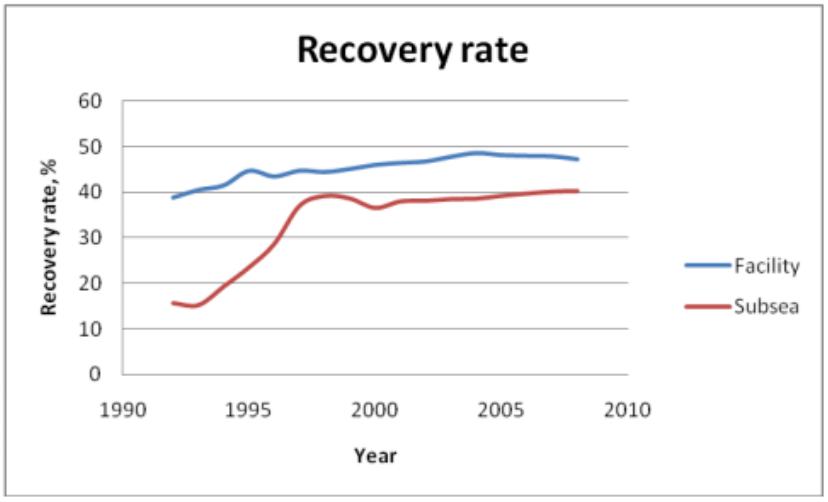

Figure 5.3: Average recovery factors for topside operated fields vs. subsea operated fields. From Osmundsen (2011), page 5.

5.2 Subsea Well Intervention

Well intervention is an IOR strategy which alters the state of the well and/or the well geometry. The operations are carried out on a well during, or at the end of, its productive lifetime. Examples of operations that may be performed include logging, perforating, milling and underreaming to remove wellbore scale, see **Figure 5.4**. (Kratz 2011)

Subsea well interventions are observed to be limited as compared to platform well interventions, see **Figure 5.5**. This may lead to a growing value gap between platform wells and subsea wells. Poor access and technology are some of the factors limiting the subsea well interventions, thus it is a key factor to develop the knowledge and new technology (Iversen 2012). See **Figure 5.6**.

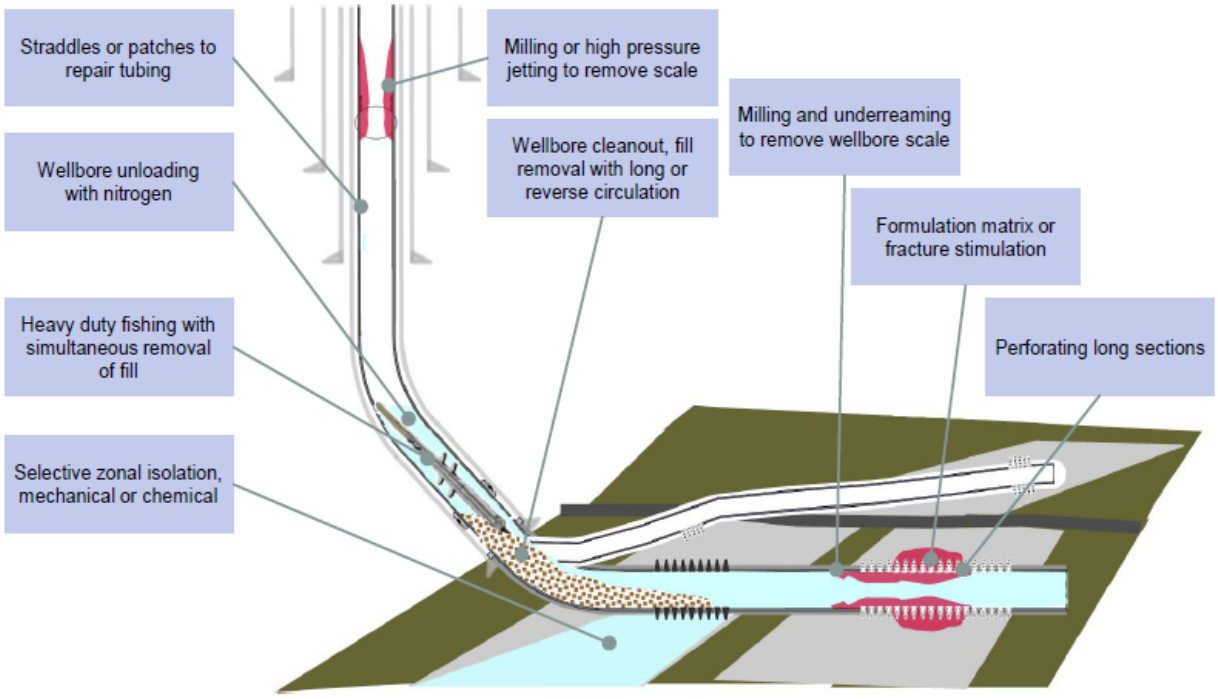

Figure 5.4: Examples of well intervention operations, from Kratz (2011), page 5.

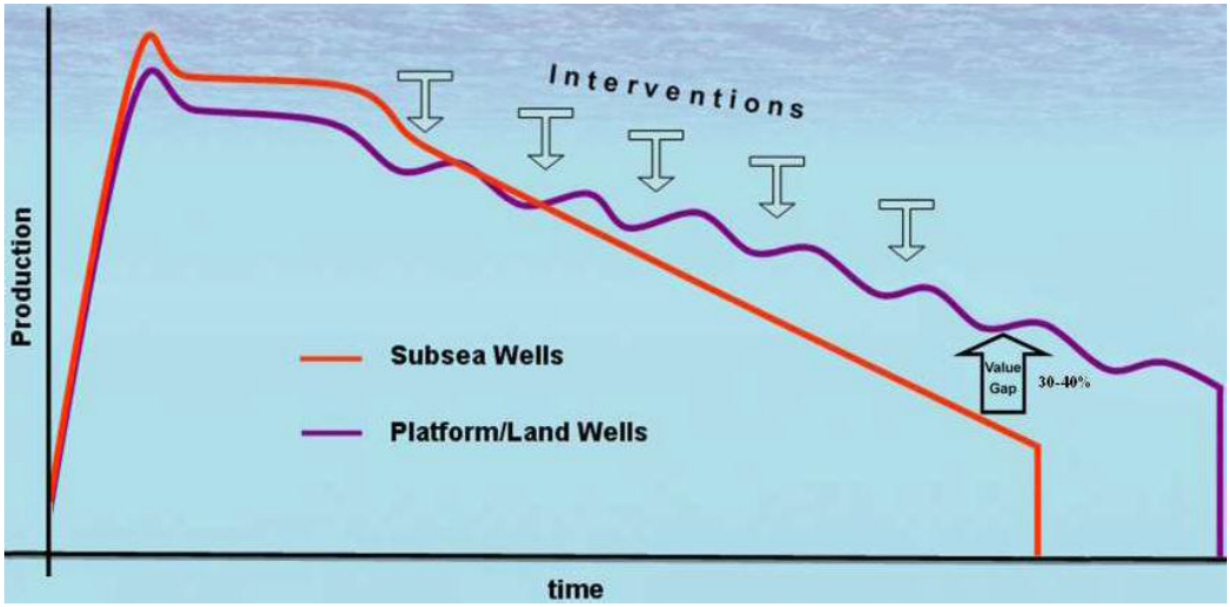

Figure 5.5: Production profile improvement on platform wells/land wells undergoing well intervention compared to subsea wells, from Haraldseide (2011), page 10.

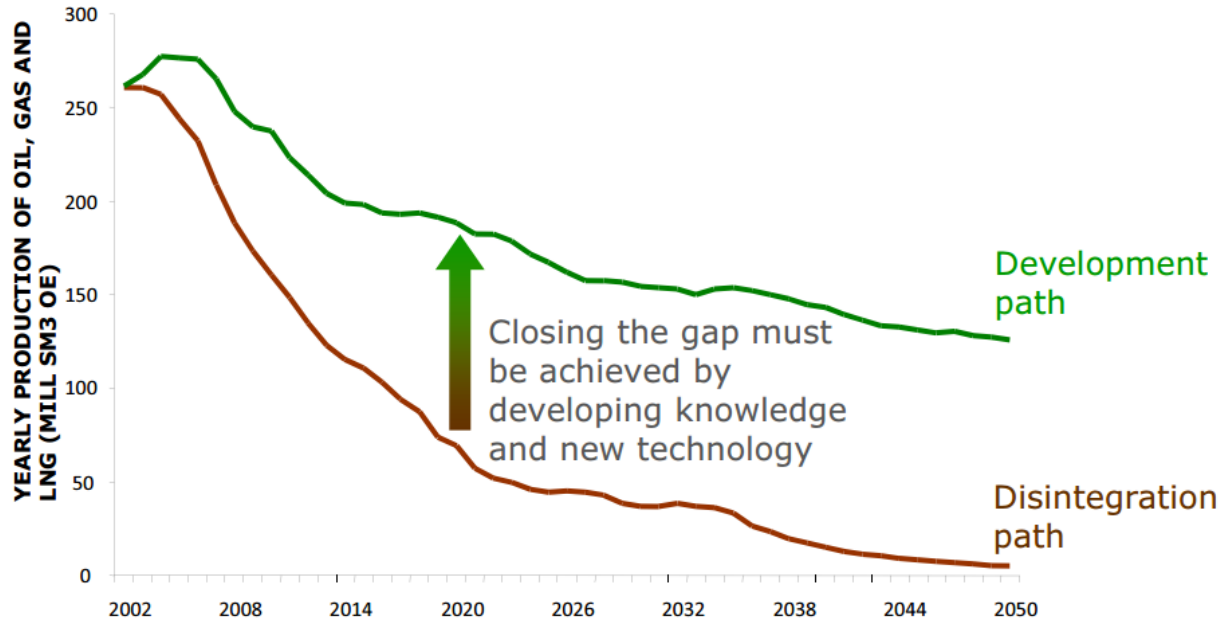

Figure 5.6: Closing the value gap may be acheived by developing knowledge and technology, from Iversen (2012).

Historically, subsea well interventions were usually performed using tethered floating drilling rigs anchored to the sea floor. As technology is developed, water depth increases, well head design evolves and well construction changes, intervention also evolves and demand grows (Kratz 2011). This implies a trend towards utilizing lighter vessels for data gathering and light interventions such as logging (Naterstad 2013). Still, well interventions of subsea developed production systems are more cost intensive than topside operated production systems. An improvement measure on a subsea well often requires five times the earnings potential than would be needed for an intervention in a platform well (Osmundsen 2011). Vessel availability, cost and the logistics involved in moving suitable vessels from field to field are some of the factors limiting operators from maintaining optimal production rates at all times (Naterstad 2013). Later commitment to IOR based on a dedicated drilling rig will normally have greater potential than platforms without such facilities or than subsea solutions where a mobile rig must be chartered each time an intervention is needed (Osmundsen 2011).

Well intervention operations are commonly divided into Light Well Intervention (LWI), Medium Well Intervention (MWI) and Heavy Well Intervention (HWI). The difference is the equipment used; which operations which can be done. The main operation methods are wireline, Coiled Tubing (CT) and jointed pipe.

5.2.1 The Drilling Riser

A drilling riser is required in conventional drilling operations and heavy well intervention operations such as recompletions. The drilling riser provides the conduit through which to run the drill string and returning drilling fluids, as well as a structure to attach hydraulic and electrical control lines for the BOP (Schlumberger 2013*a*). See **Figure 5.7**. The riser may be considered a temporary extension of the wellbore to the surface.

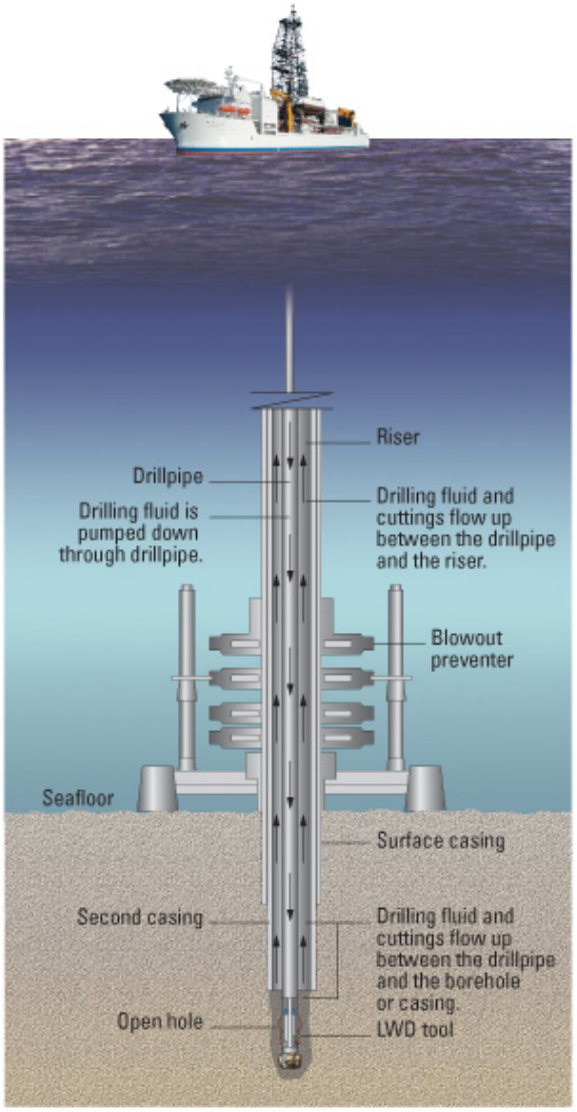

*Figure 5.7: Marine drilling riser, from Schlumberger (2013*a*).*

Only the heavier vessels and rigs are able to operate with a conventional drilling riser, due to the riser's complex constructions and weight, and that it requires a certain amount of flexibility and heave compensation in order to compensate for wave-induced motion

(Naterstad 2013). Production riser types are roughly divided into high pressure risers and low pressure risers, signifying the construction's capacity to withstand pressure. (Naterstad 2013)

Riserless Light Well Intervention (RLWI) units are vessels which perform well intervention measures with the use of cables instead of the riser. These measures are commonly referred to as RLWI. RLWI are optimal for installation and manipulation, repair and scale removal of some equipment, fluid sampling, re-perforations, zone isolation and chemical treatment. RLWI has been performed successfully in the North Sea up to 600 metres. (Haraldseide 2011)

5.2.2 Well Intervention Operations

Light Well Intervention

LWI includes wireline services using a subsea lubricator system. Subsea wireline lubricator systems do not require workover riser packages. Hence, these systems are easily used with monohull vessels. (Naterstad 2013)

Examples of wireline operations include fishing, logging, setting and retrieval of valves, installation of gas lift systems and ESP, perforations, setting or removing of plugs and gauge cuttings. The interventions performed by wireline are limited by weight and energy.

Medium Well Intervention

MWI consists of CT, performed using a workover riser package via a semisubmersible or jack-up rig. Riserless CT systems are also being developed, to further decrease the cost of subsea well intervention and allow monohull vessels to use this technology. (Sandheep & DeWalt 2003)

Examples of CT operations include fishing, logging, perforating, acidizing/stimulating, proppant fill, nitrogen injection, Through Tubing Rotary Drilling (TTRD) and cementing.

Heavy Well Intervention

HWI involves jointed pipe operations using derricks and hydraulic workover units, both of which requires the use of conventional rigs and a conventional riser (Naterstad 2013).

Examples of jointed pipe operations include fishing, plugging and abandonment, acidizing/stimulating, setting and retrieval of valves, perforating, TTRD and cementing.

Figure 5.8 illustrates examples of vessels and rigs which may be used to perform LWI, MWI and HWI.

Some intervention methods are limited depending on equipment or downhole conditions. For example, some fish may be retrievable by wireline, while others may not. **Table 5.1**

shows a brief comparison of intervention conveyance methods, taken from *Subsea Well Intervention Operations on the Norwegian Continental Shelf* (Naterstad 2013).

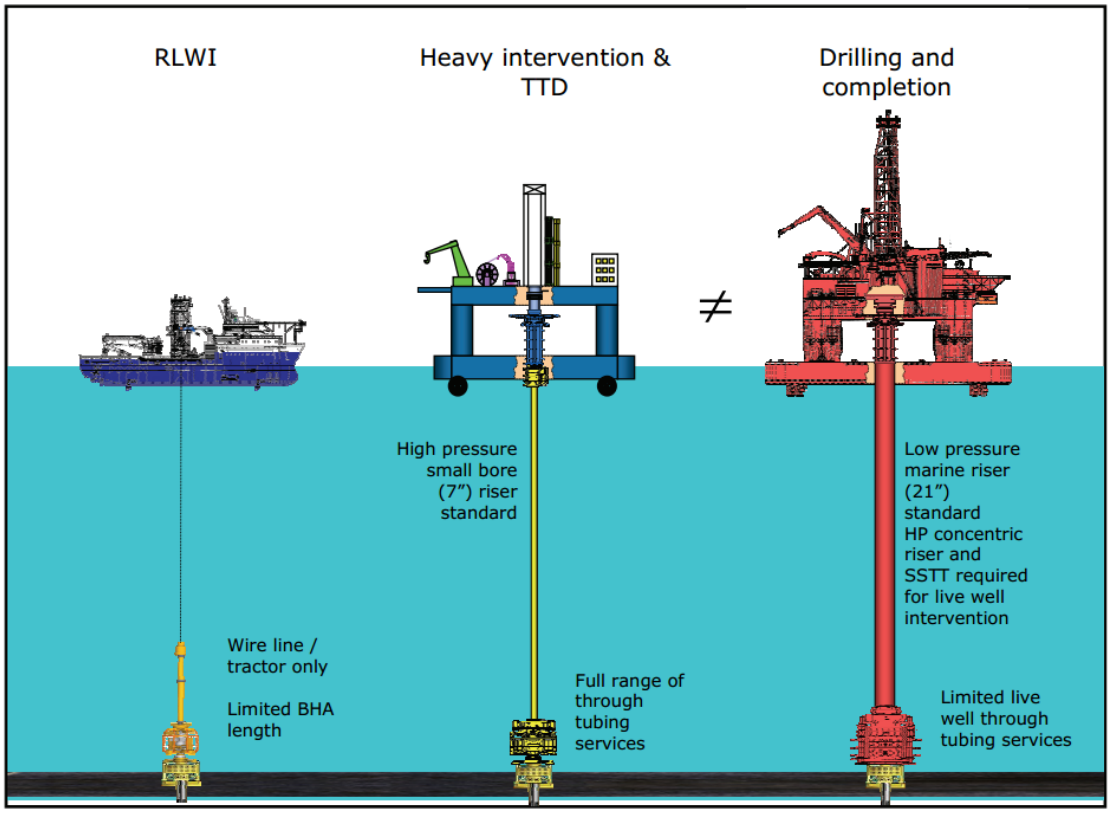

Figure 5.8: Examples of vessels and rigs which may be used to perform different well intervention measures, from Fjærtoft & Sønstabø (2011), page 8.

Table 5.1: Comparison of intervention conveyance methods, from Naterstad (2013), page 25.

Intervention Measure	Wireline	Coiled Tubing	Jointed Pipe
Borehole Surveys/logging			
Casing Leak/Repair			
Electrical Submersible Pumps	Limited	Limited	
Fishing	Limited		
Fluid Displacement			
Gas Lift Valves			
Horizontal Well Sand Control			
Paraffin/Asphaltene Precipitation/Hydrate Obstructions	Limited		
Perforating			
P&A	Limited	Limited	
Remedial Cementing			
Re-Perforating			
Sand Control/Gravel Pack			
Sand Washing			
SCSSV Failure (Tubing Pull Repair)		Limited	
SCSSV Failure (Wireline Repair)	Limited	Limited	
Setting/Pulling Tubing Plugs			
Stimulation			
Tubing/Packer Failure			
Water Shut-Off			
Zonal Isolation			

Legend:
Not applicable at present
Limited functionality at present
Full functionality

5.2.3 Well Intervention Measures

Infill Drilling

Once a field has produced for some time, it might be desirable to drill additional wells, sidetrack existing wells, replace damaged wells, or convert existing wells to multi-lateral wells in order to improve the recovery. This is commonly referred to as infill drilling (Naterstad 2013). Infill drilling increases the reservoir-to-well-exposure, hence increasing the reservoir drainage area, and enables widely spaced reservoir compartments to be targeted, optimizing economic extraction of oil and gas. Infill drilling might not be

possible using conventional drilling technology if depletion of the reservoir has reduced the reservoir pressure to the point where the mud window is closed. (Naterstad 2013)

Sidetracking can be done at different locations in the well. A sidetrack can be made through existing reservoir completions in order to drain the same reservoir. Making a multilateral well, or a new sidetrack, can be done by placing a whipstock in the existing well and kick off in another direction. Milling of the existing casing at the kick off point is necessary. The whipstock can be perforated afterwards to open up for production from both wells.

Through-Tubing Drilling and Completion (TTDC) is a generic term for drilling sidetracks in existing producers and injectors, and covers both Coiled Tubing Drilling (CTD) and TTRD (jointed pipe), including installing the associated lower completion, typically liners or screens, see **Figure 5.9**. (Statoil 2008)

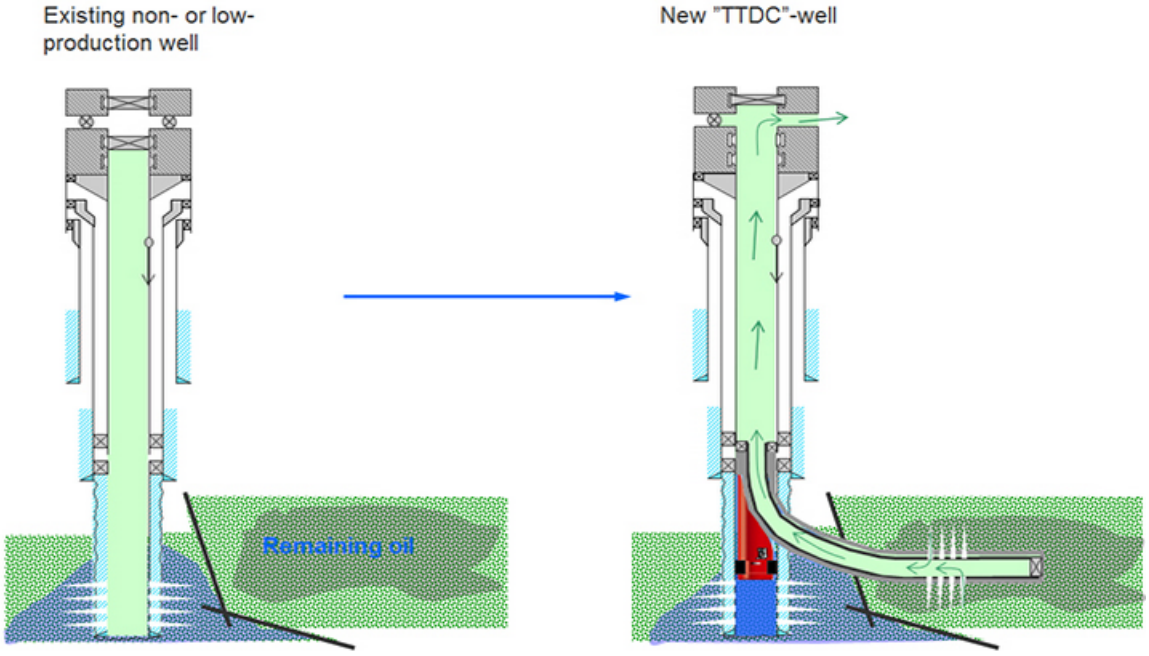

Figure 5.9: Illustration of a sidetracked well with through-tubing drilling, from Statoil (2008).

Through-tubing drilling is a slim-hole side-tracking technique currently used on offshore wells to inexpensively drill marginal targets, with a kick-off point in existing production liner or completion tubing. The main advantage of the technology is that new reservoir sections can be reached without having to remove the existing X-mas tree, the completion or the production casing, thereby reducing operational time significantly compared to a "standard" slot recovery or side-track (Statoil 2008). TTDC-wells are particularly useful for accessing pockets of isolated oil and gas in mature fields.

Through tubing drilling has limited reach, due to sliding friction and the buckling limit of the tubing used; TTRD has a limited reach of 3500 ft from kick-off point, while CTD has

a limited reach of approximately 2500 ft (Naterstad 2013).

Acid Squeeze

The potential of a well may be limited due to skin damage. Skin damage may be induced by drilling fluids, clean-up fluids and the interaction of clay with water. Formation rocks contain clay, which has a tendency to swell in contact with water. Skin damage induces reduced rock permeability near wellbore.

Squeeze is an application of pump pressure to force a treatment fluid, for example acid, or slurry into a planned treatment zone. The intention of acid treatments is to dissolve the sediments and mud solids that are inhibiting the permeability of the rock and stimulate the productivity of the well (Naterstad 2013). In most cases, a squeeze treatment will be performed at downhole injection pressure below that of the formation fracture pressure. In high-pressure squeeze operations, performed above the formation fracture pressure, the response of the formation and the injection of treatment fluid may be difficult to predict. (Schlumberger 2014*m*)

Acid squeeze is done by using carefully placed specialized tools fitted on a CT string or a drill pipe string. It can also be performed using supply vessels with appropriate tanks and pumps, pumping the well full of chemicals. (Naterstad 2013)

Scale Removal

Scale is defined as a deposit or coating on the surface of the metal, rock or other material. It is caused by a precipitation of solids due to a chemical reaction with the surface (usually $CaCO_3$ and/or $BaSO_4$), a change in pressure and/or temperature, or a change in the composition of a solution. In severe conditions scale creates a significant restriction, or even a plug, in the production tubing, see **Figure 5.10**. (Schlumberger 2014*l*)

*Figure 5.10: Scale can severely impede flow by clogging perforations or forming a thick lining in the production tubing, from Schlumberger (2014*l*).*

As scale precipitates accumulate, the effective diameter of the tubing decreases, causing pressure loss along the well and associated reduced productivity. Scale can be removed, either by using milling tools fitted on a drill string, CT string or wireline, or chemical treatment of the well, depending on the composition and severity of the precipitates. (Naterstad 2013)

Methanol and Glycol Injection

Gas hydrates are a well-known problem in natural gas processing and transmission pipelines when natural gas and water exist at specific conditions. This is particularly true at high pressures and low temperatures (Moshfeghian & Taraf 2008). One of the methods to prevent hydrates from forming is by injecting alcohols and/or glycols into the gas stream to move the hydrate-formation conditions to lower temperatures and higher pressures (inhibition). The inhibitor may be distributed as aqueous phase, vapor hydrocarbon phase or liquid hydrocarbon phase.

Methanol and Glycol (MEG) may be used as inhibitor. In a typical MEG regeneration prevents hydrates from forming (Moshfeghian 2007). The purpose of the injected MEG is not to "dehydrate" the gas, but to prevent formation of hydrates. The MEG absorbs only a small amount of water vapor from the gas with normally used MEG concentrations, 80-85 weight%. (Moshfeghian 2007)

Perforations

To perforate a well is to create holes in the casing or liner to achieve efficient communication between the reservoir and the wellbore. Formation fluids may enter the production tubing, or materials may be introduced to the annulus through the holes. The characteristics and placement of the perforations can have significant influence on the productivity of the well (Schlumberger 2014*h*). Therefore, it is important to ensure efficient creation of the appropriate number of perforations, perforation size and orientation. The perforations are usually made by means of projectiles, discharging jets or shaped explosive charges (Naterstad 2013). A perforating gun assembly with the appropriate configuration of shaped explosive charges is lowered downhole, either by means of wireline, tubing or coiled tubing.

Recompletion

Many wells have multiple productive zones. The need for recompletion rises after the well has produced all of the oil or gas from the original completed zone (U.S. Emerald Energy Company 2012). It is common practise to complete one zone at a time, to avoid production from several layers and introducing the possibility of crossflow (Naterstad 2013). Due to pressure reduction in the already produced zone, the well is normally recompleted in a zone above the initial completion. This is usually the least complicated and least expensive method. (U.S. Emerald Energy Company 2012)

The process of recompletion is similar to completing the original well. In the act of replacing the original completion interval and preparing a different reservoir interval in the same producing well, the existing tubing is pulled, followed by plugging off the previously producing zone. The new zone is perforated and a new production tubing is placed. (U.S. Emerald Energy Company 2012)

Hydraulic Fracturing and Pulse Fracturing

Hydraulic fracturing involves injection of a fluid with a relatively low rate of loading. This results in a two-winged vertical fracture extending outward from the well, approximately 180° apart and oriented perpendicular to the least principle rock stress. The fluids usually contain water, proppant and a small amount of nonaqueous fluids designed to reduce friction pressure while pumping the fluid into the wellbore.

The potential penetration of the hydraulic fracture can be tens to hundreds of meters (in tight shales) due to the creation of a single fracture and the ability to pump large volumes of fluids at relatively low rates (Advanced Resources International 2013). Hydraulic fracturing creates high-conductivity communication with a large area of formation and bypasses any damage that may exist in the near-wellbore area.

Pulse fracturing is characterized by peak pressures exceeding both the maximum and minimum in-situ stresses, also creating a radial fracture pattern. Pulse fracturing involves much rapid energy discharge, creating a series of vertical fractures, up to 7-8 m in length (in tight shales), propagating radially outward from the wellbore (Advanced Resources International 2013).

The primary difference between hydraulic fracturing and pulse fracturing is the rate at which energy is applied to the formation to create fractures. See **Figure 5.11**.

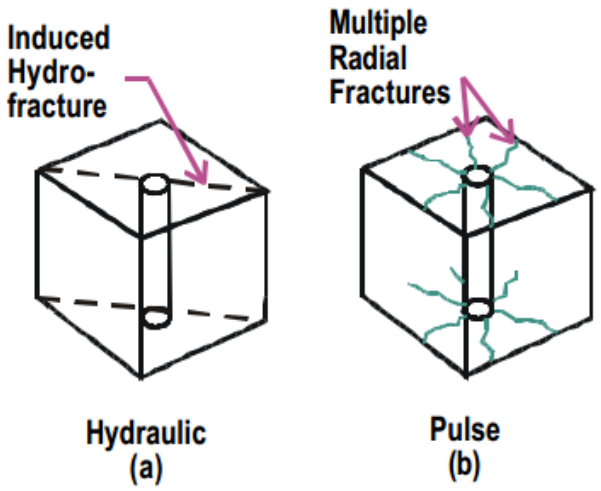

Figure 5.11: Comparison of created fracture geometries for rock fracturing techniques, from Advanced Resources International (2013), page 3.

6 Jette

The Jette field lies within production license PL027D (Lysne & Nakken 2013), in block 25/7 and 25/8, 180 km west of Haugesund and six km south of the ExxonMobil operated Jotun field. The location is shown in **Figure 6.1**. Det Norske Oljeselskap ASA is the operator with an ownership of 70%, and their partner, Petoro, has an ownership of 30% (Winther 2013). The field is divided into Jette North and Jette South.

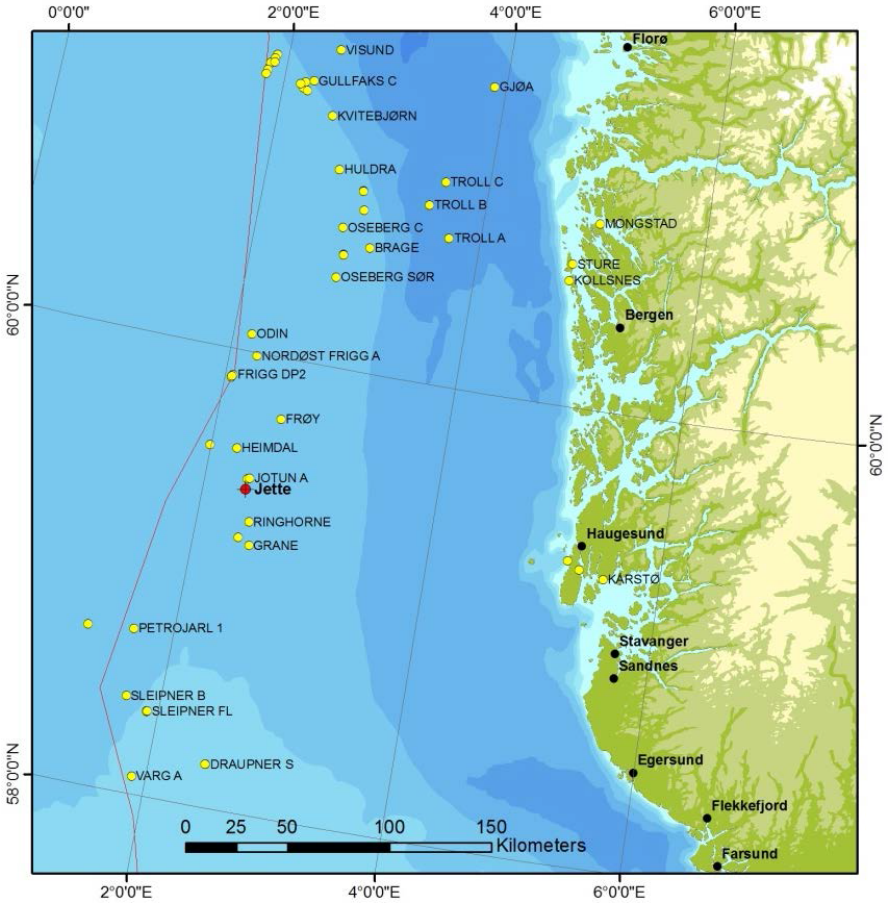

Figure 6.1: The Jette field is located 180 km west of Haugesund, and six km south of the Jotun field. From Rodrigues et al. (2013a), page 12.

The exploration wells, 25/8-17 and 25/8-17 A, proved oil and gas in the Paleocene sandstones, Heimdal formation, in the *Jetta* prospect in October/November 2009. Well 25/8-17 showed an undersaturated oil column of 27 m at a vertical depth of 2100 m, and the sidetrack well 25/8-17 A showed a thin gas cap over the oil column (Brenna et al. 2012). The water depth is 126-128 m, with a relatively flat sea bottom (Winther 2013). The field is developed with two horizontal wells, well 25/8-D-1 AH T3 and 25/8-E-1 H, hereafter referred to as Well D and Well E respectively. Both of the wells are drilled in Jette South, due to unexpected challenges while drilling (Winther 2013).

The Jette field is in the Heimdal Formation, in the Rogaland Group. It is of Cenozoic age, 56-66 million years. (Winther 2013)

6.1 Geology

The Rogaland Group, consisting of Baler, Sele, Lista, Heimdal and Ty formations, is at an estimated depth from 1892 m True Vertical Depth (TVD) Mean Sea Level (MSL) to 2170 m TVD MSL (Brenna et al. 2012). Jette is producing from the distal parts of the Paleocene Heimdal formation, a sand-rich, deep-marine, turbidity system in the Upper Heimdal formation (Winther 2013). This is part of the same formation as the Tau West structure produced at Jotun (Lorentzen 2013). The shale in the Sele and Lista formations poses as the cap rock, with a thickness of 80-100 m. (Nakken et al. 2010)

Jette is structurally downfaulted from the Utsira High, and is a combination of a structural- and a stratigraphical trap (Brenna et al. 2013*b*). As Jette, Jotun contains both differential compaction traps and a stratigraphical trap (Winther 2013). These are seen as Elli and Elli South four-way dip closures and Tau West in **Figure 6.2**. The stratigraphical trap in Jette is observed towards the main fault in north-east, in the Jette/Tau area, as the sands pinch out. Several faults were initially located at Jette, but there is a high degree of uncertainty with regards to faults (Lorentzen 2013). See **Figure 6.3**.

6.1.1 Stratigraphy

The lithologies in Jette include claystone, tuffacecous claystone, sandstone, siltstone and local limestone stringers, with main facies roughly divided into High Density Turbidities (HDT), Low Density Turbidities (LDT), green shales and black shales.

The reservoir facies at Jette reflect the settling environment, a deep-marine, turbidity system, where the different submarine fan systems are separated by biostratigraphically correlatable and laterally extensive anoxic black shale intervals. These intervals mark the periods of basin shutdown. The submarine fan systems are characterized as amalgamated sandy debris and high density turbidities are interbedded with turbidite. The depositional setting of the reservoir sands are strongly influenced by sandstone mounding of the underlying Ty- and lower Heimdal formation along the main fault trend at Jette. (Brenna et al. 2013*b*)

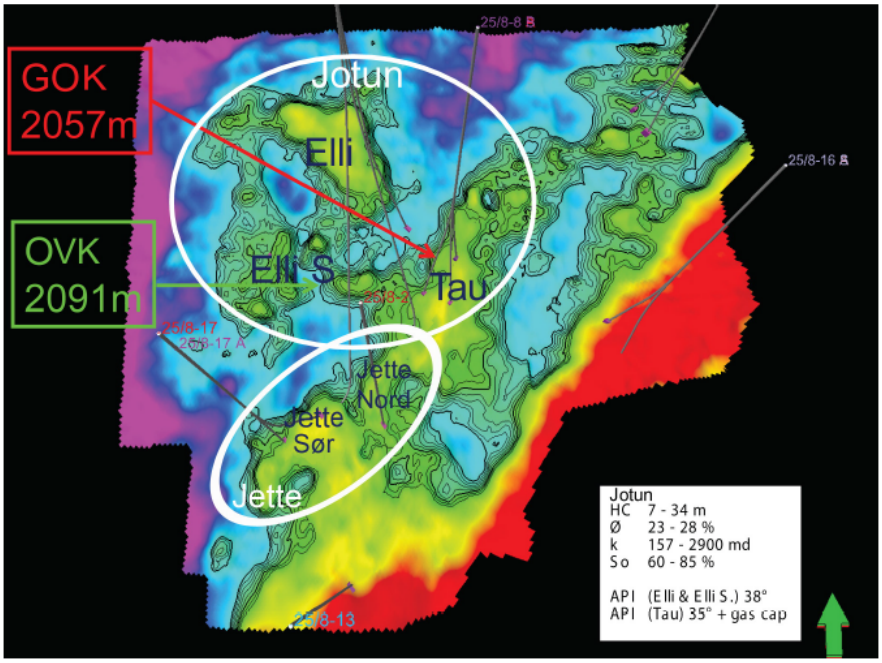

Figure 6.2: Jette area map. The Jotun/Tau/Jette closures are drawn and parameters for the Jotun field listed, from Brenna et al. (2012), page 15.

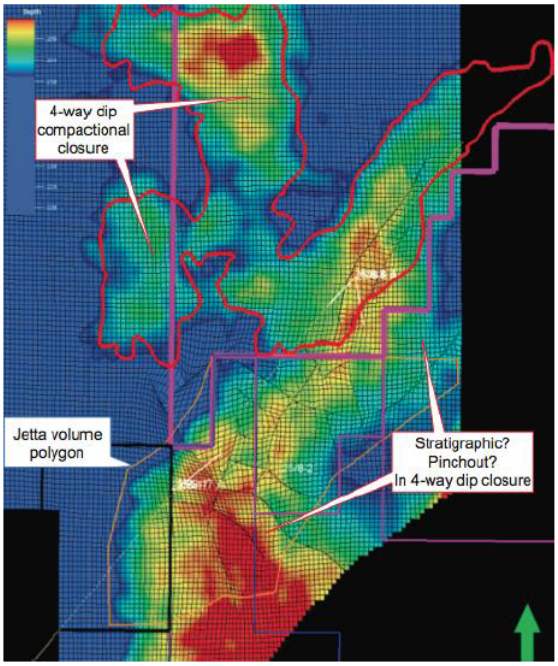

Figure 6.3: Trap configuration of Jette and Jotun including possible faults, from Lorentzen (2013), page 33.

The periodic black shale intervals are identified in both logs and seismic data, and are recognized as zone boundaries. Sand injections are observed in the shale layers, which may provide considerable vertical connectivity allowing effective vertical drainage while areally extensive basin muds retard water break through (Brenna et al. 2013*b*). Pockets of sands may also be found, sealed with black shale.

The HDT sand is recognized as the main reservoir facie, and is believed to be characteristic for both Z1 and Z2 layers. It is of good reservoir quality, with massive, well sorted, amalgamated turbidities. The LDT is of moderate reservoir parameters, and is associated with turbidite flow, lower energy, finer grained turbidities and classical non-amalgamating turbidities (Brenna et al. 2013*b*).

The thicknesses of the periodic layers vary from 4-10 m.

6.2 Reservoir

The highly heterogeneous reservoir is found at approximately 2060 m TVD MSL. The permeability of the reservoir sands are in mD region. The targeted sands, Z1 and Z2 layer, pinches out towards north-east. The Oil-Water Contact (OWC) is defined at 2091 m TVD MSL, and the questionable Gas-Oil Contact (GOC) is expected at 2068 m TVD MSL.

Based on observations from neighbouring fields, which are assumed to have the best pressure support in the North Sea (Winther 2013), it is expected water-drive at Jette, resulting in that the initial reservoir pressure is maintained throughout the production period. As the reservoir depletes, the water will move in from the aquifer below and displace the oil. The initially found gas cap at Jette is not expected to give any pressure support. This is based on the uncertainty whether there exists a gas cap or not. This is discussed further in **Section 6.6**.

As seen in **Figure 6.4** the blue arrows indicate aquifer support from west and the white outlines indicate estimated drainage areas (Winther 2013).

The initial reservoir pressure and temperature is 196.7 bara and 83.6 °C. The GOR is estimated to 80-100 Sm^3/Sm^3, and the B_o to 1.346 Rm^3/Sm^3. The Bubble Point Pressure (P_{BP}) was initially assumed to be 172.3 bara, and as of today (11.02.2014) estimated to 114.7 bara. This rises questions as to the existence of the gas cap.

Both the net gross and the porosity is smaller than what are estimated at the Jotun field, indicating poorer reservoir quality. The net gross is 20-26% and the porosity is assumed to be 24-25%. kh is estimated with a geometric average of 14-27 $mD * m$ (Winther 2013). **Table 6.1** summarizes the reservoir parameters of Jette.

The latest resource estimate indicates Stock Tank Oil Initially In Place (STOIIP) of 11.2 MSm^3, and technical recoverable reserves of 1.039 MSm^3 (Lorentzen 2013).

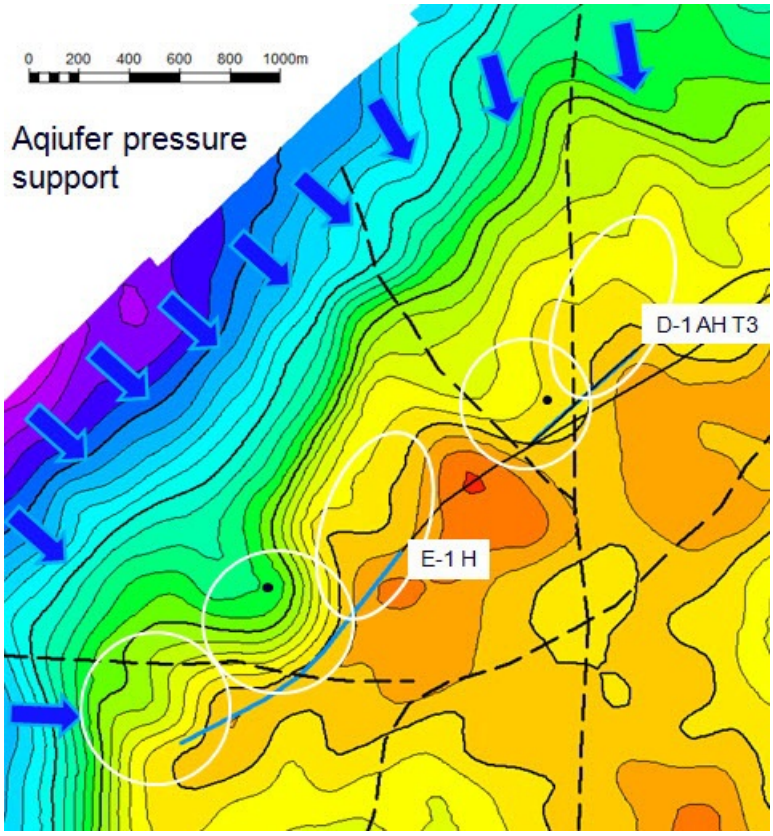

Figure 6.4: Aquifer pressure support in the Jette field. The blue arrows indicate aquifer support from west, and the white outlines indicate estimated drainage areas. From Winther (2013), page 33.

Table 6.1: Reservoir parameters.

Parameter	Unit
Reservoir pressure	196.7 bar
Bubblepoint pressure	114.7 bar
Reservoir temperature	83.6 °C
Porosity	0.25
Oil density	838.6 kg/m^3
Water density	1,041 kg/m^3
Salinity	60,000 mg/l

6.3 Field Development

The Jotun field is located around six km north of Jette. Jotun has been in production since 1999 and is of this date (11.02.2014) in late tail production. The status of Jotun and its nearby location affected the chosen development of Jette; Jette was found to be

of insufficient size to warrant topside production facilities, thus it would not have been profitable to produce without the already existing infrastructure in the area. Jette was developed as a subsea structure with two satelite wells tied back to Jotun B with a six km long pipeline. The production from both Jotun and Jette are commingled at Jotun B, and transferred to Jotun A for processing and export (Winther 2013). The oil in the two fields are similar in composition, which made the chosen development easier. The connection of the two wells from Jette extends the lifetime of the Jotun field.

The production from the wells is through two 8 in. pipelines, tied to the Pipeline End Manifold (PLEM), see **Figures 6.5** and **6.6**. The commingled production is then routed through a 8 in. pipeline, connected to a 12 in. vertical riser at Jotun B. Topside Jotun B the diameter of the pipeline is reduced back to 8 in., which may be an unfortunate design as it is a very effective slug generator. At Jotun B the rates of oil, gas and water are measured at the Multiphase Flow Meter (MPFM), before it is routed through either a 10 in production line or a 10 in. test line to the FPSO unit Jotun A.

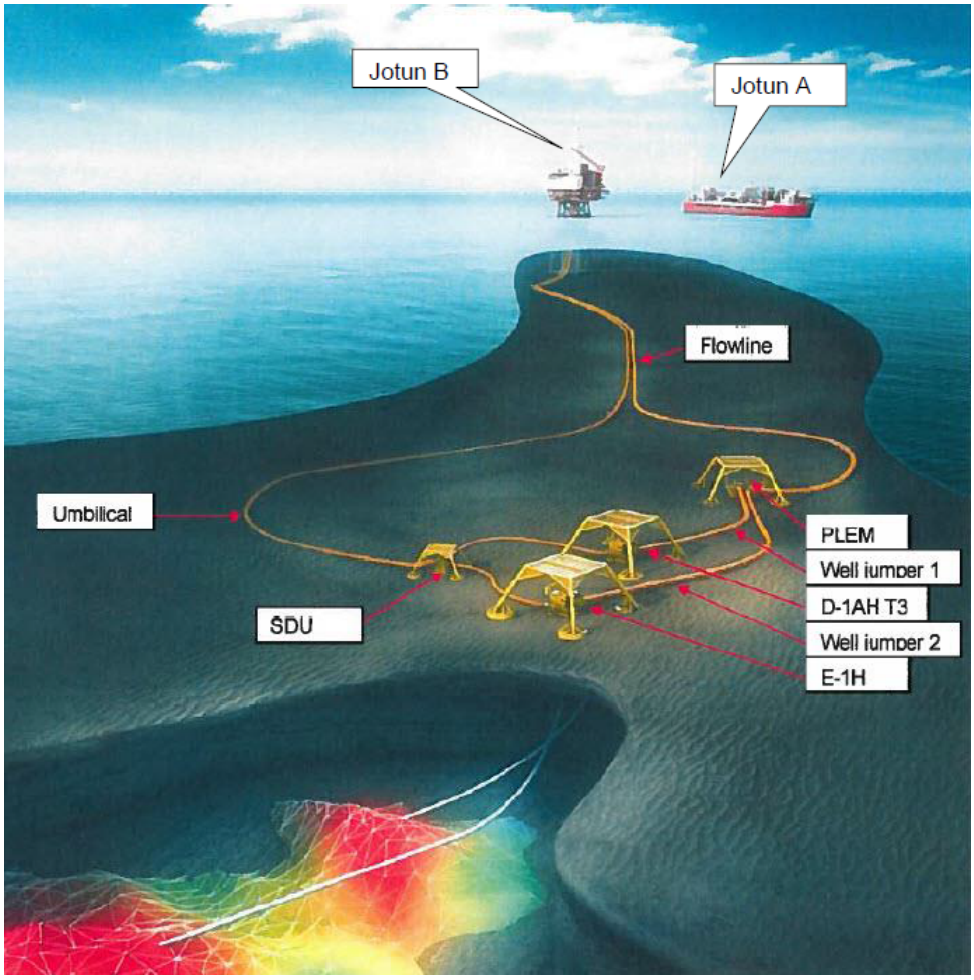

Figure 6.5: Jette field layout, from Krogstad & Barbier (2014), page 4.

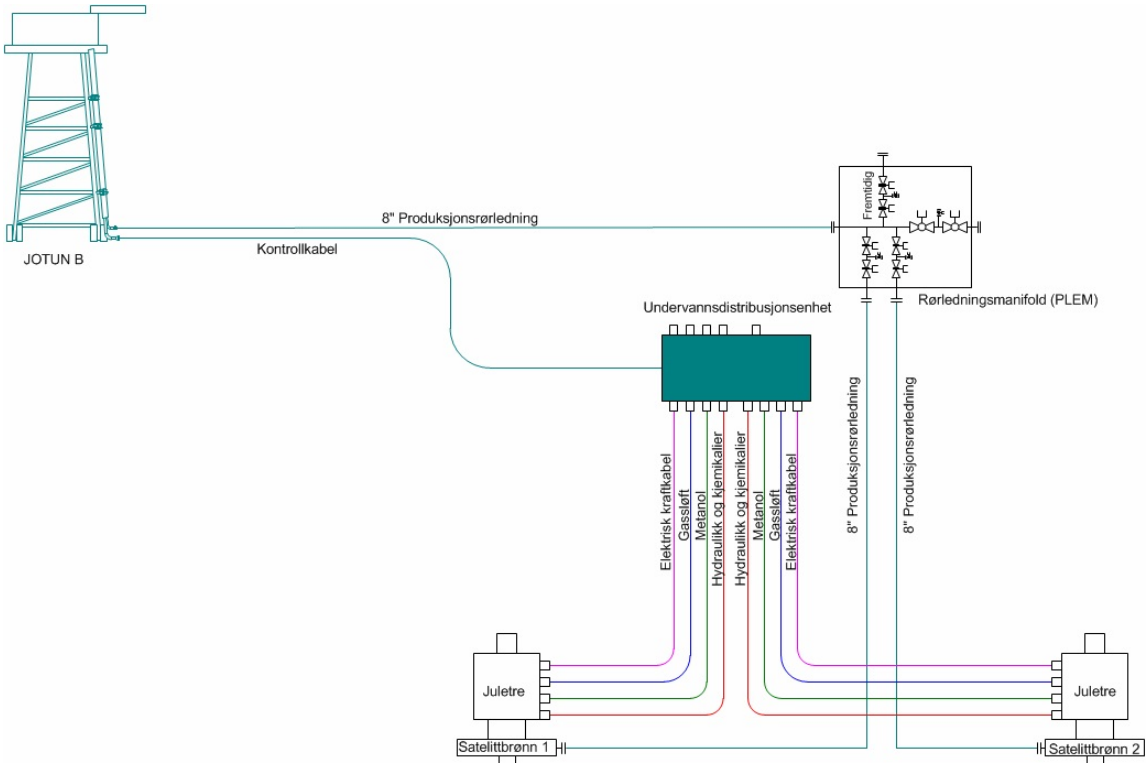

Figure 6.6: Field overview over the subsea installations, from Brenna et al. (2011), page 4.

Gas lift is installed in both the wells. The two wells can share a total gas lift rate of 200 000 Sm^3/day, where the highest gas lift rate is to the well which will give the highest production (Winther 2013). A gas lift allocation is performed every third month to optimize the gas lift process. The gas in the gas lift comes from Jotun B (Winther 2013). Jette started to produce in May 2013 and has, with the current tie-in arrangement, an estimated lifetime of 10 years.

6.3.1 Wells

The main objective was to develop the field with two horizontal producers, 25/8-A-1 AH in Jette South and 25/8-B-1 H in Jette North, to produce oil from the upper reservoir zones, that is layer Z1 and Z2 (Brenna et al. 2012). The initial plan of 25/8-D-1 AH was to land the well at a vertical depth of 2100 m TVD Rotary Kelly Bushing (RKB) and drill horizontally for 1974 meters to the planned Target Depth (TD) at 4499 m Measured Depth (MD) RKB. Well 25/8-B-1 H was planned to be drilled after 25/8-D-1 AH to obtain more information about the field and update further horizontal well trajectory. The initial plan was to land the well at a vertical depth of 2100 m MD RKB and drill horizontally for 1634 meters to the planned TD at 4217 m MD RKB. Geosteering was vital for both wells to ensure as much sand as possible in these intervals due to shallow, thin sand layers.

(Brenna et al. 2012)

Challenges during drilling of both the horizontal wells led to that both the wells were drilled in Jette South. Jette South was prioritized based on an assessment of the sands here were better defined; of better reservoir quality (Winther 2013). The description of Well E, in **Section 6.4**, is taken from the project *Productivity Index in Horizontal Wells* (Winther 2013). Both the wells were drilled with oil based mud.

6.3.2 Gas Lift System

The gas used for gas lift comes from the Jotun field. The injection gas is conveyed down the tubing-casing annulus and enters the production train through the deep set Gas Lift Valve (GLV). See **Figure 6.7**.

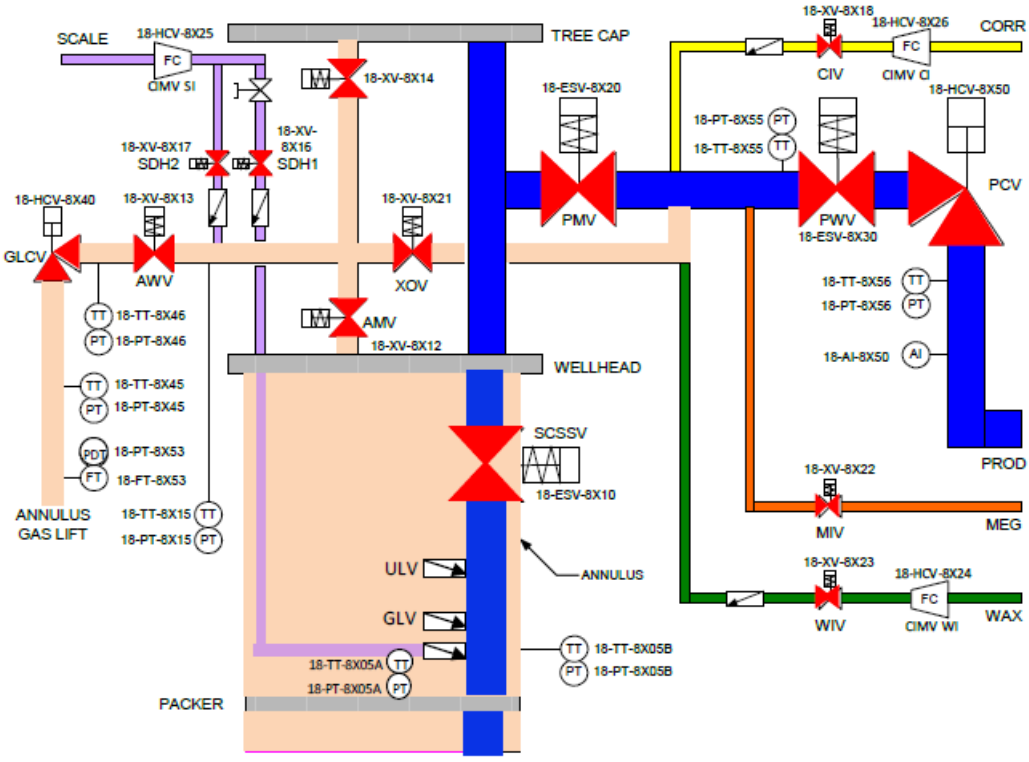

Figure 6.7: Flow chart Jette subsea, from Brenna et al. (2013a), page 11.

6.4 E-1 H

Well E is the longest of the two production wells. It was originally planned that this well were to be drilled in Jette North, but due to difficulties and better reservoir quality it was

drilled in Jette South. Both production wells are shorter than planned due to formation stability problems during drilling and completion.

The inclination of the well is approximately 86 degrees. Its horizontal section is mainly in Heimdal Z2 and a short interval in the clay rich Heimdal Z5. (Winther 2013)

6.4.1 Well Completion

An 9 1/2 in. openhole section of 1220 m was drilled in Well E and the total length was completed with standalone mesh screens and Inlet Control Devices (ICD's). Packers were not installed in Well E due to difficulties during the completion. The standalone mesh screens were installed to prevent sand production. See **Appendix C** for figure of completion of the well.

Well E is currently gas lifted with one unloading valve located at 968.21 m TVD RKB and one main injection valve at 1514.35 m TVD RKB. The lift gas can deliver a maximum pressure of 135 bar. (Winther 2013)

6.5 D-1 AH T3 Well

25/8-D-1 AH was drilled as a side track to the observation well 25/8-D-1 H to TD at 3794 m MD. Due to severe hole collapse problems and not being able to circulate, the first production well proved unsuitable to be completed as a producer (Brenna et al. 2012). Numerous issues lead to the drilling of two more side-tracks, in which the last was considered successful, well 25/8-D-1 AH T3. 3535 m MD RKB, TD, was reached on the 29th of August 2012.

It was observed severe overbalance during drilling, 120 bar, and Equivalent Circulation Density (ECD) was 1.53-1.54 Specific Gravity (SG), using WARP mud. The WARP was displaced with Low-Solids Oil-Based Mud (LSOBM) in order to clean the well while setting the screens (Rodrigues et al. 2013*a*). Numerous attempts of running screens were made, but due to experienced tight spots the screens were set at 2977 m MD RKB with a hanger at 1804.3 m MD RKB. A triconic bit with a single run motor was a part of the completion, and was left at 2977 m MD RKB (Rodrigues et al. 2013*a*). This lead to a shorter reservoir section than intended of approximately 500 m, from 2418.50 m MD RKB to 2799 m MD RKB.

6.5.1 Well Completion

Even though an 8 1/2 in. openhole section of 1115 m was drilled in Well D, only 560 m was completed. A 5 1/2 in. production tubing was installed, and the well was completed with standalone metal mesh screens with inflow control devices and three slip-on swell packers. Ezeeglyder centralizers are on all joints. Due to the difficulties during drilling and completion, only two of the packers are situated in the openhole section, while the

uppermost swell packer is placed inside the 9 5/8 in. production casing. Morphisis swellable packers were used, with a maximum differential pressure of 35 bar. Som zonal isolation is obtained due to the installation of swell packers. The depth of the three packers are described in **Table 6.2**. The standalone mesh screens were installed to prevent sand production. See Appendix C for figure of completion of Well D.

Table 6.2: Depth of the three swellable Morphisis packers. Maximum differential pressure per packer is 35 bar.

Packer	Measured Depth	True Vertical Depth
# 1	2153 m MD RKB	2013 m TVD RKB
# 2	2546 m MD RKB	2099 m TVD RKB
# 3	2821 m MD RKB	2110 m TVD RKB

The well is gas lifted with one unloading valve at 1034.86 m TVD RKB and one main injection valve at 1588.34 m TVD RKB. The lift gas can deliver a maximum pressure of 135 bar (Winther 2013).

6.5.2 Well Clean-up

At the stage of the packer setting, the swell packer had been in the well for 5-6 days, mostly exposed to LSOBM. It is expected that the swell packers may have expanded to the Outer Diameter (OD) of the well, with this time of exposure. Together with the OD centralizers on each screen joint at the lower completion, the swell packers introduce restrictions to mud returns through the annulus. This is particularly the case of the uppermost swell packer which was placed in the 9 5/8 in. casing. (Lysne & Nakken 2013)

In order to displace mud in the well, the reservoir section was displaced to LSOBM using a 2 7/8 in. inner string Drill Pipe (DP) with swab cups and stinger. In the mud displacement period a pressure increase of 10 bar, from 120 bar to 130 bar, was observed while maintaining circulation at 500 Liters Per Minute (LPM) over a two hour period (Naterstad 2013). When pulling the string out of the polished bore receptacle, the pumping pressure, while pumping at 290 LPM, decreased from 85 to 22 bar (Lysne & Nakken 2013). This implies that a pressure loss of 63 bar was recorded from the mud motor, bit and sand screen assembly at this stage. The magnitude of this pressure loss is by far higher than what is recorded earlier in the operational sequence (Naterstad 2013).

The well was left with LSOBM until clean-up before production. Well cleaning prior to production is established by reviewing production data and fluid density logs. **Figure 6.8** shows produced liquid volumes from the well and pipeline during clean-up. **Figure 6.9** shows fluid density profiles between the wellhead pressure sensor and downhole P/T-gauge. Figure 6.9 are supposed to show peaks in the vicinity of the fluids in the well at the commencement of clean-up (Lysne & Nakken 2013).

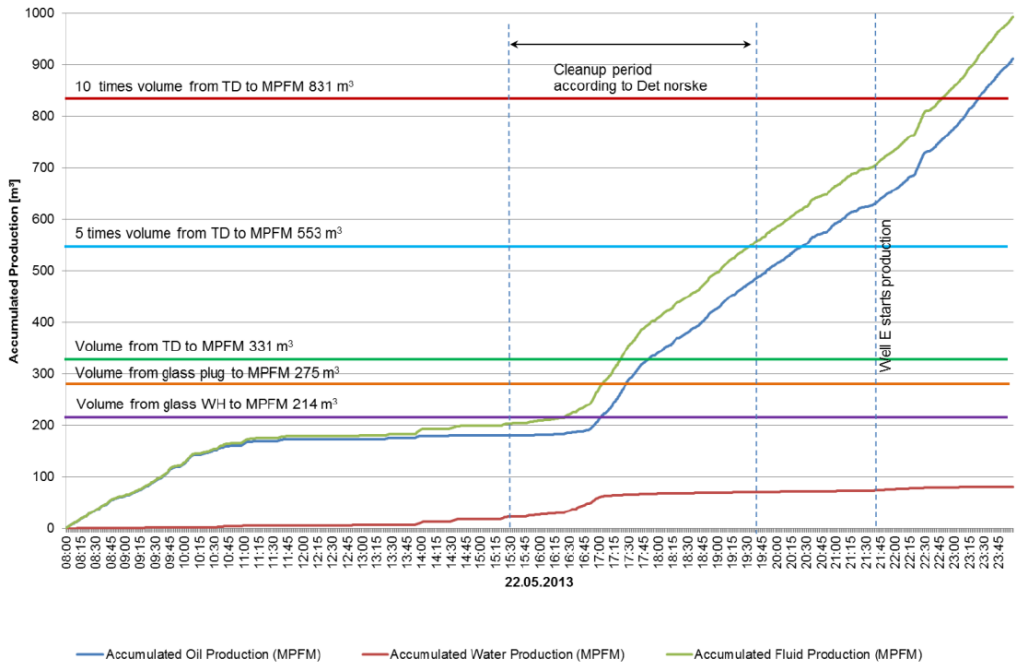

Figure 6.8: Produced liquids at Jotun B (MPFM) compared to volumes in Well D and the pipeline to Jotun B, from Lysne & Nakken (2013), page 24.

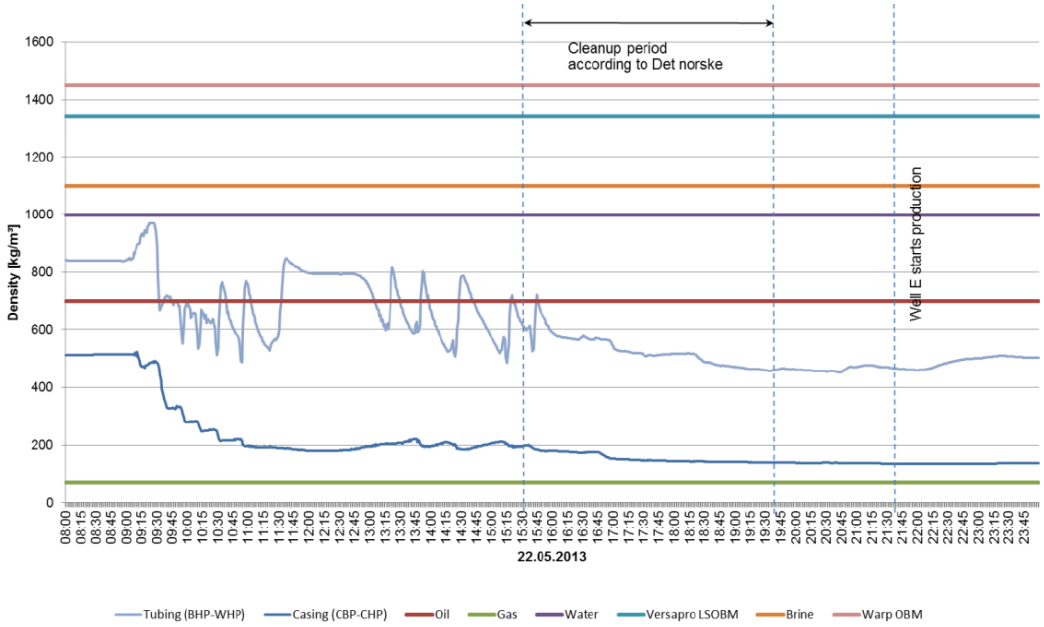

Figure 6.9: Density of fluid in tubing (BHP-WHP) and annulus (CBP-CHP) between wellhead an P/T-gauge compared to densities of fluids in Well D at start of clean-up, from Lysne & Nakken (2013), page 25.

CBP is the Casing Bottom Pressure and CHP is the Casing Head Pressure. The figures indicate that the clean-up period may have been far too short. Figure 6.9 do not show any peaks in the density, which may indicate that the drilling and completion fluids have largely been left downhole. The fluids may be produced over time.

6.6 Production

The recovery strategy is based on reservoir depletion, combined with gas lift on the wells. Water injection is not considered, as it is assumed a strong pressure support from the underlying aquifer. **Table 6.3** specifies the design capacity of the commingled production from Jette which can be processed at Jotun A.

Table 6.3: Design capacity of the commingled production from Jette.

Production parameter	Field design capacity
Maximum oil rate	3,500 Sm^3/day
Maximum fluid rate	5,500 Sm^3/day
Maximum total gas production	400,000 Sm^3/day
Minimum arrival pressure at Jotun B	20 Sm^3/day
Maximum water production	5,000 Sm^3/day
Total gas lift rate	200,000 Sm^3/day

The subsea chokes are not fully open, but in some kind of choke back position at all times. This is not very effective and prevents the wells from producing to their potential (Winther 2013). It is not expected any problems with precipitation of wax or hydrates during production, as the gas used for gas lift has been dried prior to injection (Lorentzen 2013). The umbilicals, as seen in the completion schemes in Appendix C, supplies methanol to prevent hydrate deposition during maintenance stops. Hydrates in the pipeline may form at 9 °C at Jette [1]. Sand production is recognized as a challenge during the production due to low permeability and high drawdown.

6.6.1 Production History

The commingled oil, water and gas rates at Jette from 19th of May 2013 to April 2014 are given in **Figure 6.10**. The coloured area below the curves are commingled liquid production rate. The framed areas in Figure 6.10 are periods of build-up testing.

Since the start of production on the 19th of May 2013, the Jette field has experienced several challenges. Challenges were initiated already at the development of the field in regards drilling and completion of the wells. The challenges experienced during production led to studies of production optimization and well intervention, which has helped clarify

[1] Personal communication with Marit Kristin Krogstad. April 2014. Trondheim: Weatherford Petroleum Consultants AS

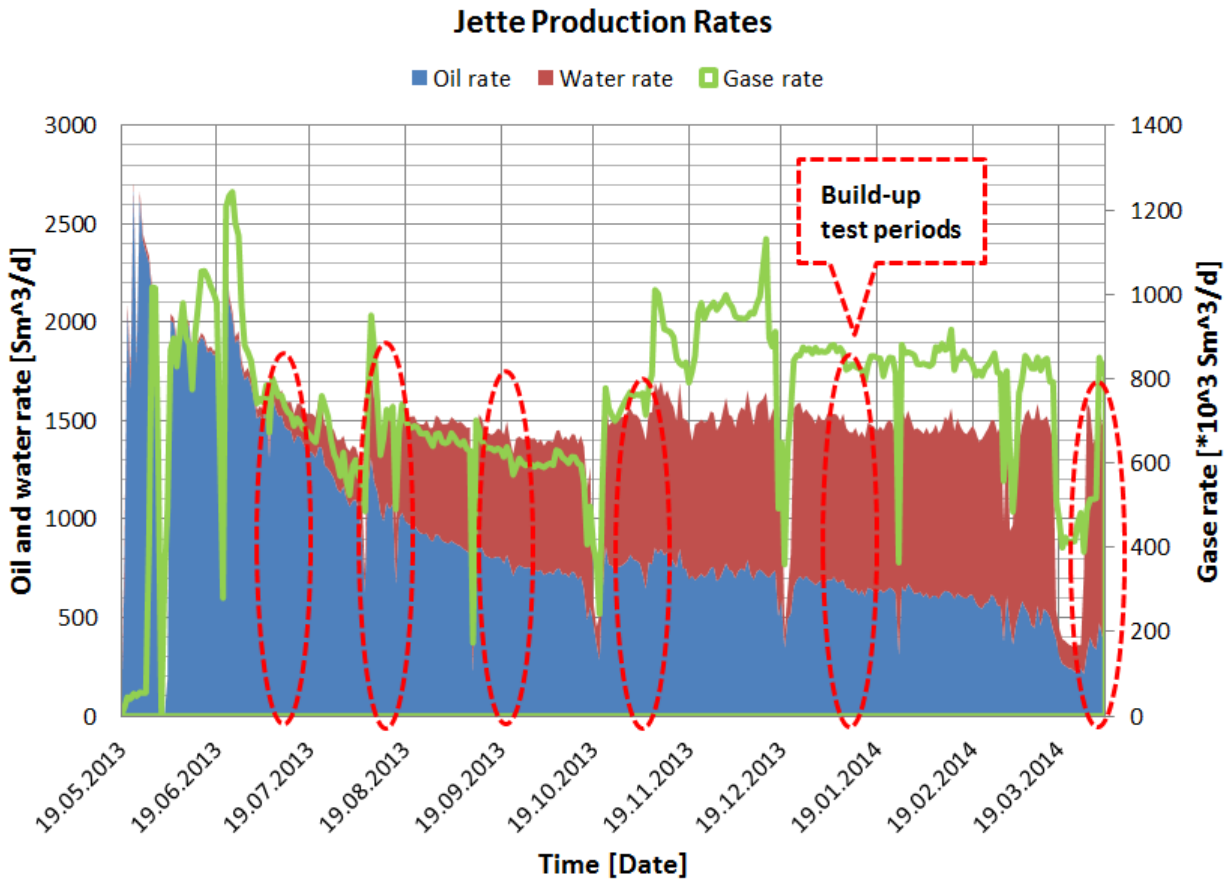

Figure 6.10: Commingled oil, water and gas rates at Jette, from May 2013 to April 2014. The coloured area below the curves are liquid production rate. The green line shows the commingled gas production rate. The framed areas indicate periods of build-up testing.

problems and given a better understanding of the characteristics of the field. Some of the measures taken in the study is the analysis of build-up tests and fluid sampling.

Initial Understanding of Jette

No core samples, no downhole fluid samples of the two horizontal producers and insufficient 3D were gathered in the initial investigation. The wells were logged, but due to the lack of core samples the depth of the logs were not calibrated with the depth of core samples. The lack of important data led to an understanding of Jette as a continuation of Jotun considering geology and fluid properties. The low initial investment has led to high operating costs, as challenges and a need for a better understanding rose.

The initial understanding of Jette was as a heterogeneous, high permeable Darcy sand reservoir with a questionable gas cap. A strong aquifer was assumed, as observed at the

Jotun field. Initially, ample faults were anticipated, but no faults were included in further analysis of the field and in the geological model.

During the autumn of 2013 several challenges were experienced;

- Slugging and instability in production.
- Optimization of gas lift rate due to limitations of design.
- High Water Cut (WC).
- Lower production than estimated, especially from Well D (estimated PI of 1 $Sm^3/day/bar$).
- High drawdown in Well D from start of production.

Slugging Challenge

The field was developed as seen in Figure 6.6, and the two producing wells have been completed as seen in Appendix C. The production fluids from the two wells flow through an 8 in. pipeline, and further into a 12 in. riser after the riser base. This design is unfortunate with regards to a smooth production. Liquid is not able to flow at steady rates up the riser, and is accumulated at the riser base. The accumulation leads to a flowback from the riser base into the pipeline. Gas pressure is building up behind the liquid accumulation, leading to a slug of oil and gas being pushed up the riser. (Winther 2013) The pressure fluctuations due to the slugging may affect the gas lift system; for periods there is no production registered by the MPFM at Jotun B. When the slug enters the 12 in. riser from the 8 in. pipeline, the velocity is reduced to 44% of the velocity in the pipeline (Lysne & Nakken 2013). As the slug flows up through the riser, the gas piston behind it is working its way through the liquid slug, making the liquid sweep out less efficient than if the riser was 8 in. The reduced diameter back to 8 in. at the top of the riser effectively reduces the velocity of the liquid slug and let the gas bypass even more liquid. This event may be observed in **Figures 6.11** and **6.12**.

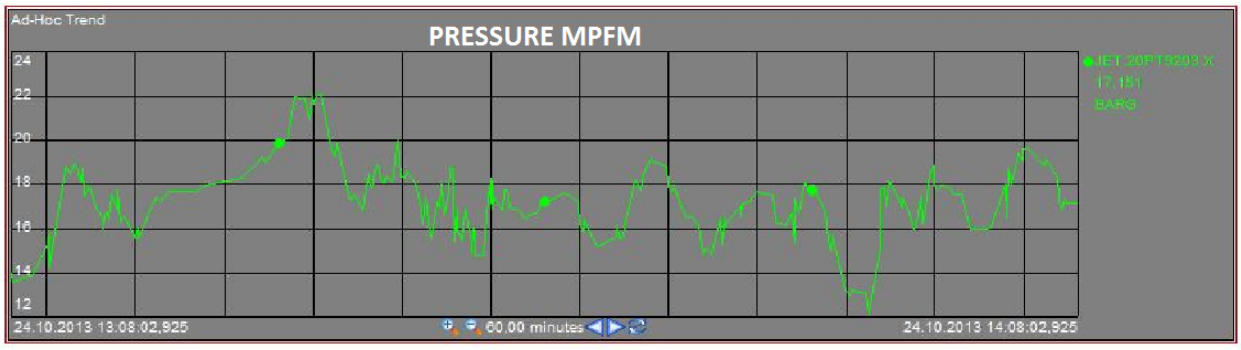

Figure 6.11: Pressure fluctuations observed at the MPFM, 24.10.2013. From Lysne & Nakken (2013), page 30.

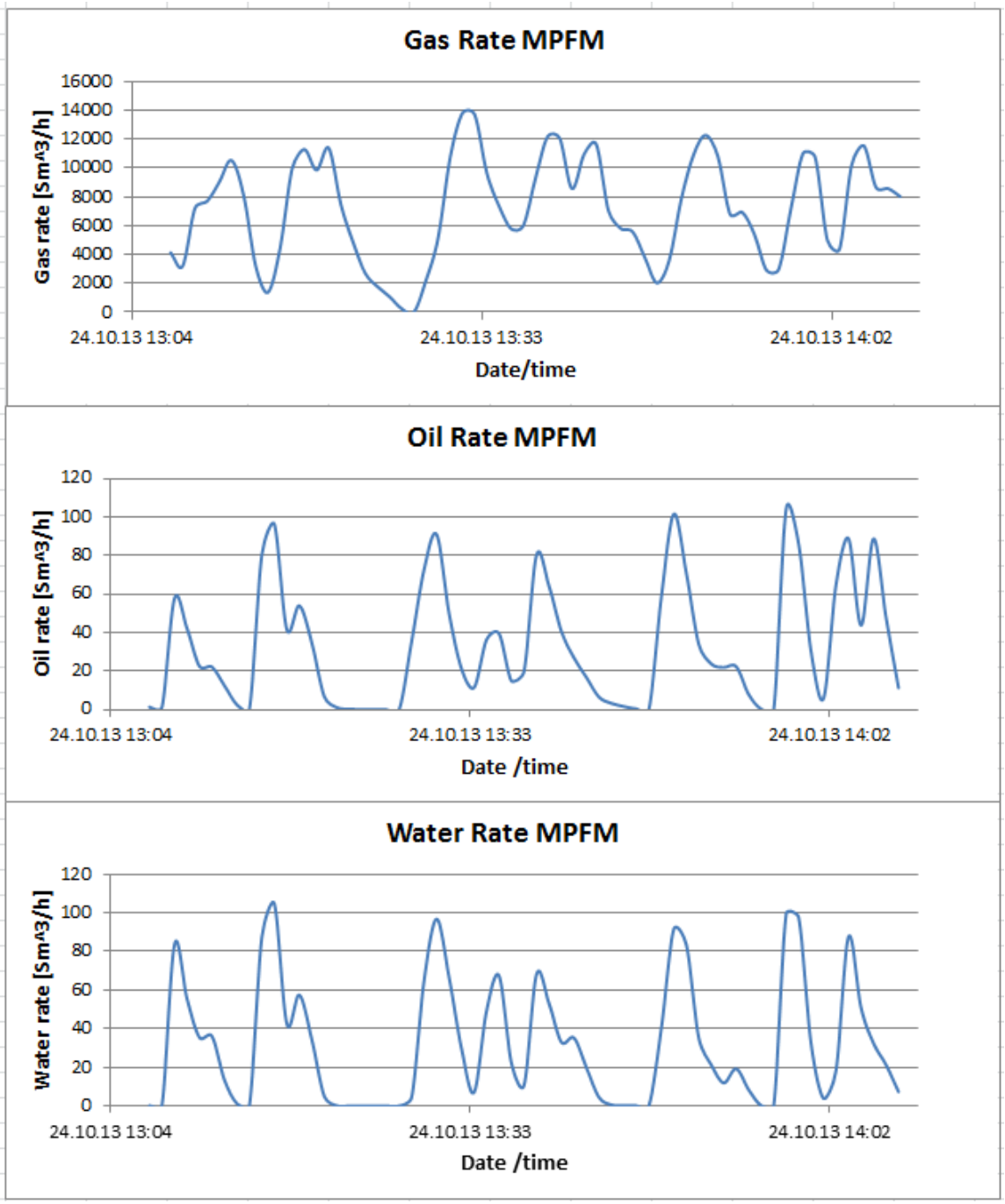

Figure 6.12: Oil rate, water rate and gas rate measured at the MPFM, 24.10.2013. The fluctuations indicate slugging.

Figures 6.11 and 6.12 indicate slugging. It should be noted that the gas slug behind the liquid slug has bypassed a lot of liquid as it is entering the MPFM at the same time as the liquid. The time series in the figures have a span of 60 minutes. The riser diameter has a

clear impact on productivity; after the first two slugs that can be observed in the figures, there are a period of six minutes without any liquid production from the pipeline. This is reducing the productivity potential of Jette and should be addressed in order to optimize the production.

Fluid Samples and PVT Analysis

The fluid samples taken at initial stages show a great variation in bubble point pressures and solution gas-oil ratios as seen in **Figure 6.13**.

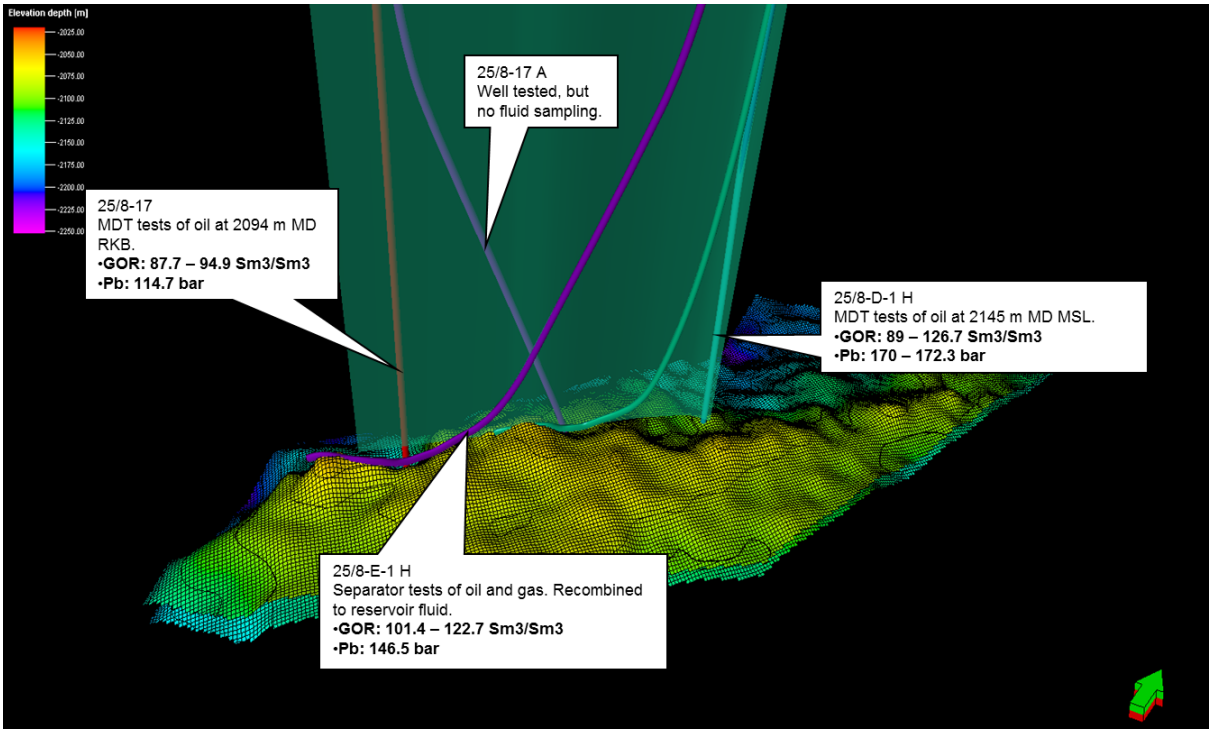

Figure 6.13: Overview of fluid samples and PVT analysis, from Lysne (2014a).

Pressure Volume Temperature (PVT) analysis from well 25/8-17 indicated a bubblepoint pressure of 114.7 bar and a solution gas-oil ratio of 87-94.9 Sm^3/Sm^3, while a separator sample taken at Jotun A indicated a bubble point pressure of 146.5 bar. Samples from well 25/8-D-1 H indicated a bubble point pressure of 172.3 bara and a GOR of 90-100 Sm^3/Sm^3. With a variation in bubblepoint pressure as high as 60 bar a high degree of uncertainty is introduced. The large variations in the PVT data may be caused by poor sampling or great variations within the reservoir. Initially, one fluid system for the entire reservoir was chosen with a GOR of 90-100 Sm^3/Sm^3 and a bubble point pressure of 172.3 bara.

The differences in PVT data may indicate that there are several fluid systems within the reservoir. This may be possible due to faults and compartmentalization.

Development of Buildup Tests

Pressure build-up tests were performed in July, August, October, December and March for both Well E and Well D, see **Figure 6.14**. The tests are of various quality due to the duration of the tests.

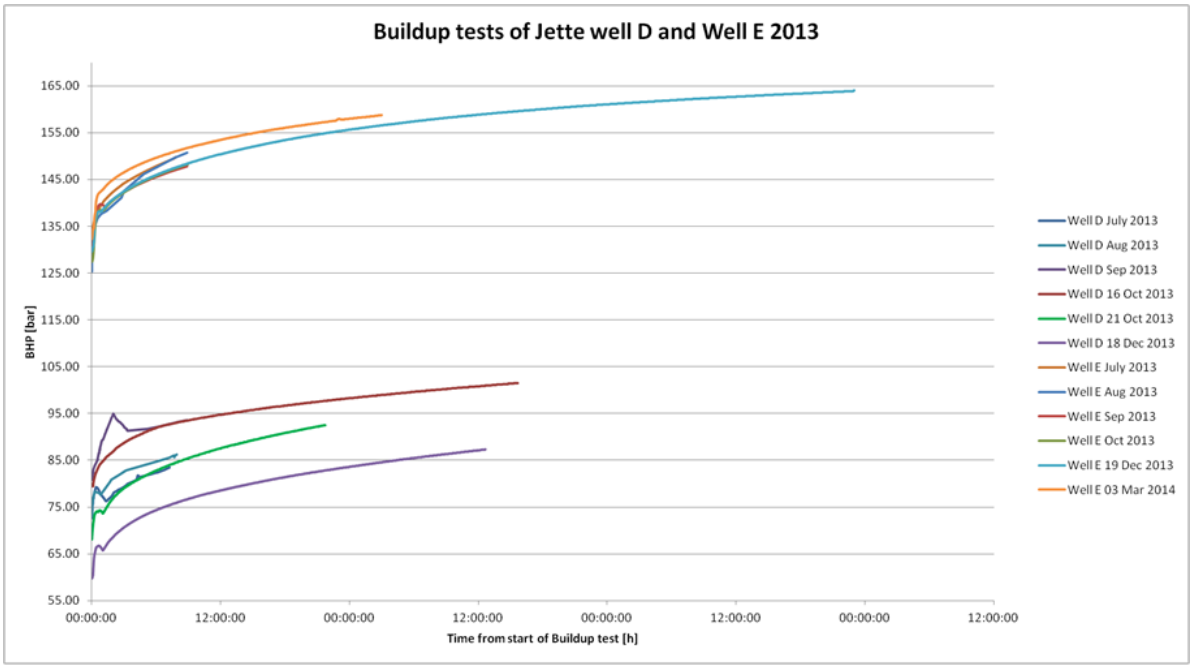

Figure 6.14: Build up tests for both Well E and Well D from July 2013 to December 2013/March 2014. The build-up tests indicate good pressure support around Well E and depletion around Well D. From Lysne (2014b).

It is observed from Figure 6.14 that all the build up tests follow the same trend. The tests for Well E may indicate good pressure support in the reservoir. This is observed by the same behaviour of the tests; all the tests builds up from the same respective pressure towards initial reservoir pressure. The tests for Well D may indicate depletion of the reservoir. This is observed by the decreasing pressures with time. All the build-up tests follow the same trend, building up with equal gradients towards different reservoir pressures. It is observed that the new reservoir pressures are lower than the previous one. In Figure 6.14 this trend may be observed by comparing the latest test, from December 2013, with earlier tests.

The build-up tests give an expression of two different, segregated systems, whereas the area around Well E experiences pressure support, while the area around Well D is being depleted. This may be attributed to the possibility of several fluid systems, where as the reservoir may be compartmentalized.

Mass Balance and Allocation

The production from the two horizontal producers are commingled, measured topside Jotun B. As there are no separate measures of each well's production (except during the multi-rate testing), it has been challenging to survey the production of each well. Build-up tests and multi-rate tests is used to estimate the productivity of each well.

The instrument measuring the gas lift rate was initially out of operating range, which led to insufficient measurements of the gas lift rates. Hence, the amount of injected gas was uncertain, and no gas mass balance could be calculated. Sensitivity studies estimated higher gas production than anticipated, which indicates higher gas lift rates and possible more gas production from the reservoir. The reservoir gas may be produced from Well D, where indications of a development towards a saturated oil reservoir has been detected.

Field Development

The field is in constant development and new challenges occur rapidly. The development is mentioned briefly below.

- October 2013: Well D had initially a PI of 1 $Sm^3/day/bar$, but after a rapid start up during build-up testing in October 2013 the PI increased to 4 $Sm^3/day/bar$. The rapid start may have loosened sand and/or remaining mud downhole.
- October 2013: The expected "*Darcy*" sands is found to have permeability in the "*milli*"Darcy range.
- October 2013: It is suspected that the productivity if Well D may suffer from poor clean-up, clogging the well and decreasing its productivity. It is also suspected that after the rapid start the well gained a longer producing interval; the well was initially suspected be clogged below the second packer, but later cleaned and clogged below the third packer. This indicates that the well mainly produce from the area around the heel.
- February 2014: Flow oscillations was observed, which may be a cause of slugging. Maintaining high gas rates in the system may be effective to suppress the flow oscillations, but high gas rates are not beneficial with regards to oil production as they may choke back the well due to high friction along the flow line. The slugging has been shown to not be severe and not detrimental to production. (Krogstad & Barbier 2014)
- February/March 2014: Well D has been shown to produce better than Well E. Well E has high water production.
- March 2014: PVT analysis, build-up tests and mass balance calculations indicates that the reservoir consists of several compartments with different fluid systems. Well E and Well D may not be producing from the same pocket; it is indicated that

the reservoir around Well E has strong pressure support from the aquifer, while the reservoir around Well D is being depleted and has probably become saturated.

- March 2014: The reservoir sand layers are below seismic resolution; the seismic indicates coherent sand layers. The latest analysis indicates incoherent sand layers.
- March 2014: In January 2014, when each well was producing alone, the simulated optimal gas lift rate with regard to production was:
  - Well E: oil production of 400 Sm^3/day with approximately gas lift rate of 96,000 Sm^3/day.
  - Well D: oil production of 290 Sm^3/day with approximately gas lift rate of 192,000 Sm^3/day.

  When both wells produce together, with optimal gas lift rates, the total oil production is 550 Sm^3/day. As it was shown that the wells produce better alone than together (choking each other), an alternating production was, in March 2014, initiated to benefit the most out of each well. During the alternating production Well D was observed to suffer with low production rate, leading to a riser temperature of 10 °C. As the temperature got critically close to the temperature of hydrate formation, 9 °C, both wells were put on production simultaneously. During the alternating production Well E had issues with high water production.
- April 2014: New and much longer build-up tests have been performed on both wells. The goal of performing longer tests is to see if possible boundaries/faults near Well D can be observed, supporting the hypothesis of a compartmentalized reservoir.

6.7 Uncertainties in the Field Development

There are a lot of uncertainties pertaining to the field and field development at Jette. This is mainly due to the lack of data; core samples and sufficient fluid samples. Data taken at an early stage deviates from the latest assumptions, indicating discrepancies. The uncertainties need to be considered in later stages and taken into account. The most important uncertainties are mentioned below.

- Initially, there where indications of a gas cap. The assumption of a gas cap was taken from the evaluations of the logs from well 25/8-17 A. Neither the build-up tests or the production data confirm the existence of a gas cap.
- The presence of faults is uncertain. Early investigations revealed indications of several faults. During the later stages, the producing area have been assumed to be virtually fault-free.
- The stratigraphy and zonation may be different than expected. For example, the shale layers may be more extensive than anticipated, and make small pockets of sands which make up small producing zones.

- The pressure support from the underlying aquifer is initially expected to be high overall the field. Shale barriers or poor transmissibillity may reduce the pressure support.

7 Productivity Evaluation of Well D

It is essential to evaluate the productivity of the well before considering to implement IOR-measures. The productivity and a sensitivity analysis may help to indicate what the well responds to and which IOR measures may be implemented. In order to be able to calculate the productivity, a better understanding of the reservoir extension, drainage area and well path are needed. This may be obtained from petrophysical logs, production data and downhole measurements.

7.1 Input Data

A better understanding of the production geometry helps in the evaluation of the productivity. It is essential to have an understanding of where the producing well is placed, how the well looks like and how big its drainage area may be.

7.1.1 Layer Thickness

Well D is estimated to produce from layer Z1 at the heel and layer Z2 in the rest of the interval. To get a better understanding of the layering, and their respective height, petrophysical logs from neighbouring wells have been evaluated. **Figures 7.1** and **7.2** show the placement of Well D and its neighbour wells; the producing Well E, the exploration wells 25/8-17 and 25/8-17 A, and the side-track well 28/8-D-1 H.

The vertical exploration wells can be used to better estimate the layer thickness than the horizontal wells, due to their normal penetration of the layers (Winther 2013). In *Productivity Index in Horizontal Wells* (Winther 2013) the thickness of Z2 near Well E was estimated. Estimated thickness of layer Z2 was 10 m. **Table 7.1** gives a summary of the height distribution of layer Z2 throughout the reservoir.

As seen in Table 7.1 and Figures 7.1 and 7.2 the Z2 layer pinches out towards north-east. When assuming a linear relationship, an average layer thickness of layer Z2 in the area of Well D is estimated to 7.7 m. As the layer thickness is based on assumptions it will carry uncertainties.

Well 25/8-17 is the most south-western well in Jette South, the region in focus. The well intersects layer Z1 at approximately 2066 m TVD MSL, as seen in **Figure 7.3**. The net

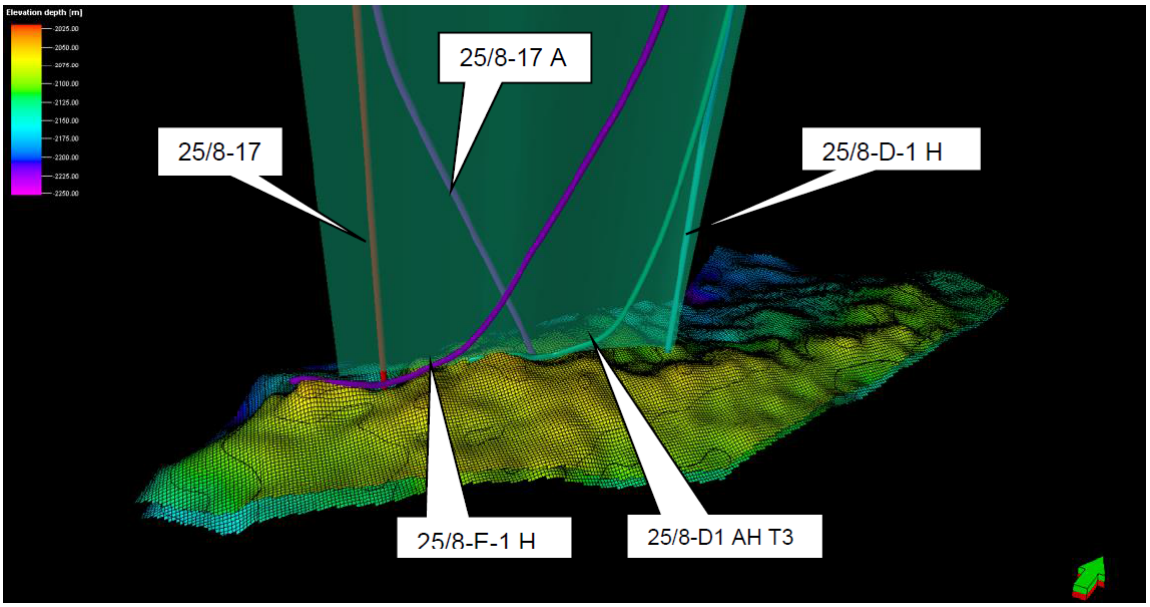

Figure 7.1: Position of the Jette wells in the Petrel model (side view). From Winther (2013), page 46.

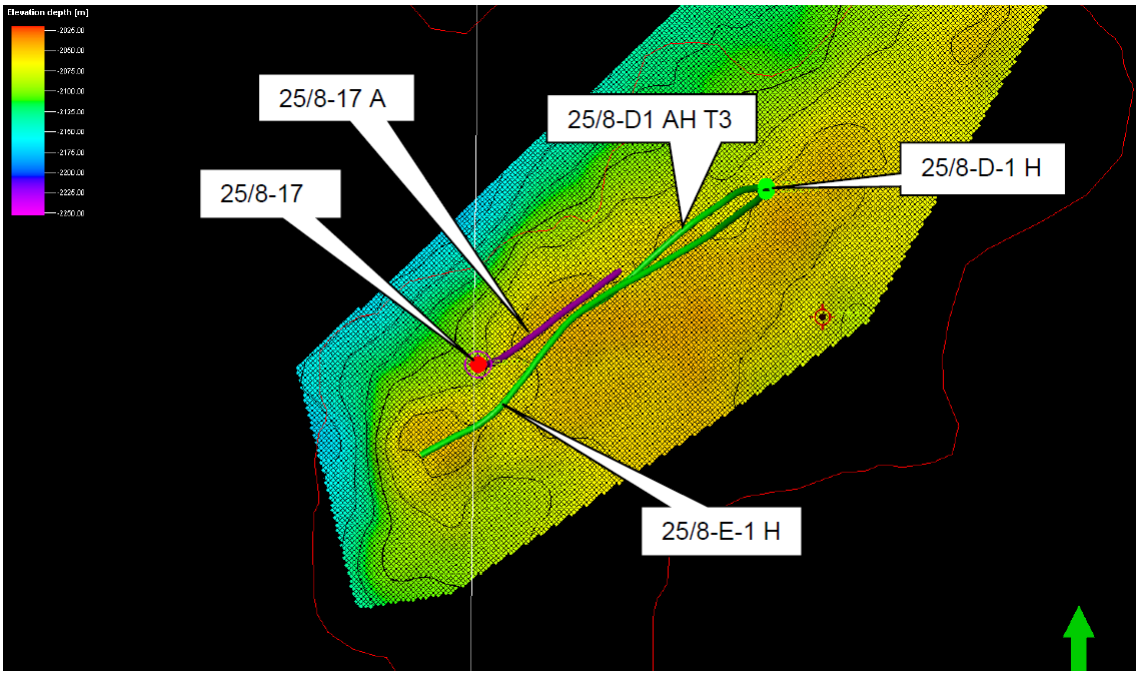

Figure 7.2: Position of the Jette wells in the Petrel model (top view). From Winther (2013), page 46.

Table 7.1: The thickness of layer Z2 in the producing Well E, the exploration wells 25/8-17 A, 25/8-17 and the side-track 25/8-D-1 H.

Well	Net height
25/8-17	20 m
E-well	10 m
25/8-17 A	7.8 m
25/8-D-1 H	5 m

pay is assumed to be 4 m from the log.

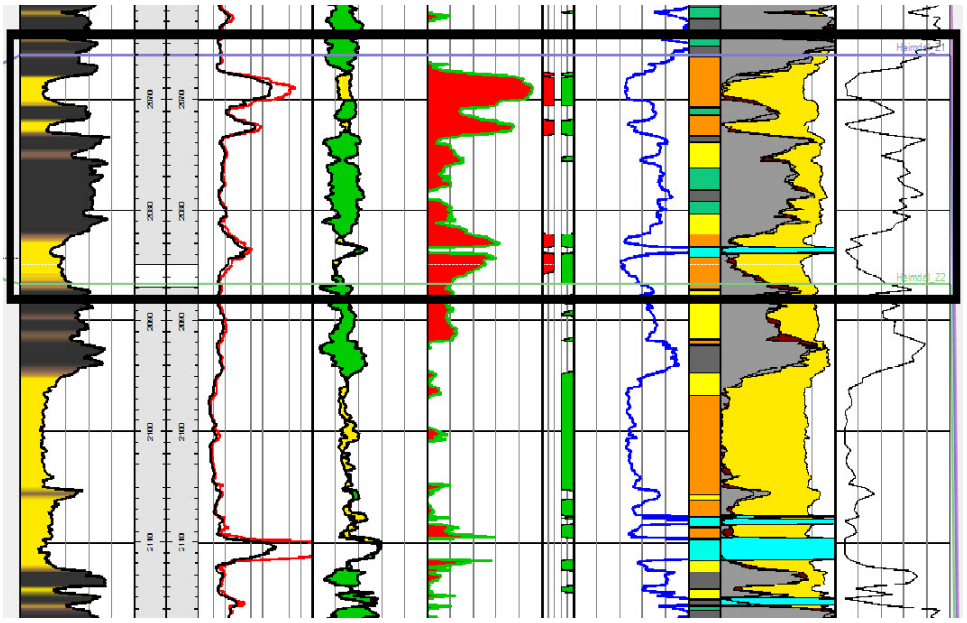

Figure 7.3: In well 25/8-17 the net pay of layer Z1 is assumed to be 4 m. From (Det Norske Oljeselskap 2013).

Well 25/8-17 A lies close to Well D. Since it is less inclined than Well D it is more appropriate to estimate layer thickness from this well than from Well D itself. As seen in **Figure 7.4** the well intersects layer Z1 at approximately 2043 m TVD MSL. The net pay is estimated from the log to 3.1 m.

Furthest north-east in Jette South is well 25/8-D-1 H. It intersects Heimdal Z1 at around 2059 m TVD MSL. The estimated net pay from the log is 1.7 m. See **Figure 7.5**.

Table 7.2 summarizes the estimated net pays from the logs.

The distribution of the layer thickness supports the theory of a pinch-out towards north-east. As seen in table 7.2, layer Z1 also pinches out towards north-east. When assuming a linear relationship, and weighting of the nearby 25/8-17 A well, an average layer thickness of Z1 in Well D is assumed to be 2.9 m.

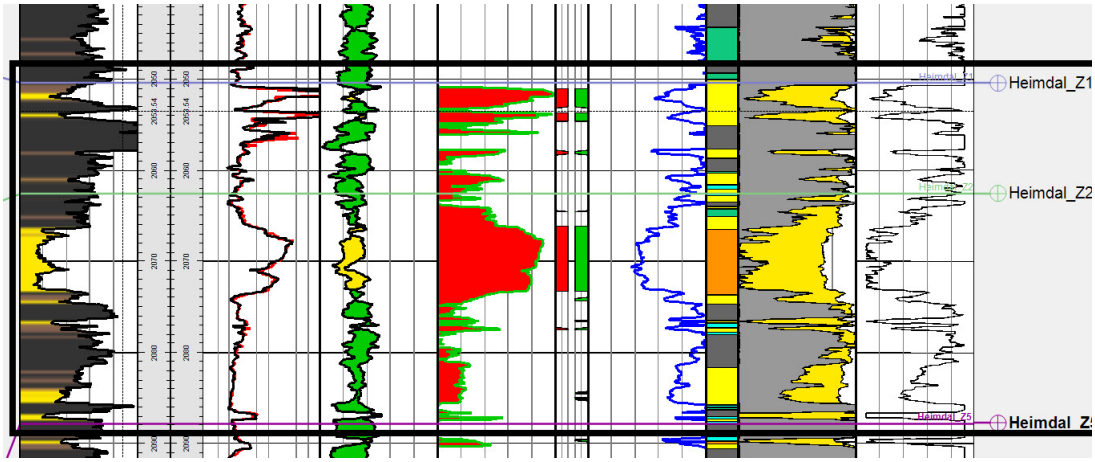

Figure 7.4: In well 25/8-17 A the net pay of layer Z1 is assumed to be 3.1 m. From (Det Norske Oljeselskap 2013).

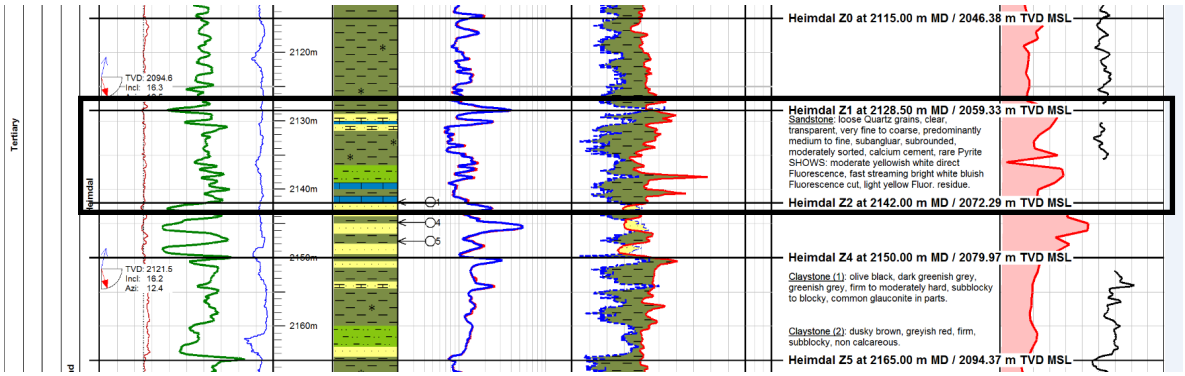

Figure 7.5: In well 25/8-17-D-1 H the net pay of layer Z1 is assumed to be 1.7 m. From (Det Norske Oljeselskap 2013).

Table 7.2: The thickness of Z1 in the exploration wells 25/8-17 A, 25/8-17 and the side-track 25/8-D-1 H.

Well	Net height
25/8-17	4 m
25/8-17 A	3.1 m
25/8-D-1 H	1.7 m

The estimated layer thicknesses of Heimdal Z1 and Heimdal Z2 for Well D is summarized in **Table 7.3**.

Table 7.3: The estimated layer thickness of Heimdal Z1 and Heimdal Z2 for Well D.

Layer	Net height
Z1	2.9 m
Z2	7.7 m

Several shale layers are observed in well 25/8-D-1 H. These layers might extend to the sand layers which Well D intersects, creating smaller sand zones and possibly sealed pockets, creating an uncertainty in the estimated net layer height.

7.1.2 Producing Length

The net pay of Well D is estimated to 240 m using the composite log. This corresponds with a visual inspection of the Computer Processed Interpretation (CPI) log. See **Figure 7.6**.

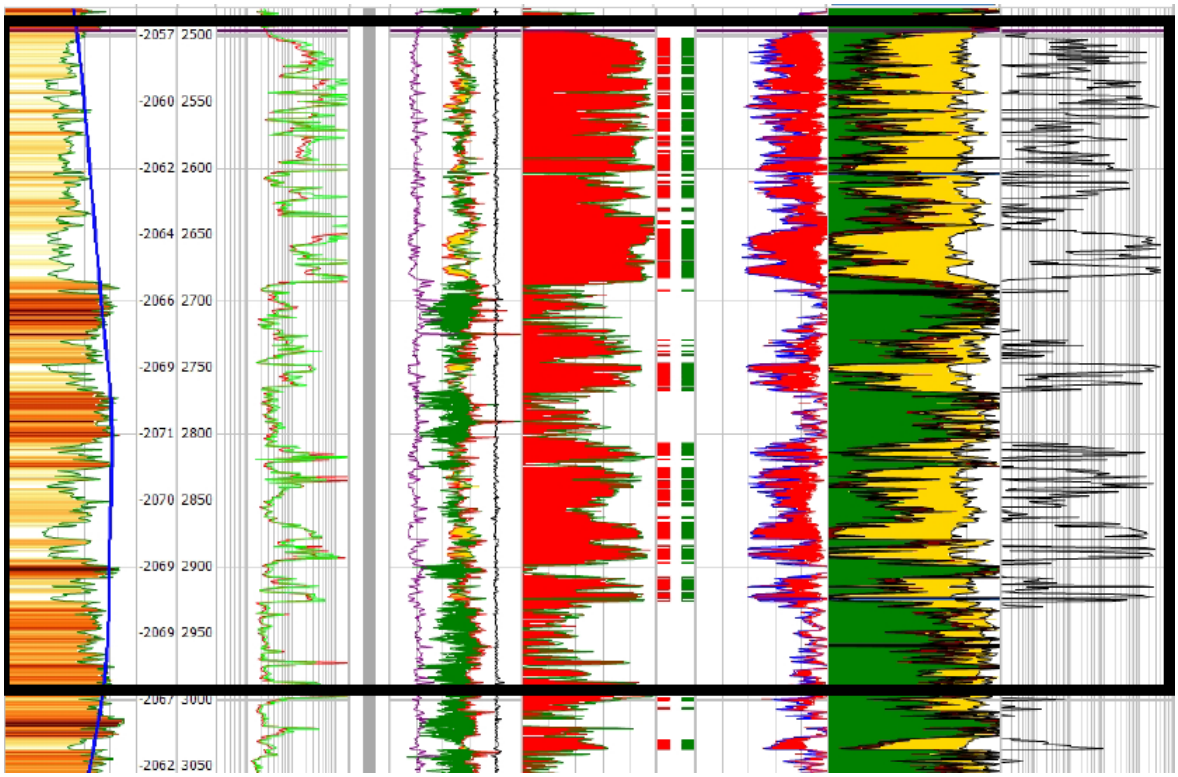

Figure 7.6: The estimated net pay is 240 m in Well D. From (Det Norske Oljeselskap 2013).

In Figure 7.6 it is observed that the net pay length of 240 m is from layer Z2, given the TVD and assumed location of the layers. The log indicates that layer Z1 in the area of

Well D is shaly, and hence not a productive zone. Well D may still produce from layer Z1, due to drawdown in the surrounding reservoir, leading to a flow from layer Z1 to the sandy intervals in layer Z2.

7.1.3 Drainage Area

The drainage area of the well is dependent upon permeability, layer height, well length, reservoir boundaries, well radius, porosity and compressibility. As there is no available seismic data which may identify closed boundaries, and the logs indicate smooth layers, the well tests have been used to estimate the minimum drainage radius.

None of the well tests taken in Well D are sufficiently long enough to reach pseudo-steady state or steady state, see Figure 6.14. Without any identification of pressure boundaries, the drainage radius, r_e, may not be found directly, but have to be estimated. In the October tests, which are the tests run longest and thus have shown to be the best so far, the radius of investigation is 140 m. This may indicate that the pressure boundaries have to be at least 140 m away from the wellbore.

The estimate of r_e will be uncertain as there is a wide range of possible drainage radii which may be assumed. The drainage radius of the well is considered to be at least 140 m. Short well length, green and black shale intrusions in the reservoir sands and poor permeability contributes to a smaller drainage area. If no faults are assumed, as initially anticipated in the Jette model, the drainage area may be bigger than with existing faults. This should be taken into consideration when evaluating the drainage area.

7.2 Well Characteristics

7.2.1 Well Path

The wellpath is highly tortuous, as can be seen in **Figure 7.7**. There is a generally high Dog Leg Severity (DLS) often surpassing 3°/30 m for relative long intervals at a time (Naterstad 2013). See framed section in **Appendix D**.

In general, DLS greater than 3°/30 m is not recommended (Naterstad 2013). The difficulties associated with doglegs which were experienced during the lower completion are mentioned below.

- The bottom hole assembly components got suck as they were pulled through some sections. This may be due to a keyseat, a worn spot caused by repeated abrasion by the drillstring in a particular location of the dogleg (Schlumberger 2014*a*).
- Difficulties to work the production liner into place may be due to the high dogleg which creates curved sections (Schlumberger 2014*a*).

- Difficulties of getting stuck during drilling may be due to friction. Excessive doglegs increase the overall friction of the drillstring (Schlumberger 2014*a*).

The tight spots that were observed during the running of the lower completion were responded to with high torque, increased weight on bit and up to 15 ton overpull. This was in order to finalize the well. Eventually, the well was only completed to 2977 m MD RKB. The attempts to work the production liner into place may have caused damage to the lower completion.

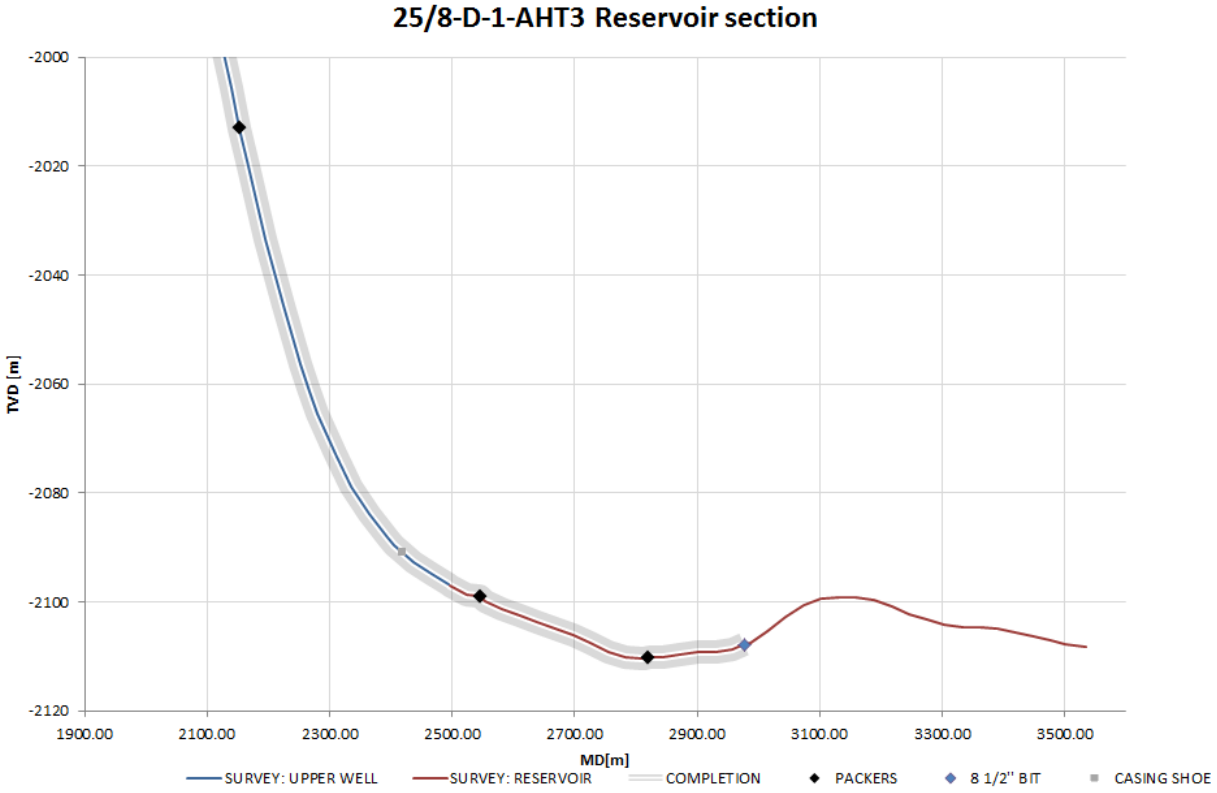

Figure 7.7: The wellpath of Well D.

7.3 Pressure Buildup Tests

Figure 7.8 shows all build-up tests in Well D since the start of production in May 2013 in detail. The drawdown differs for the different tests, as may be seen in Figure 7.8.

Segregation is seen in all the tests during the first hour after shut-in, see Figure 7.8, except in the test from 16.10.2013 to 18.10.2013. Segregation can be explained by gas bubbles from below the liquid in the liquid column which slowly rise up through the well. Due to expansion of the gas, the liquid falls down and is pushed into the reservoir. This trend is expected in a gas lift well. No such segregation, as in the first October test, may indicate

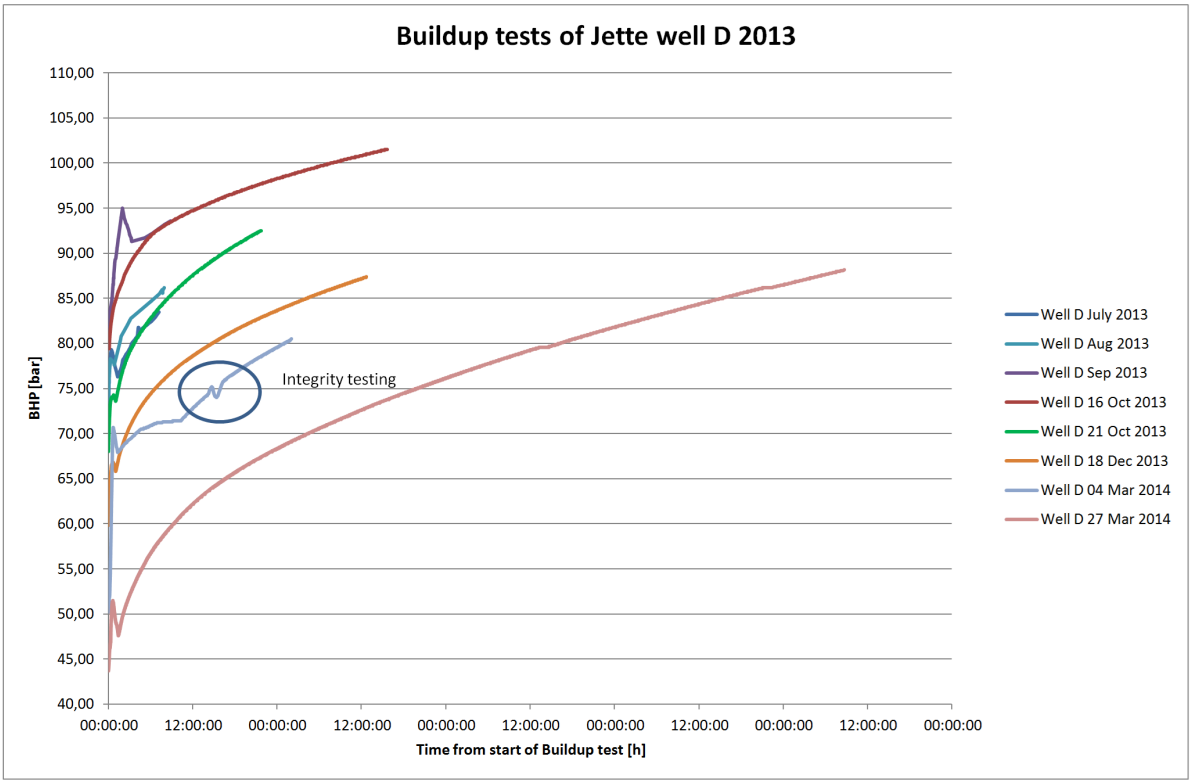

Figure 7.8: All build-up tests in Well D since start of production, from (Lysne 2014b).

a smaller liquid column and hence, a possibility of poorer oil production. This hypothesis may explain the poor repeatability of the tests. From the buildup tests it is observed that the reservoir is depleting, as mentioned in Section 6.6.

Two build-up tests were performed on Well D in October, the first from 16.10.2013 to 18.10.2013, and the second from 21.10.2013 to 22.10.2013. In the time slot between the two build-up tests, a build-up test on Well E was performed. This is seen in **Figure 7.9**.

The tests from October are the most representative tests so far (as of February 2014); the duration of the previous tests have been too short to obtain the most important parameters from the analysis. Weatherford Petroleum Consultants performed a build-up test analysis in October 2013. The tests were evaluated in PanSystem. Input parameters used in the evaluation are shown in **Table 7.4**. Production data, that is the rate history, was also used as input parameters.

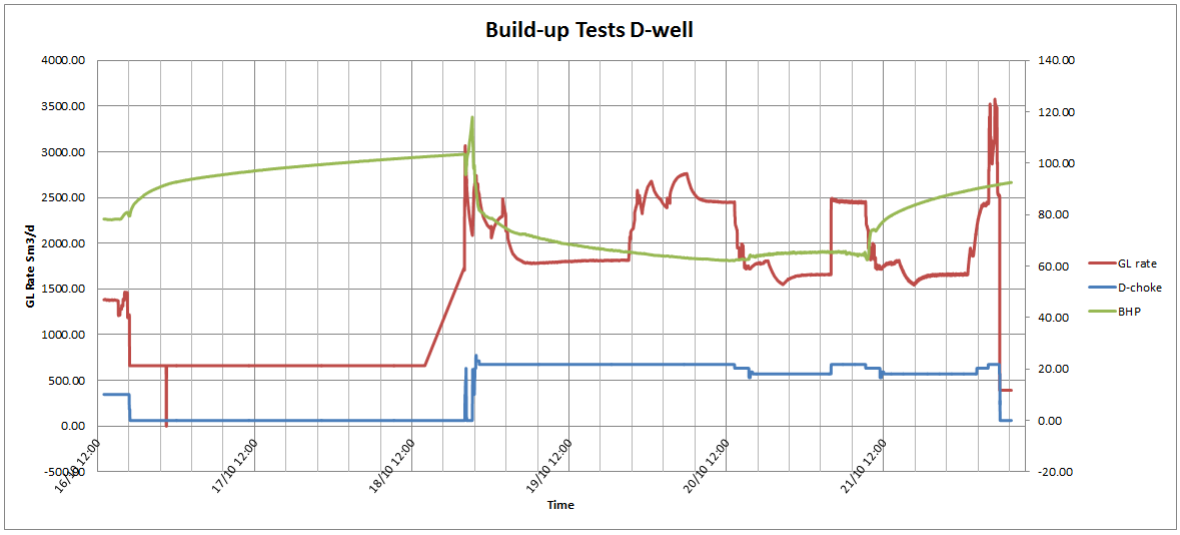

Figure 7.9: Data of Well D. Two build-up test periods are seen from 16.10.2013 to 18.10.2013 and from 21.10.2013 to 22.10.2013. In between, a build-up test on Well E was performed.

Table 7.4: Input parameters in the well test analysis.

Parameter	Data
Layer height	7.7 m
Oil Formation Volume Factor	1.346 Rm^3/Sm^3
Oil viscosity	0.567 cp
Well radius	0.108 m

Match of First Build-up Test, 16.10.2013-18.10.2013

Figure 7.10 shows the evaluation of the first build-up test.

Oscillating pressure is observed in the test period from the start to around one hour, see Figure 7.10. As the oscillation is observed so early in the test the behaviour is most likely not attributed to the reservoir itself, but may be a phenomenon in the well or near the wellbore. The effect dissipates after one hour. Due to pressure oscillations, the latter part of the test was used for matching purposes, as this was assumed to be more representative. This means that the values for vertical permeability, wellbore storage and skin are subject to a higher degree of uncertainty (Lysne & Nakken 2013). The match from the latter part of the test is given in **Table 7.5**.

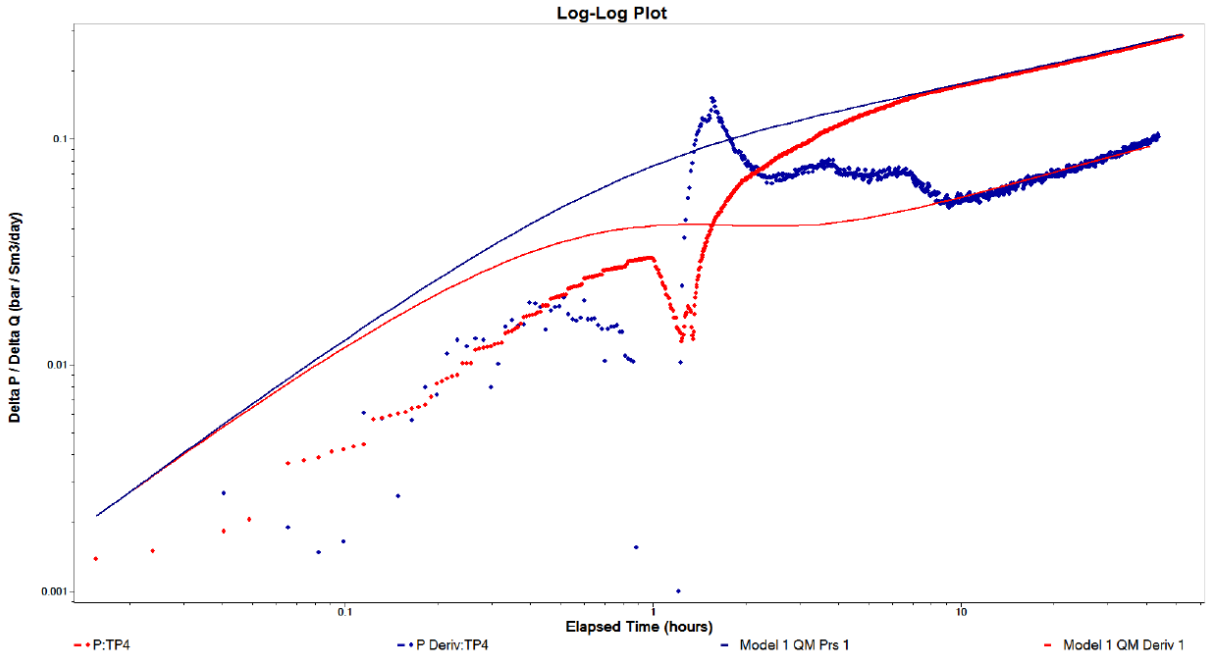

Figure 7.10: The build-up test with its evaluation, 16.10.2013-18.10.2013. From Lysne & Nakken (2013), page 55.

Match of Second Build-up Test, 21.10.2013-22.10.2013

Figure 7.11 shows the evaluation of the second build-up test.

No oscillation were observed in the second well test, see Figure 7.11. The late stage trend is the same as for the first build-up; both stop while in linear flow without indicating the start of a pseudo-radial flow. The match from the second well test is given in Table 7.5.

As may be observed in Figures 7.10 and 7.11 perfect matches could not be obtained. The mismatch might be due to changing wellbore storage effects. Also, there might be something wrong with the model, for example rate input. Pseudo-steady state or steady state regimes were not reached, due to insufficient well test duration.

The initial reservoir pressures found in the well tests deviate from the reservoir pressure measured downhole. This may indicate that the well is producing from a sealed pocket, where depletion is a major factor. With a sealed pocket, the aquifer do not give any, or little, pressure support.

The producing length found from the logs deviates from the producing length from the well tests. This may be due to wrong net-to-gross factor, uncertainties in the logs or the well test model.

The parameters obtained from the second test are more beneficial than those obtained from the first test, due to the oscillation in test 1. Still, the parameters from the analysis should

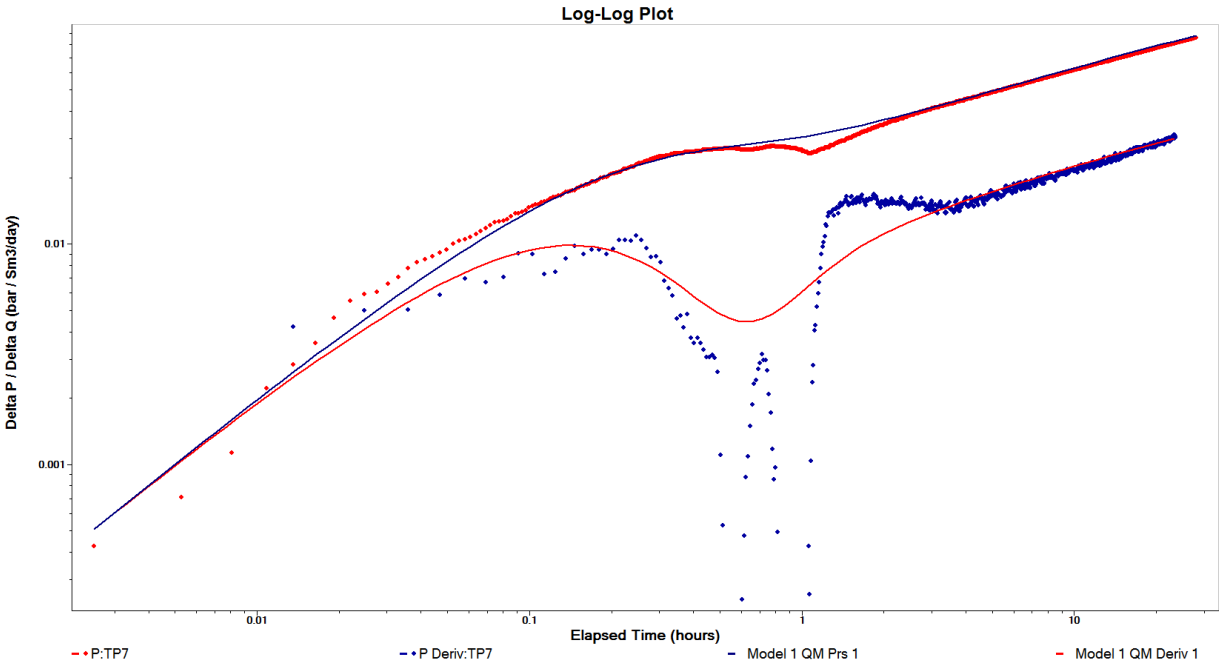

Figure 7.11: The build-up test with its evaluation, 21.10.2013-22.10.2013. From Lysne & Nakken (2013), page 56.

Table 7.5: Output parameters from PanSystem.

Parameter	Well Test #1	Well Test #2
Producing well length	300 m	300 m
Skin	5	1
Skin pressure drop	5.1977 bar	1.6365 bar
Pseudo-radial skin	-5.5395	-5.7367
Horizontal permeability	3.2 mD	13 mD
Vertical permeability	2.5 mD	4 mD
Initial reservoir pressure	160.947 bar	150.991 bar

be treated with caution as there are a lot of uncertainties in the analysis. Pseudo-radial flow do not occur in any of the two tests, giving poor estimates of k and h. This creates a non-uniqueness problem, and a range of different solutions exist, which are equally viable. The poor estimates of kh leads to poor estimates of producing well length, L, vertical permeability, k_v, and S. Due to the uncertainties and the deviation in results in the build-up tests, one, or both of them, might be wrong.

7.4 Production Data

Production data measured at surface and at P/T-gauge were used as input data when calculating the productivity index. The production data varies with time; BHP, gas lift rate and choke opening change with rate of flow. In order to find the most accurate picture of the production, that is an area without too much oscillation and varying rates, the data have been plotted, see **Figure 7.12** (Winther 2013). This may reduce the uncertainty in the choice of data. Production data from October 2013 has been used, as the longest and most qualitative pressure build up tests were performed at the point in time.

The most representative data are found when the well has produced stable for some period [1]. A stable production is found late in a given period, and also, the variations of the parameters are small. (Winther 2013)

The two framed areas are the most representative points for the multi-rate tests considering the variations in choke opening, BHP and gas lift rate, see Figure 7.12. Well E is shut in during the multi-rate tests to obtain the production data for Well D.

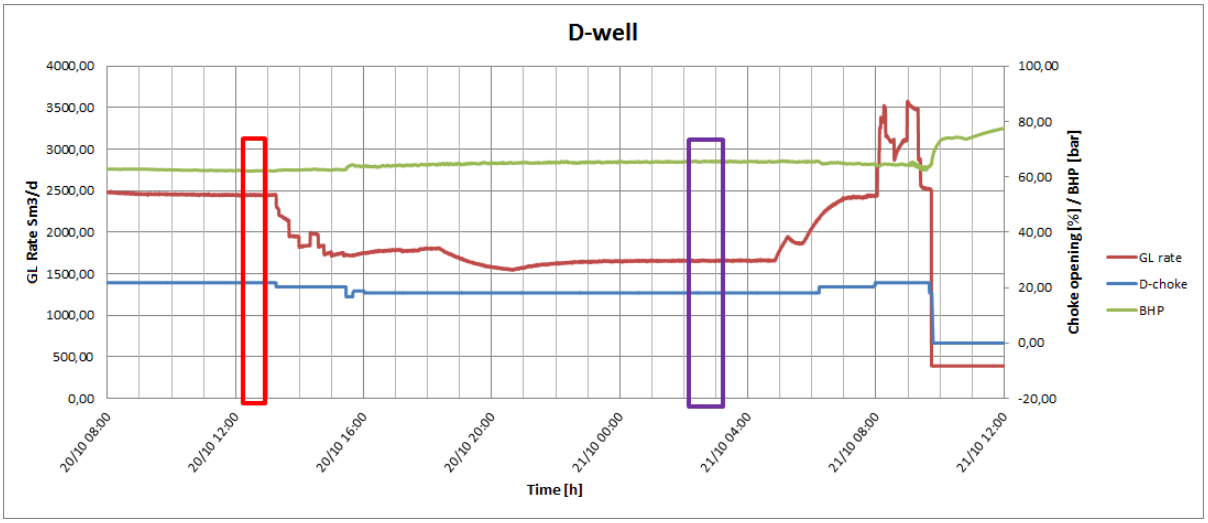

Figure 7.12: Graphics of the production data in Well D, showing the opening of the choke, the bottomhole pressure and the gas lift rate. The framed periods are the chosen multi-rate tests.

7.5 Estimation of the Productivity Index

The productivity index of Well D is calculated directly from the multi-rate tests and with the use of a pseudo-steady state model. The main difference of the two above mentioned

[1] Personal communication with Jean-Christophe Barbier. November 2013. Trondheim: Weatherford Petroleum Consultants AS

methods is the input data used in the calculations. The multi-rate tests use rate and pressure only, while the pseudo-steady state model takes the reservoir extension and properties, and production geometry into account. This assures a quality control of the calculations and the estimated PI. The build-up tests provide additional input data for the pseudo-steady state model.

To test whether the assumptions and calculations are representative, the calculated data from the multi-rate tests are used as input data in inflow- and lift performance models. The combination of these methods makes sure of quality control, and may help to find deviations from expected PI.

The analysis of the build-up tests indicate a depleting reservoir. This contradicts the initial assumption of an active aquifer giving pressure support. In the following, the PI has been calculated with both a reservoir pressure of 197 bar and 151 bar. The reservoir pressure found in the second well test is chosen as input, as it is considered the most reliable. This may give an indication on the state of the reservoir.

7.5.1 Multi-Rate Test

The PI was estimated with the use of data from two multi-rate tests in October 2013, both with a reservoir pressure of 197 bar and 151 bar. The input data and results are shown in **Tables 7.6** and **7.7**.

Productivity Index Estimated With Reservoir Pressure of 197 Bar

Table 7.6: PI calculated from the two multi-rate tests, 197 bar reservoir pressure.

Test data	FBHP	P_{res}	Liquid rate	Oil rate	Liquid PI	Oil PI
Test number	[bara]	[bar]	$[Sm^3/d]$	$[Sm^3/d]$	$[Sm^3/d/bar]$	$[Sm^3/d/bar]$
1	99	197	507	421	5.2	4.3
2	102	197	435	351	4.6	3.7

The average liquid PI is 4.9 $Sm^3/day/bar$, and average oil PI is 4.0 $Sm^3/day/bar$ for the tests with 197 bar reservoir pressure.

Productivity Index Estimated From Well Test Results

When calculating the PI with the use of the reservoir pressure found in the second well test, 151 bar, the calculated PI doubles when compared to the results found in Table 7.6, see Table 7.7.

The average liquid PI is 9.3 $Sm^3/day/bar$, and average oil PI is 7.6 $Sm^3/day/bar$ for the tests with 151 bar reservoir pressure.

Table 7.7: PI calculated from the two multi rate tests, 151 bar reservoir pressure.

Test data	FBHP	P_{res}	Liquid rate	Oil rate	Liquid PI	Oil PI
Test number	[bara]	[bar]	$[Sm^3/d]$	$[Sm^3/d]$	$[Sm^3/d/bar]$	$[Sm^3/d/bar]$
1	99	151	507	421	9.8	8.1
2	102	151	435	351	8.9	7.2

7.5.2 Pseudo-Steady State Model

Data from build-up tests, log evaluation and drilling reports are used as input in the pseudo-steady state model. The input data have been considered constant.

A rectangular drainage area and well placement are used as seen in **Figure 7.13**. The drainage areas used in the calculations are estimated from the relations discussed in **Subsection 7.1.3**.

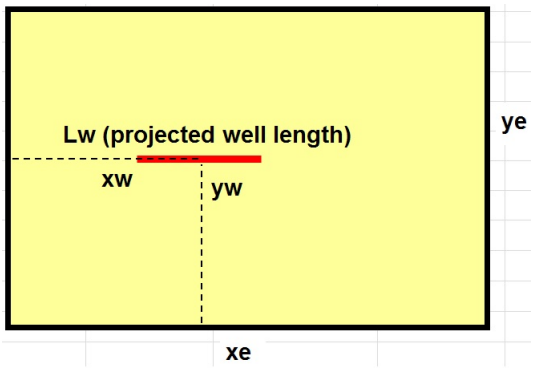

Figure 7.13: The reservoir schematic.

Productivity Index Estimated With Reservoir Pressure of 197 Bar

It is observed from the log of Well D that the well penetrates only the sand layers from Z2. This indicates that this is the producing layer. **Table 7.8** contains input data used in the pseudo-steady state model to calculate PI. Average well deviation has been used.

The data used for estimating the drainage area, see Figure 7.13, and its results, are given in **Table 7.9**. It is assumed that the well is in the middle of the producing layer, and that the oil formation volume factor and oil viscosity are constant.

Different combinations of the sides of the drainage area may give the same productivity. This may indicate that the drainage area is approximately in the area of 600.000-900.000 m^2.

Table 7.8: Input data considered constant.

Parameter	Symbol	Unit
Reservoir height	h	7.7 m
Well radius	r_w	0.108 m
Well length	L	240 m
Well deviation	θ	88 deg
Well location	z_w	3.85 m
Skin along the well	s	1
Horizontal permeability	k_h	13 mD
Vertical permeability	k_v	4 mD
Oil Formation Volume Factor	B_o	1.346 Rm^3/Sm^3
Oil viscosity	μ_0	0.567 cp

Table 7.9: Productivity Index calculated with a pseudo-steady state model.

x_e	y_e	x_w	y_w	Drainage area	PI_{oil}	C_A
$[m]$	$[m]$	$[m]$	$[m]$	$[\mathrm{m}^2]$	$[Sm^3/d/bar]$	[-]
800	800	400	400	640.000	3.9	31.0

Productivity Index Estimated From Well Test Results

The results from the second well test are used as input in the pseudo-steady state model. See **Table 7.10**. Average well deviation has been used.

Table 7.10: Input data considered constant.

Parameter	Symbol	Unit
Reservoir height	h	7.7 m
Well radius	r_w	0.108 m
Well length	L	300 m
Well deviation	θ	88 deg
Well location	z_w	3.85 m
Skin along the well	s	1
Horizontal permeability	k_h	13 mD
Vertical permeability	k_v	4 mD
Oil Formation Volume Factor	B_o	1.346 Rm^3/Sm^3
Oil viscosity	μ_0	0.567 cp

With a reservoir depleting as rapidly as found in the well tests it is expected that the actual drainage area of the well may be smaller. It is assumed that the well is in the middle of the producing layer, and that the oil formation volume factor and oil viscosity is constant.

The small drainage area indicates a poor reservoir-to-well exposure.

Table 7.11: Productivity Index calculated with a pseudo-steady state model.

x_e	y_e	x_w	y_w	Drainage area	PI_{oil}	C_A
$[m]$	$[m]$	$[m]$	$[m]$	[m^2]	$[Sm^3/d/bar]$	[-]
300	300	150	150	90.000	7.5	31.0

It is observed that the PI estimates from the multi-rate tests correlates with that of the pseudo-steady state model.

7.6 Inflow Performance Relation

The Inflow Performance Relationship (IPR) curves and the Tubing Performance Relationship (TPR) curves have been simulated and matched by using the WellFlo modeling tool. The OLGA Steady State model has been used for flow correlation of the lower and upper completions of the well, and the IPR curves are based on a Vogel model with coefficient of 0.2. The TPR curves are generated on the basis of the flowing conditions from each of the tests (Winther 2013). Two simulations have been performed, one based on a reservoir pressure of 197 bar and estimated well length from logs, and one based on the results from the second well test.

Productivity Index Estimated With Reservoir Pressure of 197 Bar

Table 7.12 shows the input data used in the WellFlo model.

Table 7.12: Input data used in the model in WellFlo, 197 bar reservoir pressure.

Test	Liquid rate	WC	Gas lift rate	GOR	GOR & GL	PI liquid	BHP	P_{res}
#	$[Sm^3/d]$		$[Sm^3/d]$	$[Sm^3/Sm^3]$	$[Sm^3/Sm^3]$	$[Sm^3/d/bar]$	[bar]	[bara]
1	507	0.17	100 471	99	238	5.2	62.19	197
2	435	0.19	76 776	105	218	4.6	65.5	197

The BHP is measured at P/T-gauge. The Bottomhole Temperature (BHT) is 83.6 °C in both tests. Note that a constant reservoir pressure, no depletion, is assumed for all cases.

The IPR curve describes the inflow performance from the reservoir. From the inflow performance curve the maximum flow rate, or Absolute Open Flow (AOF), performance may be found, which is obtained with maximum drawdown. The AOF from the reservoir is 650-750 m^3/day for both the tests. See **Figures E.1** and **E.2**, in **Appendix E**.

Figures 7.14 and **7.15** show the inflow- and lift performance curves for both multi-rate tests. The inflow curve has an initial pressure of 166 bar, the static pressure at P/T-gauge.

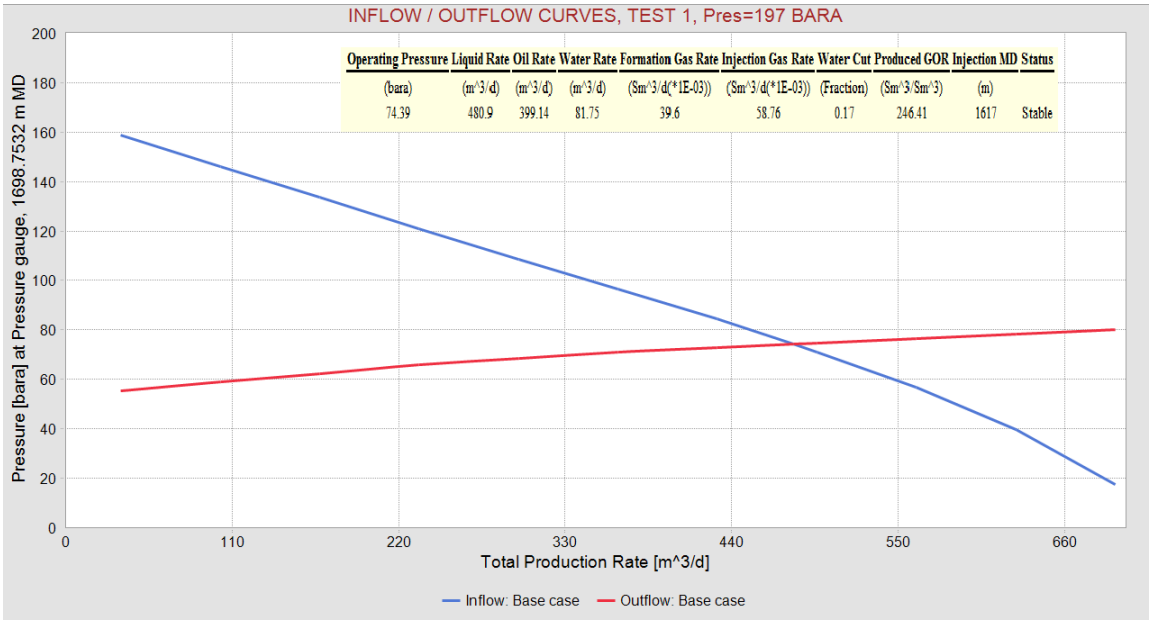

Figure 7.14: Inflow- and lift performance curves. The inflow curve is the blue line and the lift performance curve is the red line. First multi-rate test, reservoir pressure is 197 bar. From WellFlo (Weatherford 2012b).

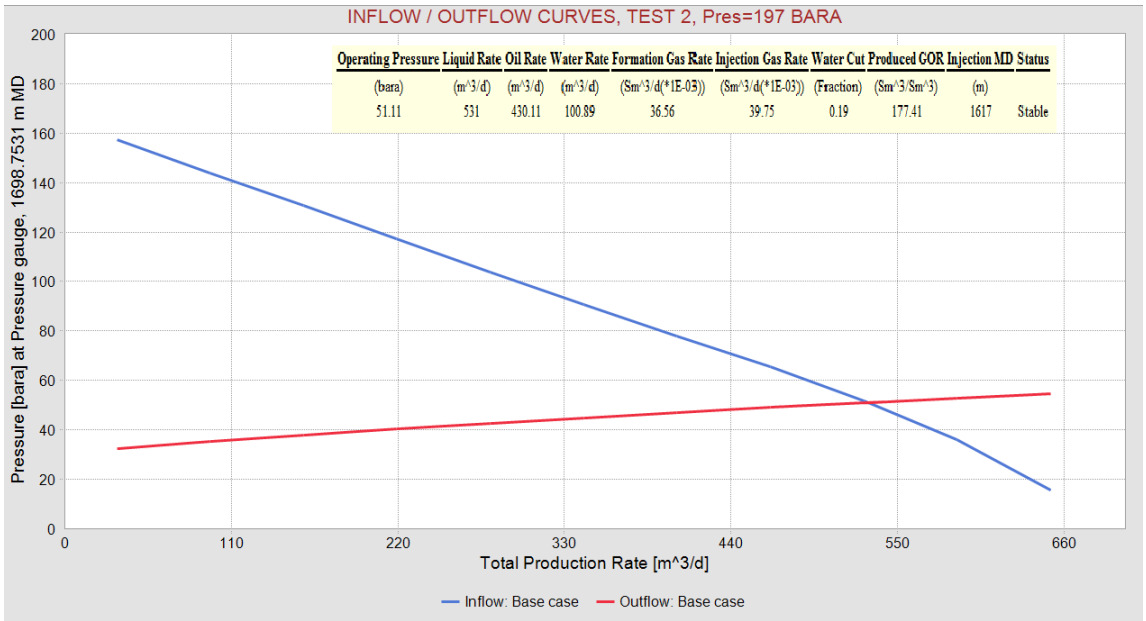

Figure 7.15: Inflow- and lift performance curves. The inflow curve is the blue line and the lift performance curve is the red line. Second multi-rate test, reservoir pressure is 197 bar. From WellFlo (Weatherford 2012b).

Productivity Index Estimated From Well Test Results

Table 7.13 shows the input data used in the WellFlo model.

Table 7.13: Input data used in the model in WellFlo, 151 bar reservoir pressure.

Test	Liquid rate	WC	Gas lift rate	GOR	GOR & GL	PI liquid	BHP	P_{res}
#	$[Sm^3/d]$		$[Sm^3/d]$	$[Sm^3/Sm^3]$	$[Sm^3/Sm^3]$	$[Sm^3/d/bar]$	[bar]	[bara]
1	507	0.17	100 471	99	238	9.8	62.19	151
2	435	0.19	76 776	105	218	8.9	65.5	151

The BHP is measured at P/T-gauge. The BHT is 83.6 °C in both tests.

The AOF from the reservoir is 900-930 m^3/day for both the tests. See **Figures E.3** and **E.4** in Appendix E. Maximum drawdown is 151 bar.

Figures 7.16 and **7.17** show the inflow- and lift performance curves for both multi-rate tests. The inflow curve has an initial pressure of 120 bar, the static pressure at P/T-gauge.

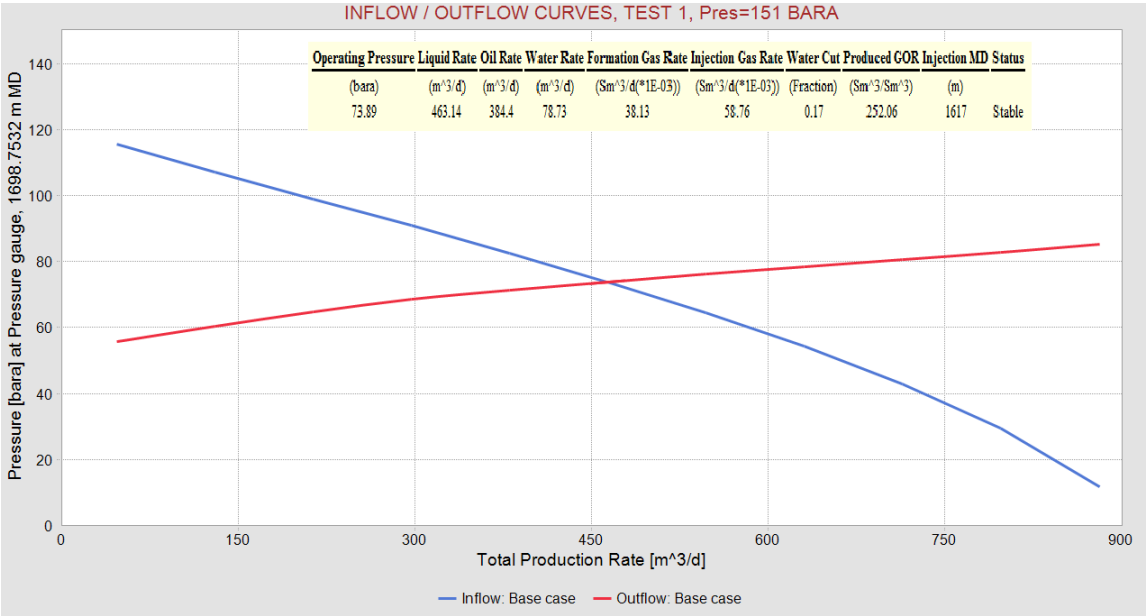

Figure 7.16: Inflow- and lift performance curves. The inflow curve is the blue line and the lift performance curve is the red line. First multi-rate test. From WellFlo (Weatherford 2012b).

As seen in figures 7.14, 7.15, 7.16 and 7.17 the calculated operating points, the intersection between the IPR and TPR curves, do not coincide with the measured data. Both calculated rates and downhole pressures deviate from the measurements at P/T-gauge and the MPFM.

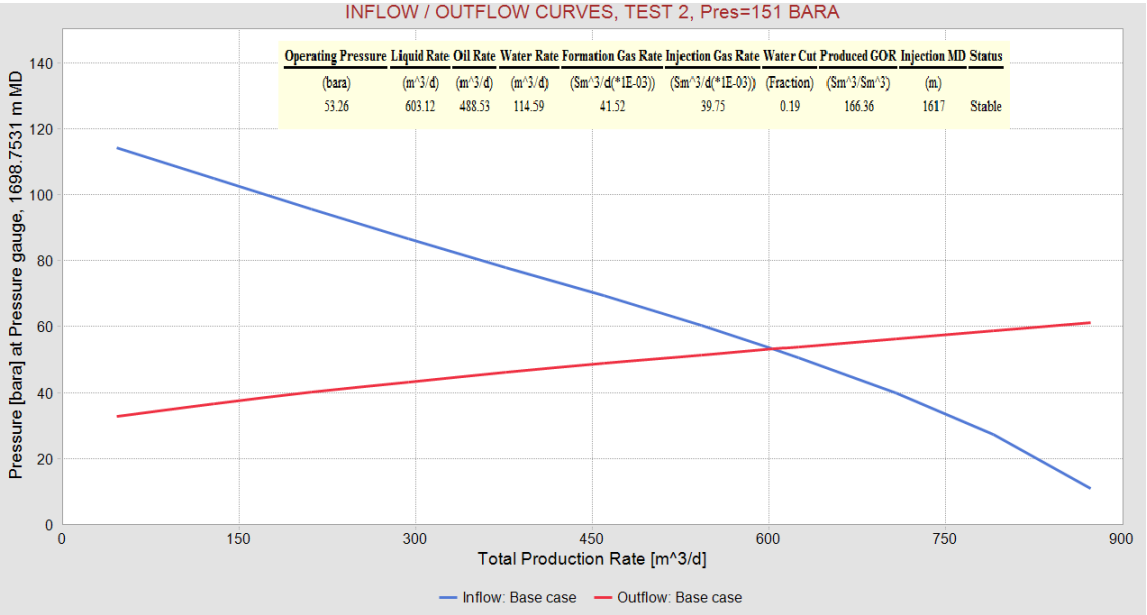

Figure 7.17: Inflow- and lift performance curves. The inflow curve is the blue line and the lift performance curve is the red line. Second multi-rate test. From WellFlo (Weatherford 2012b).

The deviation is as much as 20% for the BHP. A sensitivity analysis is performed in Section 7.8.

7.7 Uncertainties

In the project report *Productivity Index in Horizontal Wells* (Winther 2013) a similar productivity calculation was performed on Well E. Some of the uncertainties mentioned below are from that respective project.

Reservoir Parameters

- An uncertainty in drainage radius may lead to an uncertainty in drainage area as the drainage area is estimated from the drainage radius. The shape of drainage area also contributes to an uncertainty in the drainage area.
- The layer thicknesses, used as input data in PanSystem, are estimated from logs. The layer thickness is proportional to the horizontal permeability; this may lead to an uncertainty in the horizontal well permeability found from the analysis of the build-up tests.
- The logs from the nearby wells may not be representative for estimating the layer thickness in Well D. There might be faults, anticlines or compartmentalization, indicating that the layers do not follow the "trend" in the area around Well D.

- Measured initial temperature and pressure are average values. These may vary within the reservoir, and affect the fluid parameters and drawdown.

Fluid Parameters and Composition

- Rate history: the oil production rate history is an important parameter in a build-up test model, as it is used to calculate the horizontal permeability. An error in the rate history may affect the results of the build-up test analysis. With only the cumulative production rate given, the rate history carries high uncertainties.
- Production data: the measurement of the production data may be uncertain due to uncertainties in flow measurement devices. Major factors contributing to the flow measurement uncertainties are fluid flow condition, construction tolerances in meter components, uncertainty of secondary devices/instrumentation, data reduction and computation, predictability in defining the physical properties of the fluid, and tolerances in prediction of coefficient of discharge. These systems should have a lower uncertainty than $\pm 10\%$. (LEVON-Group et al. 2009)
- Viscosity, gas solubility, flow rate, fluid density, and oil and water saturation are fluid parameters which vary with temperature and pressure. These parameters may contribute to uncertainties in the calculations, as average values are used.
- Uncertainties in reservoir pressure lead to different drawdown and PI values. This may lead to wrong assumptions in permeability, reservoir extension, aquifer support and geology in the area around Well D.

Wellbore Geometry

- Irregularities, tortuosity, in the wellbore may lead to possible uncertainties in its dependent parameters. These parameters are for example well radius and fluid flow friction loss. Friction loss in the horizontal section is ignored in the calculations of the PI, which leads to a slightly higher drawdown. This may lead to too optimistic PI estimates. The observed dog leg of Well D is high, indicating that this may cause some wrong estimates.
- The deviation of the well may vary with the length of the well, and in the previous calculation an average deviation is used. As will be shown in the sensitivity analysis, the productivity index is highly dependent upon the well deviation. The deviation will also vary due to tortuosity in the wellbore.
- In addition to varying well deviation along the well, the reservoir layer height may vary. This may lead to an uncertainty in the well location, and the drainage area if no-flow boundaries are assumed. The shape factor may also change.
- The mechanical skin may have another value than estimated. This may affect the productivity of the well.

Models

The equations and software used might carry uncertainties as they follow certain correlations.

- Equations are simplified and theoretical, not taking changes over time into account.
- The software, WellFlo and PanSystem, calculate the best possible match with regards to the input parameters. The match in data may not be good and give uncertain output data.
- Uncertainties in CPI logs as these are computer processed.
- The lack of information from the two well tests, the difference in segregation and the mismatch may create uncertainties in output values. The lack of information of when and/or where pseudo-radial flow occurs, in PanSystem, may create uncertainties in the horizontal permeability, vertical permeability, producing well length and skin.

7.8 Sensitivity Analysis

7.8.1 Inflow Performance Relation

Well Head Pressure (WHP) and subsea choke opening are normally used as allocation parameters to allocate the oil production rate. At the Jette field, there are a few circumstances preventing the use of these two parameters. The primary reason is that gas lift will by far exceed the WHP and the choke opening effect. It is possible to have a large range of oil production rates from a well and yet a constant WHP due to the gas lift. The chokes should be in a maximum open position after start-up, and the flow from the wells should rather be controlled by gas lift. (Winther 2013)

At Jette it can be assumed that there is a strong relationship between gas lift rate and liquid production. It can also be assumed that with a given productivity index for the well, the pseudo-steady state liquid production is directly proportional to the drawdown. Hence, it is recommended to use BHP and/or gas lift rate as allocation parameters. There are reasons to believe that liquid production rate is strongest linked to gas lift rate since the BHP will change with water cut. (Winther 2013)

The challenge in Well D is to get a match with the BHP. The same trend of pressure match is observed for both reservoir pressures and their respective PI; from multi-rate test 1, the BHP is found to be too high and the producing rates too low, while in multi-rate test 2 the BHP is found to be too low and the rates too high. This may indicate that the gas lift rates or GOR are not correct. A sensitivity analysis were done at the tests, altering the gas lift rate, the GOR and the Inner Diameter (ID) of the well. It is assumed that the previously calculated PI's are correct.

The sensitivity analysis for the different parameters, with associated plots are shown in Appendix E, in **Subsection E.2.1**. It is observed in the figures that by altering the gas lift rates and the GOR a good match may be obtained. Altering the ID has little impact on the results.

Gas Lift Rates

Figures 7.18 and **7.19** summarize the results from the sensitivity analysis.

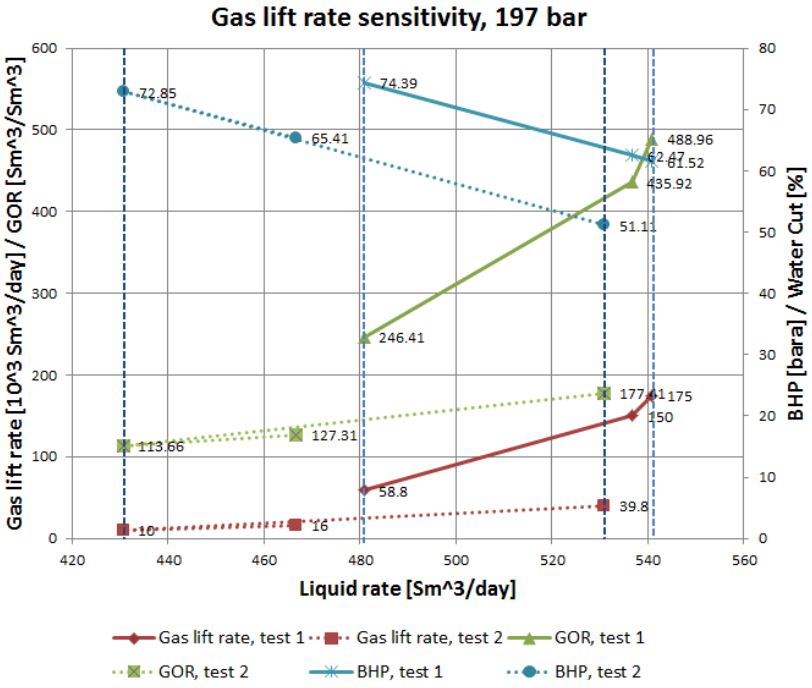

Figure 7.18: Gas lift rate sensitivity, for both tests with 197 bar reservoir pressure.

Gas-Oil Ratio

Figures 7.20 and **7.21** summarize the results from the sensitivity analysis.

Inner Diameter in Reservoir Section

Figures 7.22 and **7.23** summarize the results from the sensitivity analysis.

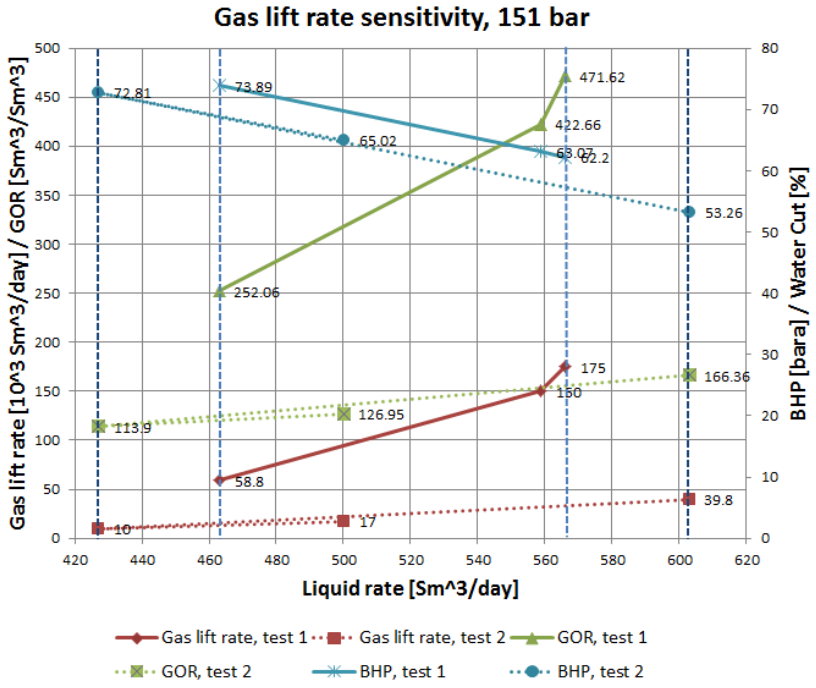

Figure 7.19: Gas lift rate sensitivity, for both tests with 151 bar reservoir pressure.

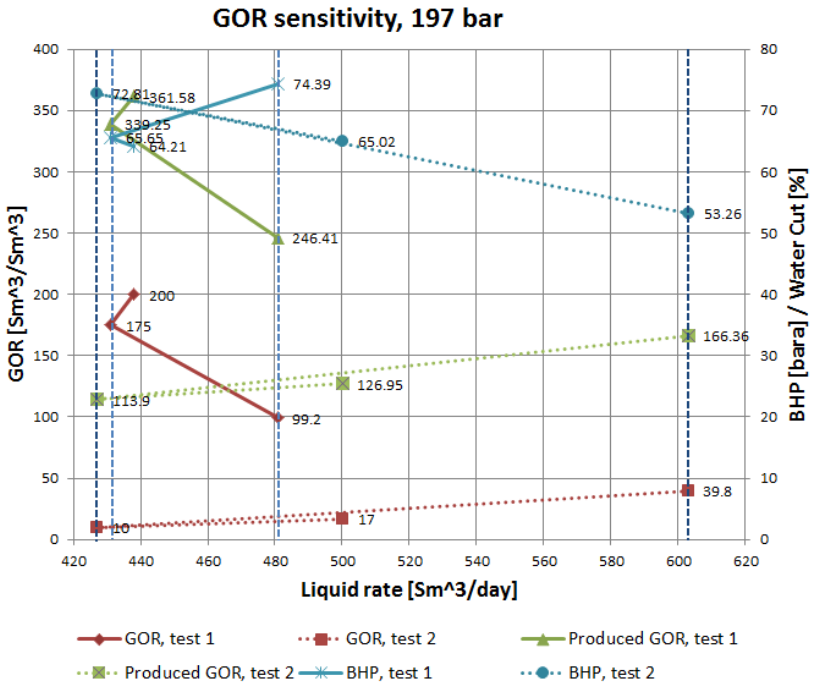

Figure 7.20: GOR sensitivity, for both tests with 197 bar reservoir pressure.

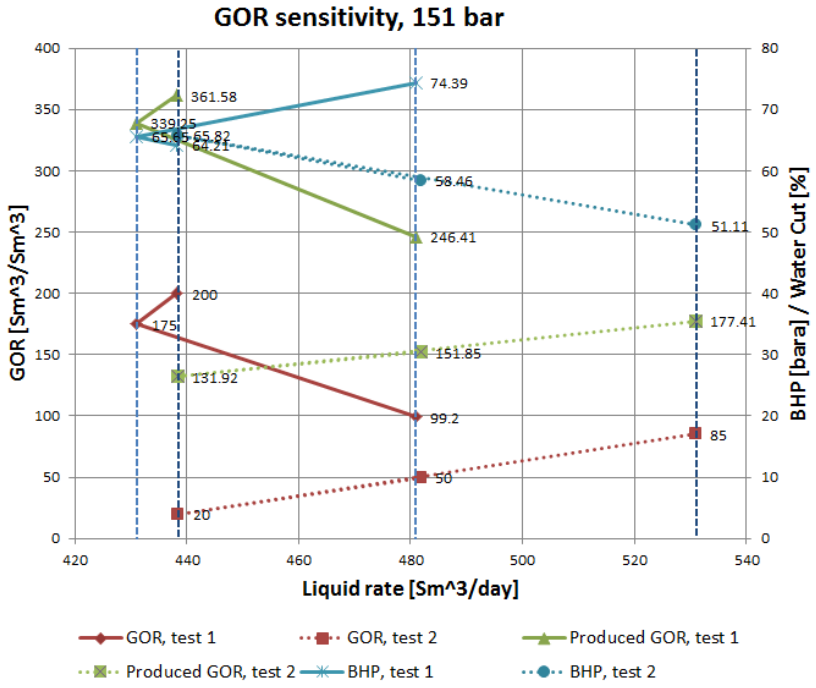

Figure 7.21: GOR sensitivity, for both tests with 151 bar reservoir pressure.

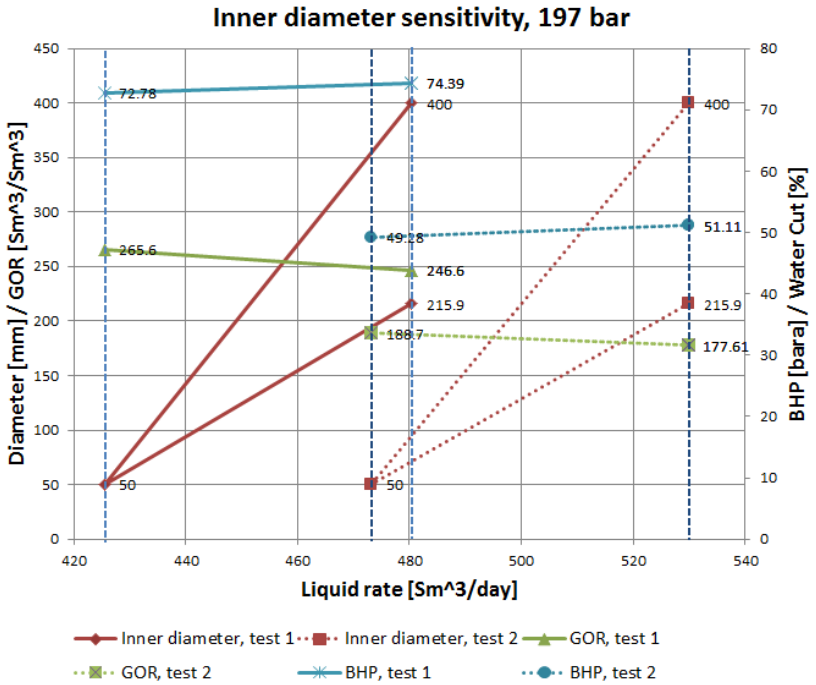

Figure 7.22: Inner diameter sensitivity, for both tests with 197 bar reservoir pressure.

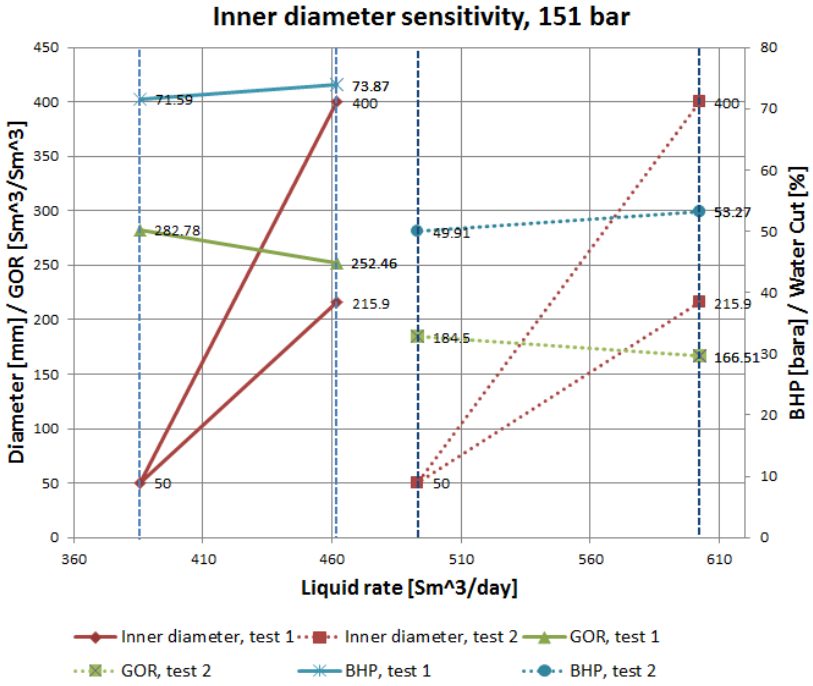

Figure 7.23: Inner diameter sensitivity, for both tests with 151 bar reservoir pressure.

7.8.2 Pseudo-Steady State Model

Sensitivity analysis has been performed at both the tests with reservoir pressure of 151 bar and 197 bar, with the use of the pseudo-steady state model. The drainage area, formation height, well deviation, skin along the well, horizontal permeability and vertical permeability were altered in the analysis. It was found that formation height, horizontal permeability and well deviations are the sources of the highest uncertainty. The uncertainty varies from 20% to 230% for these parameters. The high uncertainties show how important it is to estimate the PI with different methods to be able to confirm/deconfirm hypotheses.

The sensitivity analysis for the different parameters, with associated plots are shown in Appendix E, in **Subsection E.2.2**. **Figures 7.24** and **7.25** summarize and show the sensitivities relative to each other. In the figures it is seen that the formation height, well deviation and horizontal permeability have the highest deviation. The sensitivity analysis is presented in spider plots.

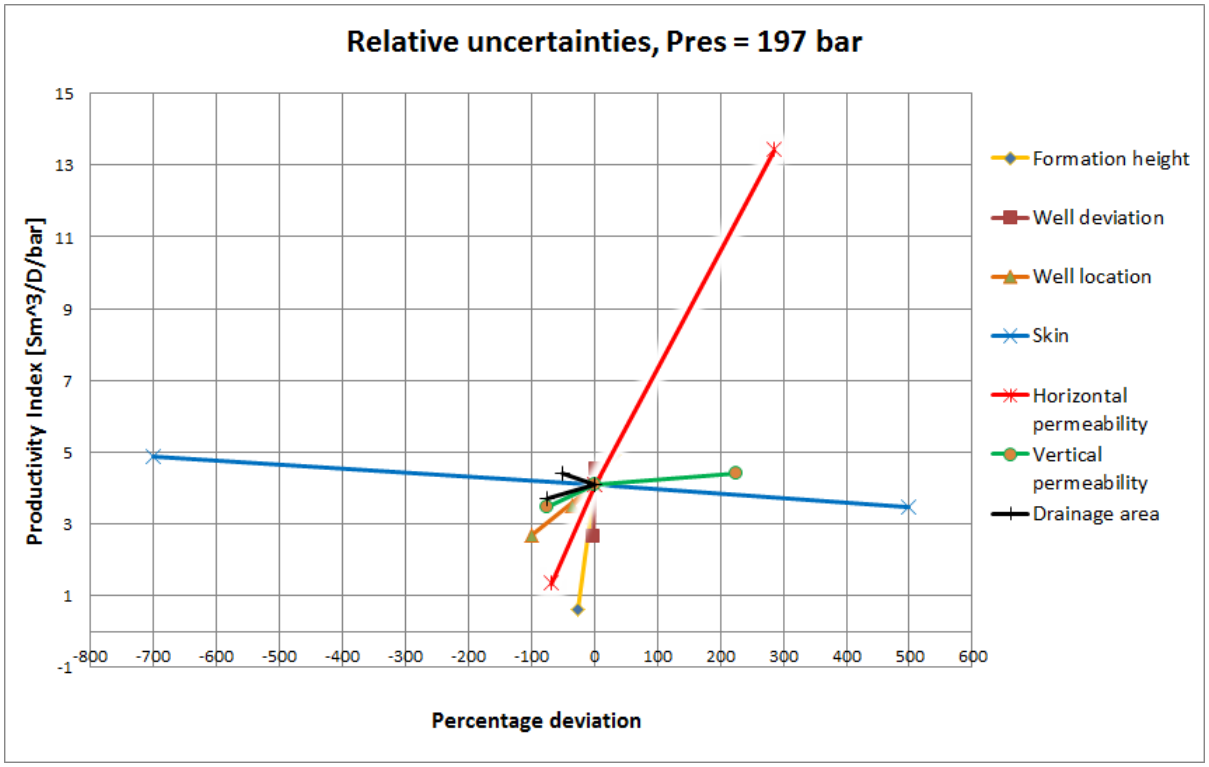

Figure 7.24: The figure shows the sensitivities relative to each other, with a reservoir pressure of 197 bar. It is seen that formation height, well deviation and horizontal permeability have the highest deviation.

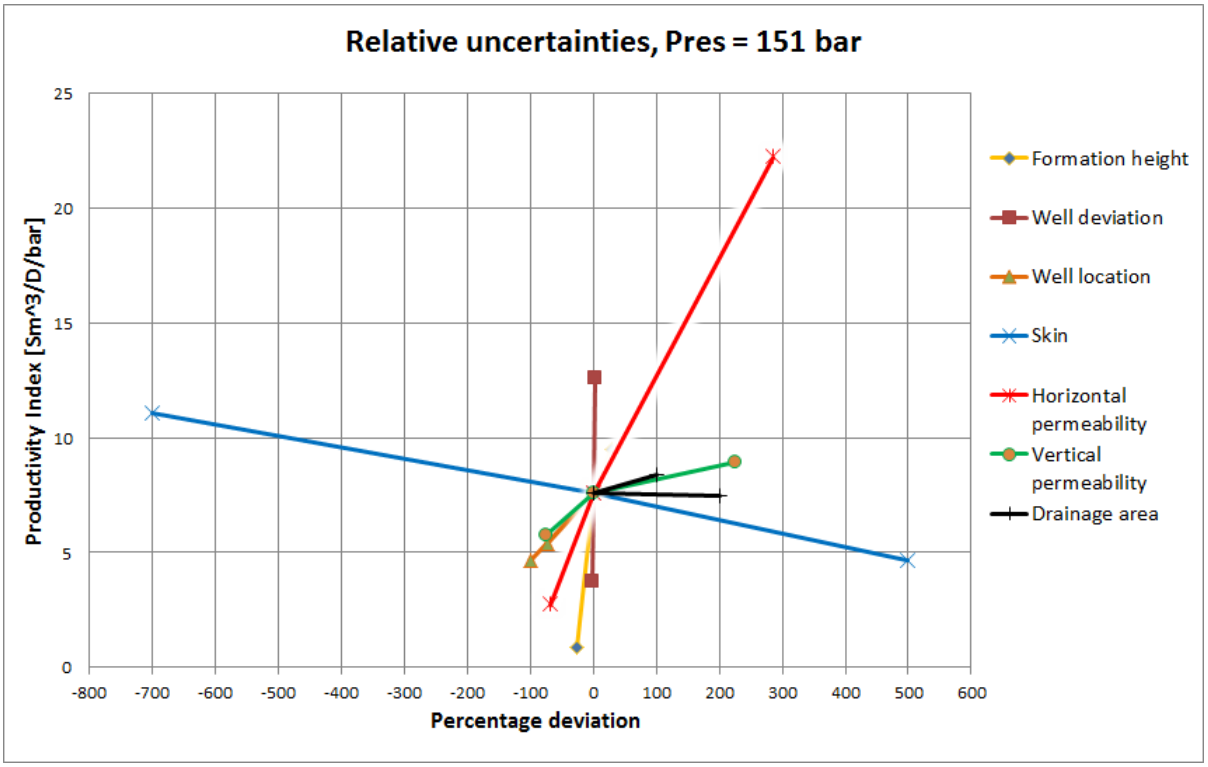

Figure 7.25: The figure shows the sensitivities relative to each other, with a reservoir pressure of 151 bar. It is seen that formation height, well deviation and horizontal permeability have the highest deviation.

7.9 Results and Hypotheses

Tables 7.14 and **7.15** summarize the calculated oil PI from the multi-rate tests and the pseudo-steady state model, both for a reservoir pressure of 197 bar and 151 bar.

Table 7.14: Productivity index calculated with different methods, reservoir pressure of 197 bar.

Method	Average oil PI
Multi-rate test	4.0 $Sm^3/day/bar$
Pseudo-steady state model	3.9 $Sm^3/day/bar$

As seen from Table 7.14 the PI deviates with 2.5%. In Table 7.15 the PI deviates with 1.3%.

The build-up tests gave conflicting results from the estimated initial reservoir pressure, with a reservoir pressure of 150-160 bar. As a part of the quality control two cases were evaluated in the calculation of the PI; a case with reservoir pressure of 197 bar and a

reservoir pressure of 151 bar. The latter offer a smaller drawdown and hence, a higher PI-value.

Table 7.15: Productivity index calculated with different methods, reservoir pressure of 151 bar.

Method	Average oil PI
Multi-rate test	7.6 $Sm^3/day/bar$
Pseudo-steady state model	7.4 $Sm^3/day/bar$

A match was obtained for both cases from the multi-rate tests, mathematical model and IPR evaluation. It is observed that to be able to obtain a match, the gas lift rates or GOR have to be increased drastically, with up to 200%. This indicates that the allocation of these two parameters may be poor, and/or that the measurements are uncertain. Hypotheses for the cause of the poor PI and uncertainties in regards reservoir pressure are listed below.

- The sand screens may be plugged due to the long exposure to LSOBM and difficulties during the completion, as described in **Section 7.1** and Section 6.5. The PI may be lower due to a higher mechanical skin.
- While drilling the reservoir section of Well D, the ECD was in the range of 1.53 to 1.54 SG. This corresponds to about 120 bar overbalance while drilling with WARP mud. However, the build-up tests do not give a skin value that represents the induced formation damage. In case of plugged sand screens, the formation damage skin derived from the build-up analysis will also be influenced by the pressure drop across the screens. The skin caused by the plugged sand screens will most likely be dominant, that is much greater that the formation skin.
- The results from the two build-up tests differ from each other. The results may indicate that one, or both, of the tests are poor, or that something has happened in between. The poor clean-up described in Section 7.1 implies that amounts of drilling and completion fluids may be produced during production. Some drilling and completion fluids may have been produced during the clean-up, leading to different results in the analysis. A clean-up of the well may lead to longer producing length in the well, and hence, a greater PI.
- The well might be located in a closed compartment, isolated from the rest of the reservoir, and the aquifer. The presence of faults and compartments may explain the poor PI and the small drainage area estimated from the pseudo-steady state model, and hence, the low oil rate, the low WC and the reservoir pressure obtained from the well tests. Faults may also explain the difficulties during drilling, as the tension increases in the proximity of the faults. An isolation of the producing zone leads to depletion of that respective zone.
- The well may be packed off below the middle swell packer due to poor clean-up and plugged sand screens. The large amounts of drilling and completions fluids that have

not been cleaned up may be located in the toe of the well, below the middle swell packer. Consequently, the sands above this swell packer may be the zone that have contributed to production of the well. If this sand is only a thin upper sand layer in the formation, the sand can potentially have been partially depleted. From the logs, it is observed that this upper sand is less favourable compared to the sands below the swell packer. This leads to a smaller PI value due to smaller producing length and drainage area.

- The swell packers, which have a maximum differential pressure of 35 bar, may collapse in presence of high pressure differential and contribute to production in periods. This may lead to variations in observed PI.
- There might be wax or buildup of scale in the well constricting the flow due to reduced tubing diameter, and hence smaller BHP and lower producing rates.

7.10 Measures to Improve the Productivity Index

It is clear that the well has a poor PI due to complications during completion and poor clean-up giving a short effective producing well length and poor drainage area. The PI is assumed to improve with the implementation of well intervention measures. An evaluation of the challenges in the well and possible measures are discussed below.

- If Well D is located in a compartment, hydraulic/pulse fracturing may be an opportunity to open up for production in surrounding sand layers. The perforations will most likely be long enough to penetrate the surrounding shale, reaching sands. On the other hand, the fracturing may lead to increased water production if the fractures reaches the OWC, and is thus not considered beneficial in the long run.
- Acid squeeze and scale removal may reduce the effect of plugging and/or poor clean-up. $CaCO_3$ is highly soluble in HCl, hence acidizing may remove particles clogging intake jets in the ICDs. These measures may increase the PI of the well. These measures are considered to be beneficial.
- Infill drilling, either by re-drill and re-completing the original well path of Well D, drilling a side-step or making a multilateral may be good option. Infill drilling and/or optimization of well placements and completions may give increased reservoir-to-well exposure, thus be able to produce from the surrounding sands.

8 Simulation Model

To increase the accuracy of simulation models it is required to increase the number of grid blocks. Very large numbers of grid blocks are impractical when performing dynamic simulations due to the amount of computations required to solve the flow equations (Lorentzen 2013). A model with less grid blocks will reduce the simulation time and increase model performance.

The simulation model provided by Det Norske Oljeselskap ASA was upscaled to obtain a reduction in run time. Upscaled models will always try to mimic the basecase. The resulting upscaled model has a good match in oil production rate, cumulative production of phases and average field pressure compared to the basecase model provided by Det Norske Oljeselskap ASA. After a history matching process of the upscaled model, it will be used as a basecase for further simulations. The upscaled model is taken from *Dynamic Reservoir Modeling of Jette* (Lorentzen 2013).

8.1 Description of the Upscaled Model

The Jette dynamic reservoir model was upscaled in Petrel. Upscaling of properties is the process of generating an average value of each property to represent multiple fine grid blocks within one large grid block resulting from upscaling. Single phase upscaling was performed on static properties such as porosity, permeability, scaled connate water saturation and scaled maximum capillary pressure. The Jette dynamic reservoir model is based on the geological model created by Det Norske Oljeselskap. The grid was coarsened by a factor one to three, see **Table 8.1**.

Table 8.1: Layering and upscaling ratio of upscaled model.

	Basecase model		Upscaled model	
Zone	Layers	Ratio	Layers	Ratio
Z1, Z2, Z5	60	n/a	20	3
Ty Upper	5	n/a	5	1
Sum	65	n/a	25	2.6

The number of grid blocks are given in **Table 8.2**.

Table 8.2: Number of grid blocks in the upscaled model.

	Basecase model	Upscaled model
Number of grid blocks	744 510	286 350
Number of active grid blocks	478 214	247 834

The upscaled model is an adequate match of the basecase model, and the simulation time is halved. Homogenization is the main cause of mismatch between the upscaled model and the basecase (Lorentzen 2013).

Jette is modeled in three dimensions with a black oil formulation containing three phases, gas, oil and water. The reservoir is initially undersaturated, but starts producing gas as the reservoir pressure is lowered below the bubble point pressure. Simulation starts on the 20th of May 2013 and runs until 1st of January 2020. (Lorentzen 2013)

The dimensions of the upscaled model is 166x69x25. Lateral dimensions of the cells are 25 m in horizontal, X and Y, directions, and vary from around a meter to around eight meters in vertical, Z, direction. See **Figure 8.1**.

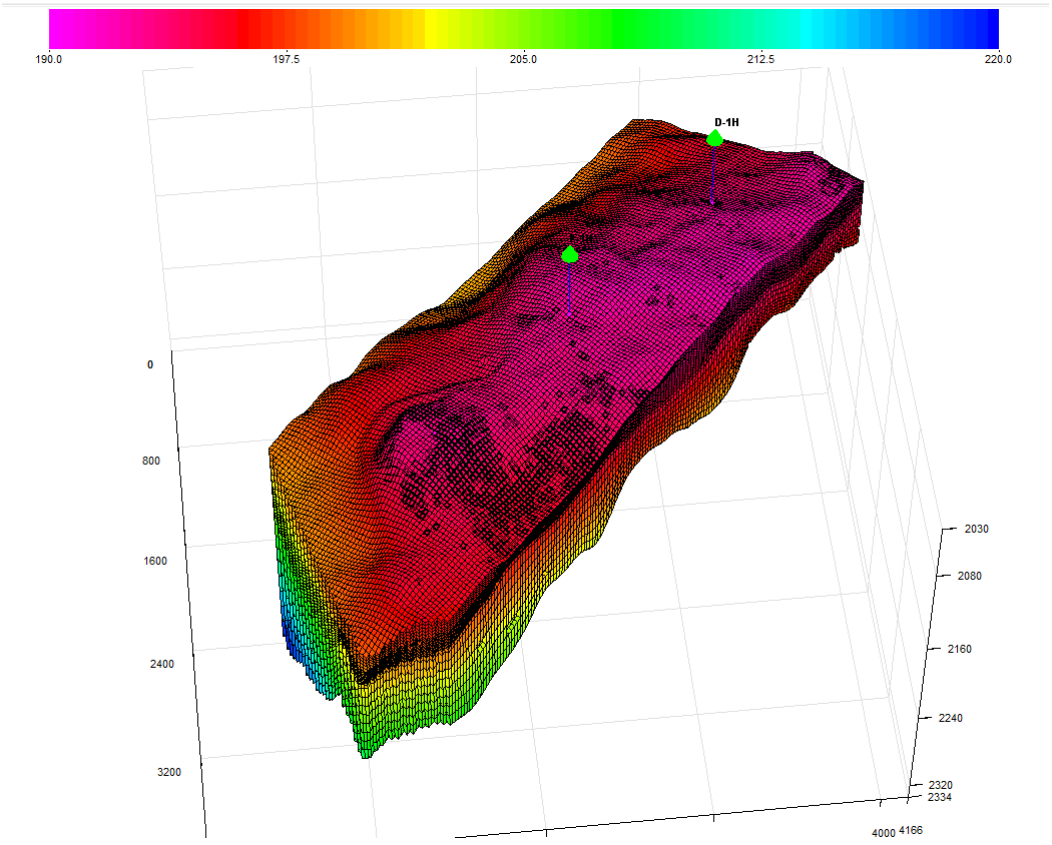

Figure 8.1: Jette upscaled simulation model illustrated with pressure, from S3GRAF (Sciencesoft 2013).

8.1.1 Geology

As above mentioned, the Jette dynamic reservoir model is based on the geological model created by Det Norske Oljeselskap. This can be seen in **Figure 8.2** where the top horizon of the dynamic reservoir model is positioned on top of the static geological model. The same features can be seen in the upscaled model.

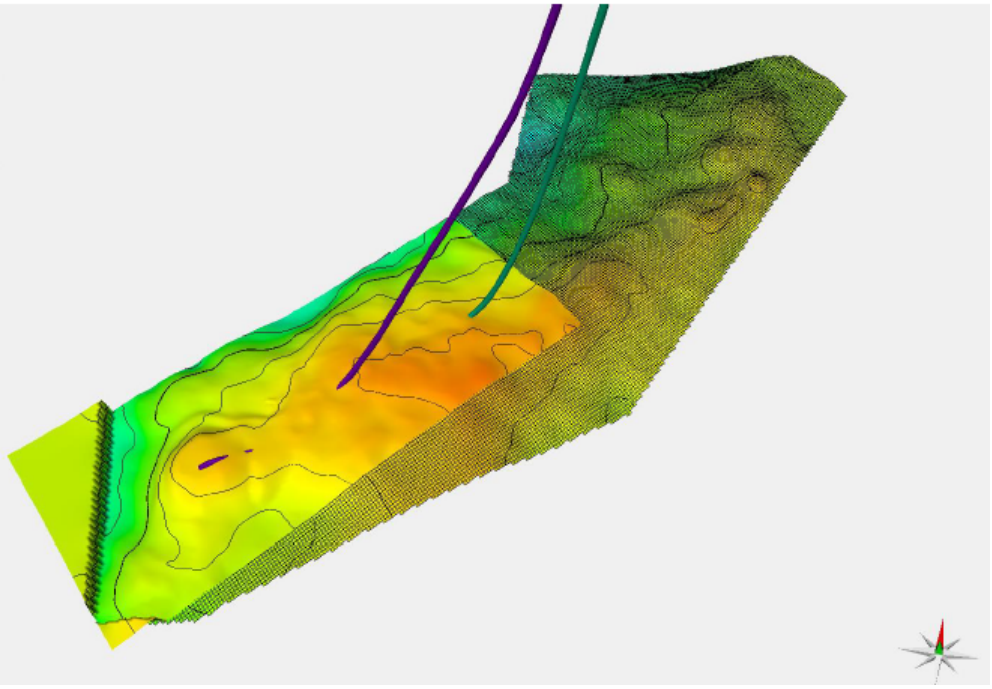

Figure 8.2: The Jette dynamic reservoir model is imposed on top of the geological model, taken from Petrel (Schlumberger 2013c).

The zone of water saturated sands and zone of cap rock are not included in the reservoir model as these will have no influence on reservoir behavior. (Lorentzen 2013)

The model is divided into six stratigraphic layers according to the characteristics of Jette's facies. The layers are seen in **Figure 8.3**.

As written in **Section 6.1** the main facies at Jette are divided into HDT, LDT, green shales and black shales. In the logs it is observed that layer Z1 contains mostly LDT sand, layer Z2 contains mostly HDT sands and also some LDT sands. Heimdal Z5 contains large amounts of black shale, and Ty Upper is a mixture of sands. Layer Z1 and layer Z2 are the most interesting zones as these are above/at the OWC. These observations are implemented in the reservoir model. The different layers are modeled with different values of permeability and porosity, where low values indicate facies of poorer reservoir characteristics and higher values of better reservoir characteristics. Thin layers of shale in between the sands are modeled with zones of lower permeability. The distribution of horizontal permeability is shown in **Figure 8.4**.

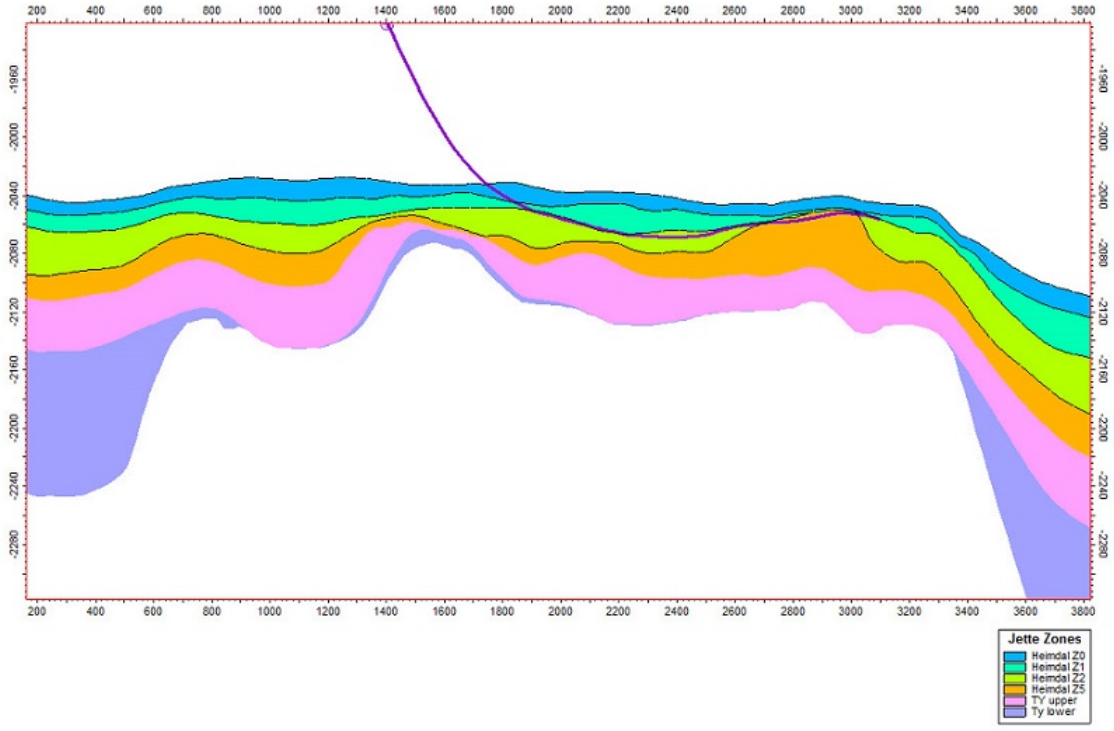

Figure 8.3: Stratigraphic layers in the reservoir model, taken from Petrel (Schlumberger 2013c).

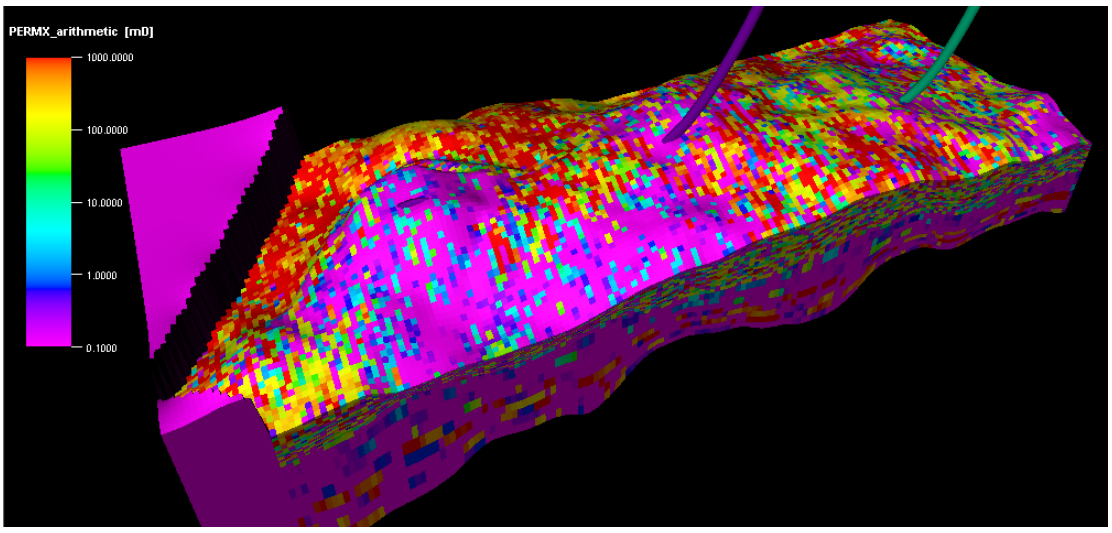

Figure 8.4: Horizontal permeability distribution in the reservoir model, taken from Petrel (Schlumberger 2013c).

Jette was initially assumed to have many faults, but these are not implemented in the model.

8.1.2 Reservoir Properties

The model is initialized with an active aquifer with an OWC at 2091 m TVD. There is no gas cap as the reservoir is estimated to be undersaturated. Bubble point pressure is estimated from the used PVT-model to 170.5 bara, reservoir pressure is 195.9 bar (at 2091 m TVD). See **Table 8.3** for model reservoir properties.

Table 8.3: Model reservoir properties.

Parameter	Unit
Reservoir pressure	195.9 bar
Reservoir temperature	82.9 °C
Bubblepoint pressure	170.5 bar
Oil density	815 kg/m^3
Water density	1,041 kg/m^3
Gas density	1.09722 kg/m^3
Salinity	60,000 mg/l
B_o	1.346 Rm^3/Sm^3
μ_o	0.506 cp
Horizontal permeability	195.8 mD
Vertical permeability	65.7 mD
Porosity	10%

The resulting oil in place from initialization is 5,974,723 Sm^3. The active aquifer is estimated to give good pressure support. Hence, the gas-oil capillary pressure is set to zero. This assumption is valid as almost no gas will evolve in the reservoir due to the reservoir being undersaturated. (Lorentzen 2013)

The model includes two producing horizontal wells, well E-1H and well D-1H. The wells have Vertical Flow Performance (VFP) tables included to account for the flow between reservoir and surface due to production by use of gas lift. The wells are connected to the grid according to the well trajectory entered in the geological model. Well efficiencies are included to be 89.9% the first year of operations and 92.8% after this period. Both wells are producing from layer Z2. The skin factor is set to 0.

8.2 Representation of Jette

The upscaled model was scaled according to the basecase model and not to the Jette production data, hence the model might not represent the real Jette production. **Figures 8.5**, **8.6**, **8.7** and **8.8** show comparisons between the upscaled model and the

real measured data. Figure 8.5 shows the field liquid production rate, Figure 8.6 shows the field oil production rate, and Figures 8.7 and 8.8 show the wells bottom hole pressures. In the upscaled model historic data are used as input to August 2013.

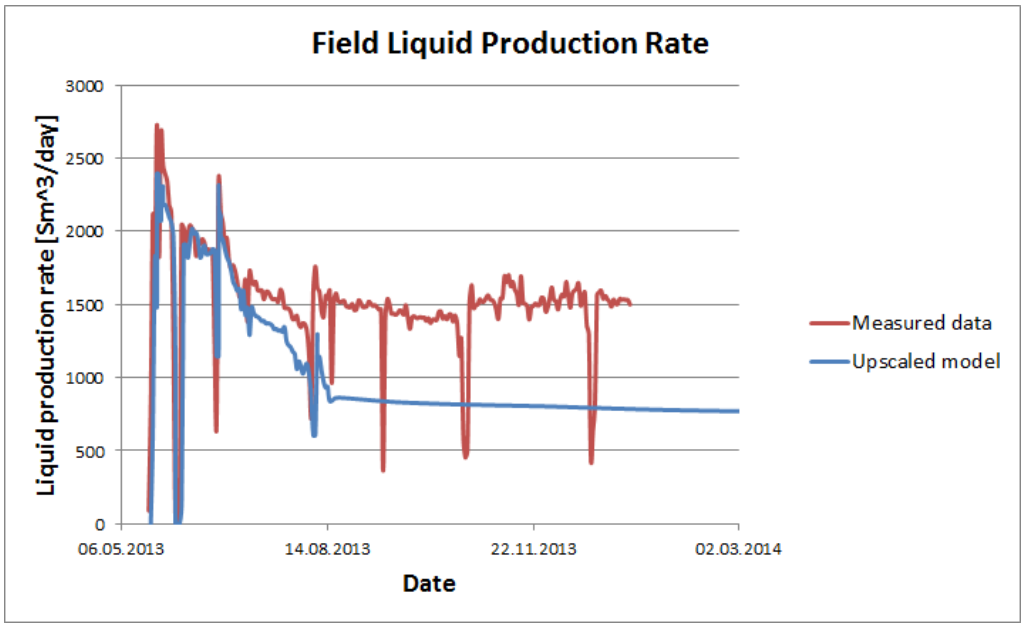

Figure 8.5: A comparison of the field liquid production rate from the upscaled model and the measured data. The upscaled model differs from the measured data.

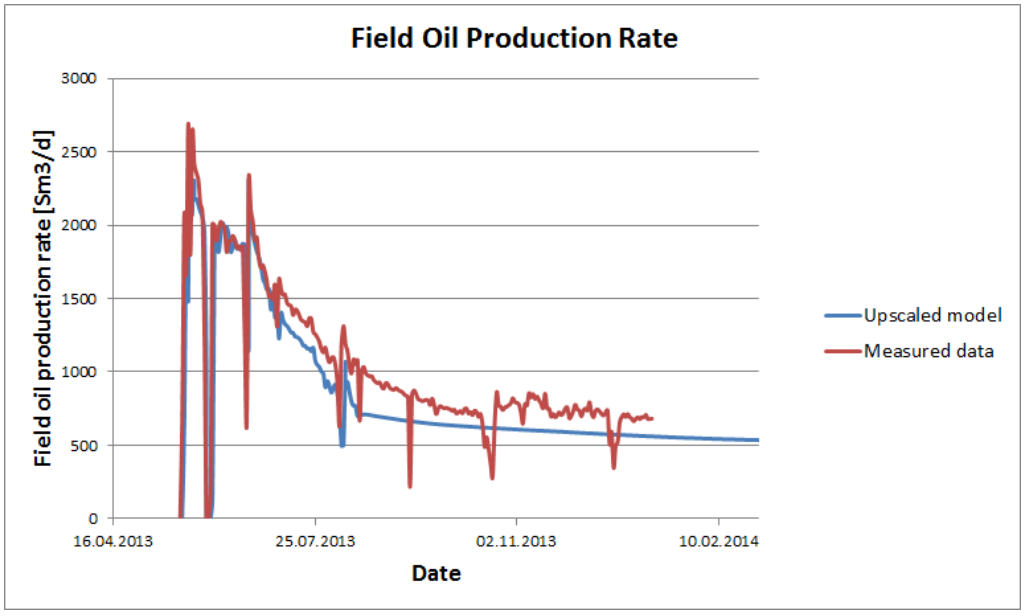

Figure 8.6: A comparison of the field oil production rate from the upscaled model and the measured data. The upscaled model differs from the measured data.

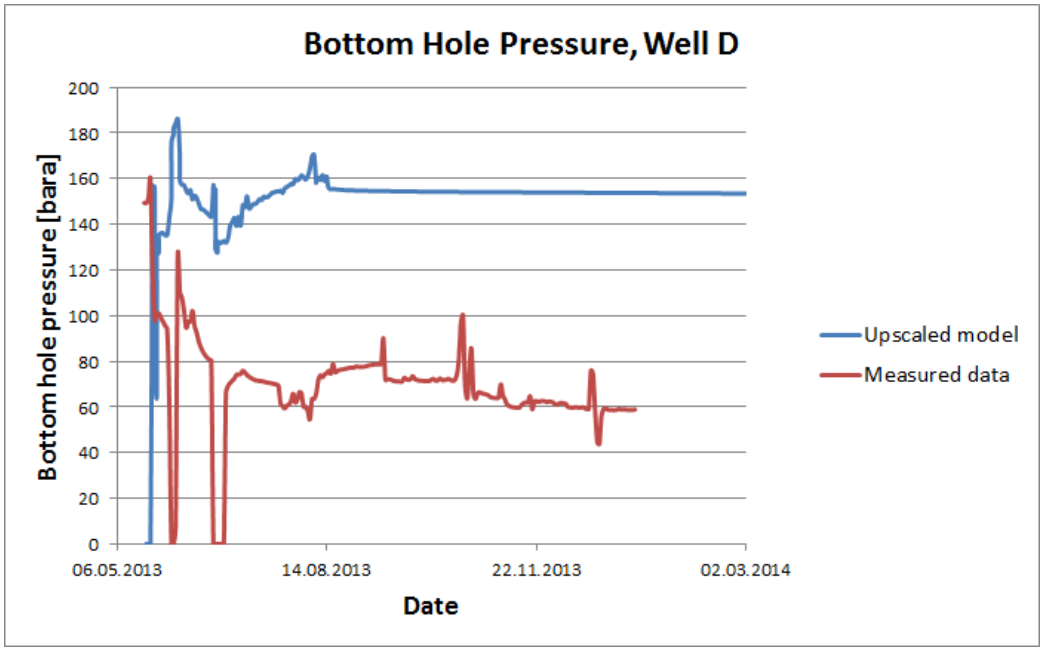

Figure 8.7: A comparison of the bottom hole pressure in Well D from the upscaled model and the measured data. The upscaled model differs from the measured data.

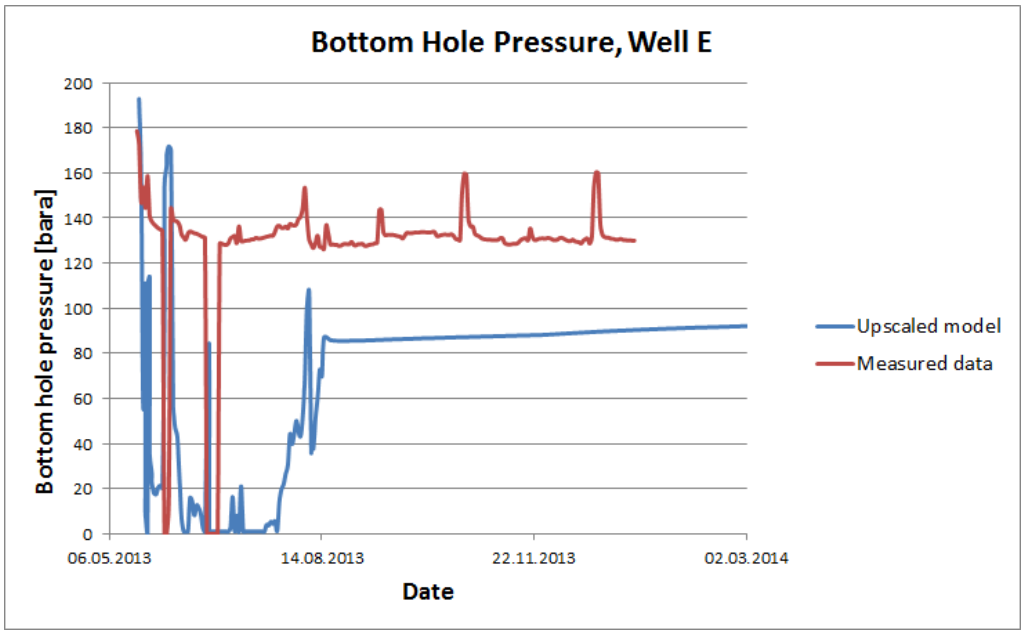

Figure 8.8: A comparison of the bottom hole pressure in Well E from the upscaled model and the measured data. The upscaled model differs from the measured data.

As seen in the plots, it is observed that the results of the upscaled model differs from the measured data, despite historic data as input. It is also observed in the model that Well D

has too low WC in comparison with real production data. This may imply that the model itself is not representable for the Jette field.

8.3 Uncertainties

The current reservoir model is not a good match compared to the observations at the Jette field, and need improvements in initialization before further use. Uncertainties in the model are listed below.

- The permeability of the reservoir is assumed too high. The average horizontal permeability in the upscaled model is 195.8 mD and the average vertical permeability in the upscaled model is 65.7 mD, whereas the estimated horizontal permeability is 13 mD and the estimated vertical permeability is 4 mD, taken from well test analysis.
- The assumed location of the wells in the reservoir may be incorrect. This will be an uncertainty in all simulation models and is not explicit for this model. It may lead to wrong predictions of stratigraphy and geological characteristics, and in production rates.
- The effect of the aquifer may not be representative.
- Geostatistics have been used to populate the grid. This may lead to a wrong distribution of permeability and porosity.
- The PVT model used for the initialization may be incorrect. An incorrect PVT model may contribute to a wrong bubble point pressure and hence, gas in the reservoir.
- The VFP tables for the wells may be incorrect, not giving the right combination of production rates and pressures in the system.

History matching of the model may reduce the uncertainties, and give a model more alike the Jette field.

9 Validation and History Matching

There are ample factors that may affect the estimated cumulative production and production rates found with simulation due to the set-up of the model. The input data used in a model is often subjective and chosen at a certain time where there may not be sufficient data. As these input data may offer great uncertainty, they need to be validated based upon the latest data.

The initial model was found to be a poor reservoir model as compared to the production history of Jette and the development of knowledge. The model does not include faults and fractures, several fluid systems or the depletion of the reservoir around Well D. The initial model is not representative for the Jette field, but an *imaginary* Jette field. Without the new knowledge of the field, the initial model was still found to be too positive with regards to permeability and not representative for the observed production data. In the initial model, the drainage area around Well E, and its productivity, is too pessimistic, and the drainage area around Well D, and its productivity, is too optimistic.

As the initial model was intended to be representative for Jette, the model will be used for future simulations after it is finalized. In order to finalize the model for simulations and reduce the uncertainties, a coarse history match of the upscaled model was performed. In addition to implementing updated PVT data and lift curves, the model has been made more realistic in regards to permeability and productivity of the two producing wells. No changes have been made to the faults, amount of fluid systems or the aquifer support.

9.1 PVT

The original PVT model input in the simulation model is based on a mixture of three Modular formation Dynamics Tester (MDT) samples from pilot well 25/8-17-D-1 H. The mixture was to give a representative average of the oil in place. Data from the original PVT model used to initialize the reservoir model is given in **Table 9.1**.

With a modelled bubble point pressure of 170 bara (in the upscaled model) an inconsistency is observed between the simulated and real production data. The results from the simulation show a higher produced gas rate than what is measured at Jotun B, with the gas lift rate taken into account. Thus, it is likely that the bubble point pressure in the PVT model is too high, which introduces uncertainties in the simulation model.

Table 9.1: Data from the original PVT model from pilot well 25/8-17-D-1 H.

Parameter	Symbol	Unit
Reservoir pressure	p_{res}	195.7 bara
Reservoir temperature	T_{res}	82.9 °C
Bubble point pressure	p_{bp}	172.3 bara
Solution gas-oil ratio	R_{so}	125 Sm^3/Sm^3
Oil Volume Factor	B_o	1.346 Rm^3/Sm^3
Gas Oil Ratio	GOR	90-100 Sm^3/Sm^3
Oil density	ρ_o	691 kg/m^3
Oil viscosity	μ_o	0.399 mPa*s

Other fluid samples taken earlier show a great variation in bubble point pressure and solution gas-oil ratio as seen in Figure 6.13.

The fluid sample from the observation well 25/8-17 was chosen as input in the new PVT model. The mentioned fluid sample is (as of 11.04.2014) one of the most tested samples, that is Constant Mass Expansion (CME) test, viscosity measurement, Differential Liberation Expansion (DLE) and multistage separation test. The main results from the PVT analysis is given in **Tables 9.2**, **9.3**, **9.4** and **9.5**. It is estimated that these tests are more representative as the bubble point pressure is lower and hence, more representative for the production data.

Table 9.2: Single stage separation.

Bottle no.	Sampling depth	GOR	ρ_{STO}	M	Gas gravity
	[m MD RKB]	[Sm^3/Sm^3]	[kg/m^3]	[kg/kgmol]	
TS-101404	2094	87.7	838.6	195.4	0.980

Table 9.3: Constant mass expansion of MDT oil sample.

Bottle no.	T_{RES}	P_{BP}	κ	Viscosity at P_{BP}
	[°C]	[bar]	[bar^{-1}]	mPas
TS-101404	83.6	114.7	$2.048*10^{-4}$	0.518

Table 9.4: Differential liberation expansion.

Bottle no.	R_s	B_o at P_{BP}	ρ_{RESO}	M	Calc. density at P_{BP}
	[Sm^3/Sm^3]	[m^3/Sm^3]	[kg/m^3]	[kg/kgmol]	[kg/m^3]
TS-101404	94.6	1.3678	844	202.3	708.5

The results from the PVT tests were used as input parameters in PVTsim and PVTflex in order to make PVT models to be used in both ECLIPSE and WellFlo. When matching

Table 9.5: Three stage separation.

Bottle no.	GOR/R_s	$B_o at P_{BP}$	ρ_{STO}	M	Calc. density at P_{BP}
	[Sm^3/Sm^3]	[m^3/Sm^3]	[kg/m^3]	[kg/kgmol]	[kg/m^3]
TS-101404	81.9	1.310	836.5	190	710.3

the PVT models the aim is to match the data from the PVT analysis. Description of the work flow in PVTsim and PVTflex can be found in **Appendix F**. Results of the PVT modeling are shown in **Table 9.6**.

Table 9.6: Data from the new PVT model after analysis.

Parameter	Symbol	Unit
Reservoir pressure	p_{res}	196.7 bara
Reservoir temperature	T_{res}	83.6 °C
Bubble point pressure	p_{bp}	117.3 bara
Oil density	ρ_o	816.7 kg/m^3
Oil viscosity	μ_o	0.764 mPa*s
Oil formation volume factor	B_o	1.164 Rm^3/Sm^3

As seen in Table 9.6, the two PVT models are quite similar. The bubble point is the largest change, with a deviation of approximately 60 bar.

9.1.1 Uncertainties

- The fluid sample might not be the most representative for both the wells. If the reservoir is compartmentalized, separating the two producing wells, there may be different fluid parameters for the fluid produced from the two wells.
- As the model is not perfectly identical to the MDT sample, but deviates with some per cents, the new parameters may contribute to further uncertainties during simulation.
- Uncertainties from the analysis of the MDT sample will follow in the PVT model.

9.1.2 PVT Modeling Software

PVTsim

PVTsim (calsep 2013), developed by calsep, is one of the industry's leading PVT simulation packages. PVTsim allows the possibility to combine reliable fluid characterization procedures with robust and efficient regression algorithms to match fluid properties and experimental data. The fluid parameters may be exported to produce high quality input data for reservoir, pipeline and process simulators. (calsep 2008)

PVTsim is compatible with Schlumberger's reservoir simulation software ECLIPSE.

PVTflex

PVTflex software (Weatherford 2012*a*) is a simulation engine based on industry-accepted theory applied to well-defined algorithms which result in the capability to predict the relevant fluid properties. The design of the software enables engineers to develop and manage accurate fluid descriptions which can be shared among other *Field Office* application modules to ensure consistent and improved calculations. That is, PVTflex is compatible with Weatherford's Field Office *WellFlo* software. (Weatherford 2013*a*)

9.2 Lift Curves

VFP tables, or lift curves, in Eclipse offer the most flexible, and potentially the most accurate, means of determining the pressure drop across each segment of the well. Interpolating the pressure drop from a table is considerably faster than calculating it from a multi-phase flow correlation. VFP tables should be constructed for a representative length of tubing at the appropriate angle of inclination, using a suitable multi-phase flow correlation. Standard VFP tables give the BHP as a function of flow rate, the Tubing Head Pressure (THP), the water and gas fractions, and optionally the Artificial Lift Quantity (ALQ) (Schlumberger 2012*b*). VFP tables normally describe the combined effect of friction and hydrostatic pressure losses along the representative length of tubing.

Two new lift curves have been made with the use of the WellFlo modeling tool; one for Well D and one for Well E.

Fluid parameters, reference depth, reservoir characteristics, wellbore deviation and equipment, gas lift data, and surface characteristics have been used as input parameters when building the lift curves in WellFlo. The work flow is described in **Appendix G**. The latest PVT model, described in **Section 9.1**, is used as PVT input.

The lift curves are exported as an ECLIPSE input file. The lift curves will, as earlier mentioned, be used to determine the pressure drop.

9.2.1 Results of New Lift Curves

The lift curves have been validated by a comparison with the original lift curves from Det Norske Oljeselskap. The input data used when comparing the lift curves, and the comparison of the lift curves for Well D are shown in **Figure 9.1**.

As seen in subfigure 9.1a the new lift curves for Well D are more pessimistic than the original lift curves for lower rates. At higher rates, the original lift curves are more pessimistic, contributing to a higher pressure drop.

The comparison of the lift curves, and the input data used when comparing the liftcurves, for Well E are shown in **Figure 9.2**.

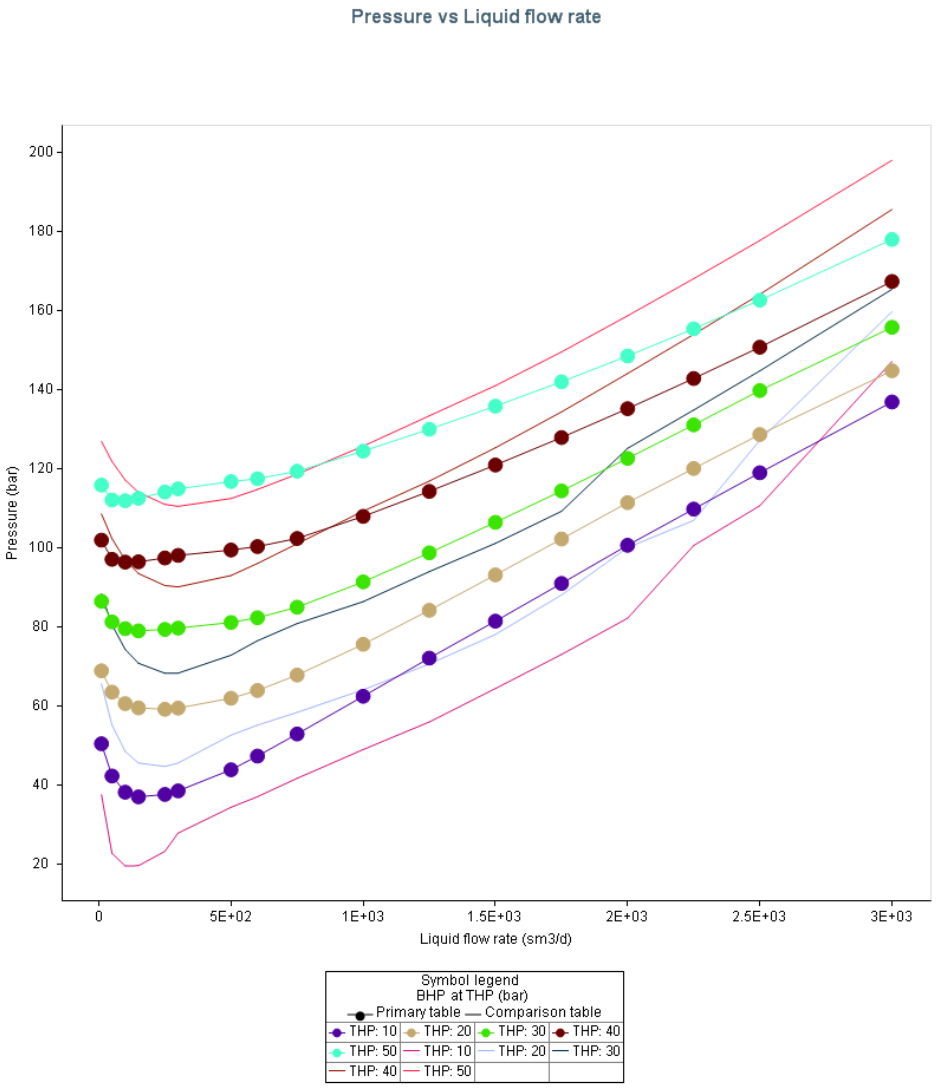

(a) Comparison of lift curves. The primary table is the new lift curve.

Water cut	0.2	sm3/sm3
Gas oil ratio	248.74	sm3/sm3
GRAT	39798	sm3/d

(b) Input data used for comparison.

Figure 9.1: Comparison of the new lift curves and the original lift curves by Det Norske Oljeselskap. Well D. Taken from Petrel (Schlumberger 2013c).

Figure 9.2a shows that the new lift curves for Well E are quite similar to the original lift curves. At the smallest THP the new lift curves are slightly more pessimistic than the original. As the THP normally is higher than that, the most pessimistic curves will not

affect the pressure drop.

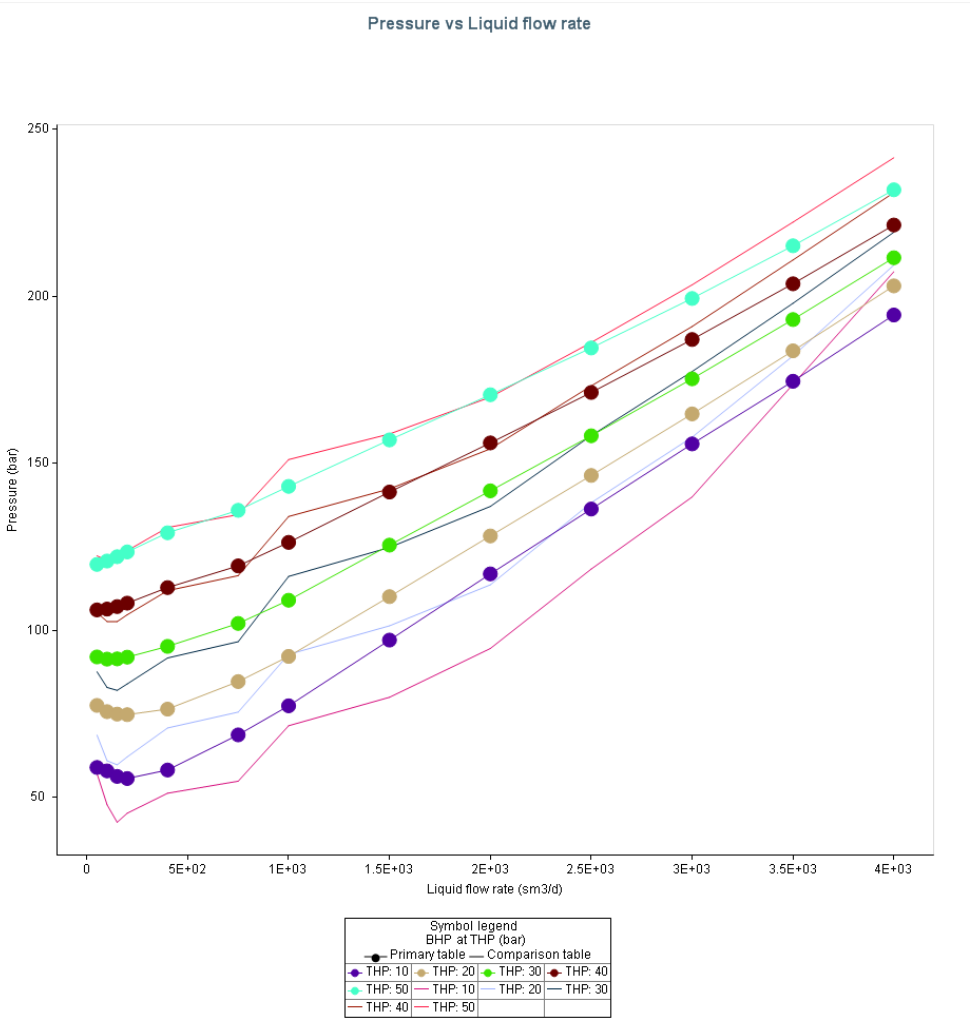

(a) Comparison of lift curves. The primary table is the new lift curve.

Water cut	0.6	sm3/sm3
Gas oil ratio	248.74	sm3/sm3
GRAT	99495	sm3/d

(b) Input data used for comparison.

Figure 9.2: Comparison of the new lift curves and the original lift curves by Det Norske Oljeselskap. Well E. Taken from Petrel (Schlumberger 2013c).

The pressure drop in both wells calculated with the new lift curves also corresponds well with the pressure drop calculated with the mechanical flow equation for pipelines.

9.2.2 Validation of New Lift Curves

In ECLIPSE, the lift curves will be used to calculate the BHP in both wells, while the THP is the constraint. With a fixed THP at 30 bara the new and the original lift curves have been compared in regards to BHP, total oil production and liquid production rate. See **Figures 9.3** and **9.4**.

Figure 9.3: Comparison of the new lift curves and the original lift curves by Det Norske Oljeselskap. Well D. The black lines show the BHP, the blue lines show the liquid production rate and the red lines show the total oil production.

The original lift curves for Well D give higher pressure drop in the wellbore, leading to a lower calculated BHP (at 01.01.2020 22.6% lower). This leads to greater liquid production rate, and greater total oil production. The original lift curve for Well D is more pessimistic than the new according to pressure drop, but more positive in regards production, see Figure 9.3.

For Well E, the lift curves are quite similar giving production results with small deviation, see Figure 9.4. The BHP in the new lift curves, at 01.01.2020, is 1.0% lower than for the original lift curves. The total oil production, while using the new lift curves, is 0.8% higher.

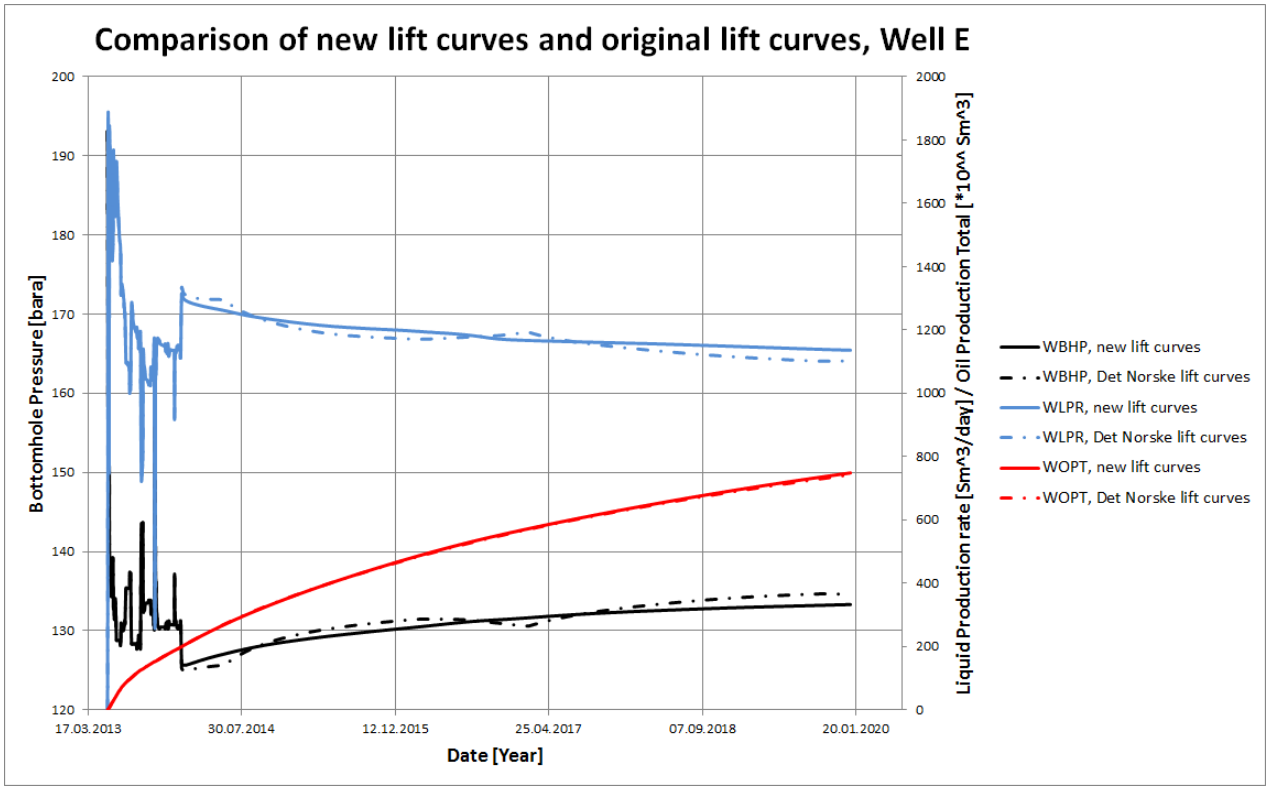

Figure 9.4: Comparison of the new lift curves and the original lift curves by Det Norske Oljeselskap. Well E. The black lines show the BHP, the blue lines show the liquid production rate and the red lines show the total oil production.

9.2.3 Uncertainties

- The implementation of the models in WellFlo may be too simplified, hence not representative for the real case.
- The input parameters from the multi-rate tests may be uncertain, leading to propagating uncertainties in the model.
- WellFlo might carry uncertainties as it follow certain correlations.
- The measurement of the production data may be uncertain due to uncertainties in flow measurement devices.
- The friction factor in the wells may differ, giving uncertainties in pressure drop due to friction.
- The PVT model may not be representative. Uncertainties from the PVT model will follow in the calculations of the pressure drop from the lift curves.

9.2.4 Lift Curve Modeling Software

WellFlo

Weatherford's Field Office WellFlo software (Weatherford 2012*b*) is a well-modelling application with design and analysis features for both naturally flowing and artificially-lifted wells (Weatherford 2013*b*). It incorporates calculations for multiphase flow through pipes, restrictions and other well components such as completions, pumps and gas-lift valves. The software supports an extensive catalogue of well equipment including tubing, casing, gas-lift valves, motors, cables, ESP and Progressing Cavity Pumps (PCP) from various manufacturers. (Weatherford 2013*b*)

9.3 History Matching of Model

As the model is not representative for the Jette field, a coarse history matching process has been performed in order to better represent the well's production history. In addition to implementing a new PVT model and lift curves, the permeability around the wells and the well productivity have been controlled by the use of multipliers. The alterations have been made in ECLIPSE. The history match is described below.

- A new PVT model, as described in Section 9.1, was implemented.
- New lift curves for the two horizontal wells were implemented. The lift curves are described in Section 9.2.
- Well E was found to be too pessimistic from the simulation model. In order to increase its production both the horizontal and vertical permeability in the sands around Well E were doubled by the use of permeability multiplier. The productivity of the well was increased with the use of the keyword $WPIMULT$.
- It was indicated in the production history in Section 6.6 that parts of Well D is blocked, non-producing intervals. Parts of the well was cleaned in October 2013 by a rough start-up following a shut-in, giving a better production. This measure was implemented in the completion data of the well, and is observed by the small "peak" in production in October 2013, see **Figure 9.9**. The well was initially completed down to the second swell packer (2546 m MD RKB), and opened up down to the third swell packer (2821 m MD RKB) in October 2013.
- Well D was found to be too optimistic from the simulation model. In order to decrease its production both the horizontal and vertical permeability in the sands around Well D were halved by the use of a permeability multiplier. The productivity of the well was decreased with the use of the keyword $WPIMULT$.

Figures 9.5, **9.6**, **9.7** and **9.8** show comparisons of the field liquid production rates, the field oil production rates, and the bottom hole pressures in Well D and Well E, between the

upscaled model, the history matched model and measured data. In the history matched model historic data are used until January 2014. The production is constrained by THP, which is considered to be the least varying parameter.

A good match of the field liquid production rate is observed in Figure 9.5. The rate from the history matched model is slightly pessimistic compared to the measured data which may, indicated from Figure 9.6, be caused by low WC. Figure 9.6 indicates a too positive oil production rate as compared to the measured data. The bottom hole pressures, seen in Figures 9.7 and 9.8, are almost spot on. This is expected as the model is controlled with BHP in the historic period. Water production is not matched.

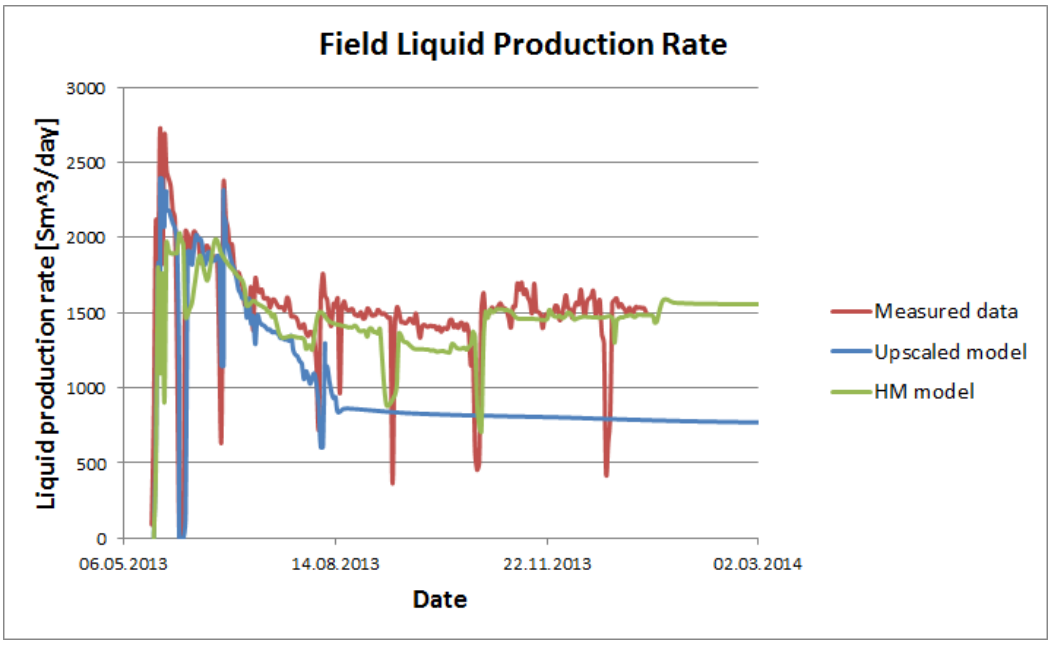

Figure 9.5: A comparison of the field liquid production rate of the measured data, the upscaled model and the history matched model.

It is observed that the history matched model gives a better match given the measured data than the upscaled model. The deviation in drawdown is found to be $\pm$ 10%; qualifying to be a coarse history match, making the model usable for further simulations. As the match is considered to be sufficient given the constraints of model quality, the history matched model will be used in future simulations in this thesis. It should be noted that as the model do not, given the production history and findings, represent the Jette field any more, the following IOR measures simulated with this model will be assumed to represent a *Jette X* case.

Figure 9.9 and **Figure 9.10** show the production data of the new basecase model when simulated to 01.01.2020. The production data are given for Well D and the field.

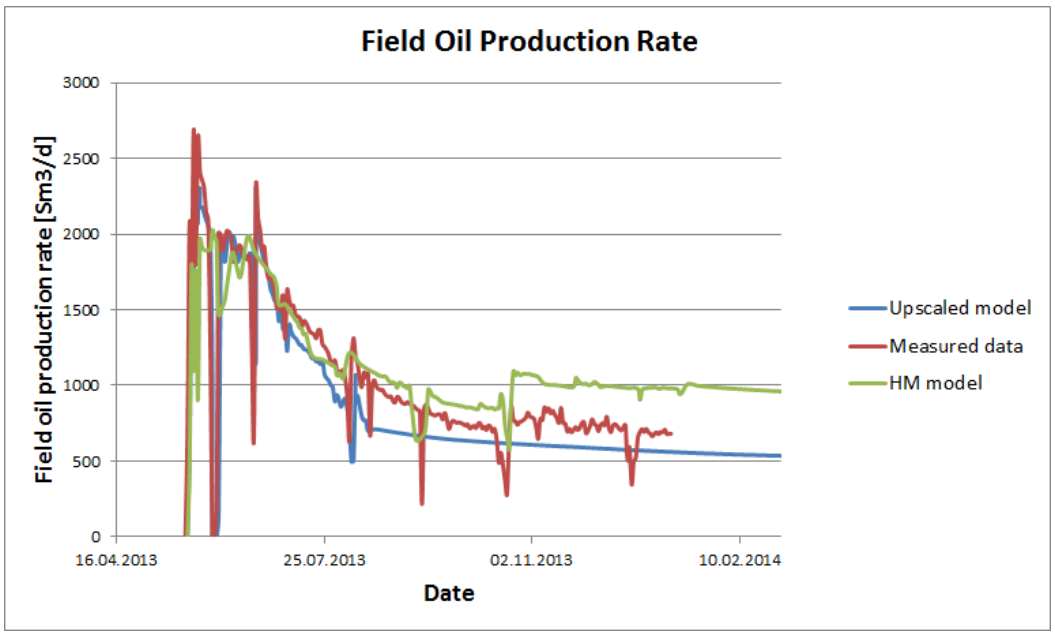

Figure 9.6: A comparison of the field oil production rate of the measured data, the upscaled model and the history matched model.

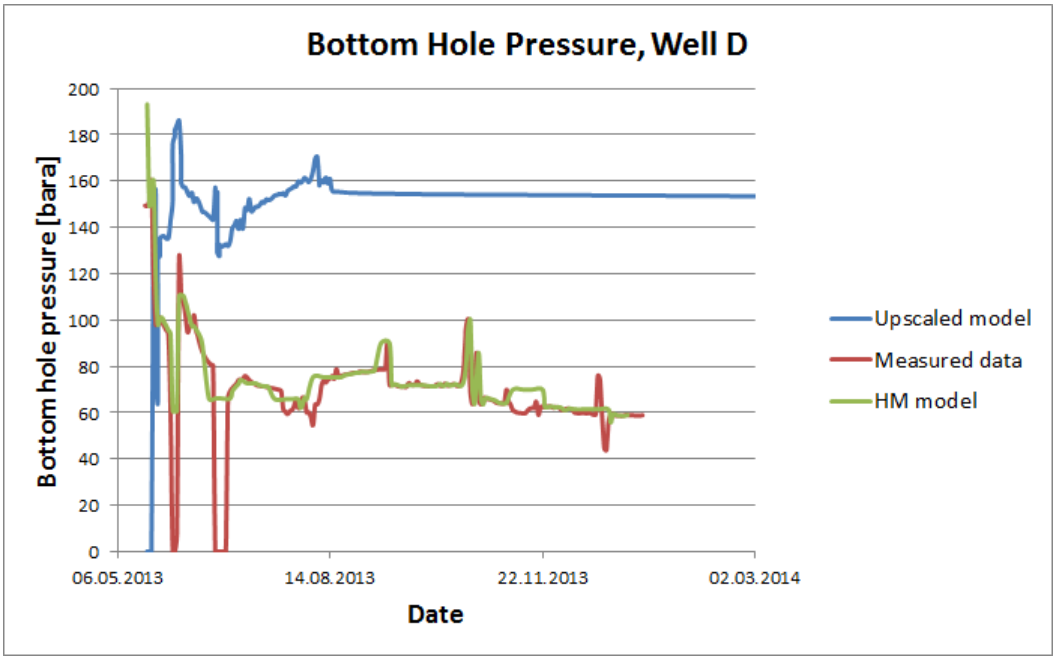

Figure 9.7: A comparison of the bottom hole pressure in Well D of the measured data, the upscaled model and the history matched model.

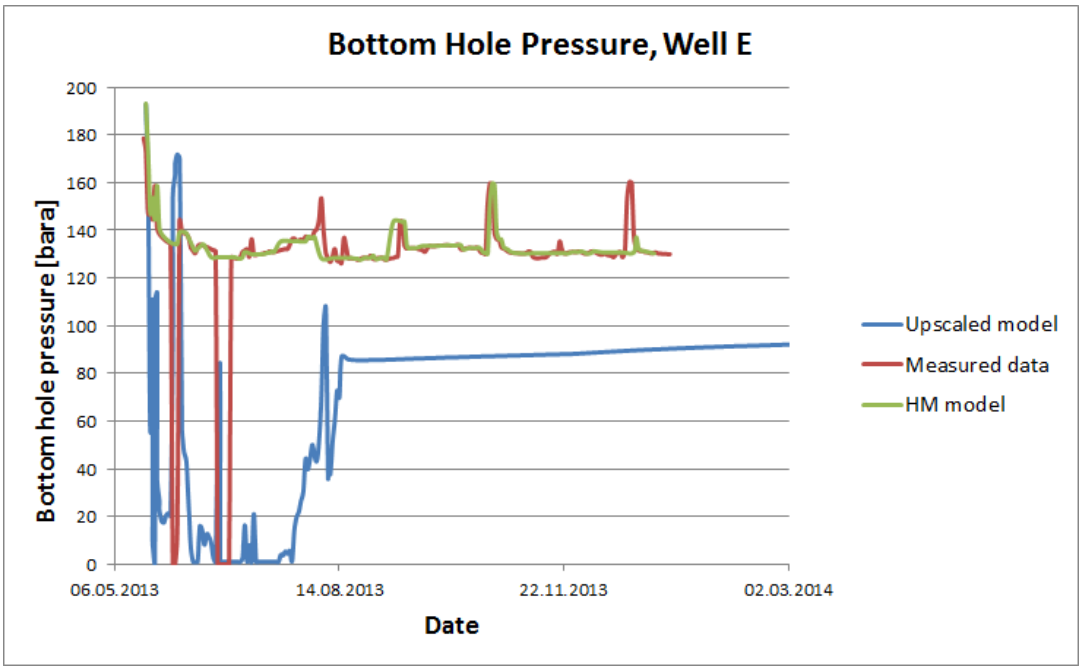

Figure 9.8: A comparison of the bottom hole pressure in Well E of the measured data, the upscaled model and the history matched model.

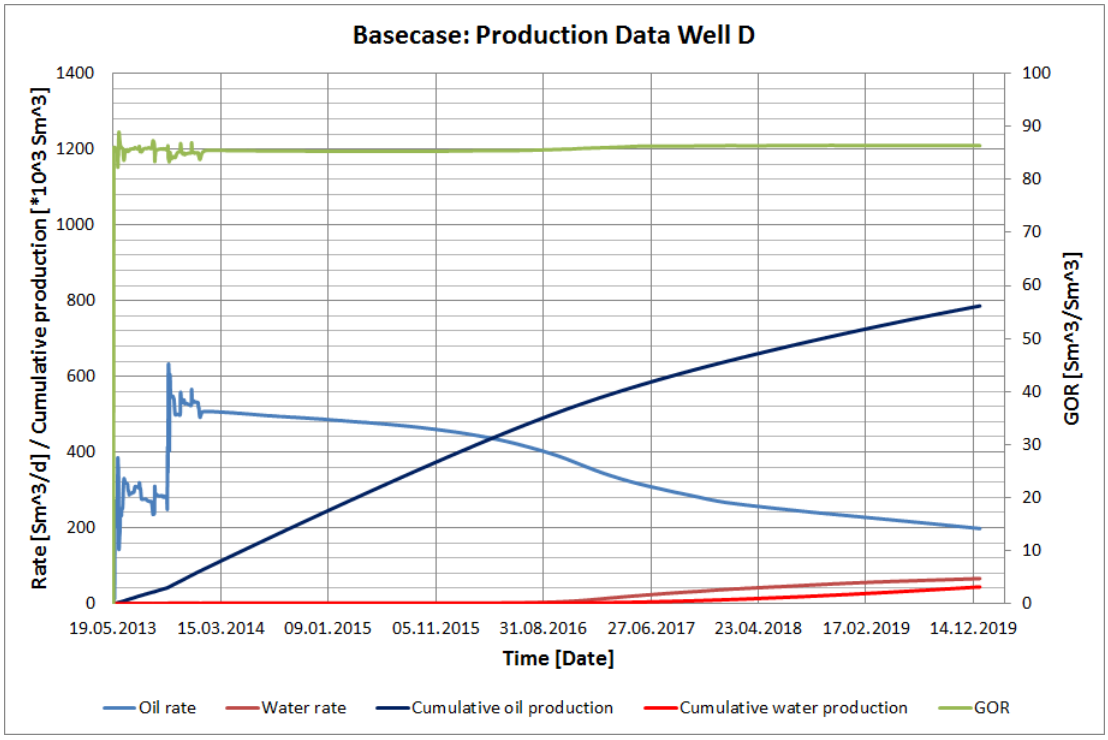

Figure 9.9: Oil rate, water rate, GOR, cumulative oil production and cumulative water production for the basecase model of Well D.

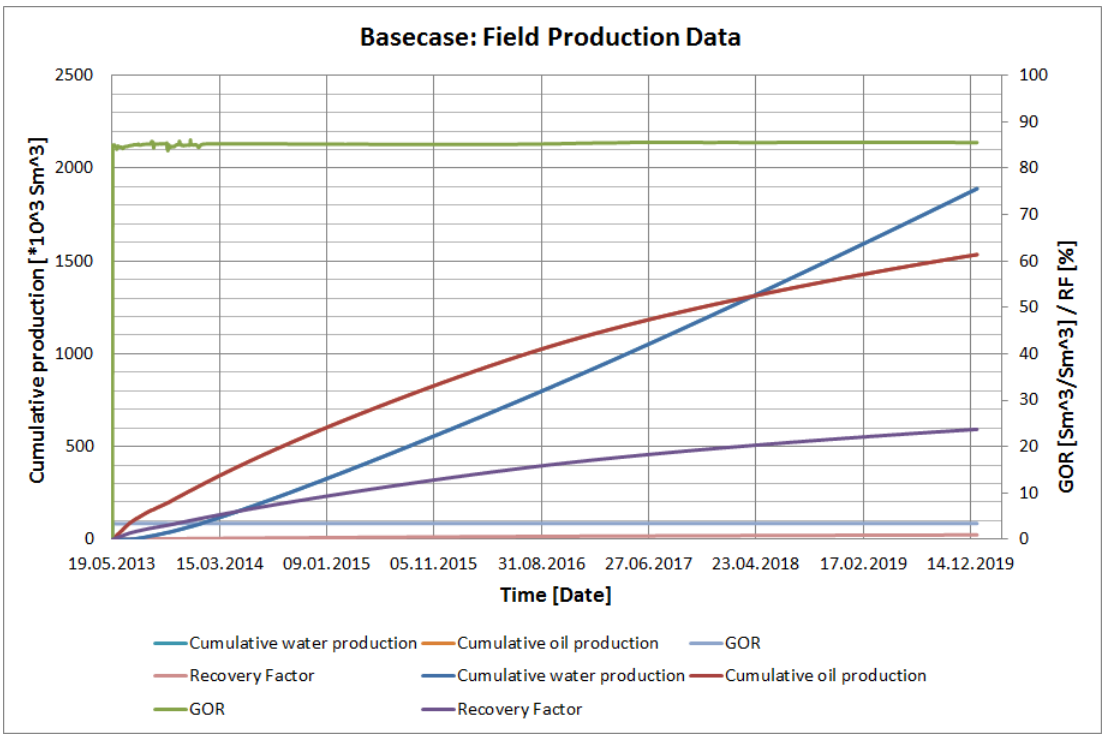

Figure 9.10: GOR, recovery factor, cumulative oil production and cumulative water production for the basecase model of the field.

10 Well Design

The evaluation of the productivity in Well D indicates a need for implementing improved oil recovery operations. In **Section 7.10** the well intervention operations, described in **Section 5.2**, were evaluated for Well D. The evaluation indicates that infill drilling and acidizing may improve the PI of the well. Multilaterals may increase the reservoir-to-well exposure, improving the drainage area of the wells. Acidizing may clean the well, giving longer inflow area to the well.

The laterals are designed in Petrel (Schlumberger 2013*c*). The procedure is described in **Appendix H**. The only alteration regarding the laterals in the input files for simulation are in the file with completion data.

The focus in the design of the wells have been on the well path in the reservoir layers itself, and not outside the reservoir layers. The well path from the main well to the connections in the reservoir layers may be different than what is shown in the following figures.

10.1 Reservoir Properties and Drilling Targets

The targeted sands around Well D, layer Z1 and Z2, are estimated to have net pay thicknesses of 1-8 m. Shale intervals are observed in the sands. In terms of thicknesses, the main targets seem to be quite narrow.

The ability to hit these targets depend on good stratigraphic control, a reliable geomodel and the accuracy of directional surveying while drilling. Keeping the well within the pay intervals throughout the whole length of the reservoir section may be a challenge. An overall risk evaluation will evaluate the uncertainties.

As it is indicated that the reservoir consists of several compartments and fluid systems having different reservoir pressures, the possibility of drilling into depleted zones involves an extra wellbore instability risk during drilling. Depletion of the reservoir will magnify both the effective stresses acting around the borehole as well as the stress anisotropy. Normally depletion and induced stress changes lead to a greater risk of borehole failure both in terms of collapse and induced fracturing. (Nakken et al. 2010)

Depletion calls for a lower mud weight and/or Managed Pressure Drilling (MPD) systems, to be used to avoid formation damage due to filtrate invasion. However, due to the stress

alterations the necessary reduction in mud weight may not be permissible due to the increase in effective stresses and their anisotropy. Consequently, depletion narrows the applicable mud weight window. (Nakken et al. 2010)

Reservoir depletion also increases the risk of sand production and may thus limit well productivity either through flow restrictions induced by sand control measures or by sand-free rate limitations for perforated liner completions (Nakken et al. 2010). The low permeability around Well D, and its high drawdown, increases the risk of sand production.

10.1.1 Targets

The targets for the multilaterals are shown in **Figure 10.1**. The zones with the most oil accumulation, that is being the most attractive targets, are situated towards the north, west and east of Well D.

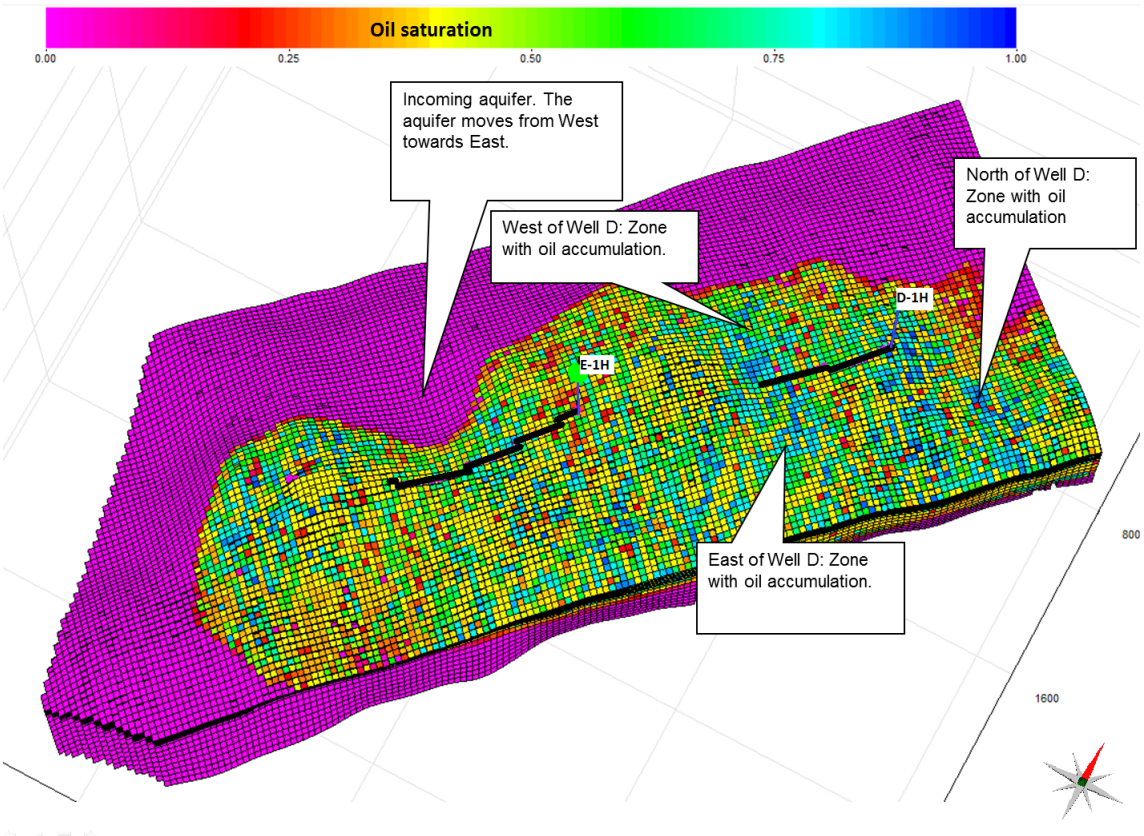

Figure 10.1: The figure shows the oil saturation at Jette and possible targets. The aquifer moves from west towards east. Taken from S3GRAF (Sciencesoft 2013).

In order to maximize pay zone exposure and avoid premature water break-through, it is important to maintain distance to the OWC, placing the wells high up in the layers and

also with distance to the active aquifer coming from west.

10.2 Drilling and Completion

Zones with high oil accumulation were targeted when designing multilaterals. Two wells with a single lateral were designed, north of Well D and east of Well D, and two multilaterals were designed. The two multilaterals are east of Well D and west of Well D.

When making the multilateral wells, side-tracks are drilled from the original well. In order to make the multilaterals, the tubing in Well D has to be pulled followed by placing a whipstock. The side-tracks are kicked off in another direction. Perforating the whipstock afterwards opens up Well D for production.

TTDC is not possible for Well D as the tubing is 5 1/2 in. only. The small size of the tubing makes it impossible to drill through, and still obtain a hole of sufficient size [1].

10.2.1 Well Completion

The proposed well completions are based on experience from the Jette production wells and other subsea wells. The objective is to make the well design as simple as possible. Different completion solutions have been considered as shown in **Appendix I**. The different completion options are openhole completions with screens and swell packers (like the completion of Well D), a barefoot completion, and a cemented and perforated liner completion. The suggested completion options and completion sketches are made simple meant to serve as options and illustrations. The technicalities regarding the completions are not the main focus.

Case 1: Single Lateral North

Oil accumulation was shown north-east of Well D, see Figure 10.1, which has been estimated to be a good area for a lateral. In order to maximize pay zone exposure and avoid premature water break-through, the lateral was placed high up, in layer Z1. It is not expected to experience early water break-through from the aquifer, as the aquifer is coming in from the west. **Figure 10.2** shows the location of the lateral relative to Well D. **Figure 10.3** shows the lateral and Well D relative to each other, seen from the east side.

The well is assumed to kick-off from Well D in the 9 5/8 in. casing, below the gas lift mandrel and P/T-gauge. The length of the lateral in the reservoir section is 700 m, with the last point at 3176.4 m MD RKB.

[1] Personal communication with Jafar Abdollahi. April 2014. Trondheim: Weatherford Petroleum Consultants AS

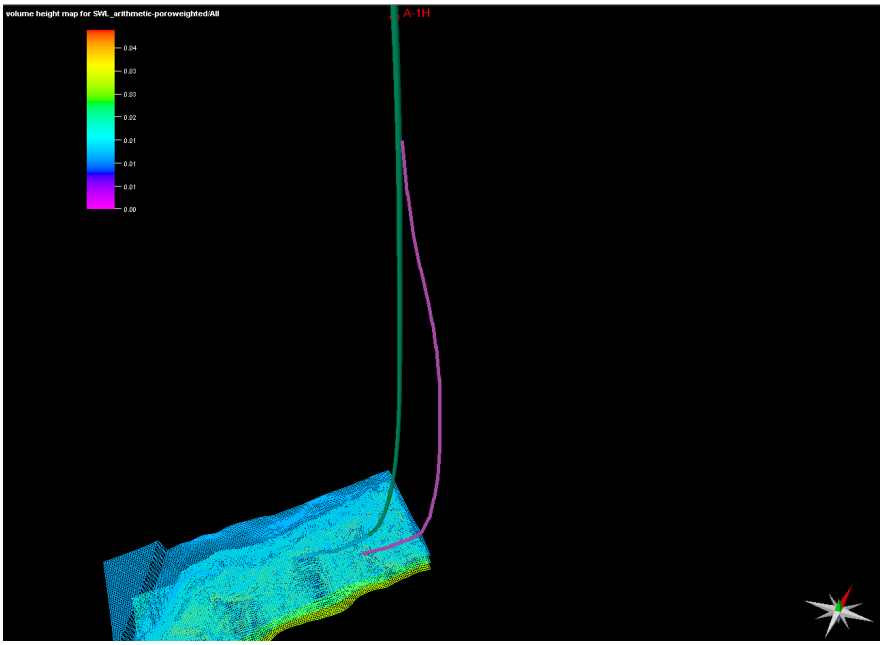

Figure 10.2: The location of the lateral towards north (purple well) relative to Well D, viewed from the top. The side-track is kicked-off from Well D. Taken from Petrel (Schlumberger 2013c).

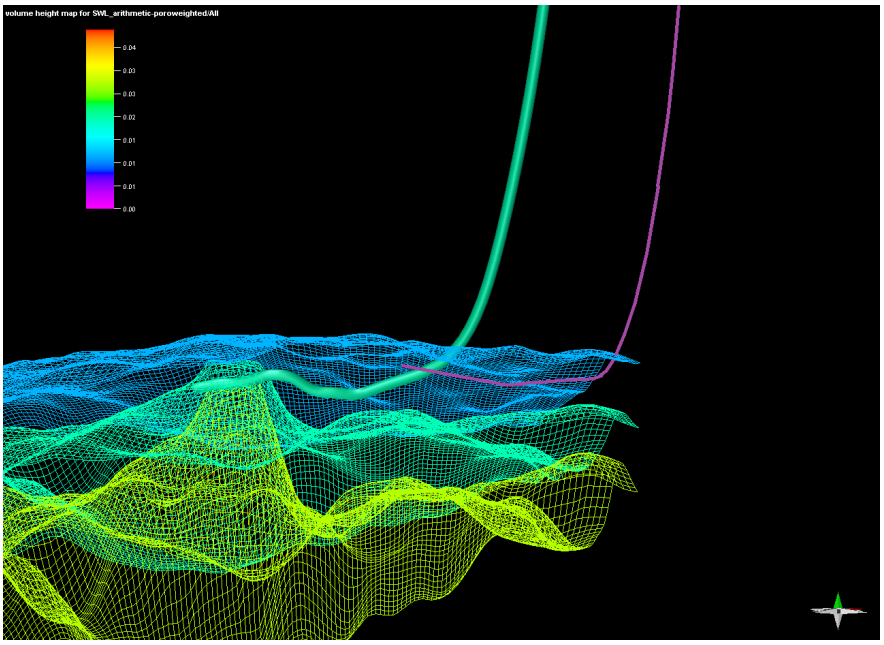

Figure 10.3: The location of the lateral towards north (purple well) relative to Well D, viewed from the side. The lateral is located high up in the productive layers. Taken from Petrel (Schlumberger 2013c).

Case 2: Single Lateral East

Oil accumulation was shown east of Well D, see Figure 10.1, which has been estimated to be a good area for a lateral. In order to maximize pay zone exposure and avoid premature water break-through, the lateral was placed high up, in layer Z1. It is not expected to experience early water break-through from the aquifer, as the aquifer is coming in from the west. **Figure 10.4** shows the location of the lateral relative to Well D. **Figure 10.5** shows the lateral and Well D relative to each other, seen from the east side.

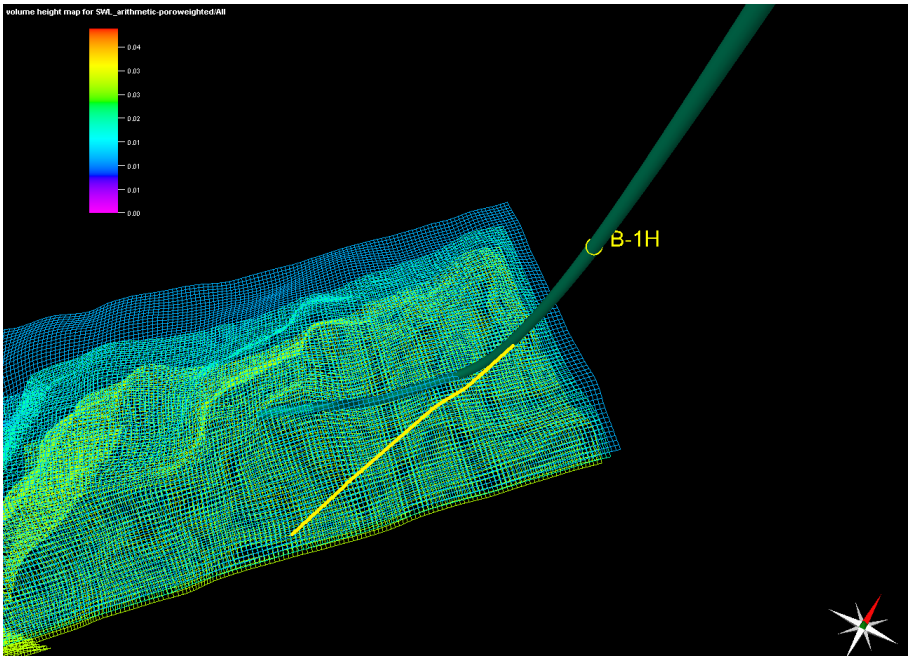

Figure 10.4: The location of the lateral towards east (yellow well) relative to Well D viewed from the top. The side-track is kicked-off from Well D. Taken from Petrel (Schlumberger 2013c).

The well is assumed to kick-off from Well D in the 9 5/8 in. casing, below the gas lift mandrel and P/T-gauge. The length of the lateral in the reservoir section is 1100 m, with the last point at 3568.7 m MD RKB.

Two completion options are suggested for Case 1 and Case 2, described below.

Option 1: New lateral completed as original Well D; standalone metal mesh sand screens, ICD's and swell packers.

Option 2: New lateral completed with a cemented and perforated liner.

Option 1 is assumed to be the best choice as sand production is recognized as a challenge in the production. High drawdown and low permeability contributes to sand production. See Appendix I for completion sketches.

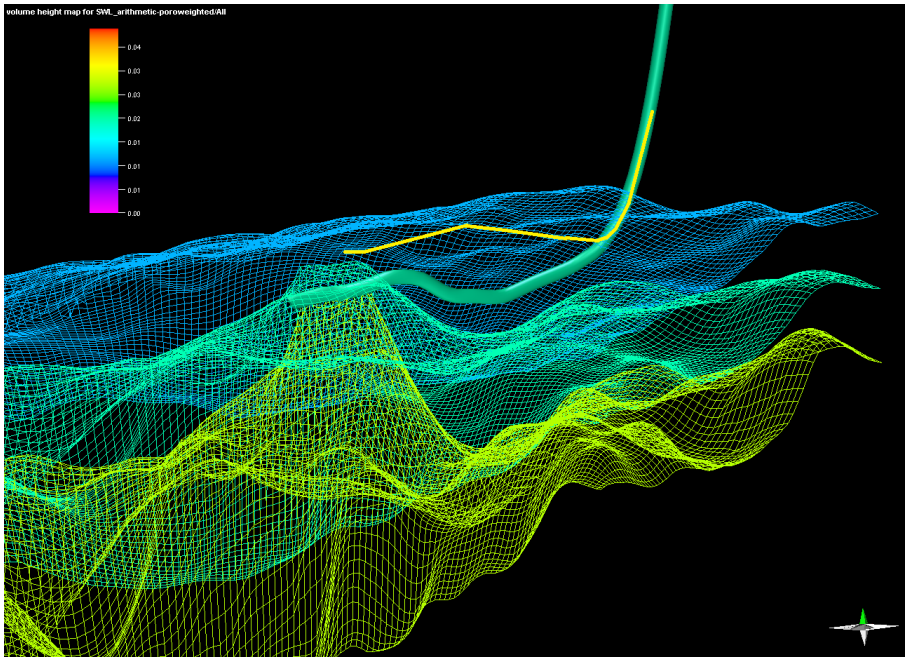

Figure 10.5: The location of the lateral towards east (yellow well) relative to Well D, viewed from the side. The lateral is located high up in the producing layers. Taken from Petrel (Schlumberger 2013c).

Case 3: Multilateral East

As mentioned previously, the area east of Well D has been estimated to be a good area for a side-track due to oil accumulation. A multilateral was designed to penetrate this area, with one lateral in layer Z2 and one lateral in layer Z1. **Figure 10.6** shows the location of the multilateral relative to Well D. **Figure 10.7** shows the multilateral and Well D relative to each other, seen from the north and in open space. As seen in Figure 10.7 the well closest to Well D is in layer Z1 while the well furthest away from Well D is in layer Z2. The lateral in layer Z1 is completed in ECLIPSE as the longest of the two laterals.

The wells are assumed to kick-off from Well D in the 9 5/8 in. casing, below the gas lift mandrel and P/T-gauge. The length of the lateral placed in layer Z1 is 1000 m, with the last point at 3533.6 m MD RKB. The length of the lateral placed in layer Z2 is 300 m, with the last point at 3697.3 m MD RKB.

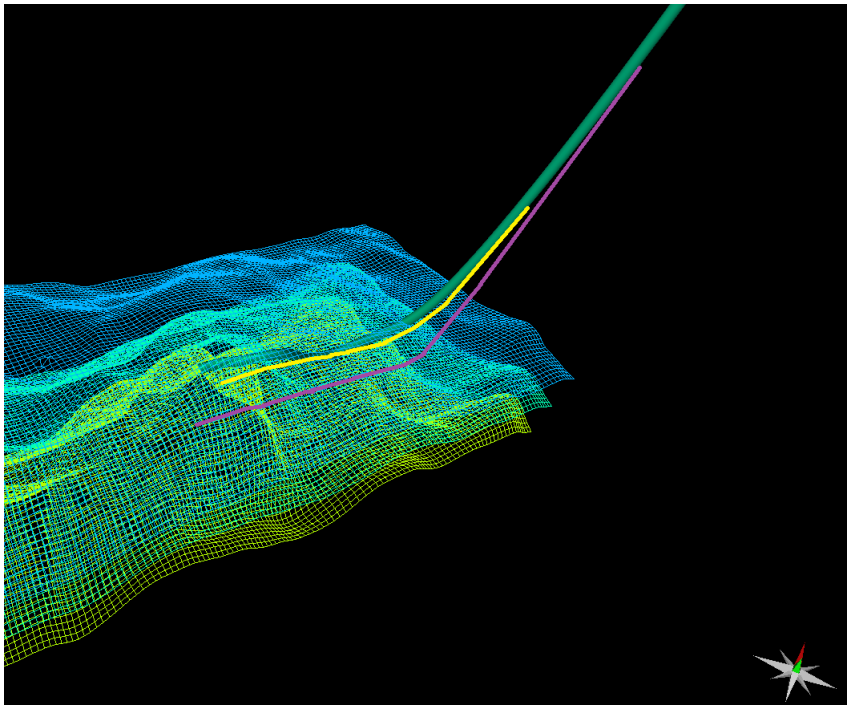

Figure 10.6: The location of the two side tracks towards east relative to Well D viewed from the top. The well pictured with a yellow line is situated in layer Z1, while the well pictured with a purple line is situated in layer Z2. Taken from Petrel (Schlumberger 2013c).

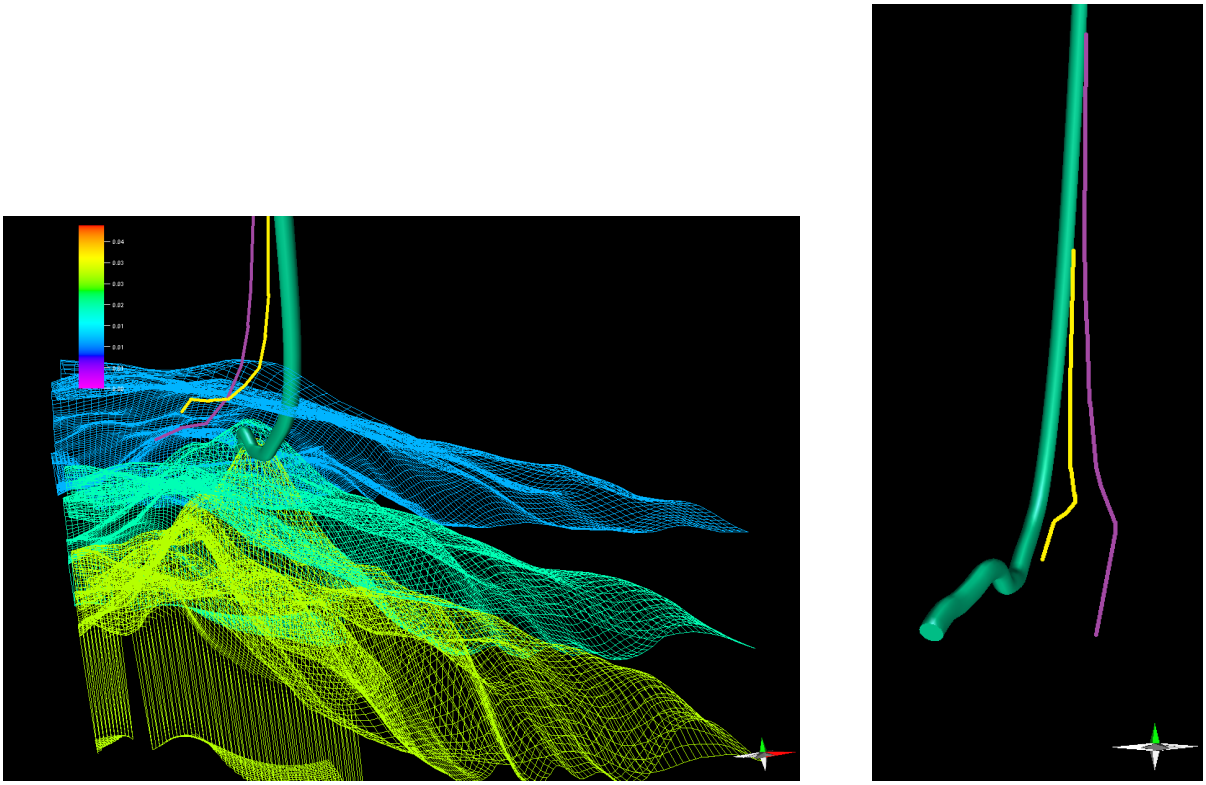

(a) Side view. *(b) Open space-view.*

Figure 10.7: The location of the two laterals towards east relative to Well D. The well pictured with a yellow line is situated in layer Z1, while the well pictured with a purple line is situated in layer Z2. Taken from Petrel (Schlumberger 2013c).

Case 4: Multilateral West

A good area for production, with sufficient oil accumulation, was shown west of Well D. The oil zone is close to the incoming water aquifer, leading to a greater risk of early water break-through. A multilateral was designed to penetrate this area, with one lateral in layer Z2 and one lateral in layer Z1. **Figure 10.8** shows the location of the multilateral relative to Well D. **Figure 10.9** shows the multilateral and Well D relative to each other, seen from the north and in open space. As seen in Figure 10.9 the well closest to Well D is in layer Z1 while the well furthest away from Well D is in layer Z2. The lateral in layer Z1 is completed in ECLIPSE as the longest of the two laterals.

The wells are assumed to kick-off from Well D in the 9 5/8 in. casing, below the gas lift mandrel and P/T-gauge. The length of the lateral placed in layer Z1 is 1000 m, with the last point at 3806.6 m MD RKB. The length of the lateral placed in layer Z2 is 300 m, with the last point at 3320.3 m MD RKB.

For both Case 4 and Case 5 the deepest lateral will be drilled first, followed by the lateral

in layer Z1. The suggested completion solutions for the multilaterals are mentioned below.

Option 1: Both laterals are completed with the same type of completion as Well D; standalone metal mesh sand screens, ICD's and swell packers.

Option 2: Both laterals are completed with a cemented and perforated liner.

Option 3: The deepest lateral is completed with the same type of completion as Well D, and the shallowest with a barefoot completion. Sand screens and packers are installed by the kick-off point of the shallowest lateral in Well D.

Option 4: The deepest lateral is completed with a cemented and perforated liner, and the shallowest has a barefoot completion. Sand screens and packers are installed by the kick-off point of the shallowest lateral in Well D.

A barefoot solution is the least expensive choice, but suffers the disadvantage that the sandface is unsupported and may collapse. The first and third completion options are considered to be the best choices as sand production is recognized as a challenge in the production. See Appendix I for completion sketches.

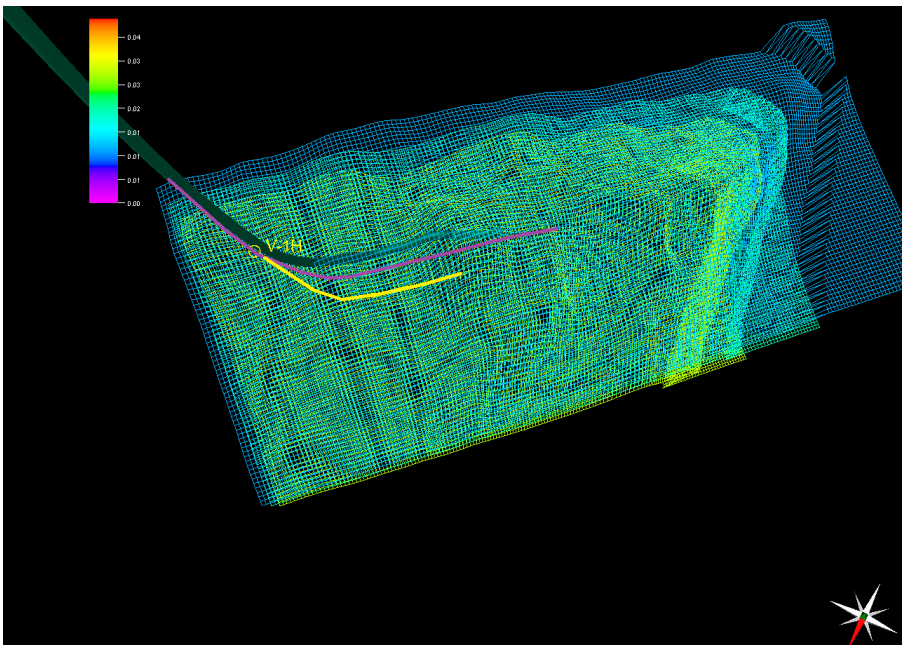

Figure 10.8: The location of the two side tracks towards west relative to Well D viewed from the top. The well pictured with a purple line is situated in layer Z1, while the well pictured with a yellow line is situated in layer Z2. Taken from Petrel (Schlumberger 2013c).

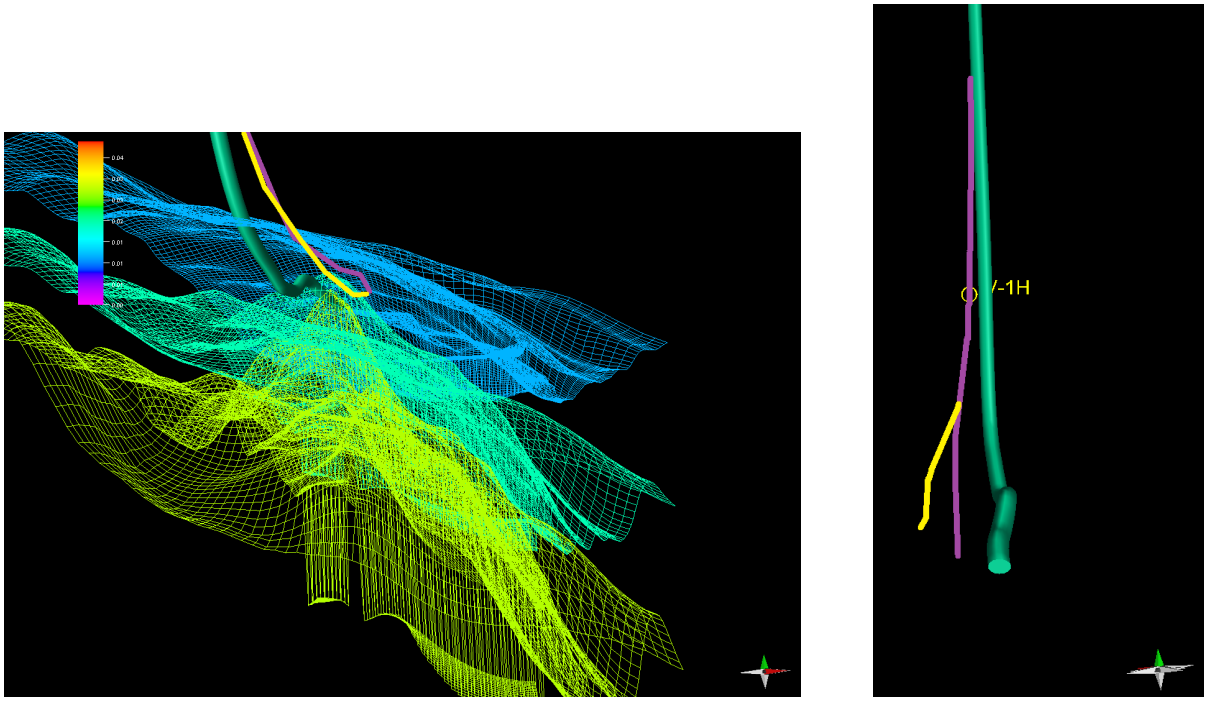

(a) Side view. *(b) Open space-view.*

Figure 10.9: The location of the two laterals towards west relative to Well D. The well pictured with a purple line is situated in layer Z1, while the well pictured with a yellow line is situated in layer Z2. Taken from Petrel (Schlumberger 2013c).

11 Implementing And Simulating Well Intervention Measures

The unfortunate design of the production system, with a 8 in. pipeline connected to a 12 in. riser, may lead to severe slugging and pressure fluctuations, and cause significant loss in production. The 12 in. riser is further connected to an 8 in. piping topside Jotun B which makes the design more unfortunate. To overcome, or reduce, the effect of slugging a replacement of the 12 in. riser with a 8 in. riser was simulated. Opening the entire well length, single-laterals, multilaterals and acidizing are measures of well intervention which have been implemented and simulated.

When simulating ECLIPSE uses average values over a longer interval of time to save time. This leads to the fact that ECLIPSE is not able to properly simulate the pressure differences in the riser when changing from 12 in. riser to 8 in. riser. Due to errors in the lift curves for pipelines found in the WellFlo program, the replacement of riser can not be simulated in WellFlo either. OLGA, being a transient simulation tool, is able to resolve the flow changes in wells and pipelines with time. The well intervention measures are simulated with the use of ECLIPSE 100, and the slugging effects in the pipeline are simulated with the use of OLGA.

11.1 Simulation Cases

11.1.1 Case 1: Single Lateral North

A side-track to Well D was designed to drain the area north of Well D. See Figures 10.2 and 10.3. The lateral is placed high up, in layer Z1, to avoid premature water break-through.

11.1.2 Case 2: Single Lateral East

A side-track to Well D was designed to drain the area east of Well D. See Figures 10.4 and 10.5. The lateral is placed high up, in layer Z1, to avoid premature water break-through.

11.1.3 Case 3: Multilateral East

A multilateral was designed to drain the area east of Well D, with one lateral in layer Z2 and one lateral in layer Z1. See Figures 10.6 and 10.7. The lateral in layer Z1 is the longest of the two laterals.

Case 3a: Well D Shut

Well D has in the production history shown to be a poor well. A scenario where Well D is shut is simulated. The two new laterals are still producing as normally.

Case 3b: Producing Layer Z1 Only

In case of early water break-through, a scenario where the lateral placed in layer Z2 is shut is simulated. This may help estimate the time of water break-through in the different layers. In Figure 10.7 this is observed by shutting of the well marked with purple color. Well D is open.

11.1.4 Case 4: Multilateral West

A multilateral was designed to drain the area west of Well D, with one lateral in layer Z2 and one lateral in layer Z1. See Figures 10.8 and 10.9. The lateral in layer Z1 is the longest of the two laterals.

Case 4a: Well D Shut

Well D has, in the production history, been shown to be a poor producing well. A scenario where Well D is shut is simulated. The two new laterals are still producing as normally.

Case 4b: Producing Layer Z1 Only

Early water break-through is suspected in the lateral placed in layer Z2. This is due to the aquifer coming in from the west towards east. A scenario where the lateral placed in layer Z2 is shut is simulated in order to see the effect of water break-through and help estimate the time of water break-through in the different layers. In Figure 10.9 this is observed by a shutting of the well marked with yellow color. Well D is open.

11.1.5 Case 5: Open Interval

The planned and drilled well length of Well D was to 3535 m MD RKB, but the well was only completed to 2977 m MD RKB. In ECLIPSE, this is simulated by shutting the completions below 2977 m MD RKB. When simulating the production from the entire well interval all the completions are opened up in the simulation model. **Figure 11.1** shows

how Well D is located in the reservoir. The well in Figure 11.1 represents the well when all the completions are open.

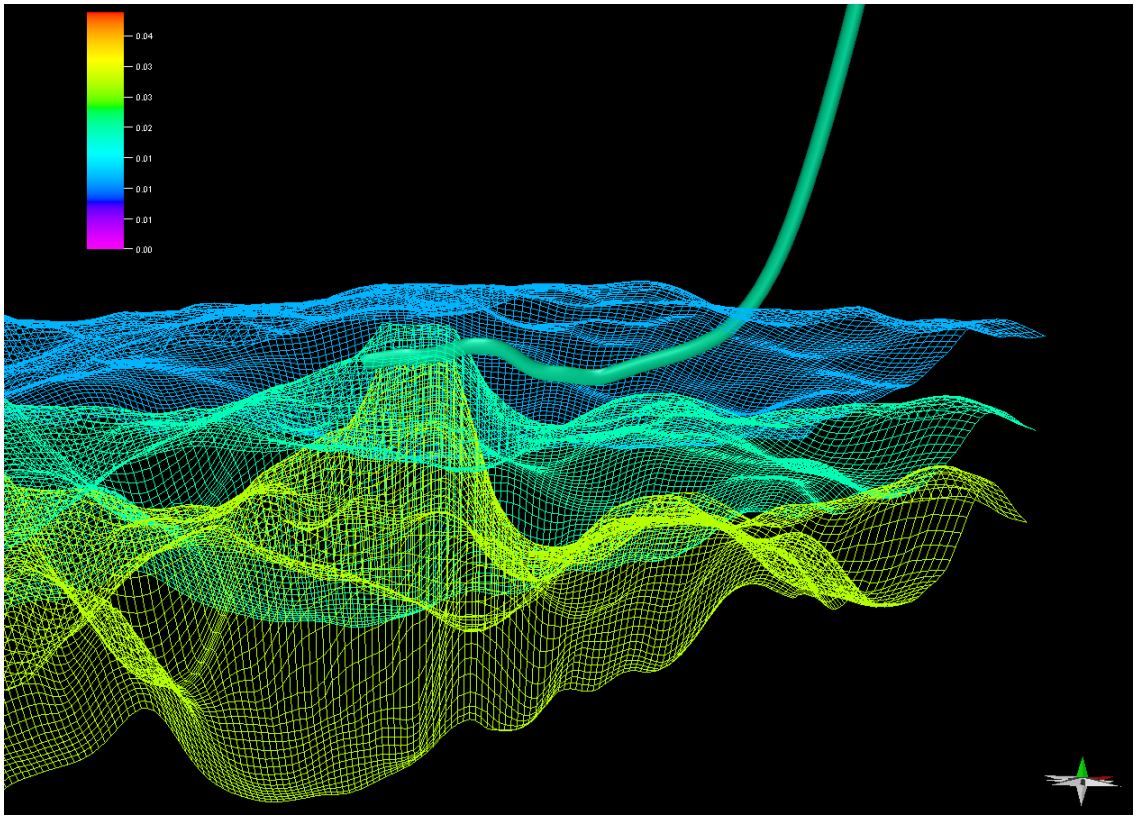

Figure 11.1: The location of Well D in the reservoir model. The well represents Well D with completed interval to 3535 m MD RKB. Taken from Petrel (Schlumberger 2013c).

The completion of the well will be as originally planned for Well D; openhole with sand screens and swell packers.

11.1.6 Case 6: Acidizing

Acid squeeze, or acidizing, may be performed in several ways, as described in **Subsection 5.2.3**. As there does not exist any proper zone isolation in Well D, acidizing will be performed by pumping the well full of chemicals, using a supply vessel. This will also be cost effective.

Acid stimulation is modelled by opening all the completions down to the triconic bit at 2977 m MD RKB, and doubling the productivity of the well. The doubling of the productivity is an assumption which carries uncertainties as the results are highly dependent upon well productivity.

11.2 Simulation Constraints

Constraints for the simulations are listed below. The history matched model has been used.

- Start date for well intervention measures is June 1, 2015. This gives a reasonable time to prepare for and implement the measures. Well D is assumed to be producing during this period.
- The wells are constraint with THP = 30 bar. The number is based on historic data, where the THP is found to be quite stable. The BHP is estimated by the use of the lift curves in the model.
- The lift curves cover the production area of the new wells.
- The liquid rate of the new wells do not exceed the capacity of the commingled production at Jotun hence, a liquid rate limit is not implemented.
- The production is simulated from the reservoir up to the well head.
- The simulations are run from 20.05.2013 to 01.01.2020.
- Open completion. No completion are taken into account.

11.3 Results From Simulation

11.3.1 Case 1: Single Lateral North

The results from the simulations for Well D and its lateral are shown in **Figure 11.2**, and the results for the field are shown in **Figure 11.3**. The results for Case 1 are summarized, and compared to the basecase, in **Table 11.1**.

With a lateral drilled towards north of Well D the simulated cumulative oil production of Well D is 1,136,200 Sm^3 at the end of simulation, 01.01.2020. As shown in Table 11.1 this implies a 44.5% increase of the basecase. The field cumulative oil production is 1,868,100 with a lateral towards north, a 21.7% increase of the basecase. The oil recovery of the field is 29% (21.7% increase from the basecase).

The water production in Well D increases with 125.6% as compared to the basecase, and has a WC at 61.0%. The increase in water production in Well D does not affect the field's water production significantly as Well D initially has a low WC.

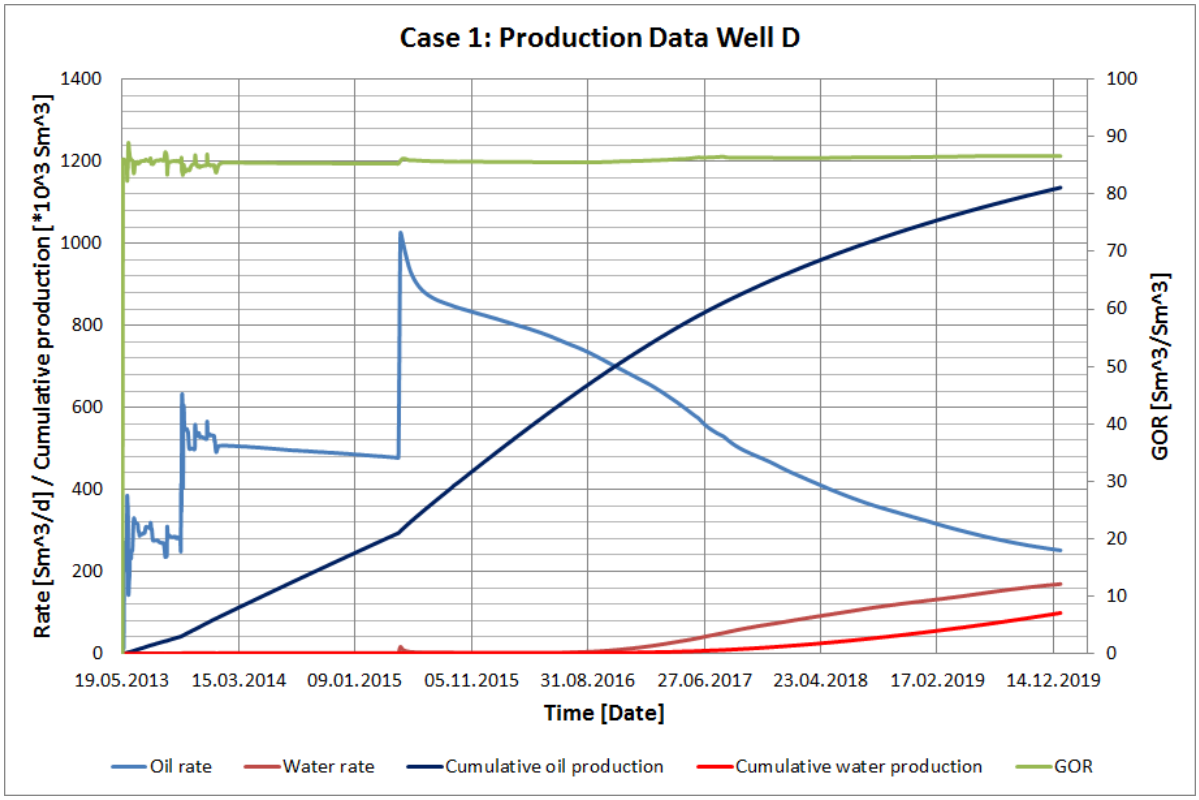

Figure 11.2: Results from Well D from the simulation with a single-lateral north of Well D. The oil rate, water rate, GOR, cumulative oil production and cumulative water production are plotted.

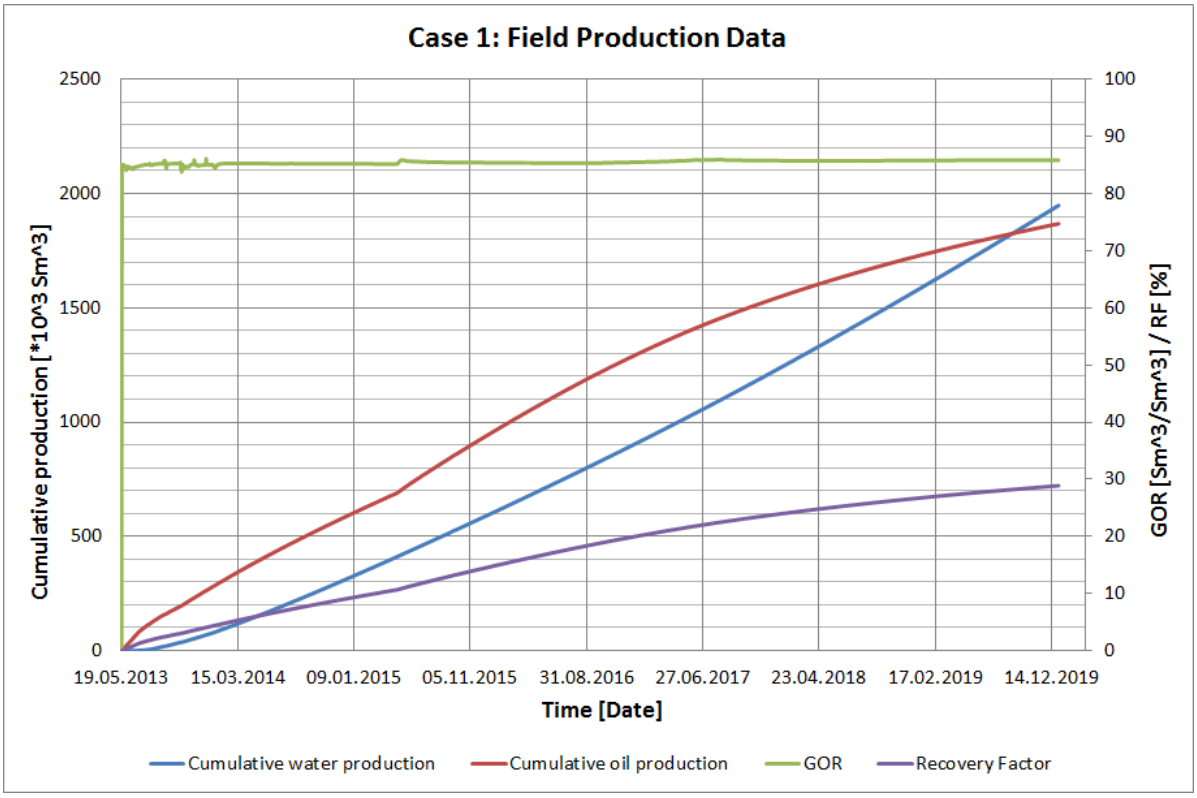

Figure 11.3: Results from the field from the simulation with a single-lateral north of Well D. The GOR, recovery factor, cumulative oil production and cumulative water production are plotted.

Table 11.1: Estimated production from Well D with a lateral towards north. The results are compared with the basecase.

Parameter	*Unit*	Basecase	Case 1	Deviation
WOPT D	Sm^3	785,658.6	1,136,201	**+44.5%**
WWPT D	Sm^3	43,661.8	99,021.8	+125.6%
WGPT D	Sm^3	6.7*10^7	9.8*10^7	+44.7%
WWCT D	*fraction*	0.25	0.40	+61.0%
FOPT	Sm^3	1,532,319	1,868,091	**+21.7%**
FWPT	Sm^3	1,878,561	1,948,082	+3.1%
FGPT	Sm^3	1.3*10^8	1.6*10^8	+21.9%
FOE	*fraction*	0.24	0.29	**+21.7%**
FGOR	Sm^3/Sm^3	85.5	85.8	+0.3%

WOPT is the Well Oil Production Total, WWPT is the Well Water Production Total, WGPT is the Well Gas Production Total, WWCT is the Well Water Cut Total, FOPT is the Field Oil Production Total, FWPT is the Field Water Production Total, FGPT is the

Field Gas Production Total, FOE is the Field Oil Efficiency (RF), and FGOR is the Field Gas-Oil Ratio.

11.3.2 Case 2: Single Lateral East

The results from the simulations for Well D and its lateral are shown in **Figure 11.4**, and the results for the field are shown in **Figure 11.5**. The results for Case 2 are summarized, and compared to the basecase, in **Table 11.2**.

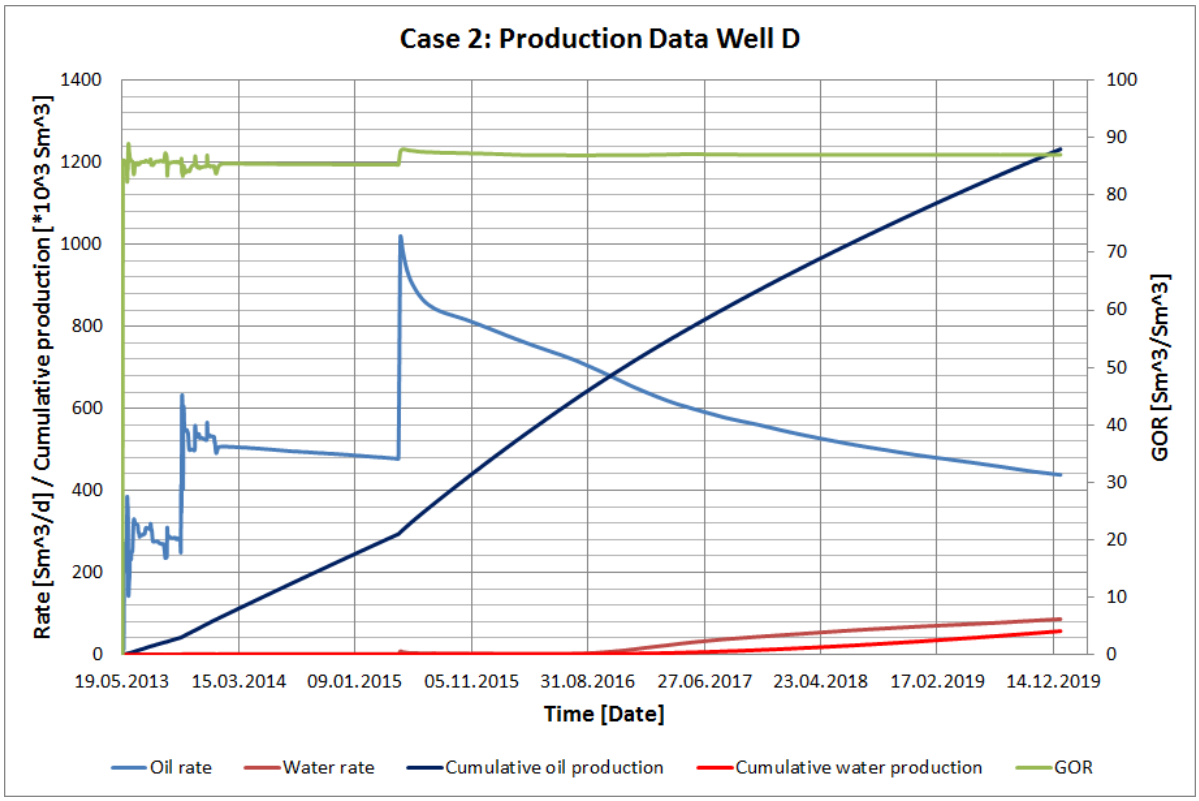

Figure 11.4: Results from Well D from the simulation with a single-lateral east of Well D. The oil rate, water rate, GOR, cumulative oil production and cumulative water production are plotted.

Well D with a lateral towards east has a simulated cumulative oil production of 1,232,400 Sm^3 at the end of simulation, 01.01.2020. This is an increase of 56.8% from the basecase, see Table 11.2. The field cumulative oil production is 1,938,000 Sm^3 (an increase of 26.3%). With an increase of 26.3% in cumulative oil production the recovery factor becomes 30.0% (26.3% increase of the basecase).

The cumulative water production in Well D increases with 30.4% as compared to the basecase. As the cumulative oil production has a significantly higher increase, the WC decreases with 34.0%.

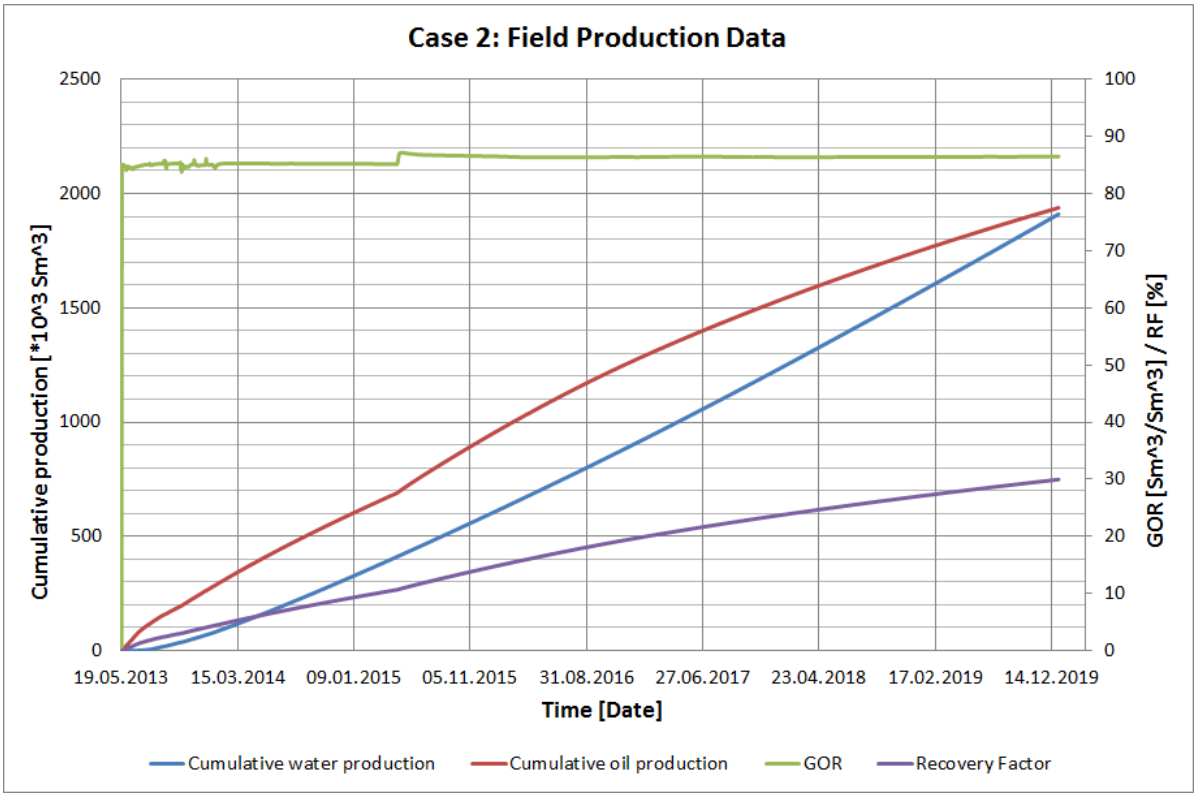

Figure 11.5: Results from the field from the simulation with a single-lateral east of Well D. The GOR, recovery factor, cumulative oil production and cumulative water production are plotted.

Table 11.2: Estimated production from Well D with a lateral towards east. The results are compared with the basecase.

Parameter	*Unit*	Basecase	Case 2	Deviation
WOPT D	Sm^3	785,658.6	1,232,350	**+56.8%**
WWPT D	Sm^3	43,661.8	57,241.6	+30.4%
WGPT D	Sm^3	6.7*10^7	1.1*10^8	+58.6%
WWCT D	*fraction*	0.25	0.16	-34.0%
FOPT	Sm^3	1,532,319	1,938,039	**+26.3%**
FWPT	Sm^3	1,878,561	1,910,164	+1.1%
FGPT	Sm^3	1.3*10^8	1.7*10^8	**+27.4%**
FOE	*fraction*	0.24	0.3	+26.3%
FGOR	Sm^3/Sm^3	85.5	86.5	+1.1%

11.3.3 Case 3: Multilateral East

The results from the simulations for Well D and its laterals are shown in **Figure 11.6**, and the results for the field are shown in **Figure 11.7**. The results for Case 3 are summarized, and compared to the basecase, in **Table 11.3**.

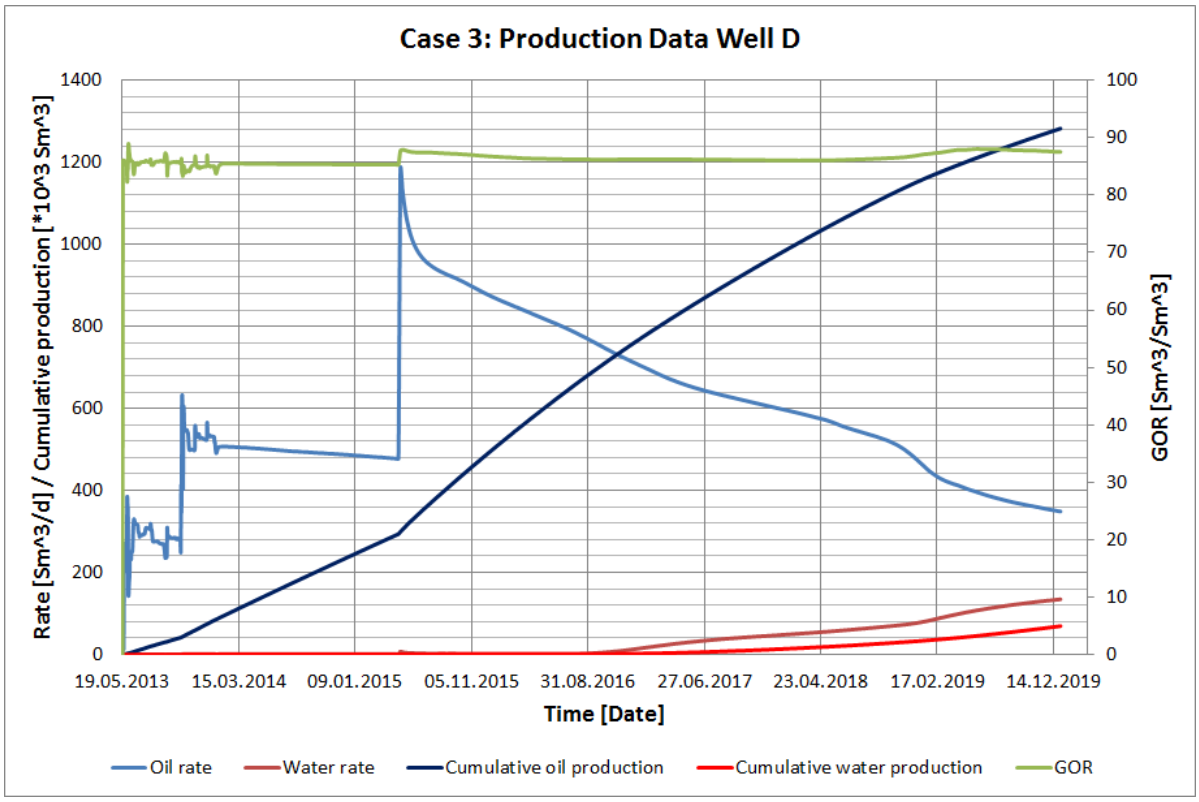

Figure 11.6: Results from Well D from the simulation with a multilateral east of Well D. The oil rate, water rate, GOR, cumulative oil production and cumulative water production are plotted.

The area east of Well D has been shown to be a good producing area with the single lateral. The multilateral towards east is expected to have a significant increase in production. As observed in Figure 11.6 the cumulative oil production, at 01.01.2020, is 1,282,700 Sm^3, which is an increase of 63.2% from the basecase. This gives a field cumulative oil production at 1,983,600 Sm^3 (29.2% increase) and a field recovery factor of 31%.

The multilateral produces slightly more water than the single lateral, with an increase of 58.0% in cumulative water production. The water cut increases with 11.6%, which gives an increase of field cumulative water production of 1.7%. This is considered negligible.

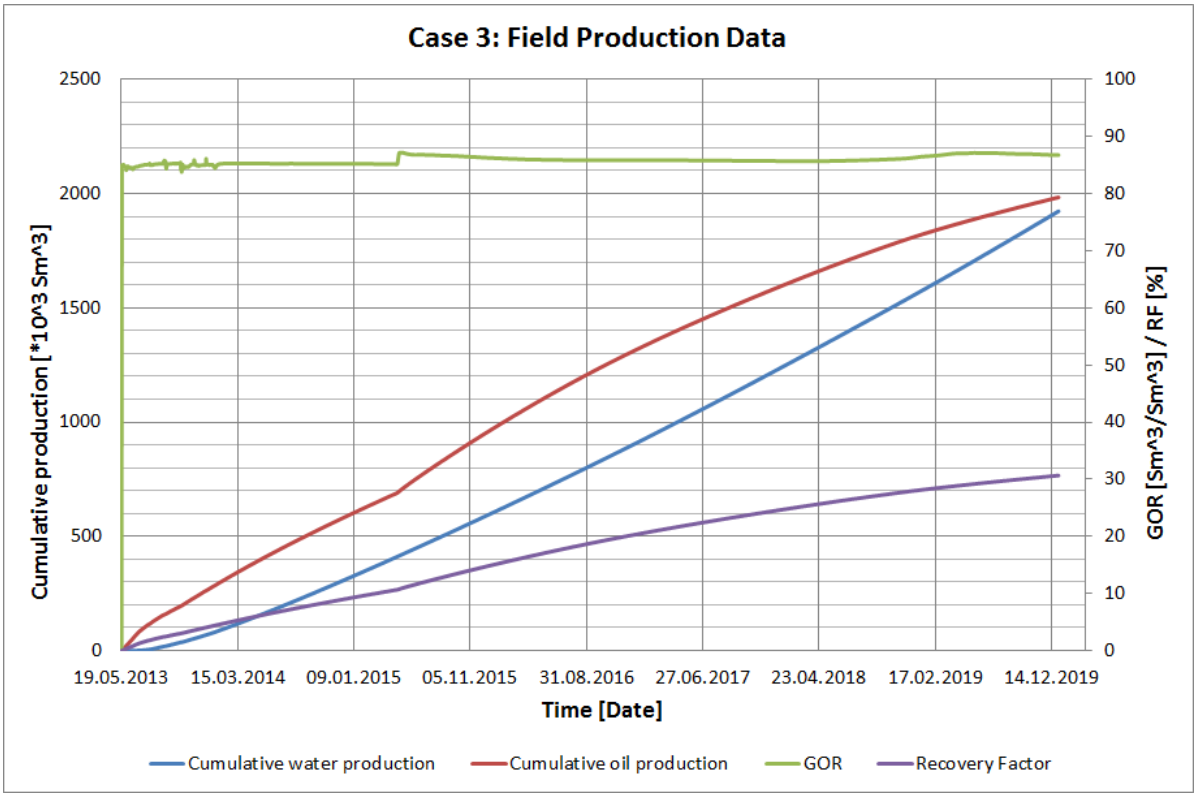

Figure 11.7: Results from the field from the simulation with a multilateral east of Well D. The GOR, recovery factor, cumulative oil production and cumulative water production are plotted.

Table 11.3: Estimated production from Well D with two laterals towards east. The results are compared with the basecase.

Parameter	*Unit*	Basecase	Case 3	Deviation
WOPT D	Sm^3	785,658.6	1,282,669	**+63.2%**
WWPT D	Sm^3	43,661.8	69,348.8	+58.0%
WGPT D	Sm^3	6.7*10^7	1.1*10^8	+64.4%
WWCT D	*fraction*	0.25	0.28	+11.6%
FOPT	Sm^3	1,532,319	1,983,612	**+29.2%**
FWPT	Sm^3	1,878,561	1,922,982	+1.7%
FGPT	Sm^3	1.3*10^8	1.7*10^8	+30.1%
FOE	*fraction*	0.24	0.31	**+29.2%**
FGOR	Sm^3/Sm^3	85.5	86.7	+1.4%

Case 3a: Well D Shut

For Case 3a the results from the simulations for Well D are shown in **Figure 11.8**, and the results for the field are shown in **Figure 11.9**. The results for Case 3a and Case 3b are summarized, and compared to the basecase, in **Table 11.4**.

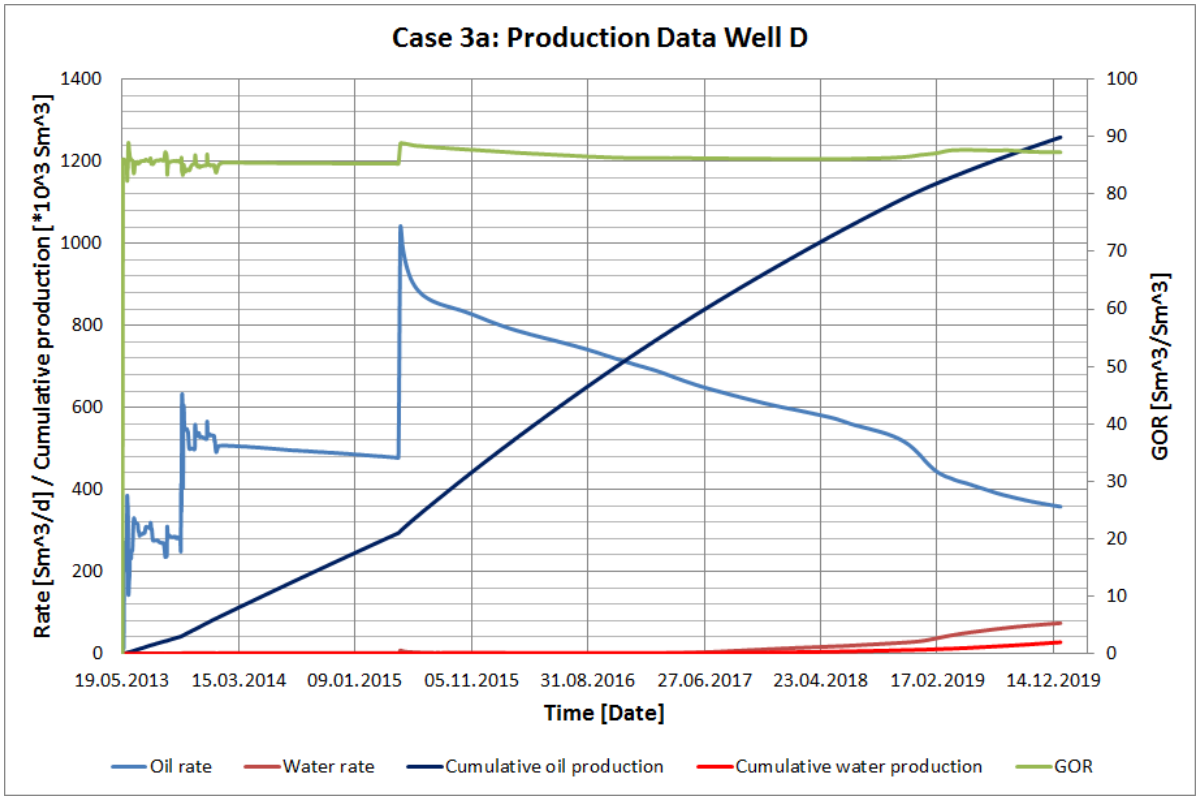

Figure 11.8: Results from Well D from the simulation with a multilateral east of Well D, with Well D shut. The oil rate, water rate, GOR, cumulative oil production and cumulative water production are plotted.

When shutting the original well a small decrease in cumulative oil production is observed, as compared to the multilateral towards east with the original well open and producing. The decrease is small, indicating that the production in the two laterals increase. Well cumulative oil production is 1,258,900 Sm^3, a 60.1% increase from the basecase. Field cumulative oil production is 1,961,000 Sm^3 (an increase of 27.6%). Field oil recovery is 30% (an increase of 27.8%).

When shutting the original well the cumulative water production decreases with 37.3%. This shows that the water moves from west towards east and hence, delaying the water break-through when shutting the well closest to the incoming aquifer. The well WC has decreased with 31.3%.

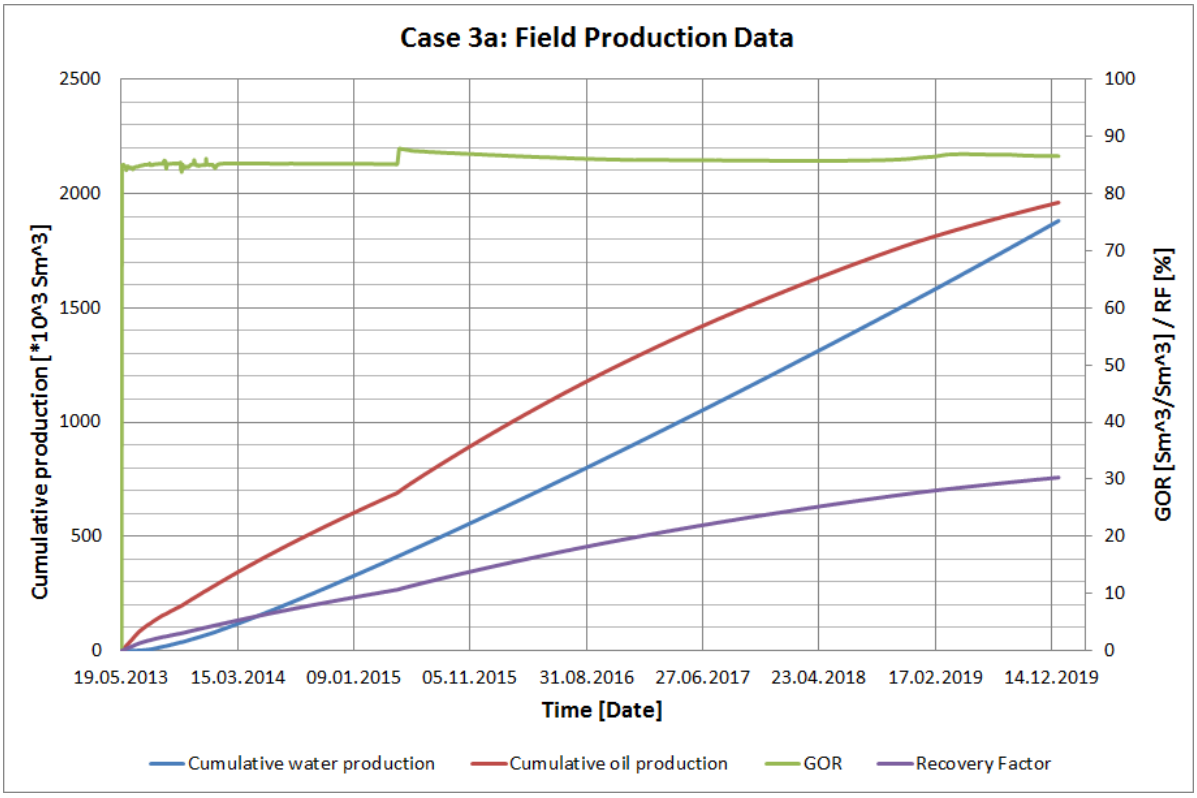

Figure 11.9: Results from the field from the simulation with a multilateral east of Well D, with Well D shut. The GOR, recovery factor, cumulative oil production and cumulative water production are plotted.

Table 11.4: Estimated production from Well D with two laterals towards east. The results are compared with the basecase.

Parameter	*Unit*	Basecase	Case 3a	Deviation	Case 3b	Deviation
WOPT D	Sm^3	785,658.6	1,258,938	**+60.1%**	1,230,516	**+56.5%**
WWPT D	Sm^3	43,661.8	27,531.6	-37.3%	65,114.0	+48.3%
WGPT D	Sm^3	$6.7*10^7$	$1.1*10^8$	+61.7%	$1.1*10^8$	+58.1%
WWCT D	*fraction*	0.25	0.17	-31.3%	0.28	+11.0%
FOPT	Sm^3	1,532,319	1,960,976	**+27.8%**	1,930,629	**+25.8%**
FWPT	Sm^3	1,878,561	1,880,962	-0.5%	1,918,849	+1.5%
FGPT	Sm^3	$1.3*10^8$	$1.7*10^8$	+28.7%	$1.7*10^8$	+26.8%
FOE	*fraction*	0.24	0.30	**+27.8%**	0.298	**+25.8%**
FGOR	Sm^3/Sm^3	85.5	86.6	+1.2%	86.6	+1.2%

Case 3b: Producing Layer Z1 Only

For Case 3b, the results from the simulations for Well D are shown in **Figure 11.10**, and the results for the field are shown in **Figure 11.11**. The results are summarized and compared to the basecase in Table 11.4.

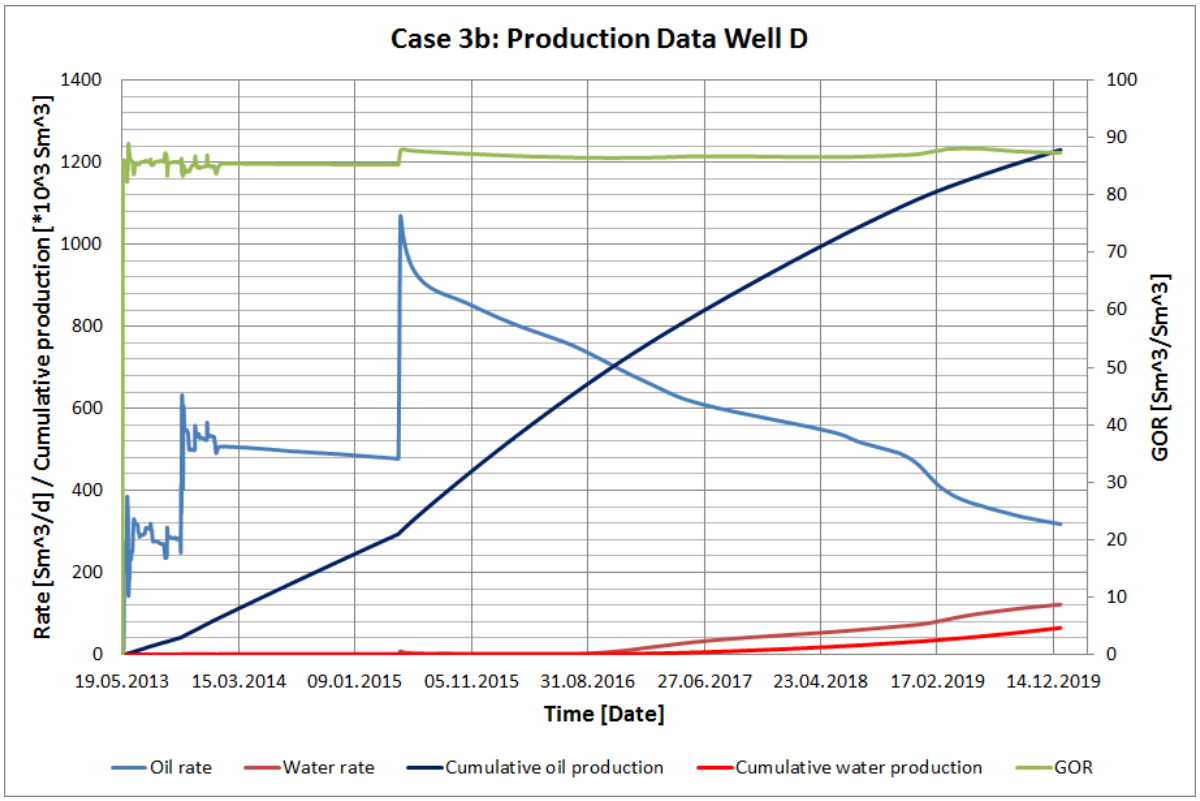

Figure 11.10: Results from Well D from the simulation with a multilateral east of Well D, with the deepest lateral shut. The oil rate, water rate, GOR, cumulative oil production and cumulative water production are plotted.

It is observed a decrease in cumulative oil production compared to both Case 3 and Case 3a when shutting the lateral placed deepest, in layer Z2. The well cumulative oil production is 1,230,500 Sm^3, an increase of 56.5% from the basecase. The field cumulative oil production is 1,930,600 Sm^3, an increase of 25.8% from the basecase, which gives an field oil recovery factor of 29.8%.

An increase in water production, as compared to Case 3a, is expected as the original lateral is in this case producing; the original lateral is placed closer to the incoming aquifer hence, experiencing earlier water break-through. The well cumulative water production has increased with 48.3% compared to the basecase, with a WC of 28%. As Well D initially has a very low water production, the increase in field cumulative water production is negligible, 1.5%.

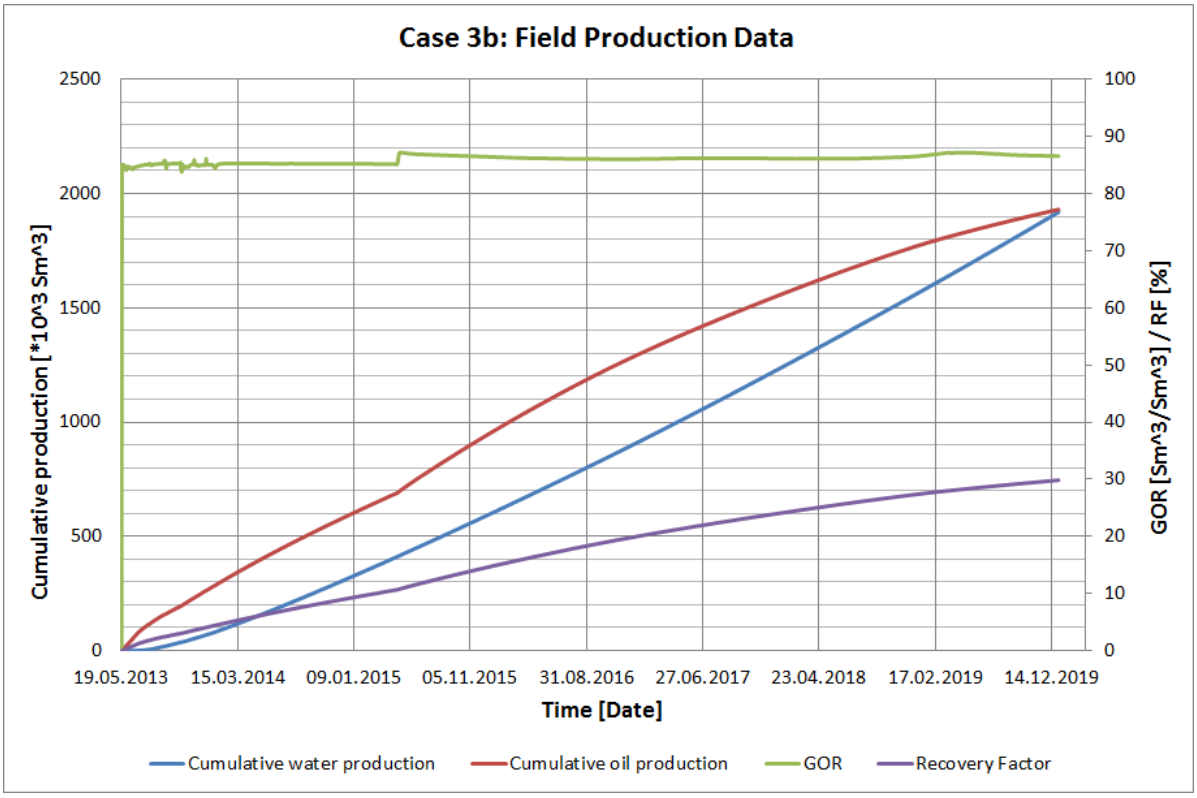

Figure 11.11: Results from the field from the simulation with a multilateral east of Well D, with the deepest lateral shut. The GOR, recovery factor, cumulative oil production and cumulative water production are plotted.

11.3.4 Case 4: Multilateral West

The results from the simulations for Well D and its laterals are shown in **Figure 11.12**, and the results for the field are shown in **Figure 11.13**. The results for case 4 are summarized, and compared to the basecase, in **Table 11.5**.

In Figure 11.12 and Table 11.5 it is observed that the increase in well cumulative water production is greater than the well cumulative oil production. This indicates that with a multilateral towards west an earlier water break-through is experienced. The well cumulative oil production is 946,700 Sm^3 (20.4% increase of the basecase), and the well cumulative water production is 139,000 Sm^3 (216.8% increase of the basecase). The well WC is 41%. Field cumulative oil production increases with 9.4% from the basecase which gives a field recovery factor of 26% (an increase of 9.4% from the basecase). The field cumulative water production increases with 5.2%, which is considered as negligible.

The multilateral towards west is expected to have a poorer oil production than the multilateral towards east due to the close location to the incoming aquifer. Also, the reservoir properties in the model may be poorer in this area.

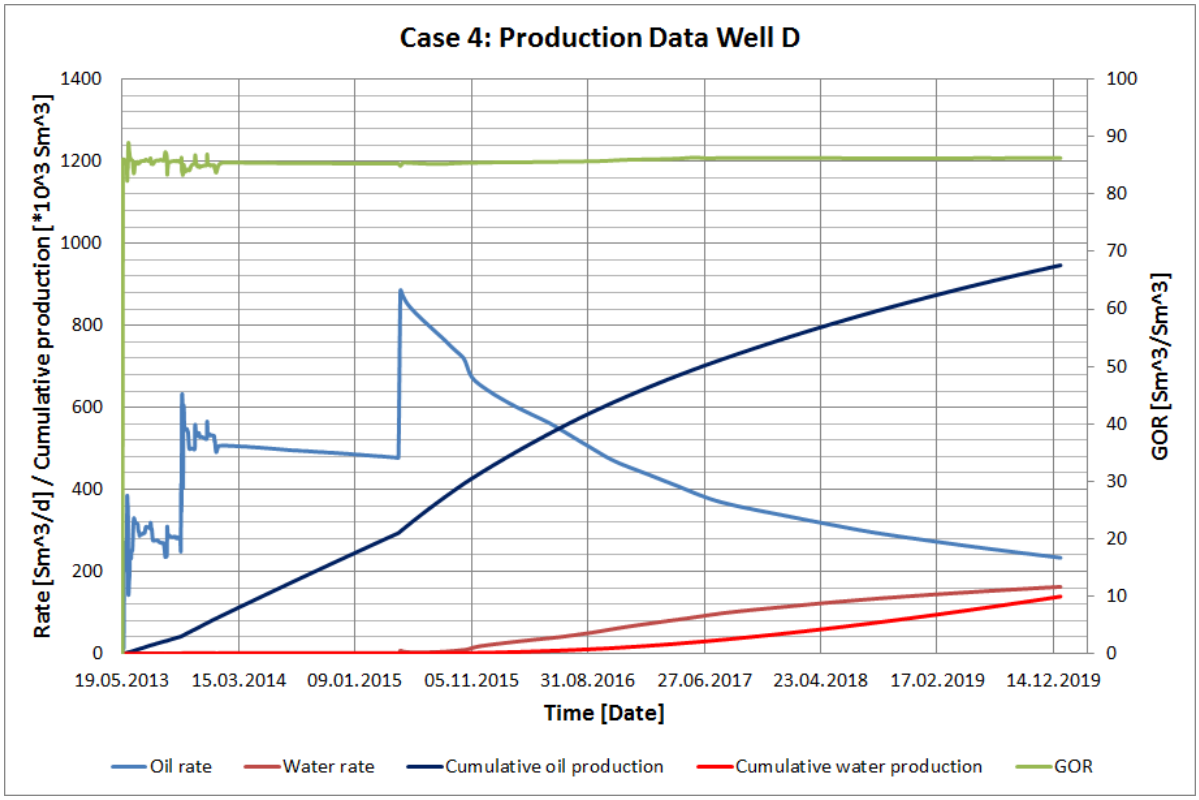

Figure 11.12: Results from Well D from the simulation with a multilateral west of Well D. The oil rate, water rate, GOR, cumulative oil production and cumulative water production are plotted.

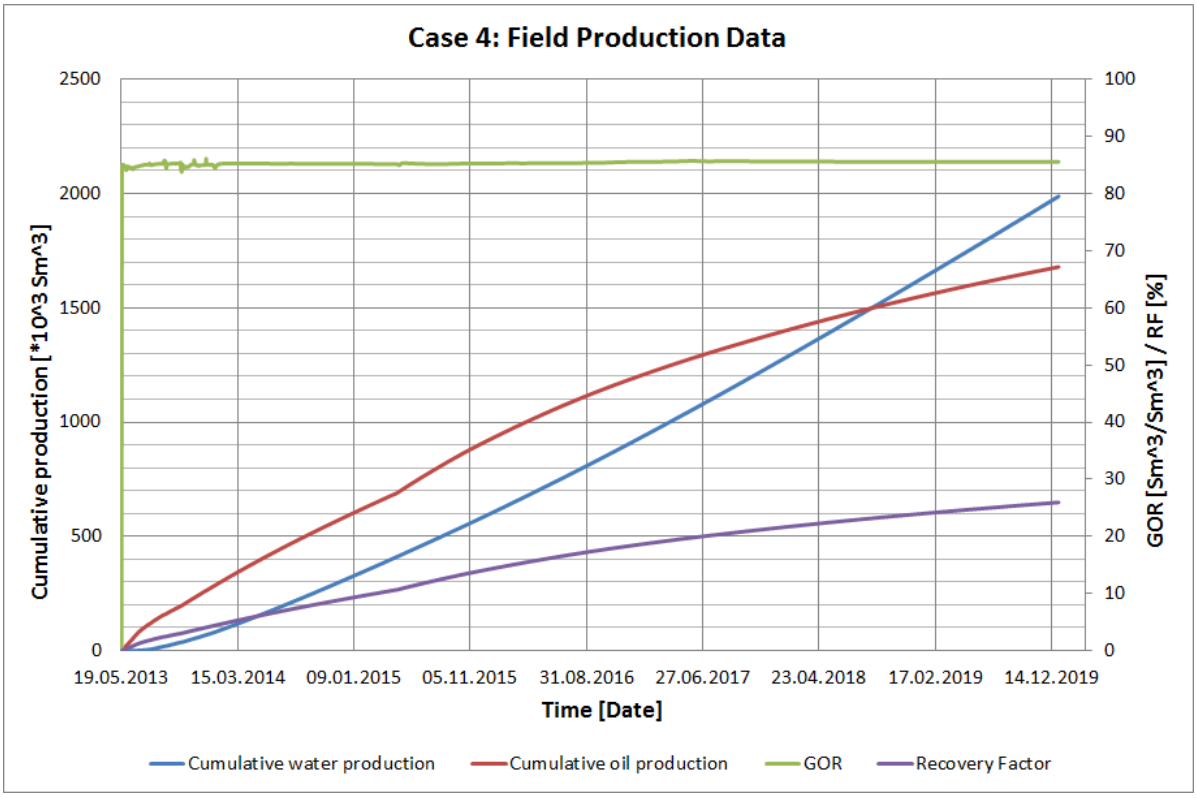

Figure 11.13: Results from the field from the simulation with a multilateral west of Well D. The GOR, recovery factor, cumulative oil production and cumulative water production are plotted.

Table 11.5: Estimated production from Well D with two laterals towards west. The results are compared with the basecase.

Parameter	*Unit*	Basecase	Case 4	Deviation
WOPT D	Sm^3	785,658.6	946,744.3	**+20.4%**
WWPT D	Sm^3	43,661.8	139,060.8	216.8%
WGPT D	Sm^3	6.7*10^7	8.1*10^7	+20.5%
WWCT D	*fraction*	0.25	0.41	+64.4%
FOPT	Sm^3	1,532,319	1,678,768	**+9.4%**
FWPT	Sm^3	1,878,561	1,987,902	+5.2%
FGPT	Sm^3	1.3*10^8	1.4*10^8	+9.4%
FOE	*fraction*	0.24	0.259	**+9.4%**
FGOR	Sm^3/Sm^3	85.5	85.6	0.0%

Case 4a: Well D Shut

For Case 4a the results from the simulations for Well D are shown in **Figure 11.14**, and the results for the field are shown in **Figure 11.15**. The results for Case 4a and Case 4b are summarized, and compared to the basecase, in **Table 11.6**.

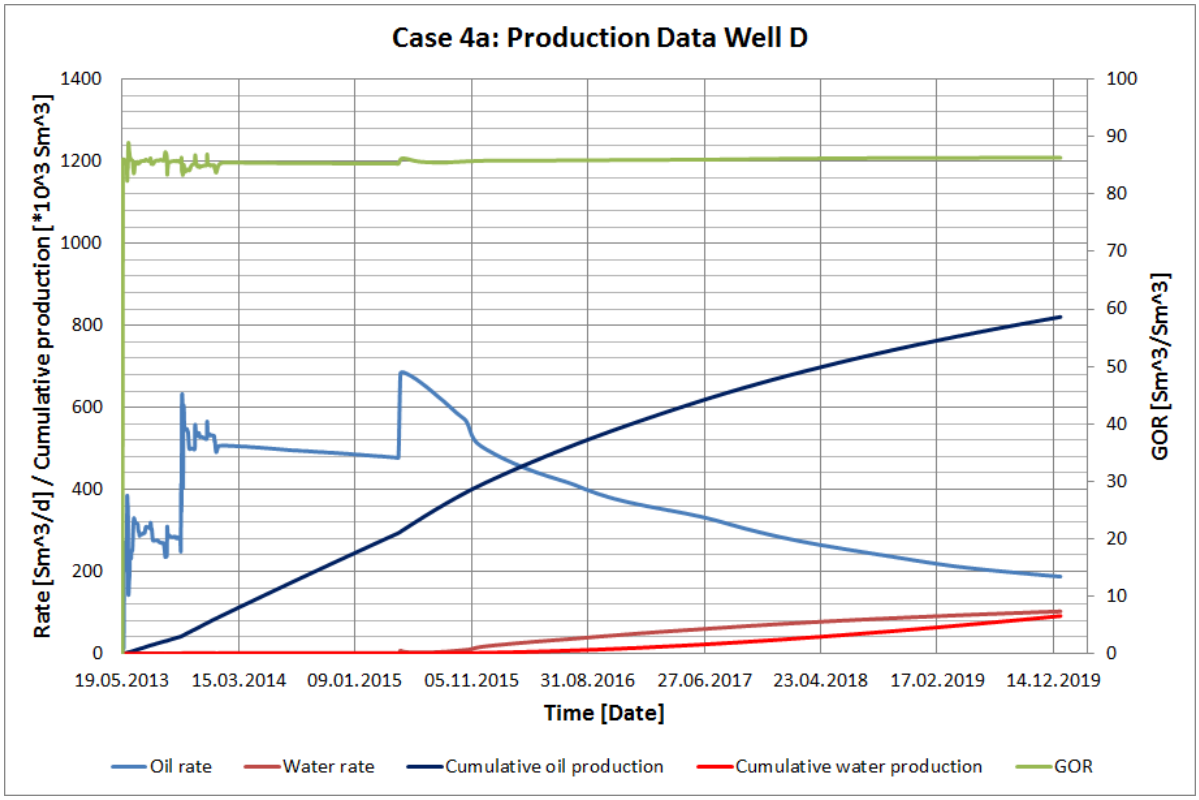

Figure 11.14: Results from Well D from the simulation with a multilateral west of Well D, with Well D shut. The oil rate, water rate, GOR, cumulative oil production and cumulative water production are plotted.

In the case with the original well shut, the well cumulative oil production decreases as compared to the multilateral with Well D producing. The well cumulative oil production is 820,800 Sm^3, an increase of 4.4% from the basecase. The field cumulative oil production increases by 1.6% from the basecase, giving a field oil recovery factor of 24%. This is an increase of 1.6% from the basecase.

The cumulative water production increases more than the cumulative oil production. Well cumulative water production increases with 108.7% compared to the basecase, giving an increase in well WC of 41.8%. The field cumulative water production increases with 2.6%.

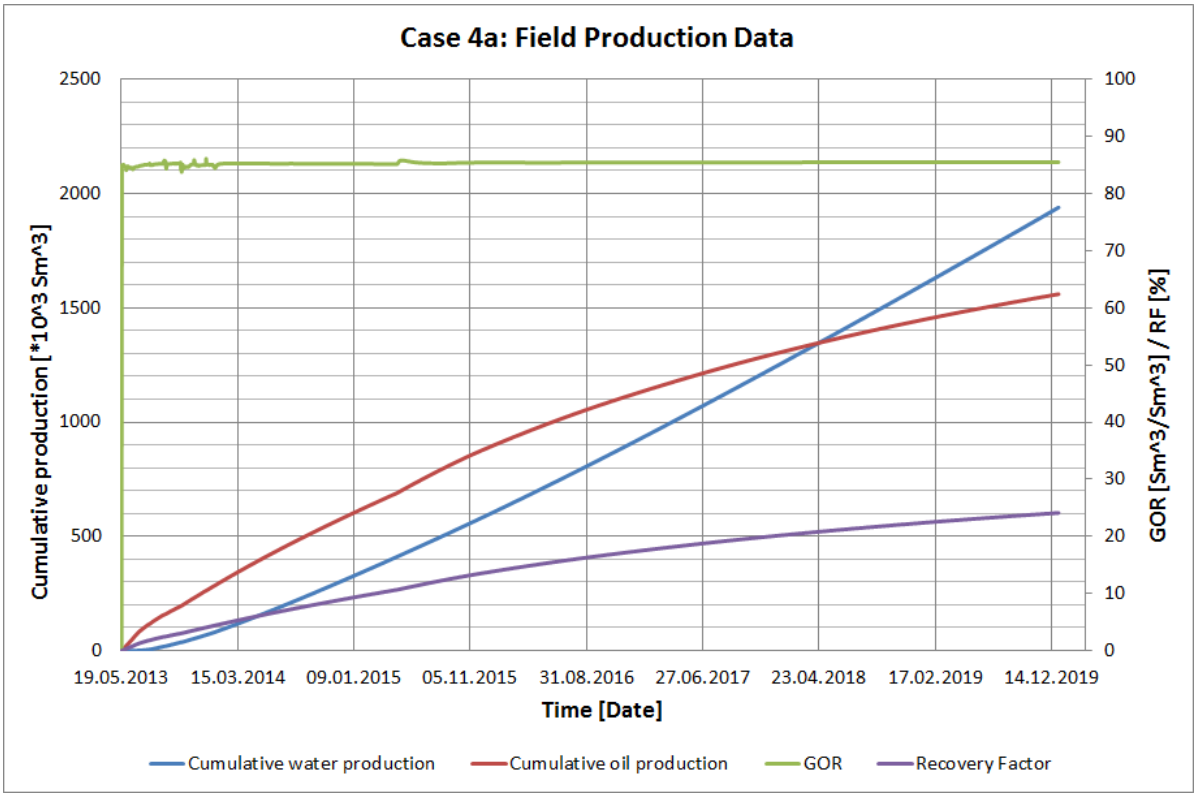

Figure 11.15: Results from the field from the simulation with a multilateral west of Well D, with Well D shut. The GOR, recovery factor, cumulative oil production and cumulative water production are plotted.

Table 11.6: Estimated production from Well D with two laterals towards west. The results are compared with the basecase.

Parameter	*Unit*	Basecase	Case 4a	Deviation	Case 4b	Deviation
WOPT D	Sm^3	785,658.6	820,784.4	**+4.4%**	988,546.8	**+25.7%**
WWPT D	Sm^3	43,661.8	91,611.4	+108.7%	98,924.1	+125.3%
WGPT D	Sm^3	$6.7*10^7$	$7.0*10^7$	+4.5%	$8.5*10^7$	+25.8%
WWCT D	*fraction*	0.25	0.35	+41.8%	0.34	+36.9%
FOPT	Sm^3	1,532,319	1,560,060	**+1.6%**	1,697,781	**+10.7%**
FWPT	Sm^3	1,878,561	1,939,235	+2.6%	1,951,102	+3.2%
FGPT	Sm^3	$1.3*10^8$	$1.3*10^8$	+1.7%	$1.5*10^8$	+10.7%
FOE	*fraction*	0.24	0.24	**+1.6%**	0.262	**+10.6%**
FGOR	Sm^3/Sm^3	85.5	85.5	-0.1%	85.5	0.0%

Case 4b: Producing Layer Z1 Only

For Case 4b, the results from the simulations for Well D are shown in **Figure 11.16**, and the results for the field are shown in **Figure 11.17**. The results are summarized and compared to the basecase in Table 11.6.

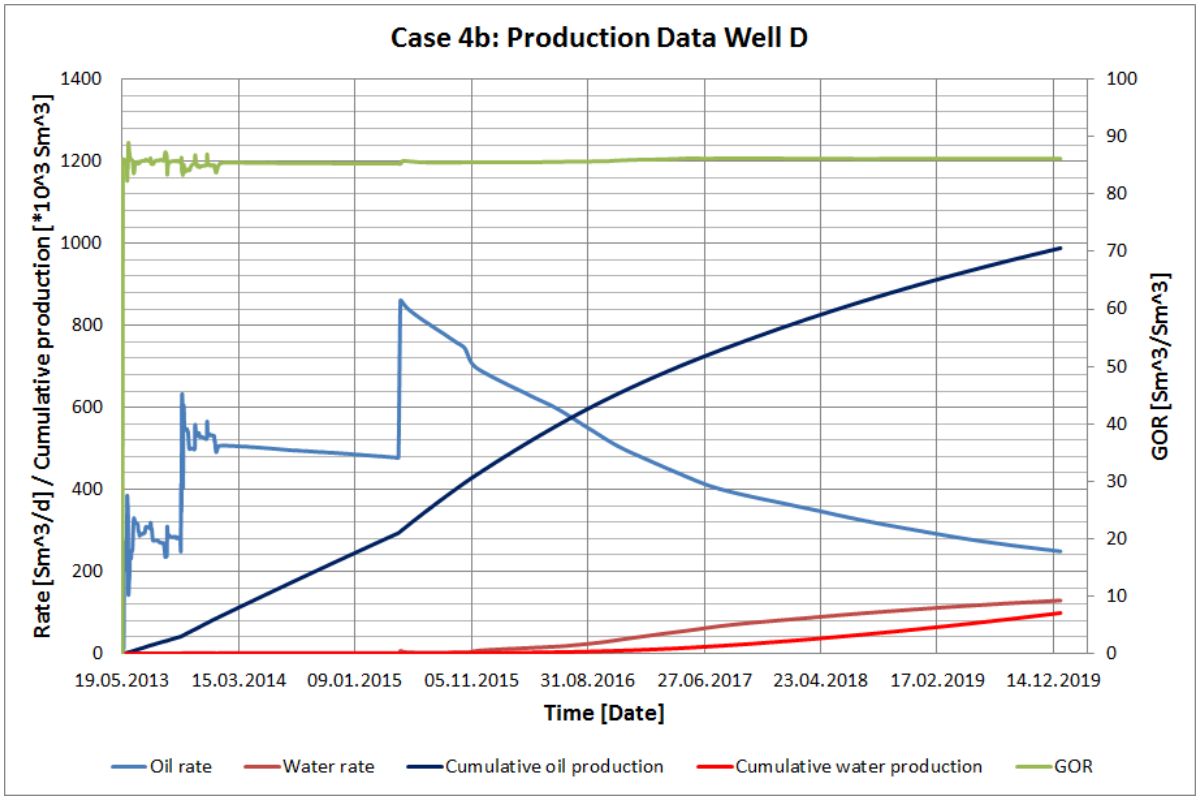

Figure 11.16: Results from Well D from the simulation with a multilateral west of Well D, with the deepest lateral shut. The oil rate, water rate, GOR, cumulative oil production and cumulative water production are plotted.

When shutting the deepest lateral, in layer Z2, the well cumulative oil production increases with 25.7% from the basecase, and the field cumulative oil production increases with 10.6% from the basecase. This gives a field oil recovery factor of 26% (an increase of 10.6% from the basecase).

The well cumulative water production increases with 125.3%, giving a WC of 34%. The WC has decreased as compared to Case 4 and Case 4a due to the higher increase in cumulative oil production. It is shown that by shutting the deepest well, more oil is produced as compared to water.

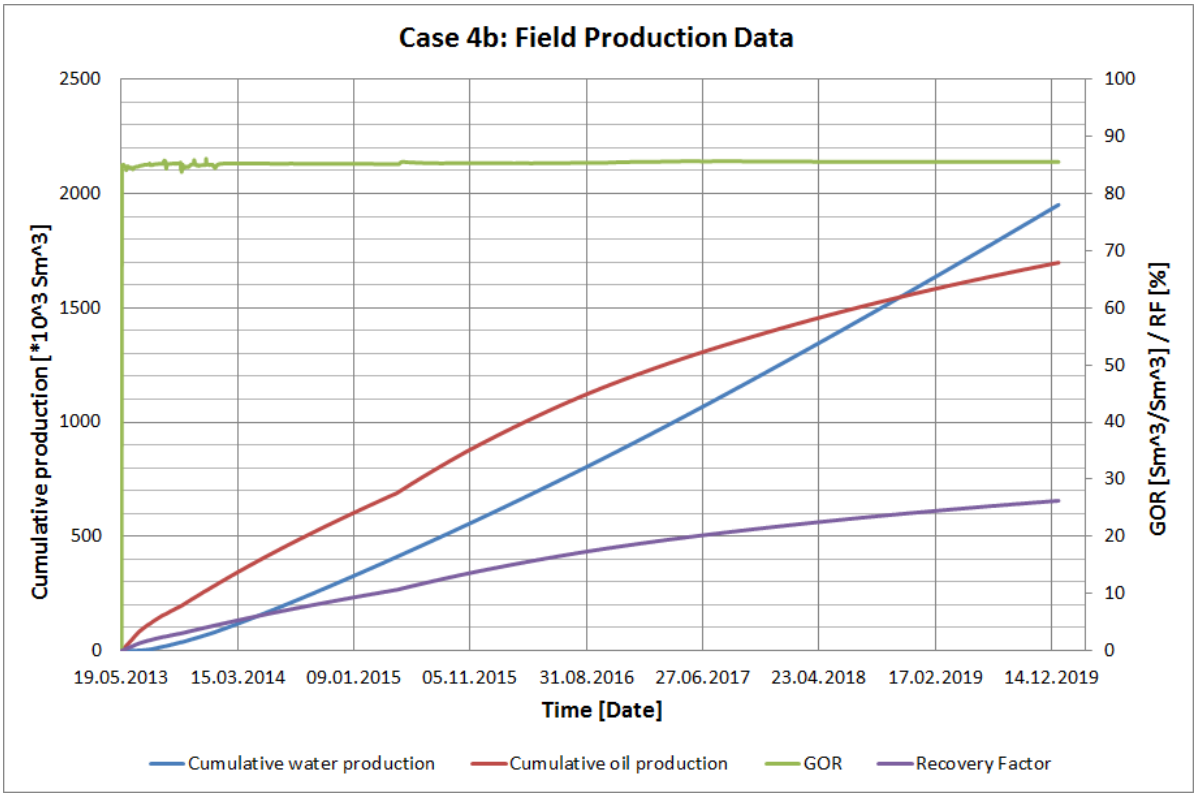

Figure 11.17: Results from the field from the simulation with a multilateral west of Well D, with the deepest lateral shut. The GOR, recovery factor, cumulative oil production and cumulative water production are plotted.

11.3.5 Case 5: Open Interval

The results from the simulations for Well D are shown in **Figure 11.18**, and the results for the field are shown in **Figure 11.19**. The results for Case 5 are summarized, and compared to the basecase, in **Table 11.7**.

As observed in Figure 11.18 and Table 11.7 opening Well D down to 3535 m MD RKB the well's cumulative oil production is 954,700 Sm^3, an increase of 21.4% from the basecase. The field cumulative oil production increases with 9.8%, giving a field oil recovery factor of 26%.

Well cumulative water production increases with 465.8% from the basecase, giving an increase of 11.0% in field cumulative water production from the basecase. The WC of the well is 51%. This is an increase of 102.7% from the basecase.

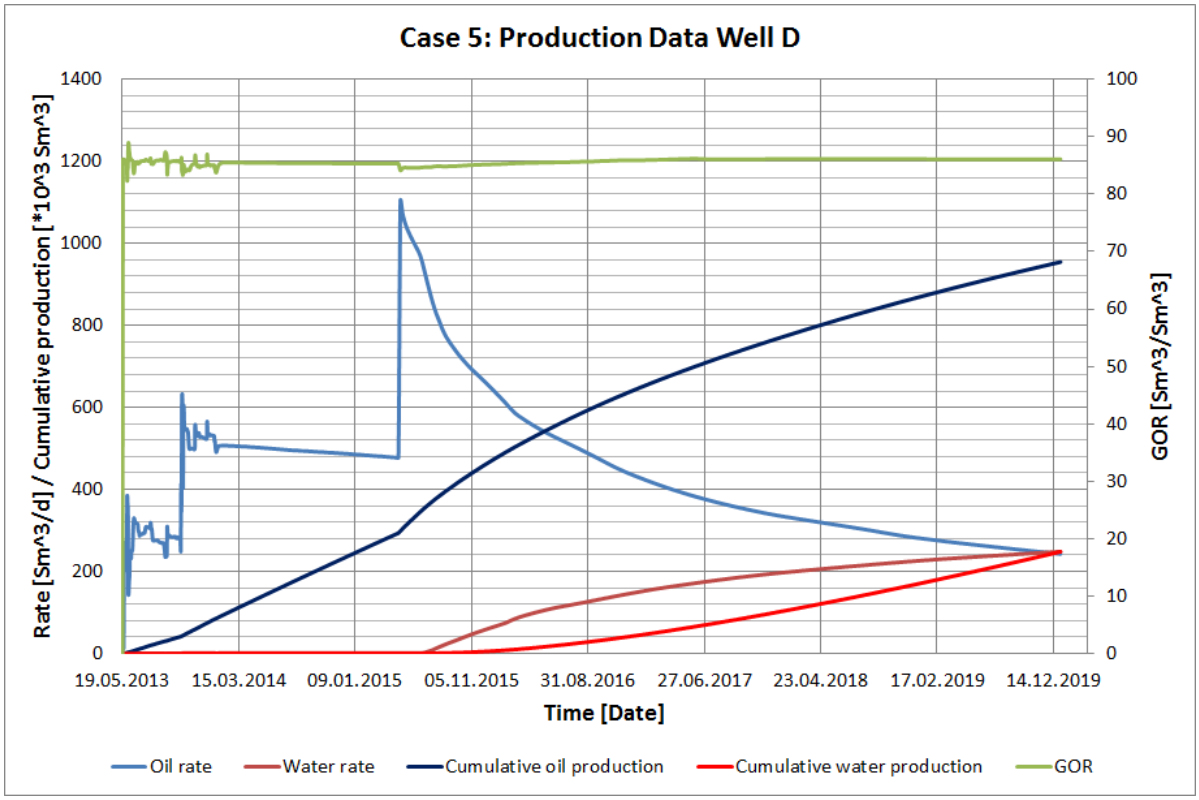

Figure 11.18: Results from Well D from the simulation of Well D opened to 3535 m MD RKB. The oil rate, water rate, GOR, cumulative oil production and cumulative water production are plotted.

The IOR measure of opening the interval down to 3535 m MD RKB is found not to be possible; the triconic bit left at 2977 m MD RKB is not millable [1]. Hence, it is not possible to drill further down, opening the well interval. As Case 5 is not possible, it will not be further discussed.

[1]Personal communication with Jafar Abdollahi and Tarje Livik Naterstad. May 2014. Trondheim: Weatherford Petroleum Consultants AS

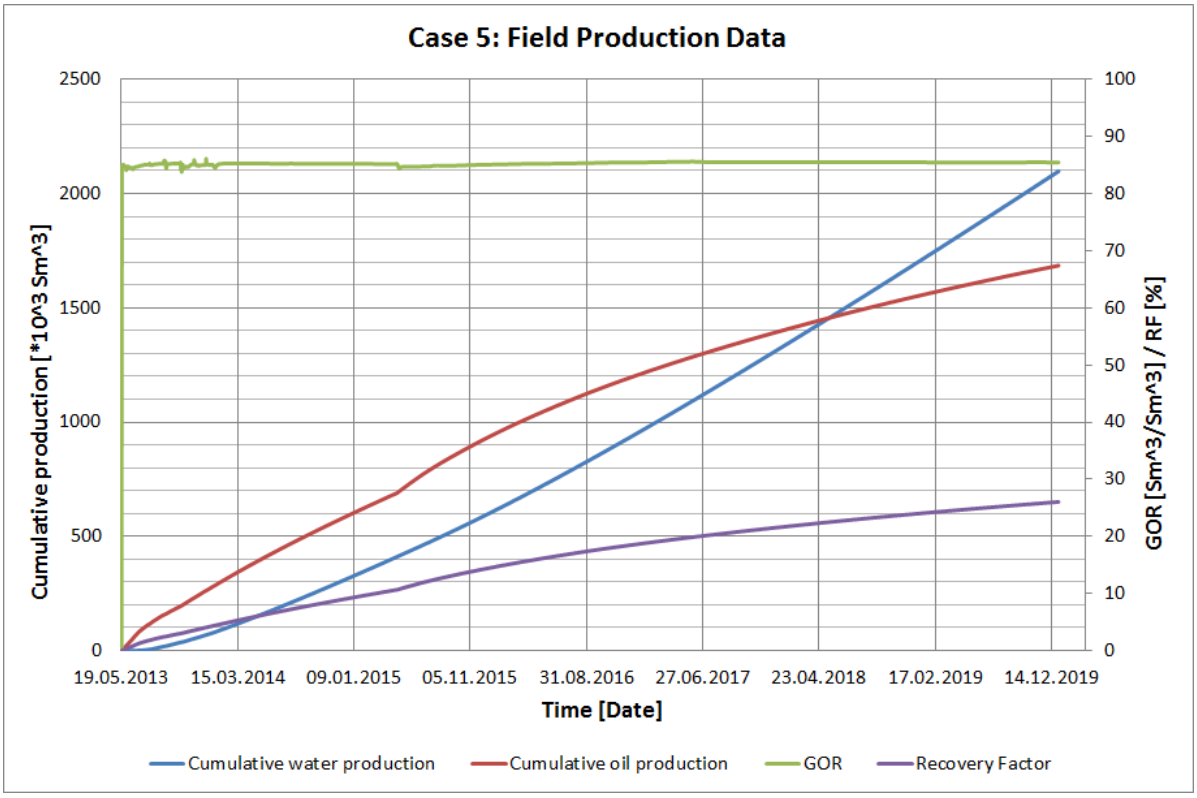

Figure 11.19: Results from the field from the simulation of Well D opened to 3535 m MD RKB. The GOR, recovery factor, cumulative oil production and cumulative water production are plotted.

Table 11.7: Estimated production from Well D with open intervall to 3535 m MD RKB. The results are compared with the basecase.

Parameter	*Unit*	Basecase	Case 5	Deviation
WOPT D	Sm^3	785,658.6	954,719.6	**+21.4%**
WWPT D	Sm^3	43,661.8	248,401.1	+465.8%
WGPT D	Sm^3	$6.7*10^7$	$8.2*10^7$	+21.2%
WWCT D	*fraction*	0.25	0.51	+102.7%
FOPT	Sm^3	1,532,319	1,684,933	**+9.8%**
FWPT	Sm^3	1,878,561	2,097,678	+11.0%
FGPT	Sm^3	$1.3*10^8$	$1.4*10^8$	+9.7%
FOE	*fraction*	0.24	0.26	**+9.8%**
FGOR	Sm^3/Sm^3	85.5	85.5	-0.1%

11.3.6 Case 6: Acidizing

The results from the simulations for Well D are shown in **Figure 11.20**, and the results for the field are shown in **Figure 11.21**. The results for Case 6 are summarized, and compared to the basecase, in **Table 11.8**.

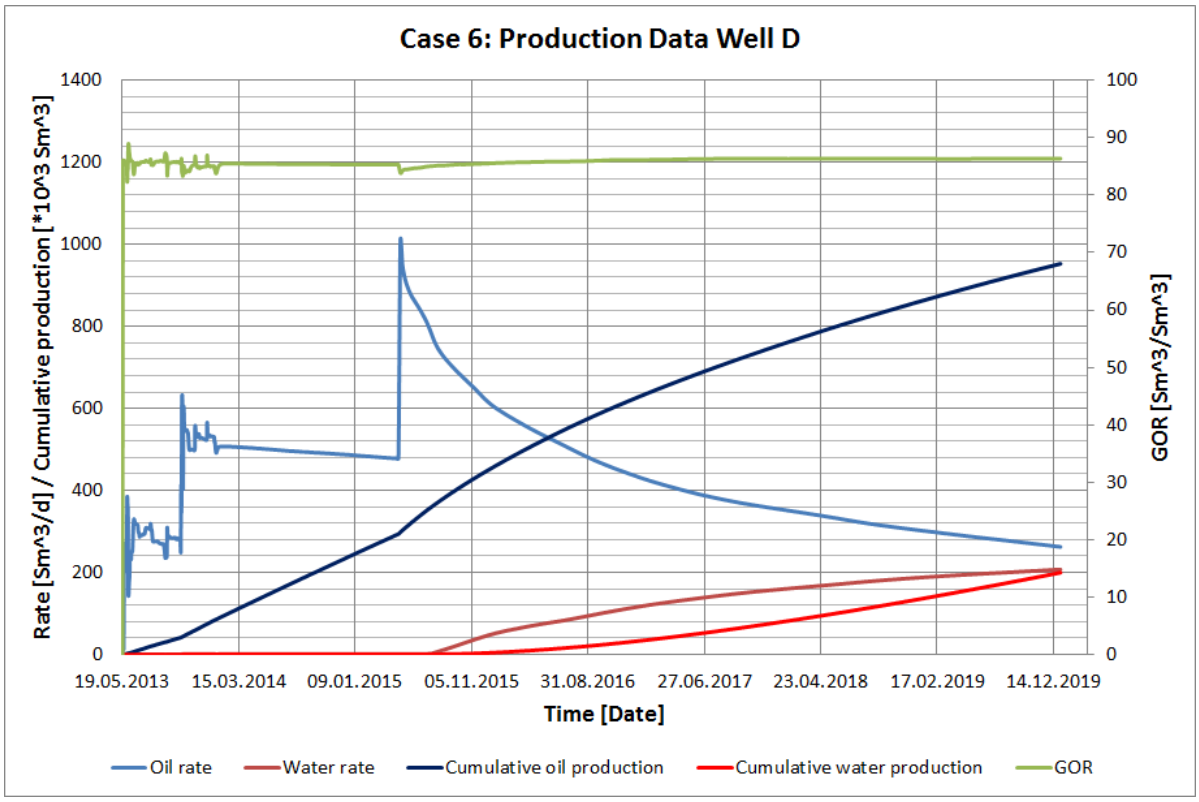

Figure 11.20: Results from Well D from the simulation of acidizing of Well D. The oil rate, water rate, GOR, cumulative oil production and cumulative water production are plotted.

The simulation of acidizing the well gives an increase in Well D's cumulative oil production of 21.1% from the basecase; the cumulative oil production is 952,900 Sm^3. The field's cumulative oil production is 1,685,300 Sm^3, an increase of 9.8% from the basecase. This gives a field oil recovery factor of 26% (which is an increase of 9.8% from the basecase).

Stimulating the well also increases the well's cumulative water production. The increase is 355.1%, giving a WC of 44%. Field cumulative water production increases with 8.4% from the basecase.

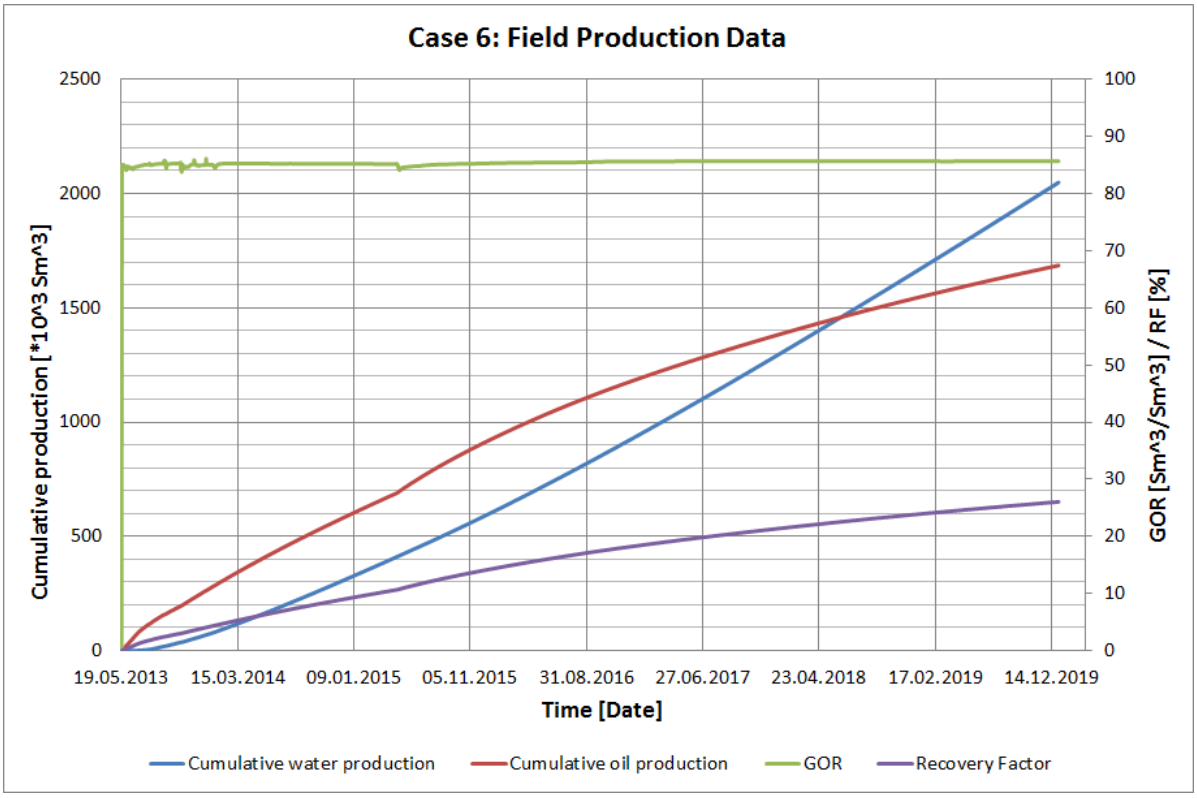

Figure 11.21: Results from the field from the simulation of acidizing of Well D. The GOR, recovery factor, cumulative oil production and cumulative water production are plotted.

Table 11.8: Estimated production from Well D after well stimulation with acid squeeze.

Parameter	*Unit*	Basecase	Case 6	Deviation
WOPT D	Sm^3	785,658.6	952,874.4	**+21.1%**
WWPT D	Sm^3	43,661.8	199,806.7	+355.1%
WGPT D	Sm^3	6.7*10^7	8.2*10^7	+21.1%
WWCT D	*fraction*	0.25	0.44	+76.8%
FOPT	Sm^3	1,532,319	1,685,299	**+9.8%**
FWPT	Sm^3	1,878,561	2,048,753	+8.4%
FGPT	Sm^3	1.3*10^8	1.4*10^8	+9.9%
FOE	*fraction*	0.24	0.26	**+9.8%**
FGOR	Sm^3/Sm^3	85.5	85.7	+0.2%

11.3.7 Productivity Indices

The productivity indices from the above cases are shown in **Figure 11.22**. The indices are used to describe the potential of the different IOR measures.

In Figure 11.22 it is observed that the IOR measure which obtains the highest PI is Case 3; multilateral towards east. Cases 3a, 3b, 2 and 1 have also shown to gain a better PI. It is observed in the figure that the PI falls quickly after the date of implementing the IOR measures. This may be due to decreasing rates and/or decreasing BHP in the wells.

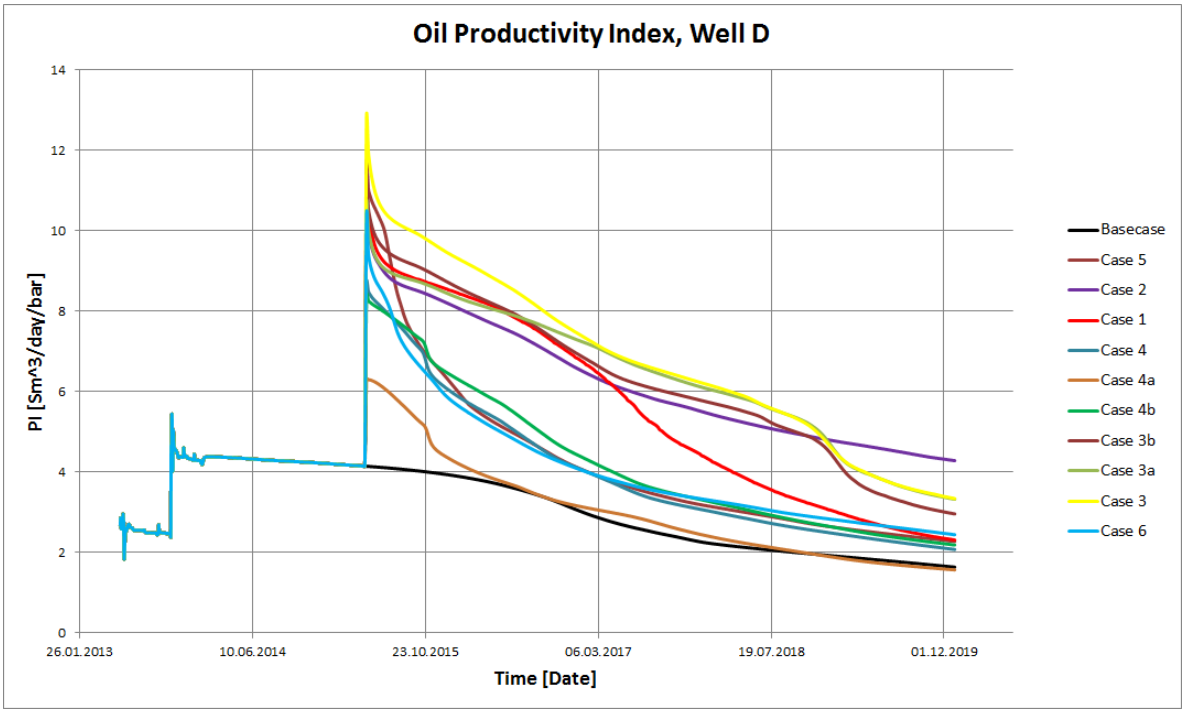

Figure 11.22: Productivity indices from the results of implementing IOR measures.

11.3.8 Results

Table 11.9 summarizes the field RF after implementing different IOR measures. In the table it is seen that Case 3 has the highest RF, and Case 4a has the lowest RF.

An economic evaluation is performed on the different cases in Chapter 12.

Table 11.9: Field oil recovery factor from the different IOR measures.

Case	Field RF	Deviation From Basecase
1	0.29	+21.7%
2	0.30	+26.3%
3	0.31	+29.2%
3a	0.30	+27.8%
3b	0.298	+25.8%
4	0.259	+9.4%
4a	0.24	+1.6%
4b	0.262	+10.6%
5	0.26	+9.8%
6	0.26	+9.8%

11.4 Slugging and Riser Evaluation

The effect of changing the riser from a 12 in. vertical riser to a 8 in. vertical riser has been simulated with the OLGA dynamic multiphase flow simulator. ECLIPSE 100 can not be used for simulating the pressure fluctuations in the riser, as the fluctuations are too small over a too short time interval. ECLIPSE uses average values hence, ignoring pressure fluctuations and slugging effects.

In OLGA turn down curves have been simulated to see the effect of the change of the riser from 12. in to 8 in.

11.4.1 Simulation Model

The simulation study has been performed by using the multiphase flow simulator OLGA 7.2.0., which is a proprietary software licensed by Schlumberger. Being a transient simulation tool, OLGA is able to resolve the flow changes in wells and pipelines with time.

Model Overview

The model is build from the pipeline geometry, and includes the flow lines from well head to PLEM and further to the MPFM at Jotun B. The pressure loss in the PLEM unit and the unknown pressure drop mechanisms between the wellhead and the Jotun B platform are modelled with a choke located at the PLEM. See **Figure 11.23**.

The 6 km long subsea tieback from the Jette wells to the riser base at Jotun B has an ID of 8 in. The riser up to Joutn B has a 12 in. ID and a length of 145 m. The flow line between PLEM and Jotun B is modelled as shown in **Figure 11.24**.

The model is made by Weatherford Petroleum Consultants.

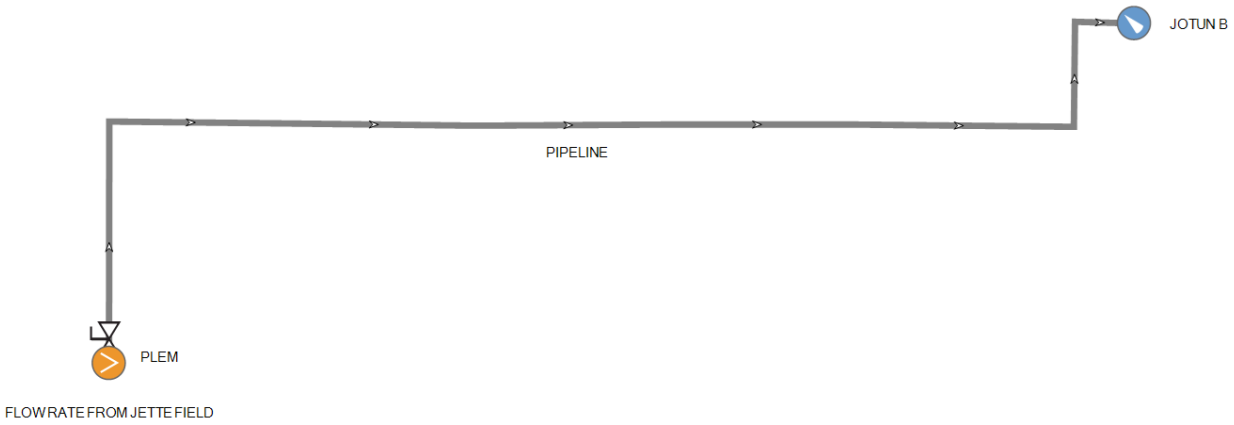

Figure 11.23: Schematics of the OLGA model. Taken from OLGA (Schlumberger 2013b).

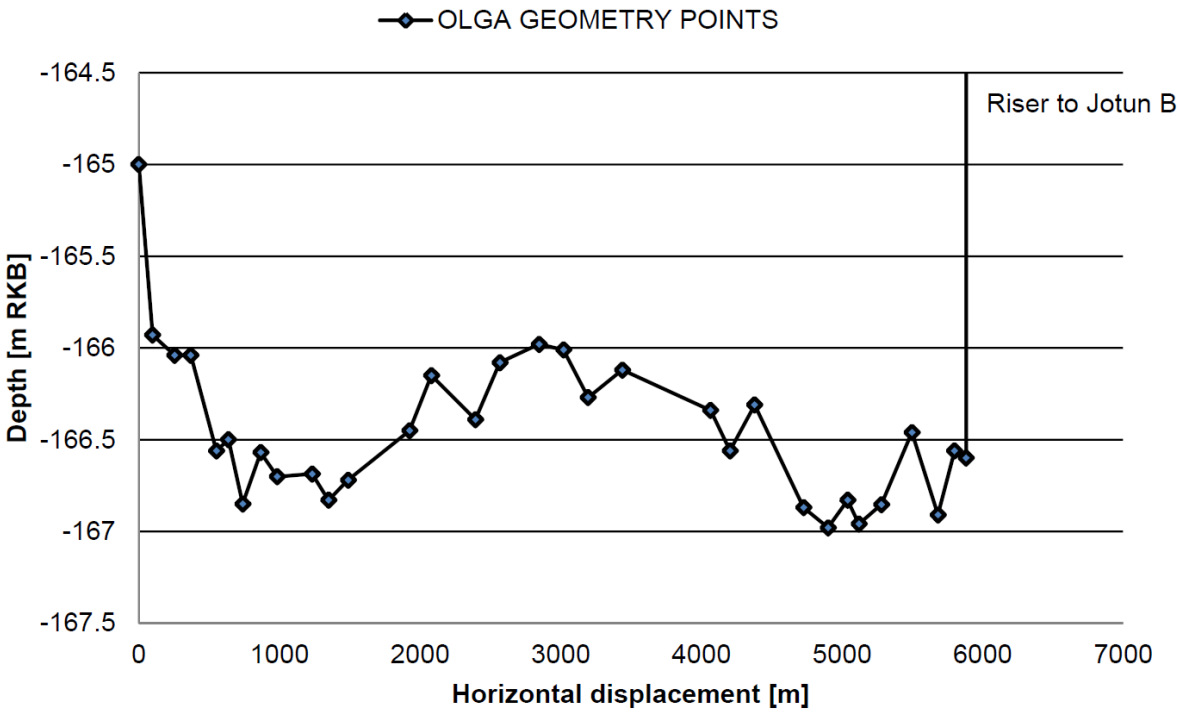

Figure 11.24: Flow line profile. Taken from Krogstad & Barbier (2014).

Simulation Input

The OLGA steady state simulation model has been used for flow correlation, with adiabatic temperature process; there is no temperature loss along the pipeline. The pressure has been fixed topside Jotun B to 20 bar, and oil rate, water rate and GOR are used as input parameters at the well head. The input parameters are taken from the basecase, 01.06.2016. That is one year after the date of implementing IOR measures.

The turn down curve has been made by simulating additional rates between 100 Sm^3/day and 3000 Sm^3/day.

11.4.2 Results

Figure 11.25 shows the turn down curves for the pipeline with a 8 in. riser and the pipeline with a 12 in. riser. It is observed in the figure that there is small differences in the pressure drop between PLEM and Jotun B. The differences are largest at low oil rates, below 1200 Sm^3/day. The small pressure drop changes indicate that, by changing the 12 in. riser to a 8 in. riser, there will not be any major changes in the observed slugging.

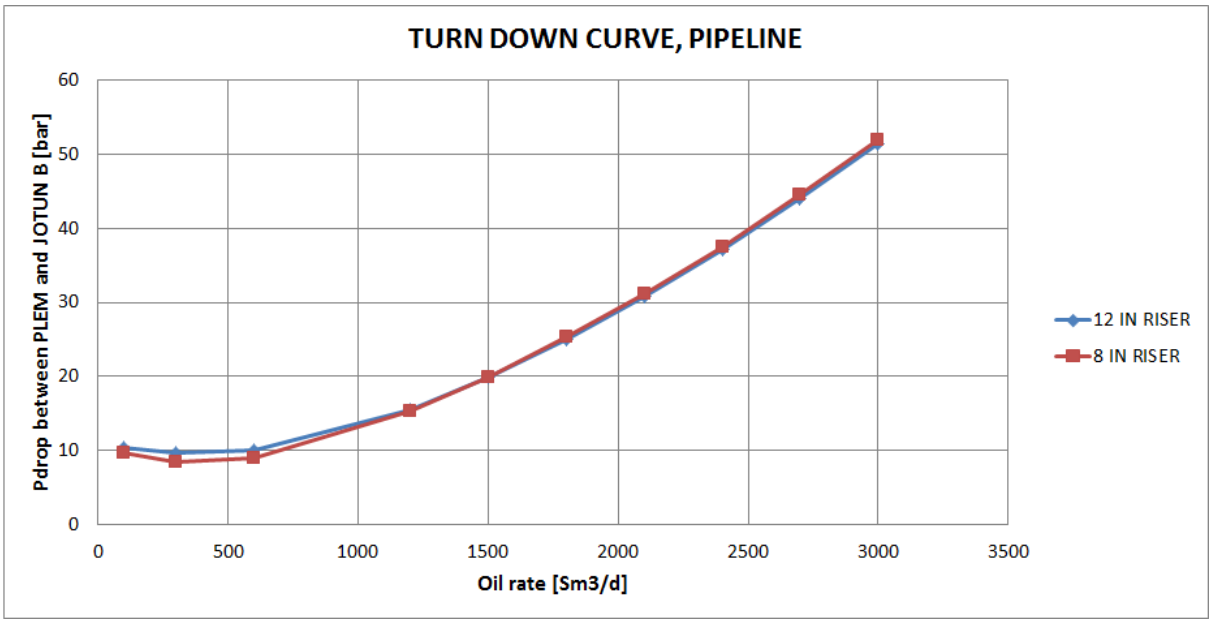

Figure 11.25: Turn down curve for both a pipeline with 8 in. riser and 12 in. riser. There is little change in pressure drop in the two risers.

The observations in Figure 11.25 indicates that there is a negligible effect of changing the riser. Hence, the IOR measures will not be simulated with a riser.

A study conducted by Weatherford Petroleum Consultants, in March 2013, found that high gas rates are effective to suppress the flow oscillations. The theoretical optimum for

Well D was found to be 96.000 Sm^3/day. This gives an oil production of 288 Sm^3/day. Such high gas rates was also found to be counter-productive with regard to oil production as they choke back the well due to high friction in the long flow line.

11.4.3 Software

OLGA Dynamic Multiphase Flow Simulator

The OLGA dynamic multiphase flow simulator (Schlumberger 2013*b*) models time-dependent behaviours, or transient flow, to maximize production potential using OLGA steady state. Transient modeling is an essential component for feasibility studies and field development design. Transient simulation with the OLGA simulator provides an added dimension to steady-state analyses by predicting system dynamics such as time-varying changes in flow rates, fluid compositions, temperature, solids deposition and operational changes. OLGA dynamic multiphase flow simulator is a Schlumberger software. (Schlumberger 2014*g*)

12 Economic Analysis

In the following chapter an economic analysis of the implementation of well intervention measures have been performed. The costs have been calculated with a model based on real data taken from Weatherford Petroleum Consultants, and the revenue have been estimated from the simulations in Chapter 11. Revenue from both oil and gas are estimated. The NPV has been calculated on the basis of the costs and revenue, and are used to evaluate the sustainability of the well intervention measures.

The costs of changing the riser have not been evaluated.

12.1 Time and Cost Estimation

The time and cost analysis at this stage has been approached by a break down of the major drilling and completion operational steps for the implementation of the well intervention measures. No learning curve is assumed in the estimates.

A probability distribution has been defined for each step by estimating the minimum required time (low or technical limit), expected or most likely (base = low x risk factor), and maximum operational time (high = base x 2). A PERT distribution has been used with end points defined by the low and high time estimates. By running a Monte Carlo simulation for all steps and distributions the final result will be an overall probability distribution for the time required to drill and complete the specific well.

The PERT distribution is a useful tool for modeling expert data. When used in a Monte Carlo simulation, the PERT distribution can be used to identify risks in projects and cost models based on the likelihood of meeting targets and goals across any number of project components. The PERT distribution can provide a close fit to the normal or log-normal distributions. Examples of the PERT distribution are seen in **Figure 12.1**.

The probability distribution for each step will include the assessed risks and unforeseen time delays due to conditions like hole instability and cleaning, directional drilling and casing/liner running problems, well control, stuck pipe, mechanical problems, etc. Waiting on Weather (WOW) is treated separately.

All inclusive day rates have been defined for drilling and completion operations. Day rates have been defined as a deterministic parameters, that is not risked.

The Authorization For Expenditure (AFE) time and cost estimate is defined as the 95% confidence limit (Nakken et al. 2010). The difference between AFE and P50 estimates define the contingency.

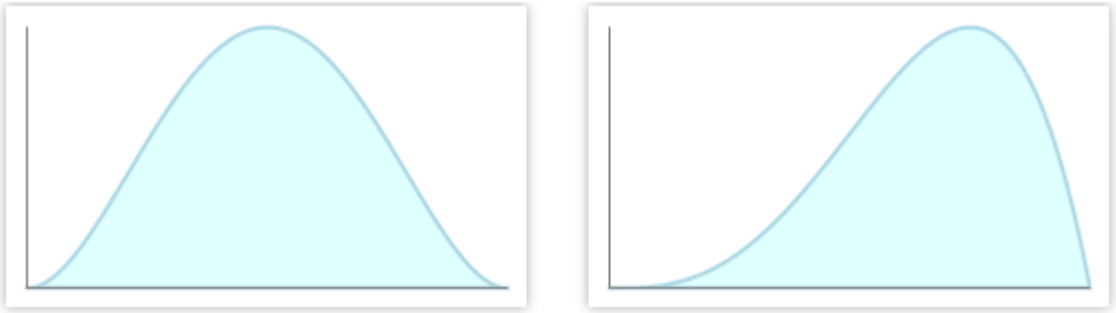

Figure 12.1: Examples of the PERT distribution. Values near the peak are more likely than values near the edges. From Vise (2000).

12.1.1 General Basis for Time and Cost Estimation

The target at the time and cost estimation at this feasibility level is an accuracy of ±30%. The rig rate assumptions given by Det Norske Oljeselskap are listed below (Nakken et al. 2010).

- Semi-submersible Drilling and Completion (DC) rig: 570,000 USD/day
- Light well intervention vessel: 200,000 - 250,000 USD/day

An exchange rate of 5.9 NOK/USD is used, rate per 14.05.2014 (Oslo Børs 2014). Experience data from Jetta, Eitri and Jotun (time and all inclusive day rate costs) have been applied with some modifications (Nakken et al. 2010). All inclusive day rates are split in drilling/completion operations. Shell has used similar spread values for their Jotun to Eitri exploration well study (Nakken et al. 2010). One may find spread rates at this level for other fields with drilling facilities at the platform. The operation days estimated in the calculations are based on experience[1].

- 5.8 MNOK / 6.4 MNOK for HWI
- 2.9 MNOK / 3.2 MNOK for LWI (assumed to be 50% of the HWI day rate[2])
- 1.5 MNOK for supply vessel [3]

[1]Personal communication with Jafar Abdollahi and Inge M. Carlsen. May 2014. Trondheim: Weatherford Petroleum Consultants AS

[2]Personal communication with Erik Iversen Nakken. May 2014. Trondheim: Weatherford Petroleum Consultants AS

[3]Personal communication with Erik Iversen Nakken. May 2014. Trondheim: Weatherford Petroleum Consultants AS

The completion costs have been raised somewhat to account for the suggested completions; premium sand screen completion with ICD's or cemented and perforated liner, downhole P/T-gauges and gas lift system. Costs associated with pre-engineering, rig mobilization/de-mobilization, Xmas tree and tubing hanger, subsea and topside facilities costs are not included. No coring or wireline/pipe conveyed logging is considered. All data acquisition is assumed performed by Measurement While Drilling (MWD) or Logging While Drilling (LWD).

12.1.2 Well Intervention Cases

Risk based time and cost estimates have been made for all the well intervention cases except Case 5 as Case 5 is considered not to be possible.

Case 1: Single-Lateral Well North

The resulting time and cost estimates for Case 1 are summarized in **Table 12.1**.

Table 12.1: Summary of risk based time and cost estimates for Case 1.

Case 1: Single-lateral North			
Time, cost and KPI estimates	Unit	Option 1	Option 2
Technical Limit (P5)	days	38	42
Expected (P50)	days	42	46
P50 Cost Estimates	MNOK	257	285
AFE (P95)	days	46	51
AFE Cost Estimate	MNOK	285	317
Drilling efficiency (P50)	m/day	130	130
Completion efficiency (P50)	days/compl.	15	19
Average daily cost (P50)	MNOK/day	6.1	6.2
Total number of meters	meters	1376	1376
Cost per meter	kNOK/m	187	207

KPI is the Key Performance Indicators. Further details on the basis for the time and cost estimation are shown in **Tables 12.2** and **12.3**.

Figures J.1 and **J.2** in **Appendix J** show the probability distribution of operation days, both completion options.

Table 12.2: Risk based time and cost estimates for Case 1 - Option 1.

Case 1 - completion option 1				Metrics			Time Distribution Assumption			Mean Estimates	
Step	Operation Description	TD (m MD RKB)	Length (m)	ROP (m/d)	Risk factor	Rate (MNOK/day)	Low (min) (days)	Base (days)	High (max) (days)	Time (days)	Cost (MNOK)
1	Rig move and positioning	0	0		1.15	5.8	2.0	2.3	4.6	2.6	15.3
2	Bullheading the well, secure the well	0	0		1.00	5.8	1.0	1.0	2.0	1.2	6.8
3	Prepare HXT	0	0		1.00	5.8	1.0	1.0	2.0	1.2	6.8
4	Rig up and test BOP, connect to riser	0	0		1.00	5.8	2.0	2.0	4.0	2.3	13.5
5	Pull tubing	0	0		1.70	5.8	1.5	2.6	5.1	2.8	16.2
5	Make up milling assembly and whipstock, RIH	0	0		1.00	6.4	1.0	1.0	2.0	1.2	7.5
6	Mill casing, clean hole, POOH	1800	0		1.20	6.4	5.0	6.0	12.0	6.8	43.7
7	Make up 8-1/2" BHA, RIH	1800	0		1.00	5.8	1.0	1.0	2.0	1.2	6.8
8	Drill 8-1/2" horizontal section to TD	3176.44	1376.44	360	1.20	5.8	3.8	4.6	9.2	5.2	30.3
9	Clean hole, scraper and spot pill	3176.44	0		1.00	6.4	1.0	1.0	2.0	1.2	7.5
10	Run screen and LC, displace OBM to packer fluid	3176.44	0		1.20	6.4	2.0	2.4	4.8	2.7	17.5
11	Set barrier in 9-5/8"	3176.44	0		1.15	6.4	1.0	1.2	2.3	1.3	8.4
12	Run upper completion	3176.44	0		1.15	6.4	3.0	3.5	6.9	4.0	25.3
13	Well clean-up to rig and testing	3176.44	0		1.00	6.4	3.0	3.0	6.0	3.5	22.4
14	Disconnect and pull BOP	3176.44	0		1.00	6.4	2.0	2.0	4.0	2.3	14.9
	WOW					6.0	0.0	1.0	10.3	2.4	14.5
	Total time & cost drilling (P50)									41.9	257.3

Table 12.3: Risk based time and cost estimates for Case 1 - Option 2.

Case 1 - completion option 2				Metrics			Time Distribution Assumption			Mean Estimates	
Step	Operation Description	TD (m MD RKB)	Length (m)	ROP (m/d)	Risk factor	Rate (MNOK/day)	Low (min) (days)	Base (days)	High (max) (days)	Time (days)	Cost (MNOK)
1	Rig move and positioning	0	0		1.15	5.8	2.0	2.3	4.6	2.6	15.3
2	Bullheading the well, secure the well	0	0		1.00	5.8	1.0	1.0	2.0	1.2	6.8
3	Prepare HXT	0	0		1.00	5.8	1.0	1.0	2.0	1.2	6.8
4	Rig up and test BOP, connect to riser	0	0		1.00	5.8	2.0	2.0	4.0	2.3	13.5
5	Pull tubing	0	0		1.70	5.8	1.5	2.6	5.1	2.8	16.2
5	Make up milling assembly and whipstock, RIH	0	0		1.00	6.4	1.0	1.0	2.0	1.2	7.5
6	Mill casing, clean hole, POOH	1800	0		1.20	6.4	5.0	6.0	12.0	6.8	43.7
7	Make up 8-1/2" BHA, RIH	1800	0		1.00	5.8	1.0	1.0	2.0	1.2	6.8
8	Drill 8-1/2" horizontal section to TD	3176.44	1376.44	360	1.20	5.8	3.8	4.6	9.2	5.2	30.3
9	Clean hole, scraper and spot pill	3176.44	0		1.00	6.4	1.0	1.0	2.0	1.2	7.5
10	Run, cement and perforate liner, displace OBM to packer fluid	3176.44	0		1.20	6.4	5.0	6.0	12.0	6.8	43.7
11	Set barrier in 9-5/8"	3176.44	0		1.15	6.4	1.0	1.2	2.3	1.3	8.4
12	Run upper completion	3176.44	0		1.15	6.4	3.0	3.5	6.9	4.0	25.3
13	Well clean-up to rig and testing	3176.44	0		1.00	6.4	3.0	3.0	6.0	3.5	22.4
14	Disconnect and pull BOP	3176.44	0		1.00	6.4	2.0	2.0	4.0	2.3	14.9
	WOW					6.0	0.0	1.1	11.4	2.7	16.0
	Total time & cost drilling (P50)									46.3	285.1

Case 2: Single-Lateral Well East

The resulting time and cost estimates for Case 2 are summarized in **Table 12.4**.

Further details on the basis for the time and cost estimation are shown in **Tables 12.5** and **12.6**. **Figures J.3** and **J.3** show the probability distribution of operation days, both completion options. See Appendix J.

Table 12.4: Summary of risk based time and cost estimates for Case 2.

Case 2: Single-lateral East			
Time, cost and KPI estimates	Unit	Option 1	Option 2
Technical Limit (P5)	days	40	43
Expected (P50)	days	44	48
P50 Cost Estimates	MNOK	268	296
AFE (P95)	days	48	53
AFE Cost Estimate	MNOK	297	328
Drilling efficiency (P50)	m/day	137	137
Completion efficiency (P50)	days/compl.	15	16
Average daily cost (P50)	MNOK/day	6.1	6.2
Total number of meters	meters	1768	1768
Cost per meter	kNOK/m	152	167

Table 12.5: Risk based time and cost estimates for Case 2 - Option 1.

Case 2 - completion option 1				Metrics			Time Distribution Assumption			Mean Estimates	
Step	Operation Description	TD (m MD RKB)	Length (m)	ROP (m/d)	Risk factor	Rate (MNOK/day)	Low (min) (days)	Base (days)	High (max) (days)	Time (days)	Cost (MNOK)
1	Rig move and positioning	0	0		1.15	5.8	2.0	2.3	4.6	2.6	15.3
2	Bullheading the well, secure the well	0	0		1.00	5.8	1.0	1.0	2.0	1.2	6.8
3	Prepare HXT	0	0		1.00	5.8	1.0	1.0	2.0	1.2	6.8
4	Rig up and test BOP, connect to riser	0	0		1.00	5.8	2.0	2.0	4.0	2.3	13.5
5	Pull tubing	0	0		1.70	5.8	1.5	2.6	5.1	2.8	16.2
5	Make up milling assembly and whipstock, RIH	0	0		1.00	6.4	1.0	1.0	2.0	1.2	7.5
6	Mill casing, clean hole, POOH	1800	0		1.20	6.4	5.0	6.0	12.0	6.8	43.7
7	Make up 8-1/2" BHA, RIH	1800	0		1.00	5.8	1.0	1.0	2.0	1.2	6.8
8	Drill 8-1/2" horizontal section to TD	3568.1	1768.1	360	1.20	5.8	4.9	5.9	11.8	6.7	38.9
9	Clean hole, scraper and spot pill	3568.1	0		1.00	6.4	1.0	1.0	2.0	1.2	7.5
10	Run screen and LC, displace OBM to packer fluid	3568.1	0		1.20	6.4	2.2	2.6	5.3	3.0	19.2
11	Set barrier in 9-5/8"	3568.1	0		1.15	6.4	1.0	1.2	2.3	1.3	8.4
12	Run upper completion	3568.1	0		1.15	6.4	3.0	3.5	6.9	4.0	25.3
13	Well clean-up to rig and testing	3568.1	0		1.00	6.4	3.0	3.0	6.0	3.5	22.4
14	Disconnect and pull BOP	3568.1	0		1.00	6.4	2.0	2.0	4.0	2.3	14.9
	WOW					6.0	0.0	1.1	10.8	2.5	15.1
	Total time & cost drilling (P50)									43.8	268.3

Table 12.6: Risk based time and cost estimates for Case 2 - Option 2.

Case 2 - completion option 2				Metrics			Time Distribution Assumption			Mean Estimates	
Step	Operation Description	TD	Length	ROP	Risk	Rate	Low (min)	Base	High (max)	Time	Cost
		(m MD RKB)	(m)	(m/d)	factor	(MNOK/day)	(days)	(days)	(days)	(days)	(MNOK)
1	Rig move and positioning	0	0		1.15	5.8	2.0	2.3	4.6	2.6	15.3
2	Bullheading the well, secure the well	0	0		1.00	5.8	1.0	1.0	2.0	1.2	6.8
3	Prepare HXT	0	0		1.00	5.8	1.0	1.0	2.0	1.2	6.8
4	Rig up and test BOP, connect to riser	0	0		1.00	5.8	2.0	2.0	4.0	2.3	13.5
5	Pull tubing	0	0		1.70	5.8	1.5	2.6	5.1	2.8	16.2
5	Make up milling assembly and whipstock, RIH	0	0		1.00	6.4	1.0	1.0	2.0	1.2	7.5
6	Mill casing, clean hole, POOH	1800	0		1.20	6.4	5.0	6.0	12.0	6.8	43.7
7	Make up 8-1/2" BHA, RIH	1800	0		1.00	5.8	1.0	1.0	2.0	1.2	6.8
8	Drill 8-1/2" horizontal section to TD	3568.1	1768.1	360	1.20	5.8	4.9	5.9	11.8	6.7	38.9
9	Clean hole, scraper and spot pill	3568.1	0		1.00	6.4	1.0	1.0	2.0	1.2	7.5
10	Run, cement and perforate liner, displace OBM to packer fluid	3568.1	0		1.20	6.4	5.2	6.2	12.5	7.1	45.5
11	Set barrier in 9-5/8"	3568.1	0		1.15	6.4	1.0	1.2	2.3	1.3	8.4
12	Run upper completion	3568.1	0		1.15	6.4	3.0	3.5	6.9	4.0	25.3
13	Well clean-up to rig and testing	3568.1	0		1.00	6.4	3.0	3.0	6.0	3.5	22.4
14	Disconnect and pull BOP	3568.1	0		1.00	6.4	2.0	2.0	4.0	2.3	14.9
	WOW					6.0	0.0	1.2	11.9	2.8	16.6
	Total time & cost drilling (P50)									**48.1**	**296.1**

Case 3: Multilateral Well East

The resulting time and cost estimates for Case 3 are summarized in **Table 12.7**. **Figures J.5- J.8** show the probability distribution of operation days, all completion options. See Appendix J.

Further details on the basis for the time and cost estimation are shown in **Tables 12.8-12.11**.

Table 12.7: Summary of risk based time and cost estimates for Case 3.

Case 3: Multilateral East					
Time, cost and KPI estimates	Unit	Option 1	Option 2	Option 3	Option 4
Technical Limit (P5)	days	60	68	57	61
Expected (P50)	days	65	74	62	67
P50 Cost Estimates	MNOK	402	457	381	409
AFE (P95)	days	72	82	69	73
AFE Cost Estimate	MNOK	441	4504	419	450
Drilling efficiency (P50)	m/day	134	135	134	134
Completion efficiency (P50)	days/compl.	35	38	32	33
Average daily cost (P50)	MNOK/day	6.2	6.2	6.1	6.1
Total number of meters	meters	1847	1847	1847	1847
Cost per meter	kNOK/m	217	247	206	221

Table 12.8: Risk based time and cost estimates for Case 3 - Option 1.

Case 3 - completion option 1				Metrics			Time Distribution Assumption			Mean Estimates	
Step	Operation Description	TD (m MD RKB)	Length (m)	ROP (m/d)	Risk factor	Rate (MNOK/day)	Low (min) (days)	Base (days)	High (max) (days)	Time (days)	Cost (MNOK)
1	Rig move and positioning	0	0		1.15	5.8	2.0	2.3	4.6	2.6	15.3
2	Bullheading the well, secure the well	0	0		1.00	5.8	1.0	1.0	2.0	1.2	6.8
3	Prepare HXT	0	0		1.00	5.8	1.0	1.0	2.0	1.2	6.8
4	Rig up and test BOP, connect to riser	0	0		1.00	5.8	2.0	2.0	4.0	2.3	13.5
5	Pull tubing	0	0		1.70	5.8	1.5	2.6	5.1	2.8	16.2
5	Make up milling assembly and whipstock, RIH	0	0		1.00	6.4	1.0	1.0	2.0	1.2	7.5
6	Mill casing, clean hole, POOH	1850	0		1.20	6.4	5.0	6.0	12.0	6.8	43.7
7	Make up 8-1/2" BHA, RIH	1850	0		1.00	5.8	1.0	1.0	2.0	1.2	6.8
8	Drill 8-1/2" horizontal section to TD	3697.25	1847.25	360	1.20	5.8	5.1	6.2	12.3	7.0	40.7
9	Clean hole, scraper and spot pill	3697.25	0		1.00	6.4	1.0	1.0	2.0	1.2	7.5
10	Run screen and LC, displace OBM to packer fluid	3697.25	0		1.20	6.4	2.2	2.6	5.3	3.0	19.2
11	Make up milling assembly and whipstock, RIH	0	0		1.00	6.4	1.0	1.0	2.0	1.2	7.5
12	Mill casing, clean hole, POOH	1750	0		1.20	6.4	5.0	6.0	12.0	6.8	43.7
13	Make up 8-1/2" BHA, RIH	1750	0		1.00	5.8	1.0	1.0	2.0	1.2	6.8
14	Drill 8-1/2" horizontal section to TD	3533.59	1783.59	360	1.20	5.8	5.0	5.9	11.9	6.8	39.3
15	Clean hole, scraper and spot pill	3533.59	0		1.00	6.4	1.0	1.0	2.0	1.2	7.5
16	Run screen and LC, displace OBM to packer fluid	3533.59	0		1.20	6.4	2.2	2.6	5.3	3.0	19.2
17	Set barrier in 9-5/8"	3533.59	0		1.15	6.4	1.0	1.2	2.3	1.3	8.4
18	Run upper completion	3533.59	0		1.15	6.4	3.0	3.5	6.9	4.0	25.3
19	Well clean-up to rig and testing	3533.59	0		1.00	6.4	3.0	3.0	6.0	3.5	22.4
20	Disconnect and pull BOP	3533.59	0		1.00	6.4	2.0	2.0	4.0	2.3	14.9
	WOW					6.0	0.0	1.6	16.1	3.8	22.6
	Total time & cost drilling (P50)									**65.4**	**401.5**

Table 12.9: Risk based time and cost estimates for Case 3 - Option 2.

Case 3 - completion option 2				Metrics			Time Distribution Assumption			Mean Estimates	
Step	Operation Description	TD (m MD RKB)	Length (m)	ROP (m/d)	Risk factor	Rate (MNOK/day)	Low (min) (days)	Base (days)	High (max) (days)	Time (days)	Cost (MNOK)
1	Rig move and positioning	0	0		1.15	5.8	2	2.3	4.6	2.6	15.3
2	Bullheading the well, secure the well	0	0		1.0	5.8	1	1	2	1.2	6.8
3	Prepare HXT	0	0		1.0	5.8	1.0	1.0	2.0	1.2	6.8
4	Rig up and test BOP, connect to riser	0	0		1.0	5.8	2.0	2.0	4.0	2.3	13.5
5	Pull tubing	0	0		1.70	5.8	1.5	2.6	5.1	2.8	16.2
5	Make up milling assembly and whipstock, RIH	0	0		1.00	6.4	1.0	1.0	2.0	1.2	7.5
6	Mill casing, clean hole, POOH	1850	0		1.20	6.4	5.0	6.0	12.0	6.8	43.7
7	Make up 8-1/2" BHA, RIH	1850	0		1.00	5.8	1.0	1.0	2.0	1.2	6.8
8	Drill 8-1/2" horizontal section to TD	3697.25	1847.25	360	1.20	5.8	5.1	6.2	12.3	7.0	40.7
9	Clean hole, scraper and spot pill	3697.25	0		1.00	6.4	1.0	1.0	2.0	1.2	7.5
10	Run, cement and perforate liner, displace OBM to packer fluid	3697.25	0		1.20	6.4	5.2	6.2	12.5	7.1	45.5
11	Make up milling assembly and whipstock, RIH	0	0		1.00	6.4	1.0	1.0	2.0	1.2	7.5
12	Mill casing, clean hole, POOH	1750	0		1.20	6.4	5.0	6.0	12.0	6.8	43.7
13	Make up 8-1/2" BHA, RIH	1750	0		1.00	5.8	1.0	1.0	2.0	1.2	6.8
14	Drill 8-1/2" horizontal section to TD	3533.59	1783.59	360	1.20	5.8	5.0	5.9	11.9	6.8	39.3
15	Clean hole, scraper and spot pill	3533.59	0		1.00	6.4	1.0	1.0	2.0	1.2	7.5
16	Run, cement and perforate liner, displace OBM to packer fluid	3533.59	0		1.20	6.4	5.2	6.2	12.5	7.1	45.5
17	Set barrier in 9-5/8"	3533.59	0		1.15	6.4	1.0	1.2	2.3	1.3	8.4
18	Run upper completion	3533.59	0		1.15	6.4	3.0	3.5	6.9	4.0	25.3
19	Well clean-up to rig and testing	3533.59	0		1.00	6.4	3.0	3.0	6.0	3.5	22.4
20	Disconnect and pull BOP	3533.59	0		1.00	6.4	2.0	2.0	4.0	2.3	14.9
	WOW					6.0	0.0	1.8	18.3	4.3	25.6
	Total time & cost drilling (P50)									**74.1**	**457.0**

Table 12.10: Risk based time and cost estimates for Case 3 - Option 3.

Case 3 - completion option 3				Metrics			Time Distribution Assumption			Mean Estimates	
Step	Operation Description	TD (m MD RKB)	Length (m)	ROP (m/d)	Risk factor	Rate (MNOK/day)	Low (min) (days)	Base (days)	High (max) (days)	Time (days)	Cost (MNOK)
1	Rig move and positioning	0	0		1.15	5.8	2.0	2.3	4.6	2.6	15.3
2	Bullheading the well, secure the well	0	0		1.00	5.8	1.0	1.0	2.0	1.2	6.8
3	Prepare HXT	0	0		1.00	5.8	1.0	1.0	2.0	1.2	6.8
4	Rig up and test BOP, connect to riser	0	0		1.00	5.8	2.0	2.0	4.0	2.3	13.5
5	Pull tubing	0	0		1.70	5.8	1.5	2.6	5.1	2.8	16.2
5	Make up milling assembly and whipstock, RIH	0	0		1.00	6.4	1.0	1.0	2.0	1.2	7.5
6	Mill casing, clean hole, POOH	1850	0		1.20	6.4	5.0	6.0	12.0	6.8	43.7
7	Make up 8-1/2" BHA, RIH	1850	0		1.00	5.8	1.0	1.0	2.0	1.2	6.8
8	Drill 8-1/2" horizontal section to TD	3697.25	1847.25	360	1.20	5.8	5.1	6.2	12.3	7.0	40.7
9	Clean hole, scraper and spot pill	3697.25	0		1.00	6.4	1.0	1.0	2.0	1.2	7.5
10	Run screen and LC, displace OBM to packer fluid	3697.25	0		1.20	6.4	2.2	2.6	5.3	3.0	19.2
11	Make up milling assembly and whipstock, RIH	0	0		1.00	6.4	1.0	1.0	2.0	1.2	7.5
12	Mill casing, clean hole, POOH	1750	0		1.20	6.4	5.0	6.0	12.0	6.8	43.7
13	Make up 8-1/2" BHA, RIH	1750	0		1.00	5.8	1.0	1.0	2.0	1.2	6.8
14	Drill 8-1/2" horizontal section to TD	3533.59	1783.59	360	1.20	5.8	5.0	5.9	11.9	6.8	39.3
15	Clean hole, scraper and spot pill	3533.59	0		1.00	6.4	1.0	1.0	2.0	1.2	7.5
17	Set barrier in 9-5/8"	3533.59	0		1.15	6.4	1.0	1.2	2.3	1.3	8.4
18	Run upper completion	3533.59	0		1.15	6.4	3.0	3.5	6.9	4.0	25.3
19	Well clean-up to rig and testing	3533.59	0		1.00	6.4	3.0	3.0	6.0	3.5	22.4
20	Disconnect and pull BOP	3533.59	0		1.00	6.4	2.0	2.0	4.0	2.3	14.9
	WOW					6.0	0.0	1.5	15.4	3.6	21.5
	Total time & cost drilling (P50)									62.2	381.2

Table 12.11: Risk based time and cost estimates for Case 3 - Option 4.

Case 3 - completion option 4				Metrics			Time Distribution Assumption			Mean Estimates	
Step	Operation Description	TD (m MD RKB)	Length (m)	ROP (m/d)	Risk factor	Rate (MNOK/day)	Low (min) (days)	Base (days)	High (max) (days)	Time (days)	Cost (MNOK)
1	Rig move and positioning	0	0		1.15	5.8	2	2.3	4.6	2.6	15.3
2	Bullheading the well, secure the well	0	0		1.0	5.8	1	1	2	1.2	6.8
3	Prepare HXT	0	0		1.0	5.8	1.0	1.0	2.0	1.2	6.8
4	Rig up and test BOP, connect to riser	0	0		1.0	5.8	2.0	2.0	4.0	2.3	13.5
5	Pull tubing	0	0		1.70	5.8	1.5	2.6	5.1	2.8	16.2
5	Make up milling assembly and whipstock, RIH	0	0		1.00	6.4	1.0	1.0	2.0	1.2	7.5
6	Mill casing, clean hole, POOH	1850	0		1.20	6.4	5.0	6.0	12.0	6.8	43.7
7	Make up 8-1/2" BHA, RIH	1850	0		1.00	5.8	1.0	1.0	2.0	1.2	6.8
8	Drill 8-1/2" horizontal section to TD	3697.25	1847.25	360	1.20	5.8	5.1	6.2	12.3	7.0	40.7
9	Clean hole, scraper and spot pill	3697.25	0		1.00	6.4	1.0	1.0	2.0	1.2	7.5
10	Run, cement and perforate liner, displace OBM to packer fluid	3697.25	0		1.20	6.4	3.0	3.6	7.2	4.1	26.2
11	Make up milling assembly and whipstock, RIH	0	0		1.00	6.4	1.0	1.0	2.0	1.2	7.5
12	Mill casing, clean hole, POOH	1750	0		1.20	6.4	5.0	6.0	12.0	6.8	43.7
13	Make up 8-1/2" BHA, RIH	1750	0		1.00	5.8	1.0	1.0	2.0	1.2	6.8
14	Drill 8-1/2" horizontal section to TD	3533.59	1783.59	360	1.20	5.8	5.0	5.9	11.9	6.8	39.3
15	Clean hole, scraper and spot pill	3533.59	0		1.00	6.4	1.0	1.0	2.0	1.2	7.5
17	Set barrier in 9-5/8"	3533.59	0		1.15	6.4	1.0	1.2	2.3	1.3	8.4
18	Run upper completion	3533.59	0		1.15	6.4	3.0	3.5	6.9	4.0	25.3
19	Well clean-up to rig and testing	3533.59	0		1.00	6.4	3.0	3.0	6.0	3.5	22.4
20	Disconnect and pull BOP	3533.59	0		1.00	6.4	2.0	2.0	4.0	2.3	14.9
	WOW					6.0	0.0	1.6	15.6	3.7	21.9
	Total time & cost drilling (P50)									63.4	388.6

Case 4: Multilateral Well West

The resulting time and cost estimates for Case 4 are summarized in **Table 12.12**. **Figures J.9- J.12** show the probability distribution of operation days, all completion options. See Appendix J.

Further details on the basis for the time and cost estimation are shown in **Tables 12.13-12.16**.

Table 12.12: Summary of risk based time and cost estimates for Case 4.

Case 4: Multilateral West					
Time, cost and KPI estimates	Unit	Option 1	Option 2	Option 3	Option 4
Technical Limit (P5)	days	59	68	56	60
Expected (P50)	days	65	75	62	66
P50 Cost Estimates	MNOK	399	460	377	405
AFE (P95)	days	71	82	68	73
AFE Cost Estimate	MNOK	439	507	415	446
Drilling efficiency (P50)	m/day	153	153	153	153
Completion efficiency (P50)	days/compl.	36	39	33	35
Average daily cost (P50)	MNOK/day	6.1	6.1	6.1	6.1
Total number of meters	meters	1470	1470	1470	1470
Cost per meter	kNOK/m	271	313	256	275

Table 12.13: Risk based time and cost estimates for Case 4 - Option 1.

Case 4 - completion option 1				Metrics			Time Distribution Assumption			Mean Estimates	
Step	Operation Description	TD (m MD RKB)	Length (m)	ROP (m/d)	Risk factor	Rate (MNOK/day)	Low (min) (days)	Base (days)	High (max) (days)	Time (days)	Cost (MNOK)
1	Rig move and positioning	0	0		1.15	5.8	2.0	2.3	4.6	2.6	15.3
2	Bullheading the well, secure the well	0	0		1.00	5.8	1.0	1.0	2.0	1.2	6.8
3	Prepare HXT	0	0		1.00	5.8	1.0	1.0	2.0	1.2	6.8
4	Rig up and test BOP, connect to riser	0	0		1.00	5.8	2.0	2.0	4.0	2.3	13.5
5	Pull tubing	0	0		1.70	5.8	1.5	2.6	5.1	2.8	16.2
5	Make up milling assembly and whipstock, RIH	0	0		1.00	6.4	1.0	1.0	2.0	1.2	7.5
6	Mill casing, clean hole, POOH	1850	0		1.20	6.4	5.0	6.0	12.0	6.8	43.7
7	Make up 8-1/2" BHA, RIH	1850	0		1.00	5.8	1.0	1.0	2.0	1.2	6.8
8	Drill 8-1/2" horizontal section to TD	3320.3	1470.3	360	1.20	5.8	4.1	4.9	9.8	5.6	32.4
9	Clean hole, scraper and spot pill	3320.3	0		1.00	6.4	1.0	1.0	2.0	1.2	7.5
10	Run screen and LC, displace OBM to packer fluid	3320.3	0		1.20	6.4	2.0	2.4	4.8	2.7	17.5
11	Make up milling assembly and whipstock, RIH	0	0		1.00	6.4	1.0	1.0	2.0	1.2	7.5
12	Mill casing, clean hole, POOH	1750	0		1.20	6.4	5.0	6.0	12.0	6.8	43.7
13	Make up 8-1/2" BHA, RIH	1750	0		1.00	5.8	1.0	1.0	2.0	1.2	6.8
14	Drill 8-1/2" horizontal section to TD	3806.55	2056.55	360	1.20	5.8	5.7	6.9	13.7	7.8	45.3
15	Clean hole, scraper and spot pill	3806.55	0		1.00	6.4	1.0	1.0	2.0	1.2	7.5
16	Run screen and LC, displace OBM to packer fluid	3806.55	0		1.20	6.4	2.4	2.9	5.8	3.3	21.0
17	Set barrier in 9-5/8"	3806.55	0		1.15	6.4	1.0	1.2	2.3	1.3	8.4
18	Run upper completion	3806.55	0		1.15	6.4	3.0	3.5	6.9	4.0	25.3
19	Well clean-up to rig and testing	3806.55	0		1.00	6.4	3.0	3.0	6.0	3.5	22.4
20	Disconnect and pull BOP	3806.55	0		1.00	6.4	2.0	2.0	4.0	2.3	14.9
	WOW					6.0	0.0	1.6	16.0	3.7	22.5
	Total time & cost drilling (P50)									65.0	399.1

Table 12.14: Risk based time and cost estimates for Case 4 - Option 2.

Case 4 - completion option 2				Metrics			Time Distribution Assumption			Mean Estimates	
Step	Operation Description	TD (m MD RKB)	Length (m)	ROP (m/d)	Risk factor	Rate (MNOK/day)	Low (min) (days)	Base (days)	High (max) (days)	Time (days)	Cost (MNOK)
1	Rig move and positioning	0	0		1.15	5.8	2	2.3	4.6	2.6	15.3
2	Bullheading the well, secure the well	0	0		1.0	5.8	1	1	2	1.2	6.8
3	Prepare HXT	0	0		1.0	5.8	1.0	1.0	2.0	1.2	6.8
4	Rig up and test BOP, connect to riser	0	0		1.0	5.8	2.0	2.0	4.0	2.3	13.5
5	Pull tubing	0	0		1.70	5.8	1.5	2.6	5.1	2.8	16.2
5	Make up milling assembly and whipstock, RIH	0	0		1.00	6.4	1.0	1.0	2.0	1.2	7.5
6	Mill casing, clean hole, POOH	1850	0		1.20	6.4	5.0	6.0	12.0	6.8	43.7
7	Make up 8-1/2" BHA, RIH	1850	0		1.00	5.8	1.0	1.0	2.0	1.2	6.8
8	Drill 8-1/2" horizontal section to TD	3320.3	1470.3	360	1.20	5.8	4.1	4.9	9.8	5.6	32.4
9	Clean hole, scraper and spot pill	3320.3	0		1.00	6.4	1.0	1.0	2.0	1.2	7.5
10	Run, cement and perforate liner, displace OBM to packer fluid	3320.3	0		1.20	6.4	5.0	6.0	12.0	6.8	43.7
11	Make up milling assembly and whipstock, RIH	0	0		1.00	6.4	1.0	1.0	2.0	1.2	7.5
12	Mill casing, clean hole, POOH	1750	0		1.20	6.4	5.0	6.0	12.0	6.8	43.7
13	Make up 8-1/2" BHA, RIH	1750	0		1.00	5.8	1.0	1.0	2.0	1.2	6.8
14	Drill 8-1/2" horizontal section to TD	3806.55	2056.55	360	1.20	5.8	5.7	6.9	13.7	7.8	45.3
15	Clean hole, scraper and spot pill	3806.55	0		1.00	6.4	1.0	1.0	2.0	1.2	7.5
16	Run, cement and perforate liner, displace OBM to packer fluid	3806.55	0		1.20	6.4	6.0	7.2	14.4	8.2	52.5
17	Set barrier in 9-5/8"	3806.55	0		1.15	6.4	1.0	1.2	2.3	1.3	8.4
18	Run upper completion	3806.55	0		1.15	6.4	3.0	3.5	6.9	4.0	25.3
19	Well clean-up to rig and testing	3806.55	0		1.00	6.4	3.0	3.0	6.0	3.5	22.4
20	Disconnect and pull BOP	3806.55	0		1.00	6.4	2.0	2.0	4.0	2.3	14.9
	WOW					6.0	0.0	1.8	18.4	4.3	25.8
	Total time & cost drilling (P50)									**74.6**	**460.1**

Table 12.15: Risk based time and cost estimates for Case 4 - Option 3.

Case 4 - completion option 3				Metrics			Time Distribution Assumption			Mean Estimates	
Step	Operation Description	TD (m MD RKB)	Length (m)	ROP (m/d)	Risk factor	Rate (MNOK/day)	Low (min) (days)	Base (days)	High (max) (days)	Time (days)	Cost (MNOK)
1	Rig move and positioning	0	0		1.15	5.8	2.0	2.3	4.6	2.6	15.3
2	Bullheading the well, secure the well	0	0		1.00	5.8	1.0	1.0	2.0	1.2	6.8
3	Prepare HXT	0	0		1.00	5.8	1.0	1.0	2.0	1.2	6.8
4	Rig up and test BOP, connect to riser	0	0		1.00	5.8	2.0	2.0	4.0	2.3	13.5
5	Pull tubing	0	0		1.70	5.8	1.5	2.6	5.1	2.8	16.2
5	Make up milling assembly and whipstock, RIH	0	0		1.00	6.4	1.0	1.0	2.0	1.2	7.5
6	Mill casing, clean hole, POOH	1850	0		1.20	6.4	5.0	6.0	12.0	6.8	43.7
7	Make up 8-1/2" BHA, RIH	1850	0		1.00	5.8	1.0	1.0	2.0	1.2	6.8
8	Drill 8-1/2" horizontal section to TD	3320.3	1470.3	360	1.20	5.8	4.1	4.9	9.8	5.6	32.4
9	Clean hole, scraper and spot pill	3320.3	0		1.00	6.4	1.0	1.0	2.0	1.2	7.5
10	Run screen and LC, displace OBM to packer fluid	3320.3	0		1.20	6.4	2.0	2.4	4.8	2.7	17.5
11	Make up milling assembly and whipstock, RIH	0	0		1.00	6.4	1.0	1.0	2.0	1.2	7.5
12	Mill casing, clean hole, POOH	1750	0		1.20	6.4	5.0	6.0	12.0	6.8	43.7
13	Make up 8-1/2" BHA, RIH	1750	0		1.00	5.8	1.0	1.0	2.0	1.2	6.8
14	Drill 8-1/2" horizontal section to TD	3806.55	2056.55	360	1.20	5.8	5.7	6.9	13.7	7.8	45.3
15	Clean hole, scraper and spot pill	3806.55	0		1.00	6.4	1.0	1.0	2.0	1.2	7.5
17	Set barrier in 9-5/8"	3806.55	0		1.15	6.4	1.0	1.2	2.3	1.3	8.4
18	Run upper completion	3806.55	0		1.15	6.4	3.0	3.5	6.9	4.0	25.3
19	Well clean-up to rig and testing	3806.55	0		1.00	6.4	3.0	3.0	6.0	3.5	22.4
20	Disconnect and pull BOP	3806.55	0		1.00	6.4	2.0	2.0	4.0	2.3	14.9
	WOW					6.0	0.0	1.5	15.2	3.5	21.3
	Total time & cost drilling (P50)									**61.5**	**376.9**

Table 12.16: Risk based time and cost estimates for Case 4 - Option 4.

Case 4 - completion option 4				Metrics			Time Distribution Assumption			Mean Estimates	
Step	Operation Description	TD (m MD RKB)	Length (m)	ROP (m/d)	Risk factor	Rate (MNOK/day)	Low (min) (days)	Base (days)	High (max) (days)	Time (days)	Cost (MNOK)
1	Rig move and positioning	0	0		1.15	5.8	2	2.3	4.6	2.6	15.3
2	Bullheading the well, secure the well	0	0		1.0	5.8	1	1	2	1.2	6.8
3	Prepare HXT	0	0		1.0	5.8	1.0	1.0	2.0	1.2	6.8
4	Rig up and test BOP, connect to riser	0	0		1.0	5.8	2.0	2.0	4.0	2.3	13.5
5	Pull tubing	0	0		1.70	5.8	1.5	2.6	5.1	2.8	16.2
5	Make up milling assembly and whipstock, RIH	0	0		1.00	6.4	1.0	1.0	2.0	1.2	7.5
6	Mill casing, clean hole, POOH	1850	0		1.20	6.4	5.0	6.0	12.0	6.8	43.7
7	Make up 8-1/2" BHA, RIH	1850	0		1.00	5.8	1.0	1.0	2.0	1.2	6.8
8	Drill 8-1/2" horizontal section to TD	3320.3	1470.3	360	1.20	5.8	4.1	4.9	9.8	5.6	32.4
9	Clean hole, scraper and spot pill	3320.3	0		1.00	6.4	1.0	1.0	2.0	1.2	7.5
10	Run, cement and perforate liner, displace OBM to packer fluid	3320.3	0		1.20	6.4	5.0	6.0	12.0	6.8	43.7
11	Make up milling assembly and whipstock, RIH	0	0		1.00	6.4	1.0	1.0	2.0	1.2	7.5
12	Mill casing, clean hole, POOH	1750	0		1.20	6.4	5.0	6.0	12.0	6.8	43.7
13	Make up 8-1/2" BHA, RIH	1750	0		1.00	5.8	1.0	1.0	2.0	1.2	6.8
14	Drill 8-1/2" horizontal section to TD	3806.55	2056.55	360	1.20	5.8	5.7	6.9	13.7	7.8	45.3
15	Clean hole, scraper and spot pill	3806.55	0		1.00	6.4	1.0	1.0	2.0	1.2	7.5
17	Set barrier in 9-5/8"	3806.55	0		1.15	6.4	1.0	1.2	2.3	1.3	8.4
18	Run upper completion	3806.55	0		1.15	6.4	3.0	3.5	6.9	4.0	25.3
19	Well clean-up to rig and testing	3806.55	0		1.00	6.4	3.0	3.0	6.0	3.5	22.4
20	Disconnect and pull BOP	3806.55	0		1.00	6.4	2.0	2.0	4.0	2.3	14.9
	WOW					6.0	0.0	1.6	16.3	3.8	22.8
	Total time & cost drilling (P50)									65.9	404.6

Case 6: Acidizing

The resulting time and cost estimates for Case 6 are summarized in **Table 12.17**. **Figure J.13** shows the probability distribution of operation days. See Appendix J.

Table 12.17: Summary of risk based time and cost estimates for the Case 6.

Case 6: Acid stimulation		
Time, cost and KPI estimates	Unit	Case 6
Technical Limit (P5)	days	15
Expected (P50)	days	17
P50 Cost Estimates	MNOK	30.5
AFE (P95)	days	20
AFE Cost Estimate	MNOK	42
Average daily cost (P50)	MNOK/day	1.8
Total number of meters	meters	2977
Cost per meter	kNOK/m	10

Further details on the basis for the time and cost estimation are shown in **Table 12.18**.

Table 12.18: Risk based time and cost estimates for Case 6.

Case 6: Acidizing				Metrics			Time Distribution Assumption			Mean Estimates	
Step	Operation Description	TD (m MD RKB)	Length (m)	LPM	Risk factor	Rate (MNOK/day)	Low (min) (days)	Base (days)	High (max) (days)	Time (days)	Cost (MNOK)
1	Vessel mobilization and positioning	0	0		1.20	1.5	6.0	7.2	14.4	8.2	12.3
2	Prepare HXT	0	0		1.00	1.5	1.0	1.0	2.0	1.2	1.8
3	Connect to HXT, prepare pumps	0	0		1.00	1.5	1.0	1.0	2.0	1.2	1.8
4	Bullheading well with acid, stimulate and shut-in	2977	2977		1.00	1.5	1.0	1.0	2.0	1.2	1.8
5	Well clean-up to rig and testing	2977	0		1.00	1.5	3.0	3.0	6.0	3.5	5.3
6	Disconnect	2977	0		1.00	1.5	1.0	1.0	2.0	1.2	1.8
	WOW					6.0	0.0	0.4	4.3	1.0	6.0
	Total time & cost drilling (P50)									**17.4**	**30.5**

12.2 Net Present Value

NPV is a formula used to determine the net present value of an investment by the discounted sum of all cash flows received from the project. The formula for the discounted sum of all cash flows can be rewritten as in **Equation 12.1**, taken from Finance Formulas (2014).

$$NPV = -C_o + \sum_{i=1}^{T} \frac{C_i}{(1+r)^i} \tag{12.1}$$

C_o is the initial investment, C_i is the cash flow, r is the interest rate and i is the time of the cash flow in years.

When a company or investor takes on a project or investment, it is important to calculate an estimate of how profitable the project or investment will be. In the formula the initial investment is a negative cash flow showing that money is going out as opposed to coming in. Considering that the money going out is subtracted from the discounted sum of cash flows coming in, the net present value would need to be positive in order to be considered a valuable investment (Finance Formulas 2014). The actual outcome may be better or worse than the estimated NPV (Jahn et al. 2008).

A simple calculation of the NPV has been performed. Taxes have not been taken into account. The initial investment, C_o, are the P50 cost estimates taken from **Subsection 12.1.2**. An exchange rate of 5.9 NOK/USD is used, rate per 14.05.2014 (Oslo Børs 2014). The interest rate has been set to 8%. The rate is taken from Strøm (2013). An oil price of 105 USD/STB and a gas price of 2.3 NOK/Sm^3 are assumed to be constant for the entire period from 2015 to the end, 2020. The prices are based on today's price trend.

Lost revenue due to the shut in of Well D in the operating period of implementing the IOR measures are not taken into account. It is assumed that Well D produces constant as estimated in the basecase, hence not choking as a consequence of the extra laterals. The

revenue is based on the increased production from the basecase. Production due to well completion are not taken into account in the revenue-estimations.

The composition of the oil and gas are not taken into account. The results from the simulations in ECLIPSE 100, that is cumulative oil and gas production, are used as data in the calculations.

The cumulative NPV of the IOR cases are shown in **Table 12.19**.

Table 12.19: Cumulative NPV for all the cases expect Case 5.

Cumulative NPV				
Case	Option 1	Option 2	Option 3	Option 4
1	968 MNOK	940 MNOK	N/A	N/A
2	1 167 MNOK	1 139 MNOK	N/A	N/A
3	1 223 MNOK	1 167 MNOK	1 243 MNOK	1 215 MNOK
3a	1 126 MNOK	1 070 MNOK	1 146 MNOK	1 119 MNOK
3b	1 032 MNOK	977 MNOK	1 052 MNOK	1 025 MNOK
4	144 MNOK	83 MNOK	166 MNOK	138 MNOK
4a	-291 MNOK	-352 MNOK	-269 MNOK	-296 MNOK
4b	212 MNOK	151 MNOK	234 MNOK	206 MNOK
6	526 MNOK	N/A	N/A	N/A

In Table 12.19 it is observed that all the cases with all completion options, except Case 4a, are found to be profitable; the NPV is positive. Case 2 and Case 3 offer the highest NPV, being the most profitable cases. Both cases are laterals towards the east of Well D. As Case 4a has negative NPV's the case is not found to be economic viable.

12.3 Risk Analysis and Decision Making

The oil and gas business involves major investments in all stages of the field life cycle. During the gaining access, exploration and appraisal stages, the expenditure does not guarantee a return, and at the development stage major investments are made in the anticipation of returns over a long period of time. Payback periods are typically long, and the project is subject to large fluctuations in key variables such as oil and gas price, and cost of services during the producing life of asset. For these reasons, it is important that careful technical and commercial risk analysis is performed when making decisions on investment in the industry. (Jahn et al. 2008)

In the following a sensitivity analysis has been performed on the NPV, altering the most important parameters. Decision trees have been made as a visual and analytical tool.

12.3.1 Uncertainties

- Oil and gas price
- Exchange rate
- Interest rate / discount rate
- OPEX
- Operation days
- Rig day rate
- Delay of IOR measures
- Reserves and production forecast. Cumulative oil and gas production
- Inflation

12.3.2 Sensitivity Analysis

In order to test the economic performance to variations in the basecase input data, sensitivity analysis was performed on the NPV. This indicates how robust the project is to variations in one or more parameters, and also highlights which of the input parameters the projects economics is more sensitive to.

A spider plot, **Figure 12.2**, shows the effect of the individual parameters. A sensitivity analysis was performed on the exchange rate, OPEX, the oil and gas price, the cumulative production and the interest rate.

It is observed in Figure 12.2 that the NPV is most sensitive to the oil price and the exchange rate.

12.3.3 Decision Making

Decision trees are often used as visual and analytical tools in decision making, as they give an overview over the outcome of the processes. Simplified decision trees have been made for cases 1-6, outlining the NPV and oil RF. **Figure 12.3** gives an overview over the current IOR cases. The decision trees are made in Microsoft Visio.

The cases have been separated in different trees, see **Figure 12.4- 12.7**. Figure 12.4 shows the decision tree for Case 1 and Case 2. Figure 12.5 shows the decision tree for Case 3. Figure 12.6 shows the decision tree for Case 4, and Figure 12.7 shows the decision trees for Case 5 and Case 6.

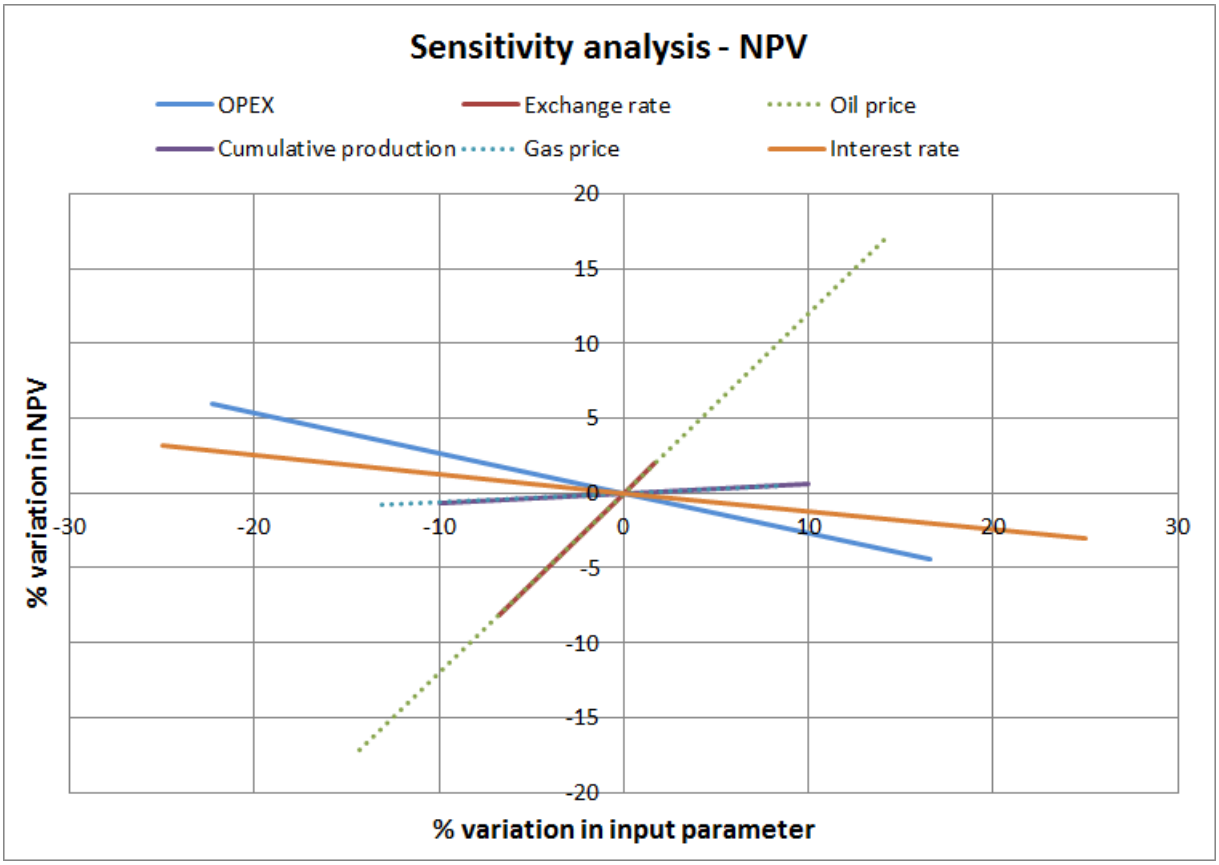

Figure 12.2: Sensitivity diagram for NPV.

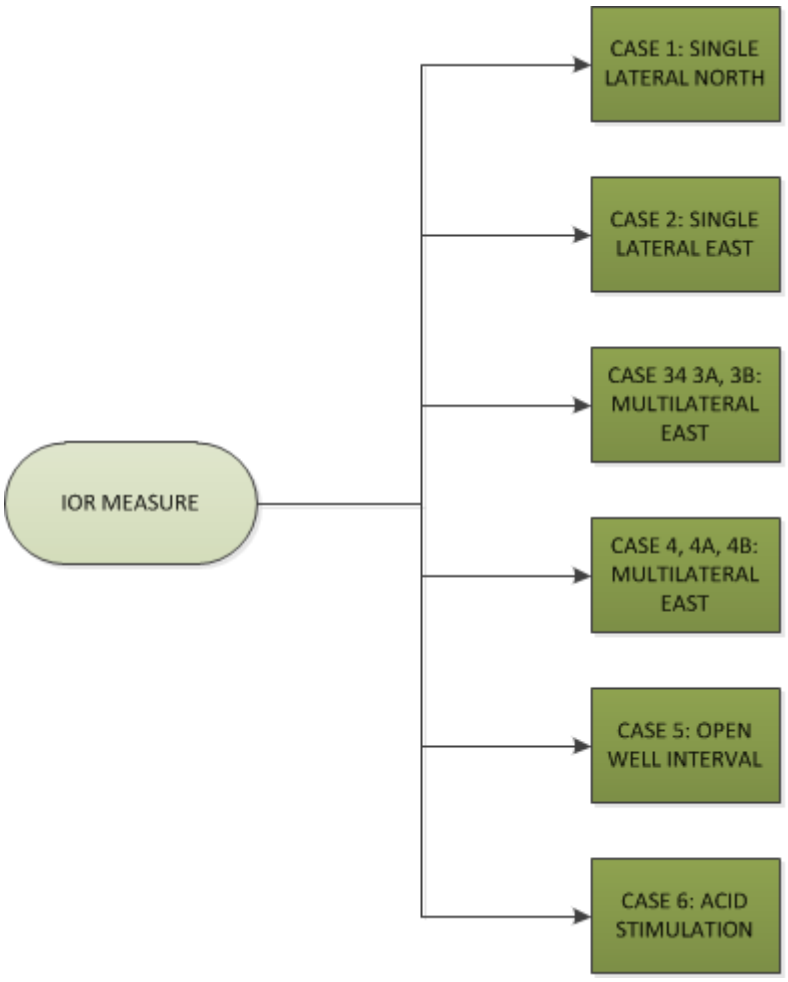

Figure 12.3: Decision making tree for the IOR measures.

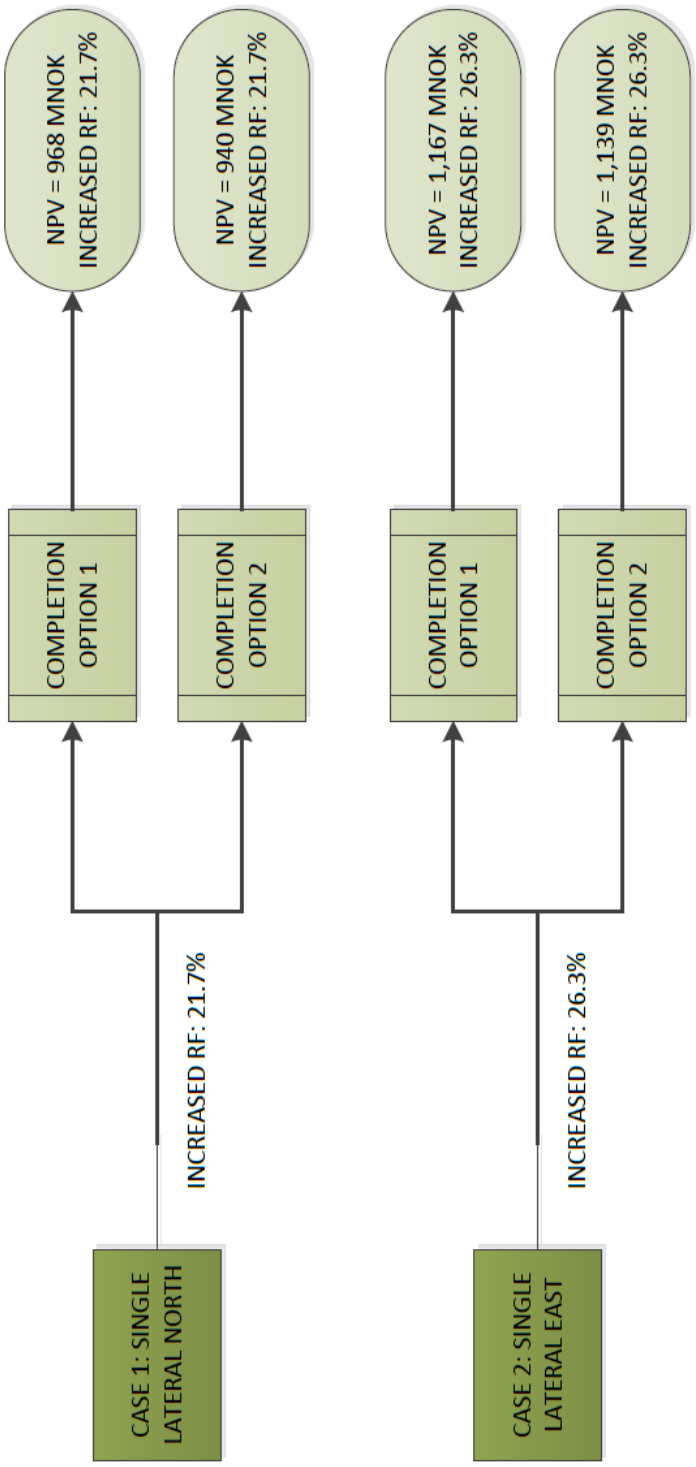

Figure 12.4: Decision making tree, Case 1 and Case 2.

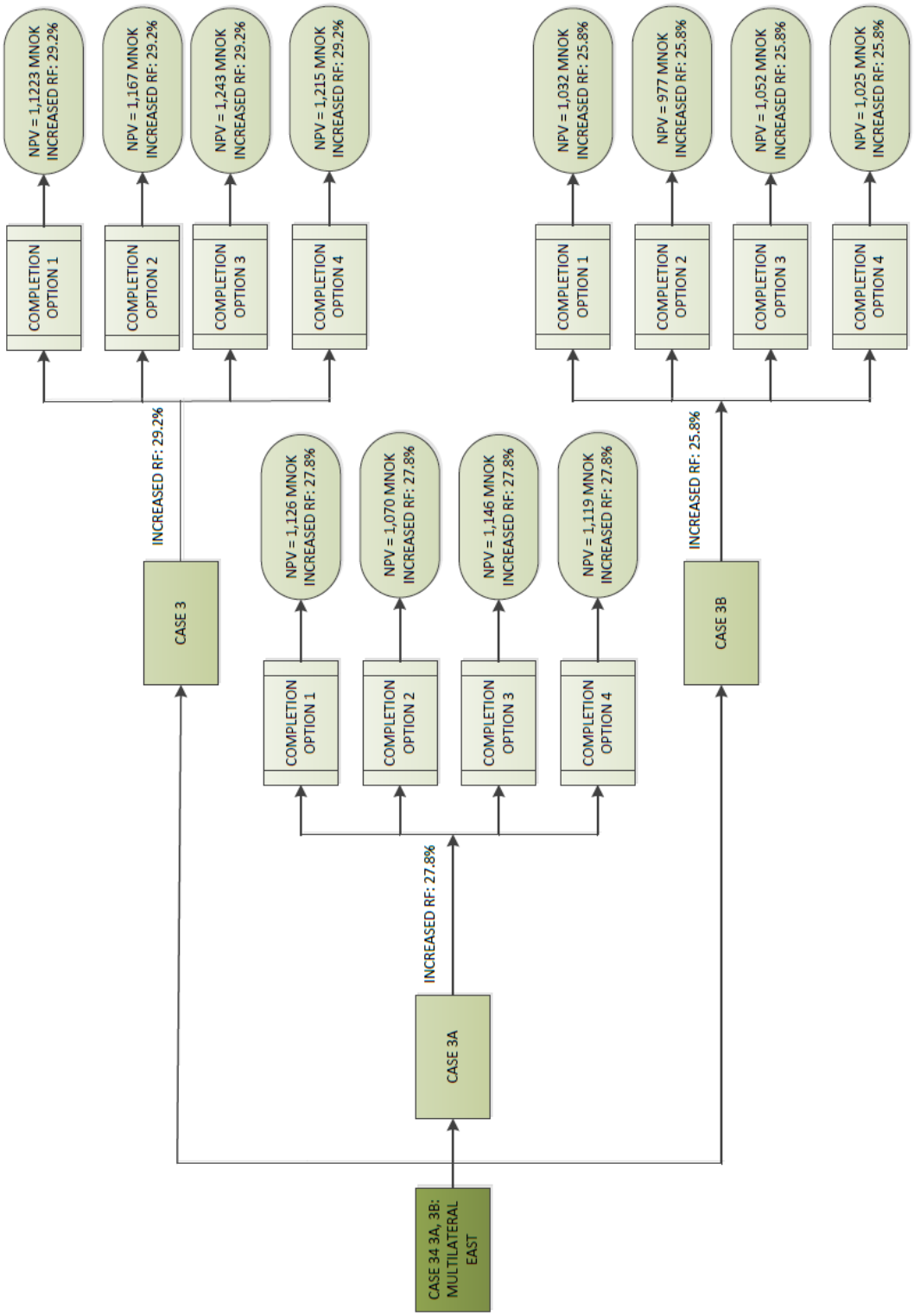

Figure 12.5: Decision making tree, Case 3.

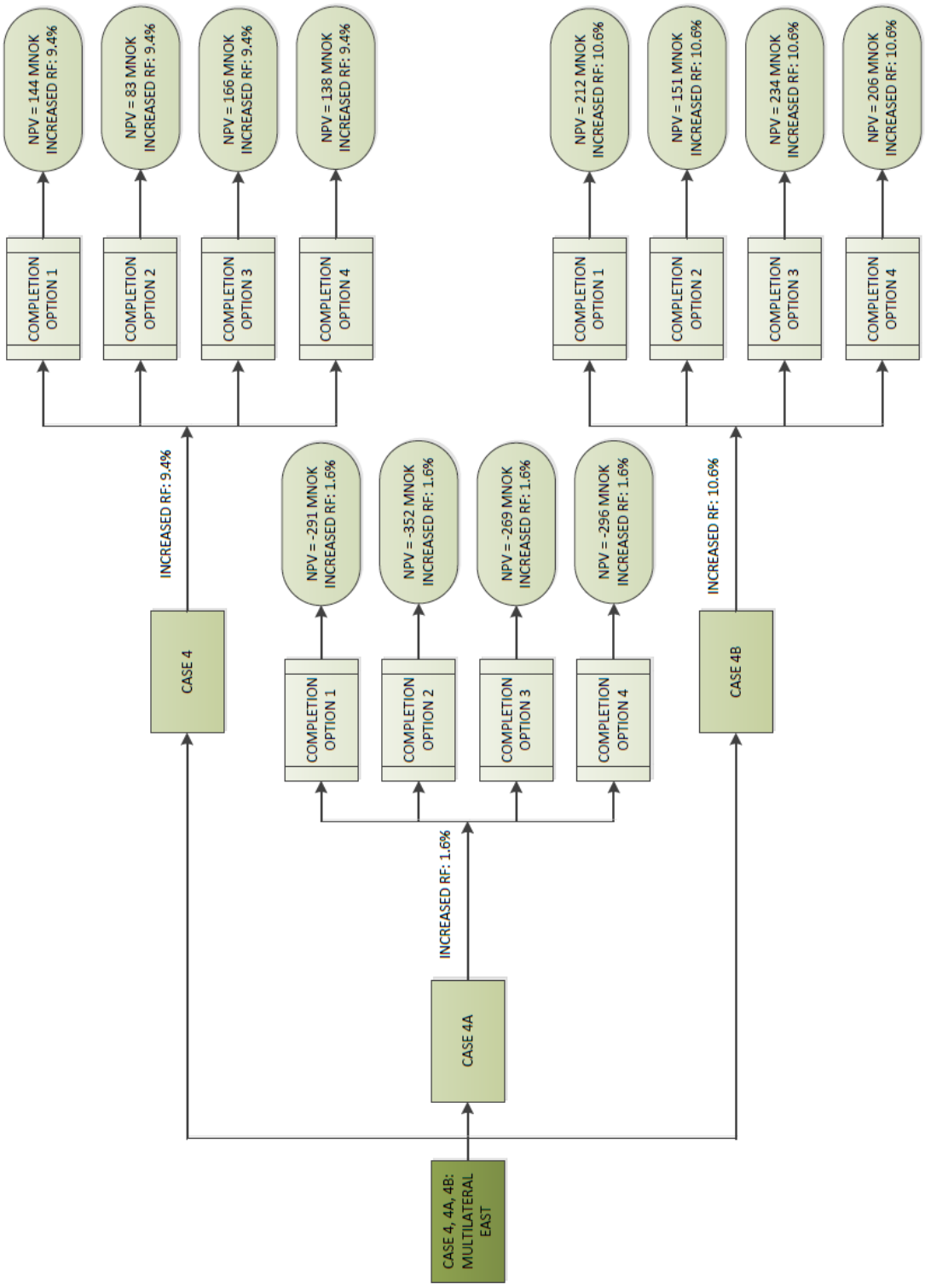

Figure 12.6: Decision making tree, Case 4.

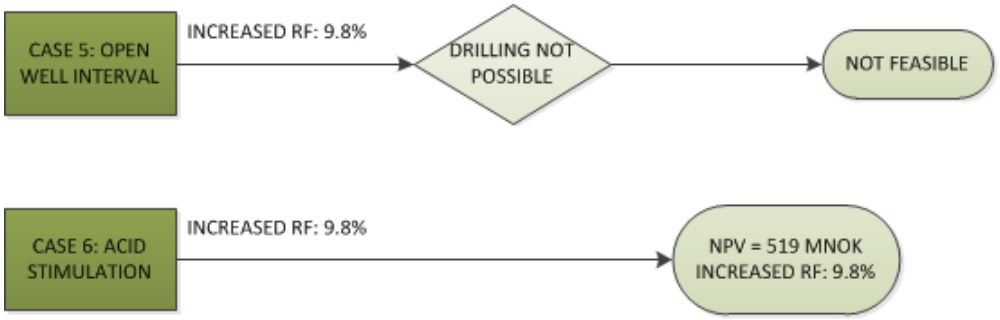

Figure 12.7: Decision making tree, Case 5 and Case 6.

12.4 Software

@Risk

@Risk performs risk analysis using Monte Carlo simulation to show how many possible outcomes there are in the spreadsheet model, and tells how likely they are to occur. It mathematically and objectively computes and tracks many different possible future scenarios, then tells the probabilities and risks associated with each different one. This means you can judge which risks to take and which ones to avoid, allowing for the best decision making under uncertainty. @Risk is a product of Palisade (Palisade 2011).

Microsoft Visio

Microsoft Visio (Microsoft 2010) is a diagramming and vector graphics application and is part of the Microsoft Office suite. The product was first introduced in 1992, made by the Shapeware corporation. It was acquired by Microsoft in 2000 (Wikipedia 2014).

13 Discussion

It is essential to evaluate the productivity of the field, the effect of the well intervention measures and estimate the NPV in order to take the decision of major investments in regards well intervention measures. Thus it is important to use the most realistic data as possible, obtaining a realistic estimate of the situation. Also, it is essential to be aware of uncertainties in the procedure.

Well intervention measures, cases with infill drilling and acid squeeze, were implemented in Well D. The cases were made using the Petrel software and the simulation propriety ECLIPSE 100, both tools of Schlumberger. A coarse history matched model were used when simulating the measures, a model in which is not considered to be representative of the Jette field. Still, the history matching has been considered as successful as it does not violate any known physical constraints.

The initialization of the simulation model was based on an initial understanding of the Jette field which contradicts the later understanding. The model was initialized with one fluid system, no faults and fractures, and an aquifer giving strong pressure support over the entire reservoir. Also, the permeability distribution was not representative for the field. Results from build-up tests, multi-rate tests and fluid sampling for PVT analysis at later stages have shown to contradict the initial understanding, leading to uncertainties in the understanding of the field. The results of the simulations will carry uncertainties, as the findings at later stages have not been implemented in the history matched model.

Well D has shown to be a challenging well, with challenges during both completion and production stages. The productivity of the well has been found to be poor, both when calculated with data from the build-up tests or the multi-rate tests with initial reservoir pressure. The contradicting data and sensitivity studies may indicate that Well D is placed in an isolated area or a shaly layer giving short intervals to produce from, or that the well is clogged. Sensitivity studies show that the PI is most sensitive to reservoir GOR, injected gas lift rate, reservoir layer height, well deviation and horizontal permeability.

The uncertainties in both the calculations of the PI and the reservoir model will affect the results from the simulations. The results from the simulations are representative for the model used, *Jette X*, but not necessarily for Jette itself. Even though the results of the simulations may not be real for the Jette field, the increase in oil RF has shown to be promising. The NPV has shown that it will be a profitable project. Even though the

performance of the well intervention measures can not be replicated perfectly to Jette due to the uncertainties, it is believed that Jette will gain promising results by implementing well intervention measures.

14 Conclusion and Recommendations

14.1 Conclusion

This thesis shows interesting and promising results regarding increased oil recovery and increased NPV of the implemented well intervention measures. To sum up the findings of this thesis the following can be made:

- The upscaled model was found to be a poor match in regards production data, hence being unrepresentative of the Jette field. After a rough history matching process of the model, the model is closer to the reality of the Jette field, but is called *Jette X*.
- The build-up tests of Well D gave conflicting results from the initial reservoir pressure, with a reservoir pressure of 150-160 bar. This gives a variation of PI from 4 $Sm^3/day/bar$ to 7.5 $Sm^3/day/bar$. This may indicate that Well D are depleting the surrounding reservoir.
- It may be indicated that there are several faults and/or fractures in the reservoir due to the observed pressure depletion around Well D. These are not implemented in the simulation model, leading to uncertainties during the simulations.
- As seen in the results the inflow- and lift performance curves do not correspond with the calculated PI's, the measured rates and BHP at P/T-gauge, given the measured gas lift rate. Altering the gas lift rate gives a match. It is observed that the oil production rate is highly dependent on gas lift rate.
- Sensitivity studies have shown that the PI is most sensitive to well deviation, horizontal permeability, reservoir layer height, gas lift rate and reservoir GOR. This show that the productivity index may change along the well length due to anisotropy, wellbore geometry and reservoir extension.
- The change of riser from a 12 in. riser to a 8 in. riser has a negligible effect on the observed slugging; the differences in the pressure drop are observed to be small. A study conducted by Weatherford Petroleum Consultants found that high gas rates are effective to suppress the flow oscillations. Such high gas rates were also found to be counter-productive with regard to oil production.
- The area east of Well D has shown to offer the best RF. Both Case 2 and Case 3 have

laterals located towards east, obtaining an increased RF of 25.8-29.2%. Case 4, with laterals west of Well D, have shown to be the case offering the lowest increased RF. Completion option 2 has, for the multilateral cases, shown to be the most expensive option.

- Case 2 and Case 3 have been found to be the most profitable cases when estimating the NPV. All cases, except Case 4a, are profitable.

14.2 Recommendations and Future Work

The recommendations and ideas for future work are summarized in the following bullet points.

- The analysis of the build-up tests gave results which must be considered highly uncertain for further use. To obtain more trustworthy results, a far longer build-up test will have to be performed. This may help reach pseudo-radial flow, and also observe potential faults.
- It is recommended to make a new and improved geologic model after a thorough analysis of faults and fractures in the field. The geologic model may serve as a base for a new simulation model. A new simulation model may be made as a network model representing the entire production system from reservoir to separator. This may help minimize uncertainties as more data points are available for comparison with model performance.
- As the flow measured topside Jotun B is commingled, it is recommended to allocate the production from both wells. This may give a better overview of the productivity from each well, and can be used to better estimate the reasons of poor production.
- It is recommended to implement the well intervention measures in a new reservoir model. This may give more certain and precise results, decreasing the uncertainties in the production and the NPV.
- The risk of drilling laterals should be evaluated, and also different completion options. This may be performed by analysing the geology and stresses in the reservoir.
- It is recommended to perform 4D seismic to obtain more data of the field.

15 Bibliography

Advanced Resources International, . (2013), 'Fracturing Technologies for Improving CMM/CBM Production'. (downloaded 18-02-2014).
URL: *http://www.epa.gov/cmop/docs/fra-technologies.pdf*

Brenna, A., Jøssund, T. & Kvilaas, G. (2011), Plan for utbygging og drift av Jette, Technical report, Det Norske Oljeselskap ASA, Trondheim, Norway (unpublished).

Brenna, A., Jøssund, T. & Kvilaas, G. (2013*a*), Driftsprosedyrer for Jette - Opprensking av brønner før oppstart, Technical report, Det Norske Oljeselskap ASA, Trondheim, Norway (unpublished).

Brenna, A., Jøssund, T. & Kvilaas, G. (2013*b*), Jette - Long Range Reservoir Management Plan, Technical report, Det Norske Oljeselskap ASA, Trondheim, Norway (unpublished).

Brenna, A., Jøssund, T., Schei, G. & Kvilaas, G. (2012), Well Planning Data Package, Technical report, Det Norske Oljeselskap ASA, Trondheim, Norway (unpublished).

calsep (2008), 'PVTsim'. (accessed 05-02-2014).
URL: *http://www.pvtsim.com/*

calsep (2013), *PVTsim.* version 21.0.0.

Dake, L. P. (2001), *Developments in Petroleum Science 36 - The Practice of Reservoir Engineering*, revised edn, Elsevier Science Ltd.

Det Norske Oljeselskap, . (2013), 'Brønner'. Projectspace database (unpublished) (accessed 01.02.2014).

Eni (2014), 'Maximize Recovery'. (accessed 31-05-2014).
URL: *http://www.eni.com/enIT/innovation − technology/technological − answers/maximize − recovery/maximize − recovery.shtml*

Eoga (2014), 'Improved Oil Recovery'. (accessed 25-02-2014).
URL: *http://www.eoga.net/about_ior.php*

Finance Formulas, . (2014), 'Net Present Values'. (accessed 13-05-2014).
URL: *http://www.financeformulas.net/NetPresentValue.html*

Fjærtoft, L. & Sønstabø, G. (2011), 'Success From Subsea Riserless Well Interventions'. Paper SPE 143296 presented at the SPE/ICoTA Coiled Tubing and Well Intervention 5-6 April 2011. (accessed 08-05-2014).
URL: *https://www.onepetro.org/conference-paper/SPE-143296-MS*

Franchi, J. (2006), *Principles of Applied Reservoir Simulation*, third edn, Burlington, Massachusetts: Gulf Professional Publishing/Elsevier.

Golan, M. & Whitson, C. (2003), *Well Performance*, second edn, tapir akademiske forlag.

Haraldseide, C. (2011), Incorporating a Human Perspective into Subsea Well Intervention (SWI) Decision Making and Work Performance at SWI vessels, Technical report, Universtity of Stavanger.

Hite, J., Stosur, G., Carnahan, N. & Miller, K. (2013), 'The Alphabet Soup of IOR, EOR and AOR: Effective Communication Requires a Definition of Terms'. Paper SPE 84908 presented at the SPE International Improved Oil Recovery Conference in Asia Pacific, 20-21 October, Kuala Lumpur, Malaysia. (accessed 17-02-2014).
URL: *https://www.onepetro.org/conference-paper/SPE-84908-MS*

Iversen, M. (2012), 'Pushing the Subsea Wells Oil Recovery Factor'. (accessed 31-05-2014).
URL: *http://www.sut.org.au/perth/perthevents/presentations/*120222*subsea australasiaconference/*120222*Morten*%20*Iversen**PUSHING*%20*THE*%20*SUBSEA*%20*WELLS*%20*OIL*%20*RECOVERY*%20*FACTOR.pdf*

Jahn, F., Cook, M. & Graham, M. (2008), *Developments in Petroleum Science 55 - Hydrocarbon Exploration and Production*, second edn, Elsevier Science Ltd.

Joshi, S. (1991), *Horizontal Well Technology*, Vol. 1, PennWell Publishing Company.

Kratz, O. (2011), 'Well Intervention Overview'. (downloaded 20-02-2014).
URL: *http://phx.corporate-ir.net/ External.File?item=UGFyZW50SUQ9MTMzNzE5fENoaWxkSUQ9LTF8VHlwZT0zt=1*

Krogstad, M. & Barbier, J.-C. (2014), Jette Production Optimization and Well Intervention Study - Phase 2: OLGA Modelling of Gas Lift Sensitivities, Technical report, Weatherford Petroleum Consultants AS, Trondheim, Norway (unpublished).

Labastidas Avila, M., Lund, T., Winther, T., Itumbo, M. & Huang, Y. (2013), Enhanced Drainage Strategy and Implementation of Nano Technology in the Norne Field, Technical report, NTNU, Trondheim.

LEVON-Group, LLC & URS-Corporation (2009), 'Adressing Uncertainty In Oil And Natural Gas Industry Greenhouse Gas Inventories'. (downloaded 05-05-2014).
URL: *http://www.api.org/ehs/climate/response/upload/addressinguncertainty.pdf*

Lorentzen, K. (2013), Dynamic Reservoir Modeling of Jette, Technical report, NTNU and Weatherford Petroleum Consultants AS, Trondheim, Norway (unpublished).

Lysne, D. (2014*a*), Oppsummering av PVT data for Jette, Technical report, Det Norske Oljeselskap ASA, Trondheim, Norway (unpublished).

Lysne, D. (2014*b*), Sammenligning av buildup tester på Jette fra juli 2013 til mars 2014, Technical report, Det Norske Oljeselskap ASA, Trondheim, Norway (unpublished).

Lysne, D. & Nakken, E. (2013), Jette Production Optimization and Well Intervention Study, Technical report, Weatherford Petroleum Consultants AS, Trondheim, Norway (unpublished).

Microsoft (2010), *Microsoft Visio*. 2010 version.

Moshfeghian, M. (2007), 'MEG Injection vs. TEG Dehydration'. (accessed 24-04-2014).
URL: *http://www.jmcampbell.com/tip-of-the-month/2007/03/meg-injection-vs-teg-dehydration/*

Moshfeghian, M. & Taraf, R. (2008), 'New method yields MEG injection rate'. (accessed 24-04-2014).
URL: *http://www.ogj.com/articles/print/volume-106/issue-33/processing/new-method-yields-meg-injection-rate.html*

Nakken, E., Kiani, A., Fathalla, N., Jacobsen, K., Kruiderink, H., Bremner, R., Jørgensen, K. & Tronvoll, J. (2010), Feasibility Study For The Jetta Development Wells, Technical report, Weatherford Petroleum Consultants AS, Trondheim, Norway (unpublished).

Naterstad, T. (2013), Subsea Well Intervention Operations on the Norwegian Continental Shelft, Technical report, NTNU and Weatherford Petroleum Consultans AS, Trondheim, Norway (unpublished).

NTNU (2014), 'Introduction to ECLIPSE 100'. (downloaded 25-02-2014).
URL: *http://www.ipt.ntnu.no/ kleppe/TPG4160/ECLIPSE100.ppt*

Oljedirektoratet (2011*a*), 'Mest fra havbrunnbrønner'. (accessed 19-02-2014).
URL: *http://www.npd.no/no/Nyheter/Nyheter/2011/Mest-fra-havbunnsbronner/*

Oljedirektoratet (2011*b*), 'Muligheter og utfordinger for felt i drift'. (accessed 20-02-2014).
URL: *http://www.npd.no/publikasjoner/ressursrapporter/2011/kapittel-5/*

Oljedirektoratet (2013), 'Utbygging og drift'. (accessed 19-02-2014).
URL: *http://www.npd.no/no/Publikasjoner/Faktahefter/Fakta-2013/Kap-6/*

OSHA (2014), 'Sidetracking'. (accessed 28-04-2014).
URL: *https://www.osha.gov/SLTC/etools/oilandgas/servicing/workover.html*

Oslo Børs, . (2014), 'Kurser og marked'. (accessed 13-05-2014).
URL: *http://www.oslobors.no/markedsaktivitet/market?newtmenuCtx* = 1.0

Osmundsen, P. (2011), 'Choice of development concept - platform or subsea solution?'. (downloaded 26-02-2014).

URL: *http://www1.uis.no/ansatt/odegaard/uis_wps_econ_fin/uis_wps_2011_1_osmundsen.pdf*

Palisade (2011), *@Risk: Risk Analysis Software.* version 5.7.

Petrowiki (2014*a*), 'Artificial Lift'. (accessed 28-04-2014).
URL: *http://petrowiki.org/Artificiallift?rel* = 1

Petrowiki (2014*b*), 'Glossary: Bullheading'. (downloaded 15-15-2014).
URL: *http://petrowiki.org/Glossary%3ABullheading*

Petrowiki (2014*c*), 'Reservoir Simulation'. (accessed 25-02-2014).
URL: *http://petrowiki.org/Reservoir_simulation*

Rafiee, M. (2011), 'Model Selection and Uniqueness Analysis for Reservoir History Matching'. MS thesis, Technischen Universität Bergakademie Freiberg, Germany (accessed 31-05-2014).
URL: *http://d-nb.info/1014188369/34*

Rodrigues, D., Aune, E. & Medina, R. (2013*a*), Final Well Report, Drilling and Well Operations, Jette Well 25/8-D-1 AH T3, Technical report, Det Norske Oljeselskap ASA, Trondheim, Norway (unpublished).

Rodrigues, D., Aune, E. & Medina, R. (2013*b*), Final Well Report, Drilling and Well Operations, Jette Well 25/8-E-1 H, Technical report, Det Norske Oljeselskap ASA, Trondheim, Norway (unpublished).

Samier, P. (2011), 'Reservoir Simulation In the Oil Industry', (Published online 22nd July 2011).
URL: *http://apos-project.eu/Articles/reservoir-simulation-in-the-oil-industry.html*

Sandheep, K. & DeWalt, B. (2003), *Well intervention providers focus on completion, reservoir expertise*, Vol. 63, 3, Offshore Magazine.

Sandvik, S. & Ravnås, A. (2010), Final Report - PVT Analysis of MDT Oil Samples from 25/8-7, Jetta, Technical report, Weatherford Laboratories A/S, Trondheim, Norway (unpublished).

Schlumberger (2012*a*), *Eclipse Reservoir Engineering Software.* version 2012 2.0.0.

Schlumberger (2012*b*), ECLIPSE Technical Description - Multi-segment Wells. Version 2012.2 User manual.

Schlumberger (2013*a*), 'Drilling riser'. accessed 31-05-2014.
URL: *http://www.glossary.oilfield.slb.com/en/Terms/d/drillingriser.aspx*

Schlumberger (2013*b*), *OLGA Dynamic Multiphase Flow Simulatior.* version 7.2.0.

Schlumberger (2013*c*), *Petrel EP Software Platform.* version 2013.2.

Schlumberger (2014*a*), 'Dog Leg'. (accessed 14-02-2014).
URL: *http://www.glossary.oilfield.slb.com/en/Terms.aspx?LookIn=term%20namefilter=dog+leg*

Schlumberger (2014*b*), 'Eclipse'. (accessed 20-02-2014).
URL: *http://www.software.slb.com/products/foundation/Pages/eclipse.aspx*

Schlumberger (2014*c*), 'Enhanced Oil Recovery'. (accessed 17-02-2014).
URL: *http://www.glossary.oilfield.slb.com/en/Terms.aspx?LookIn=term%20namefilter=enhanced+oil+recovery*

Schlumberger (2014*d*), 'History Matching'. (accessed 08-04-2014).
URL: *http://www.glossary.oilfield.slb.com/en/Terms.aspx?LookIn=term%20namefilter=history%20matching*

Schlumberger (2014*e*), 'Milling'. (accessed 18-02-2014).
URL: *http://www.glossary.oilfield.slb.com/en/Terms.aspx?LookIn=term%20namefilter=milling*

Schlumberger (2014*f*), 'Multilateral'. (accessed 22-04-2014).
URL: *http://www.glossary.oilfield.slb.com/en/Terms/m/multilateral.aspx*

Schlumberger (2014*g*), 'OLGA'. (accessed 20-02-2014).
URL: *https://www.software.slb.com/products/foundation/Pages/olga.aspx*

Schlumberger (2014*h*), 'Perforate'. (accessed 26-02-2014).
URL: *http://www.glossary.oilfield.slb.com/en/Terms.aspx?LookIn=term%20namefilter=perforate*

Schlumberger (2014*i*), 'Petrel'. (accessed 05-02-2014).
URL: *http://www.software.slb.com/products/platform/Pages/petrel.aspx?tab=options*

Schlumberger (2014*j*), 'Reservoir Charcterization Model'. (accessed 24-02-2014).
URL: *http://www.glossary.oilfield.slb.com/en/Terms.aspx?LookIn=term%20namefilter=reservoir+model*

Schlumberger (2014*k*), 'Reservoir Simulation'. (accessed 24-02-2014).
URL: *http://www.glossary.oilfield.slb.com/en/Terms.aspx?LookIn=term%20namefilter=reservoir+simulation*

Schlumberger (2014*l*), 'Scale'. (accessed 08-03-2014).
URL: *http://www.glossary.oilfield.slb.com/en/Terms/s/scale.aspx*

Schlumberger (2014*m*), 'Squeeze job'. (accessed 26-02-2014).
URL: *http://www.glossary.oilfield.slb.com/en/Terms/s/squeeze_job.aspx*

Sciencesoft (2013), *S3GRAF*. version 7.2.

Skjæveland, S. M. & Kleppe, J. (1992), *Spor Monograph - Recent Advances in Improved*

Oil Recovery Methods for North Sea Sandstone Reservoirs, Vol. 1, Norwegian Petroleum Directorate.

Statoil (2008), 'Through tubing drilling and Completion'. (accessed 26-02-2014).
URL: *http://www.statoil.com/en/technologyinnovation/optimizingreservoirrecovery/advanceddrilling/through%20tubing%20drilling/pages/throughtubingdrilling.aspx*

Strøm, T. (2013), 'Interest rate'. Lecture notes on Discounting and Deflating. TPG5110 Petroleum Economics. NTNU, Trondheim, Norway.

UiS (2014), 'Increased oil recovery'. (accessed 08-04-2014).
URL: *http://www.uis.no/research-and-phd-studies/research-areas/oil-gas-and-renewable-energy/petroleum-engineering/increased-oil-recovery/*

U.S. Emerald Energy Company, L. (2012), 'Recompletion'. (accessed 09-04-2014).
URL: *http://www.usemeraldenergy.com/recompletion.html*

Vise, D. (2000), 'The beta-PERT Distribution'. (accessed 13-05-2014).
URL: *http://www.riskamp.com/beta-pert*

Weatherford (2012*a*), *PVTflex Fluid Properties Modeling*. version 1.5.0.23.

Weatherford (2012*b*), *WellFlo Well Analysis*. version 2012 5.5.0.6.

Weatherford (2013*a*), 'PVTflex'. (accessed 05-02-2014).
URL: *http://www.weatherford.com/Products/Production/ProductionOptimization/Software/PVTFlexSoftware/index.htm*

Weatherford (2013*b*), 'WellFlo'. (accessed 05-02-2014).
URL: *http://www.weatherford.com/Products/Production/ProductionOptimization/Software/WellFloSoftware/index.htm*

Wikipedia (2013), 'Eclipse'. (accessed 20-02-2014).
URL: *http://en.wikipedia.org/wiki/ECLIPSE_(reservoir_simulator)*

Wikipedia (2014), 'Microsoft Visio'. (accessed 18-05-2014).
URL: *http://en.wikipedia.org/wiki/MicrosoftVisio*

Winther, T. (2013), Productivity Index in Horizontal Wells, Technical report, NTNU and Weatherford Petroleum Consultants AS, Trondheim, Norway (unpublished).

A Unit Conversion

Table A.1: Unit conversion table.

Parameter	Field Units			SI Units	
Length	1	ft	=	0.3048	m
Diameter	1	in.	=	0.0254	m
Pressure	1	psia	=	6895	Pa
Permeability	1	mD	=	10^{-9}	m^2
Volume - liquids	1	bbl	=	0.159	m^3

B Theory

Horizontal Well Technology
Productivity Index
Well Testing

3 Horizontal Well Technology

In general, a horizontal well is drilled parallel to the reservoir bedding plane. Strictly speaking, a vertical well is a well which intersects the reservoir bedding plane at 90 degrees, see Figure 3.1 [14]. If the reservoir bedding plane is vertical, then a conventional vertical well will be drilled parallel to the bedding plane, and in the theoretical sense it would be a horizontal well. Thus, while analyzing horizontal well performance, geometric configuration of the reservoir bedding planes should be considered. [14]

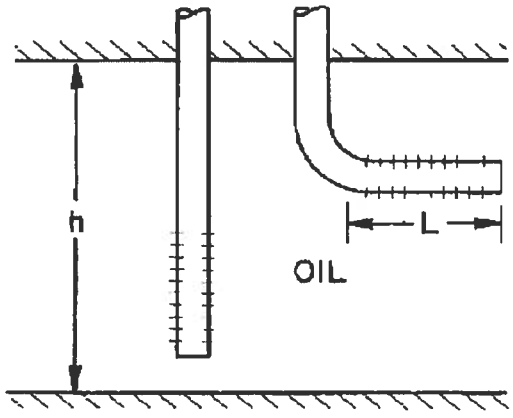

Figure 3.1: A schematic of a vertical well drilled perpendicular to the bedding plane, and a horizontal well drilled parallel to the bedding plane, from [14] page 2

Although the first horizontal wells were drilled as early as 1927, the major thrust of drilling horizontal wells started in the 1980s. With an oil price around $35 a barrel, the interest in horizontal wells was reignited. The purpose was to enhance reservoir contact and thereby enhance well productivity. [15]

Initial wells were short length wells, about 75 metres long. In 1985, the first medium radius horizontal well was drilled using a down-hole motor. Since then, using horizontal wells have become a common practice. Medium radius drilling technique is still the most commonly used drilling method [15]. The development of geosteering and mud motors have been a key technology enabling drilling of horizontal wells. As of 2008, the world's

longest horizontal well is 12.289 metres long with a 10.902 metres long horizontal section. This was an offshore well in the North Sea. [9]

3.1 Advantages and Disadvantages

In recent years, horizontal wells have been very successful in increasing productivity, adding reserves, and improving the overall cost-effectiveness of field operations.

Horizontal wells are being used in a variety of conditions; intersecting natural fractures, increasing reservoir-to-well exposure, reducing water and gas cresting, exploiting thin oil and gas zones, enhancing heavy oil recovery, tapping unswept oil, improving sweep, producing attic oil, and connecting discontinuous zones. Limited success has also been observed for thermal and low-permeability applications. [29]

Advantages

1. **Higher rates and reserves:** Higher rates and reserves as compared to vertical wells. This results in less finding costs and less operating costs per barrel of oil produced. [15]

2. **Developing costs:** For many horizontal wells, the finding (developing) cost, defined as well cost divided by well reserves, is less than the cost of buying provided producing reserves. [15]

3. **Number of wells:** To produce the same amount of oil, one needs fewer horizontal wells as compared to vertical wells. This results in reduced need for surface pipelines, locations, etc. [15]

Disadvantages

1. **High costs:** High costs as compared to a vertical well. In the U.S., a new horizontal well drilled from surface, costs 1.5-2.5 times more than a vertical well. A re-entry horizontal well costs about 0.4-1.3 times a vertical well cost. [15]

2. **Producing layers:** Generally, only one zone at a time can be produced using a horizontal well. If the reservoir has multiple pay-zones, especially with large differences in vertical depth, or large differences in permeabilities, it can be challenging to drain all the layers using a single horizontal well [15]. However, one can drill a well with stair-step, see Figure 3.2, where long horizontal portions are drilled in more than one layer, or use ICD's.

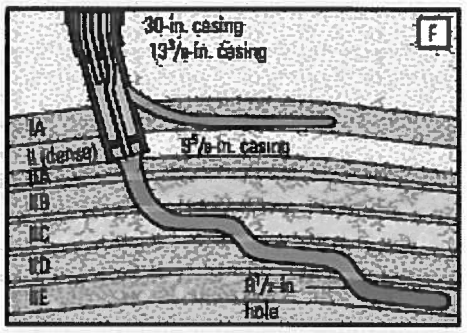

Figure 3.2: Multilateral with stair-step can be drilled to maximize horizontal footage in productive intervals and delay water breakthrough, from [24].

3.2 Important Parameters

Simplified, one can consider a horizontal well as a *turned over* vertical well. This affects characteristics of the well mainly due to pressure distribution from compaction. Some of the parameters that will be affected are the length, location of the well, anisotropy, drainage area and skin factor.

3.2.1 Well Geometry and Placement

A typical horizontal well is different from a vertical well because productivity of a well depends upon well-to-reservoir exposure. Moreover, the obtainable well length depends upon the drilling technique that has been used to drill the well. Therefore, it is essential to choose the appropriate drilling technique which will give the desired horizontal well length. [14]

Well Completion

An important consideration is well completion scheme; one can either have an open hole, insert a slotted liner, insert a liner with external casing packers, or case the hole and perforate the casing, depending upon local completion need and experience [14]. The type of completion affects the performance of the well.

Well Length

The well length is one of the most important aspects of a horizontal well, as the productivity depends upon the length of the well. A longer well has more contact with the reservoir zone and hence, increasing the drainage area.

Location in the Reservoir

The primary advantage of a horizontal well over a vertical well is the increased exposure of the pay zone. In a small reservoir zone a horizontal well may be drilled along the respective layer, obtaining contact over its entire length, whereas the vertical well can not get sufficient contact. With careful planning and successful execution, a horizontal well may obtain a bigger drainage area, and delay both gas- and water breakthrough.

Thus, well length, the well's physical location in the reservoir, the precision in drilling location, and the type of completion that can be achieved strongly depend upon the drilling method.

3.2.2 Skin

Equation 3.1 indicates that for a given positive skin factor, S, pressure drop in the skin region for a horizontal well is considerably smaller than that for a vertical well [13]. That is due to the rate, q. kh is the permeability thickness product, Δp_{skin} is pressure loss due to skin, μ is the viscosity of the fluid and B is the initial formation volume factor.

$$S = \frac{kh\Delta p_{skin}}{q\mu B} \tag{3.1}$$

This shows that for a given skin damage the stimulation treatment to remote to near-wellbore damage would have less effect on the productivity of a horizontal well than on the productivity of a vertical well [14]. Theoretically, horizontal wells can also be represented as a vertical well with large negative skin factor, i.e. highly stimulated vertical wells.

The reduced influence of near-wellbore damage on horizontal well productivity in a high-permeability reservoir also explains the reason for many successful horizontal-well-field-projects in high-permeability reservoirs. In contrast, in low-permeability reservoirs, the influence of damage on horizontal wells can be severe. [14]

Effective Wellbore Radius

The effective wellbore radius concept is used to represent the well which is producing at a rate different than that expected from the calculations based upon a drilled wellbore radius. Effective wellbore radius is the equivalent wellbore radius according to the measured production rate. Hence, damaged wells will have an effective wellbore radius less than the drilled wellbore radius, and stimulated wells will have a greater one. Thus, one can either express the damage/stimulation as a skin factor or with the use of effective wellbore radius. [34]

3.2.3 Permeability Anisotropy

In naturally fractured reservoirs, the permeability along the fracture trend is larger than in a direction perpendicular to fractures [14]. This can be correlated with an anisotropic reservoir, whereas the vertical permeability differs from the horizontal permeability. A well drilled along the low-permeability direction has the potential of a larger drainage area than a well drilled along the high-permeability direction. This indicate that good vertical permeability is essential for successful horizontal well operations. Joshi, Renard and Dupuy [14] showed that reduction in vertical permeability has the same effect as drilling a horizontal well in a thicker reservoir and reducing incremental contact area. See Figure 3.3. [29]

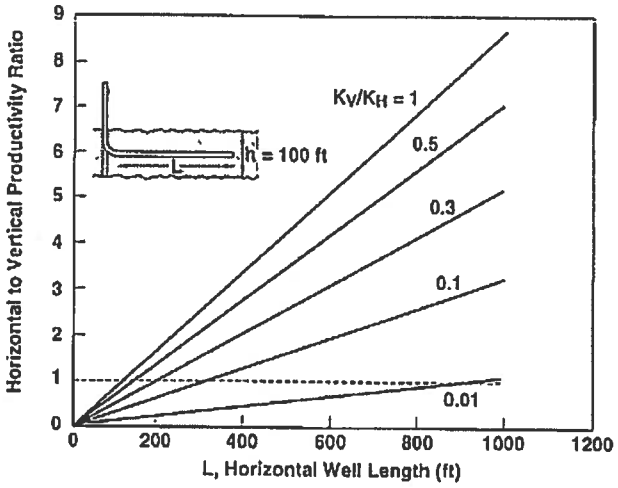

Figure 3.3: Effect of vertical permeability and horizontal well length, from [29] figure 5

In most reservoirs the vertical permeability is lower than the horizontal permeability due to compaction and pressure from the overburden. When performing reservoir analysis, vertical permeability is normally considered one-tenth or even less than one-tenth of the horizontal permeability. However, the maximum ratio is one. [14]

If one has to drill a horizontal well in a low-permeability reservoir, it is essential to create reasonable vertical permeability artificially by fracturing a horizontal well.

3.2.4 Drainage Area

A horizontal well can be imagined as a number of vertical wells drilled next to each other, and completed in a limited payzone thickness. As shown in Figure 3.4 and 3.5 each end of a horizontal well would drain either a rectangular or a circular area, with a rectangular drainage area at the center. This concept implicitly assumes that the reservoir thickness is considerable smaller than the sides of the drainage area. It is possible to calculate the

drainage area of a horizontal well by assuming an elliptic or rectangular drainage area in the horizontal plane, with each end of the well as foci of drainage area [14]. The width of the drainage area of a horizontal well may be estimated from the drainage radius of a vertical well.

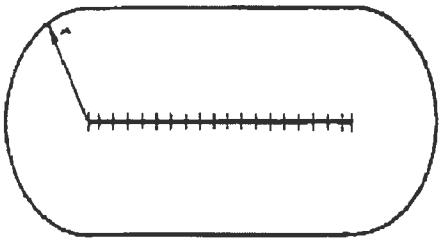

Figure 3.4: Elliptic drainage area of a horizontal well, from [14] page 62

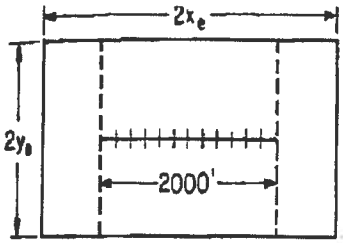

Figure 3.5: Rectangular drainage area of a horizontal well, from [14] page 57

The drainage area may be limited by geological factors such as sealing faults and impermeable layers, and reservoir parameters such as permeability. This implies that the drainage area may not be a straight-forward calculation. Elliptical and rectangular drainage shapes are a simple correlations to a real drainage area. The real drainage area will vary with reservoir factors, geological- and well factors. For a long well inside a non-rectangular drainage shape it is safest to approximate the shape with a rectangle to avoid a too optimistic estimate. [18]

4 Productivity Index

The reason for testing a well is to determine what the production rate will be if a certain backpressure is exerted at the wellhead. The productivity index as a concept is very useful for describing the relative potential of a well. It combines all rock and fluid properties, as well as geometrical considerations, into a single constant, thus making it unnecessary to consider these properties individually. [12]

4.1 Productivity Index in Horizontal Wells

The major purpose of a horizontal well is to enhance reservoir contact and thereby enhance well productivity. As a rule of thumb [14] a 1000-ft-long horizontal well can drain twice the area of a vertical well, while a 2000-ft-long horizontal well can drain three times the area of a vertical well in a given time. This indicates that the productivity index will be higher for a horizontal well compared to a vertical well. The calculation of productivity indices in horizontal wells will be more complex than those of vertical wells. Amongst the reasons for this are anisotropy, horizontal pressure drop and change of skin factors.

4.1.1 Important Factors

The calculation of the productivity index is highly affected by the type of well. In addition to be dependent upon the characteristics of a horizontal well, the productivity index is also affected by reservoir height, shape factor and horizontal well pressure. The characteristics of a horizontal well, drilling method, skin, permeability anisotropy and drainage area, are described in Chapter 3. These factors are important to consider.

Reservoir Height

The influence of reservoir height on horizontal wells is quite significant [14]. For a given length of a horizontal well, the incremental gain in reservoir contact area in a thin reservoir is much more than in a thick reservoir. It is important to note that the terms thick and thin are relative. Figure 4.1 shows the change in productivity of a horizontal well in a 160-acre drainage area under steady-state conditions. The top curve is for a 25-ft-thick reservoir and the bottom curve is for a 400-ft-thick reservoir.

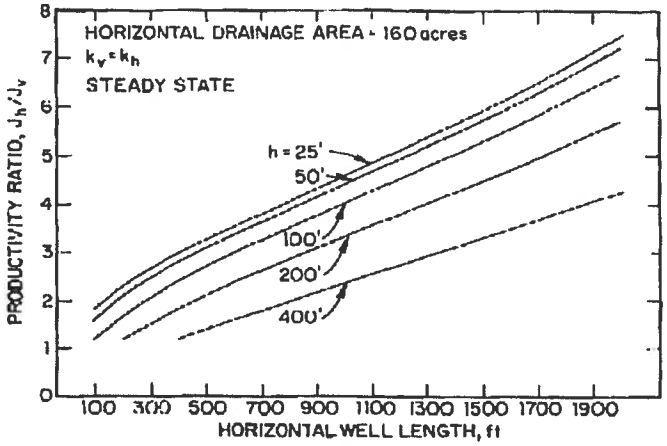

Figure 4.1: Productivity ratio of horizontal and vertical well versus well length for different reservoir thickness, from [14] page 80

Shape Factor

The shape factor, C_A, is a geometric factor, which depends upon drainage shape and the well location. Thus it accounts for the influence of well location within the drainage plane on well productivity [14]. See Appendix B for table of shape factors.

Horizontal Well Pressure

In the horizontal section of a horizontal well there will be a pressure drop, see Figure 4.2. If the horizontal wellbore pressure drop is very small as compared to the pressure drawdown from the reservoir to the wellbore, then for all practical purposes, a horizontal well can be considered as an infinite-conductivity wellbore, i.e. a wellbore at a constant pressure. In contrast, if the pressure drop through the wellbore is significant as compared to the reservoir drawdown, then reservoir drawdown along the well length would change, and therefore, production along the well length would also change. [14]

Assuming that a horizontal wellbore can be represented as a horizontal pipe, that the gravity and acceleration terms are negligible in a horizontal section of pipe, and the flow is fully developed, the equation for pressure drop would be as given in Equation 4.1 [1].

$$\Delta p = \frac{-f_m \rho v^2 L}{2gd} \tag{4.1}$$

f_m is the dimensionless friction factor, ρ is the density of the fluid, v is the velocity of fluid, g is the gravitational constant, d is the diameter of the pipe and L is the well length. The equation is in SI Units.

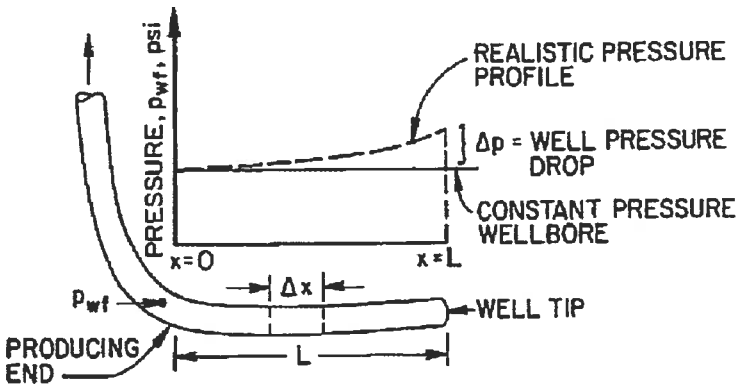

Figure 4.2: A schematic diagram of pressure loss along the well length, from [14] page 300

4.1.2 Ideal Productivity Index

Ideal Productivity Index is the index of a well with no skin alteration. The well should be undamaged/unstimulated hence, the skin = 0. With skin = 0 there will not be any pressure drop due to skin alteration in the near-well formation zone. [6]

The ideal productivity index is defined in Equation 4.2.

$$PI = \frac{q_0}{p_R - p_{wf} - \Delta p_{skin}} \tag{4.2}$$

p_{wf} is the wellbore flowing pressure, and p_R is the reservoir pressure. The pressure drop across the skin, Δp_{skin}, can be found directly from well tests or calculated with Equation 4.3 [13].

$$\Delta p_{skin} = \frac{q\mu B}{2\pi \bar{k} h} S \tag{4.3}$$

where q is the production rate, B is the volume formation factor, $\bar{k}$ is the geometric average of the vertical and horizontal permeability (see Equation 4.4) h is the height of the reservoir and s is the skin around the well. All the factors are given in SI Units hence, p_{skin} is given in *Pascal*.

$$\bar{k} = \sqrt{k_v k_h} \tag{4.4}$$

4.2 Reservoir Inflow Performance

The expression Reservoir Inflow Performance, IPR, is used customarily to define the relation between surface oil rate and wellbore flowing pressure. Bottomhole flowing pressure, p_{wf}, used in the IPR is usually expressed at the depth of mid perforations. [12]

The simplest and most widely used IPR equation is the *straight–line* IPR as seen at Figure 4.3. It states that the rate is directly proportional to pressure drawdown in the reservoir. The constant of proportionality is called the *productivity index*. The straight-line IPR is only used for undersaturated oils.

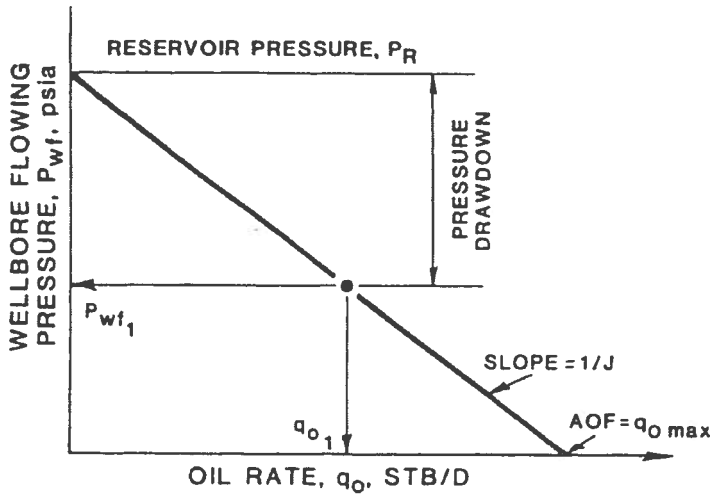

Figure 4.3: Straight-line IPR. From [12] page 30

The condition of an undersaturated oil with straight-line IPR does not apply to gases or saturated oil wells. Instead of linear rate increase with pressure drawdown, it is observed that larger-than linear pressure drops are required to increase the rate [12]. Hence, the pressure relation shows curvature pronounced at higher rates. In terms of productivity index, PI decreases with increasing drawdown.

For a well with gas lift both the inflow performance curve and the lift performance curve are considered, see Figure 4.4. The inflow curve defines the flow from the reservoir to the operating point, and the lift curve defines the flow from the operating point to the surface. The curves match at the operating point as it is a common point for both flows. The production rate is dependent on the lift performance curve. The operation point is normally at P/T-gauge.

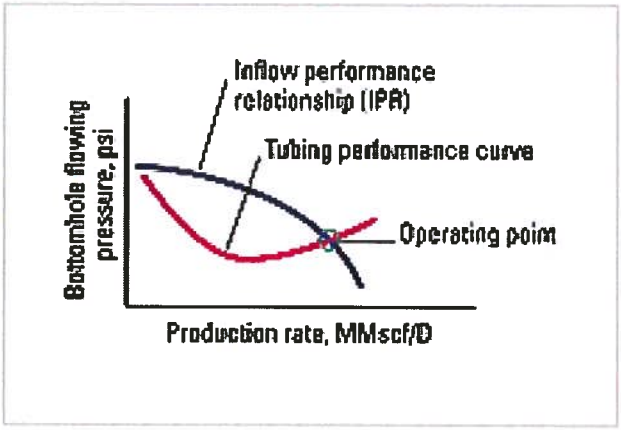

Figure 4.4: Relation between inflow and lift performance curve. From [23]

Reservoir inflow performance can be modelled in WellFlo.

4.2.1 WellFlo

The WellFlo software is a well-modelling application with design and analysis features for both naturally flowing and artificially-lifted wells. It incorporates calculations for multiphase flow through pipes, restrictions and other well components such as completions, pumps and gas-lift valves. The software supports an extensive catalogue of well equipment including tubing, casing, gas-lift valves, motors, cables, Electric Submersible Pumps (ESP) and Progressing Cavity Pumps (PCP) from various manufacturers [32], and can provide a wealth of data as below mentioned.

- Full support for both compositional and black-oil modelling with enhanced tuning
- Library of vertical and horizontal multiphase flow correlations and models
- Integrated hydrate, wax and asphaltene calculations
- Rigorous temperature modelling
- Design and analysis of many artificial-lift methods including gas-lift, ESP, PCP, plunger-lift and jet-pump
- Visualization of results

WellFlo is developed by Weatherford.

4.3 Mathematical Model

To determine the productivity index of individual layers only the drainage area, shape factor and skin value for each layer are needed. The shape factors can be approximated

from published tables, for example Dietz shape factors. For horizontal wells, even with common outer boundaries in all layers, the shape factors based on the midpoint of the well segment in each layer might differ significantly. The skin values are even more likely to vary, e.g. from changes in the well angle, layer properties and layer skin. [17]

For wells in layered reservoirs, the productivity index can be obtained by adding the individual layer productivity indices.

The following mathematical model is based on the basic definition of productivity index, Equation 4.5. A rectangular drainage area is assumed, whereas the outer boundaries are constricted by the length of the well and the drainage radius of the well. This productivity index should be used for production with pressure depletion at stable conditions. Pseudo-steady state is assumed. An assumption of a rectangular drainage area is used as it avoids a too optimistic estimate of the productivity index. [18]

4.3.1 Horizontal Wells in Closed Rectangular Reservoirs

For any well in a layered reservoir, isolated except at the wellbore, the total PI of the well can be defined by the expression

$$PI = \frac{q_0}{p_R - p_{wf}} \tag{4.5}$$

where p_R is the average pressure in the volume of the reservoir being drained by the well. The units are $STB/day/bar$ if the rate is given in STB/day and pressure in *bara*.

Under pseudosteady state conditions;

$$PI = \frac{q_0}{p_R - p_{wf}} = \frac{kh}{1.842B\mu(\frac{1}{2}\ln\frac{4A}{e^{\gamma}C_A r_w^2} + s)} \tag{4.6}$$

This is the PI in practical SI Units with pressure kPa and the permeability in μm^2, $\gamma = 0.5772156$ denotes Euler's constant, C_A is the Dietz shape factor for the well location and shape of the layer, and s is the pseudo-skin factor of the well segment within the layer. $\bar{k}$ is the geometric average of the vertical and horizontal permeability. The bottomhole flowing pressure, p_{wf}, is usually expressed at the depth of mid perforations [12].

When using the mathematical model at a real reservoir many of the input parameters in Equation 4.6 will be based on assumptions. These can therefore be varied in sensitivity studies.

5 Well testing

Pressure transient testing techniques, such as pressure buildup, drawdown, injectivity, falloff, and interference, are important parts of analysis. The testing includes generating and measuring pressure variations with time in wells and, subsequently, estimating rock, fluid and well properties [10]. Information that can be obtained from transient well tests are interwell flow capacity of a reservoir, static well pressure, extent of well damage, distance to nearest boundary, fluid volume in place and detecting heterogeneities within the pay zone [28]. All this information can be used to help analyse, improve, and forecast reservoir performance [13].

Interwell flow capacity of a reservoir is the product of the permeability times pay thickness. It is directly related to the ability of a reservoir to transmit fluids. It is used in predicting the maximum rate of production from a well. [28]

Static well pressure can be used as a measure of the stage of depletion of a reservoir. It is an essential feature in material balance calculations. The static well pressure is that pressure that would be measured if a well were shut-in for a long period of time without the external influence of adjacent wells. [28]

Extent of well damage If a well has altered permeability in the near-wellbore vicinity, then a measure of the amount of change in the near well conductivity (from the virgin state) can be computed from an analysis of transient well test data [28]. The concept of well damage or stimulation is translated into quantitative terms with the *skin effect* [13].

Distance to nearest boundary If a fault or pinchout exists near a well, then the distance to this boundary can often be calculated through an analysis of well test data. At times multiple barriers can be seen and analysed. [28]

Fluid volume in place Under certain test conditions, the volume of the fluids within the drainage area of a well can be computed from an analysis of the well test data. [28]

Detecting heterogeneities within the pay zone Such heterogeneities include man-made fractures, layered conditions, naturally fractured conditions, and lateral changes in mobility of the flowing fluids.

5.1 Horizontal wells

5.1.1 Well tests

Well test analysis of a horizontal well may be complex and on many occasions difficult to interpret. A horizontal well is difficult to analyse due to horizontal well profile, producing well length and interpretation of test results.

1. **Horizontal well profile:** Most horizontal-well-mathematical-models assume that horizontal wells are perfectly horizontal and are parallel to the top and bottom boundaries of the reservoir. In general, the drilled horizontal wellbores are rarely horizontal, but rather snake-like, see Figure 5.1 [14].

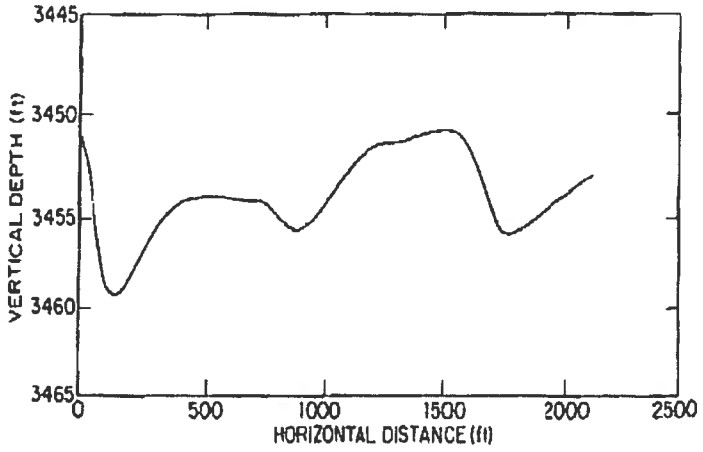

Figure 5.1: A typical horizontal well profile, from [14], page 166

   Due to the *snake* effect, one portion of the well may see the top reservoir boundary effect earlier than the remaining portion of the well, while a certain portion of the well may see the bottom reservoir boundary earlier than the remaining portion of the well. These variations along the well affect a pressure gauge inserted at the producing end of a horizontal well. [14]

2. **Producing well length:** If one wants to know whether the drilled length is also the producing length, the calculation is not straightforward, because horizontal wells exhibit negative skin factors, depending upon their lengths and reservoir properties. In practice, part of this negative skin factor is offset by the positive skin factors due to near wellbore damage and the effects of perforation density and the completion scheme. If parts of the horizontal wellbore intersect an unproductive interval, it will also appear as a positive skin factor. [14]

3. **Interpretation of test results:** In general, a test on a horizontal well where the productivity is less than expected or where one is trying to estimate whether a

horizontal well is producing at its full potential, the interpretation of test results may be challenging; it is challenging to identify the initial radial-flow period, and to estimate the mechanical skin. [15]

5.1.2 Flow regimes

Horizontal wells may exhibit five distinct flow regimes depending upon the well and reservoir geometries as described below. [21]

Early-time radial flow period in a vertical plane

Regarding a well producing at a constant rate; the early-time radial-flow regime occurs before the area drained or the pressure transient caused by this production encounters either of the top and bottom boundaries of the reservoir. See Figure 5.2.

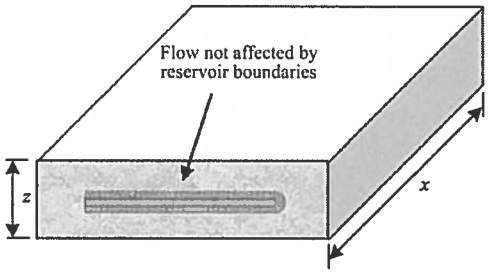

Figure 5.2: Early-time radial flow is not influenced by boundaries, from [21]

However, this flow pattern is likely to be elliptical, moving further into the reservoir at a given time in the higher-permeability x-direction than in the lower-permeability z-direction. [21] The flow is radial in the vertical plane perpendicular to the well during this flow period. [14]

From this flow period estimations of $\bar{k}$, L_w, k_z and *skin* can be obtained.

Hemi-radial

If the wellbore is much nearer one boundary than the other another flow regime, called half-radial or hemi-radial flow, may exist. It can occur immediately following the early-radial flow regime. Eventually, the area affected by the production will include the entire thickness of the reservoir. When that occurs, a linear flow pattern may develop. [21]

Early-time linear flow

If the horizontal well is long enough compared to the formation thickness, a period of linear flow may develop once the pressure transient reaches the upper and lower boundaries. [14]

The duration of the linear flow is determined by the effective well length and the horizontal permeability. This means that once the horizontal permeability is known, the effective well length may be found from the shape of half-slope in the log-log plot, see Figure 5.5. [19]

Late-time pseudo-radial flow in a horizontal plane

If the well length is sufficiently short as compared to the reservoir size, pseudo-radial flow will develop at late times. If the top or bottom boundary is maintained at constant pressure, i.e. with the existence of an active gas cap or water aquifer, then the pseudo-radial flow period will not develop. Instead, there will be a steady state flow at the late time [14]. Figure 5.3 shows early-time linear flow and late-time pseudo-radial flow in a horizontal plane.

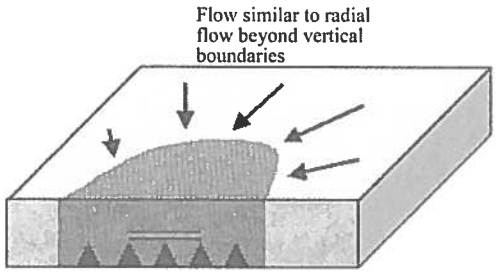

Figure 5.3: Early-time linear flow may develop after top and bottom boundaries are encountered. Late-time pseudo-radial flow begins after flow enters wellbore from beyond ends of well, from [21]

From this flow period the permeability-thickness product, kh, is determined. Thus, by estimating the layer thickness h, the horizontal permeability can be obtained. Pseudo-radial skin, S_{pr} can also be found.

Late-time linear flow

The late-time pseudo-radial flow continues until the area affected by the production reaches one of the sides of the reservoir. Once the area affected is the entire extension of the reservoir, that is when the pressure transient has reached both sides of the reservoir, late-linear flow regime begins, see Figure 5.4 [21].

5.1.3 Identifying flow regimes

The above mentioned flow regimes can be identified on a diagnostic log-log plot of the pressure change, Δp, and pressure derivative, p', against the logarithm of time. See Figure 5.5.

As seen in Figure 5.5, both early-time radial flow period in a vertical plane and late-time pseudo-radial flow in a horizontal plane are identified with zero slope. Early-time linear

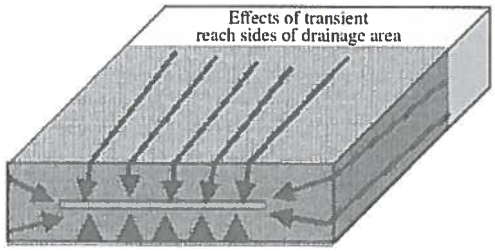

Figure 5.4: Late-linear flow includes flow from the drainage volume perpendicular to the well, from [21]

flow is identified with a 1/2 slope. Late-time linear flow, which is identified by a 1/2 slope, may happen immediately after early-time linear flow, or after late-time pseudo-radial flow. If it happens after early-time linear flow it may be challenging to identify. In the figure, late-time linear flow is not identified. This may be due to the unfortunate fact that most well test are halted prematurely, thus never reaching this period. Wellbore storage may be characterized by a unit slope. It does not imply that all these flow regimes appear in any given test, in fact, that would be rare. These are the shapes that identify the flow regimes that may appear in the test being analyzed. [21]

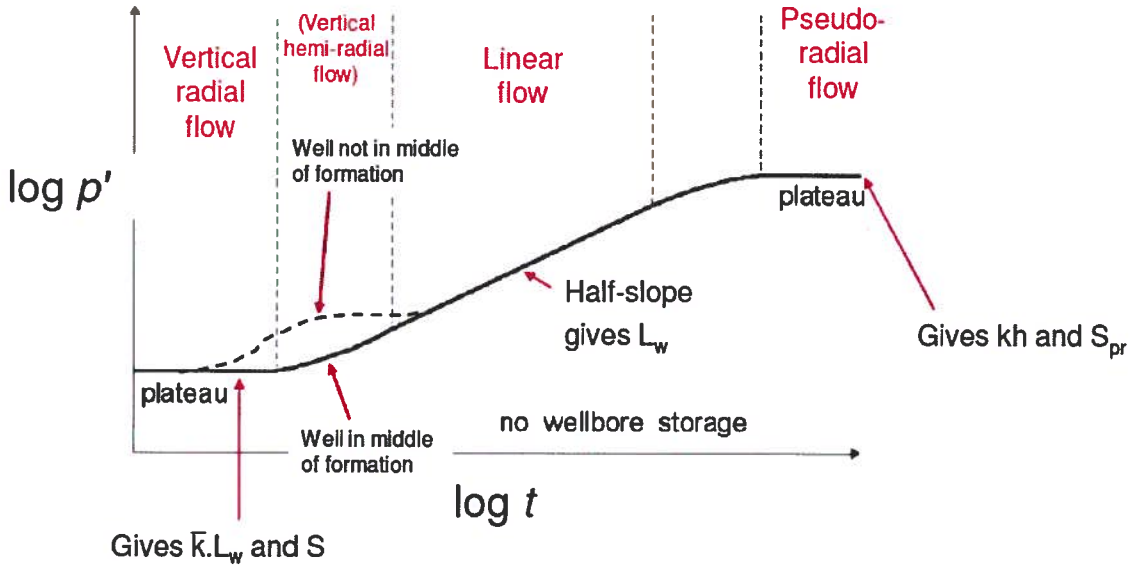

Figure 5.5: An example of the full response from a horizontal well in a homogeneous infinite acting reservoir, from [19], page 37

The shapes that may appear in a drawdown test may not appear in a buildup test because of the complex superposition of flow regimes. The best way to solve the problem is to ensure that a buildup test on a horizontal well is run with a producing time much greater than the maximum shut-in time in the test. [21]

5.2 Limitations

There are several limitations with the use of well testing which has to be considered and evaluated. The results might not be correct and hence, other sources, for example logs, have to be evaluated to get a more reliable description of the reservoir.

In practice, the application of pressure transient analysis is often limited by;

1. Insufficient data collection. [10]
2. Inappropriate application of analysis techniques. [10]
3. Failure to integrate other available or potentially available information. [10]
4. The test are not run for sufficient enough time [10]
5. Due to the nature of horizontal wells, it usually takes a substantial amount of time to reach pseudo-radial flow. In some finite reservoirs, pseudo-radial flow may never develop; i.e. reservoir boundaries start to affect pressure response before pseudo-radial flow begins to develop. Thus, the flow capacity and skin factor can not be obtained by analyzing pseudo-radial flow pressure data. [14]
6. A horizontal well may penetrate an unproducing interval, or a section of wellbore may be so damaged that fluid flow is completely blocked. Hence, the skin factor obtained via well test analysis reflects both mechanical skin and pseudo-skin, and it's difficult to find the skin of the reservoir. [14]

5.3 PanSystem

PanSystem software is one of the industy's leading well test analysis programs. It provides multiple options for models and analysis, which include industry standards as well as user-defined models for additional flexibility. PanSystem software is dedicated to transient well testing, and provides a way to simplify complex transient well testing through detailed analysis, simulation, and reporting. [31]

A pressure transient well test has the unique capacity to obtain information from within the reservoir surrounding the well. With appropriate testing and analysis techniques it can provide a wealth of data, as given below.

- Permeability of the reservoir-at-large and, in some cases, the near-wellbore region
- Completion efficiency, effective open interval size (over the life of the well)
- Reservoir structure (boundaries, heterogeneities)
- Reservoir pressure
- Nature of any pressure support

- Drainage area, connected pore volume, and initial hydrocarbons in place
- Vertical permeability, vertical communication in layered systems
- Well performance (over the life of the well)
- Communication between wells
- Deliverability and production forecast

PanSystem is developed by Weatherford.

C Well Schematics

Well schematic 25/8-D-1 AH T3/T2
Completion schematic 25/8-D-1 AH T3
Completion schematic 25/8-E-1 H

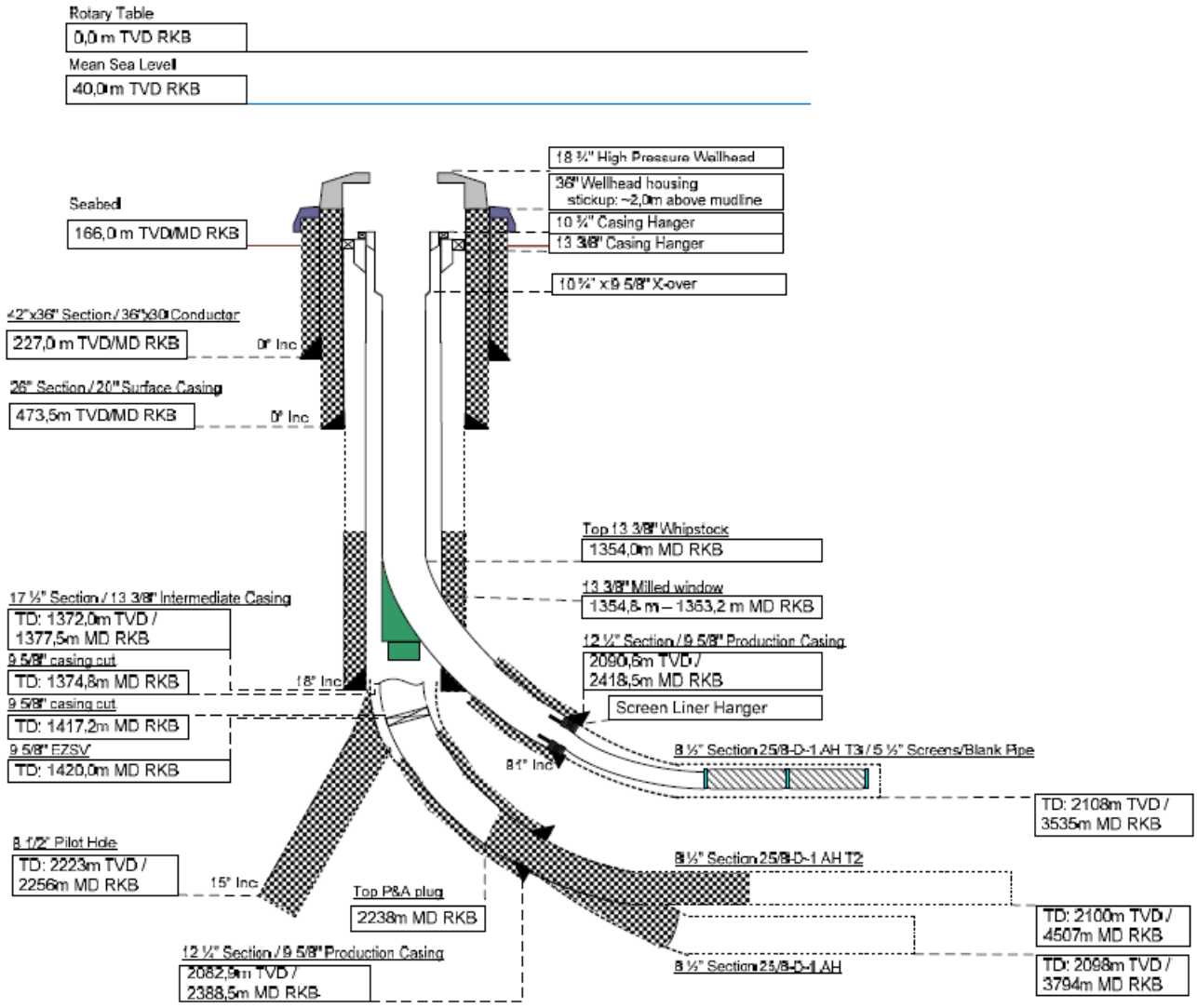

Figure C.1: Current production well 25/8-D-1 AH T3, and abandoned wells. From Rodrigues et al. (2013a).

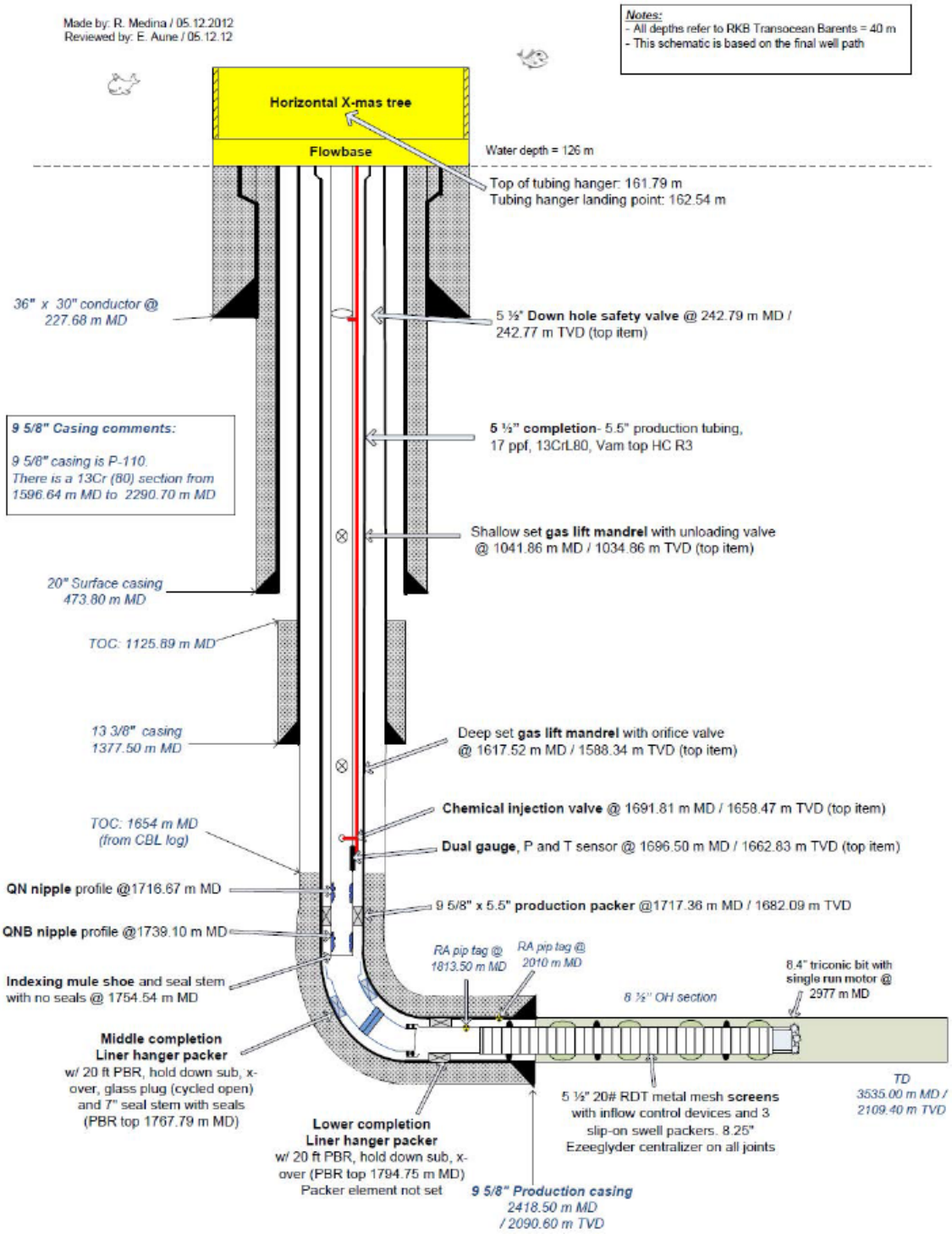

Figure C.2: Completion well schematic for 25/8-D-1 AH T3. From Rodrigues et al. (2013a).

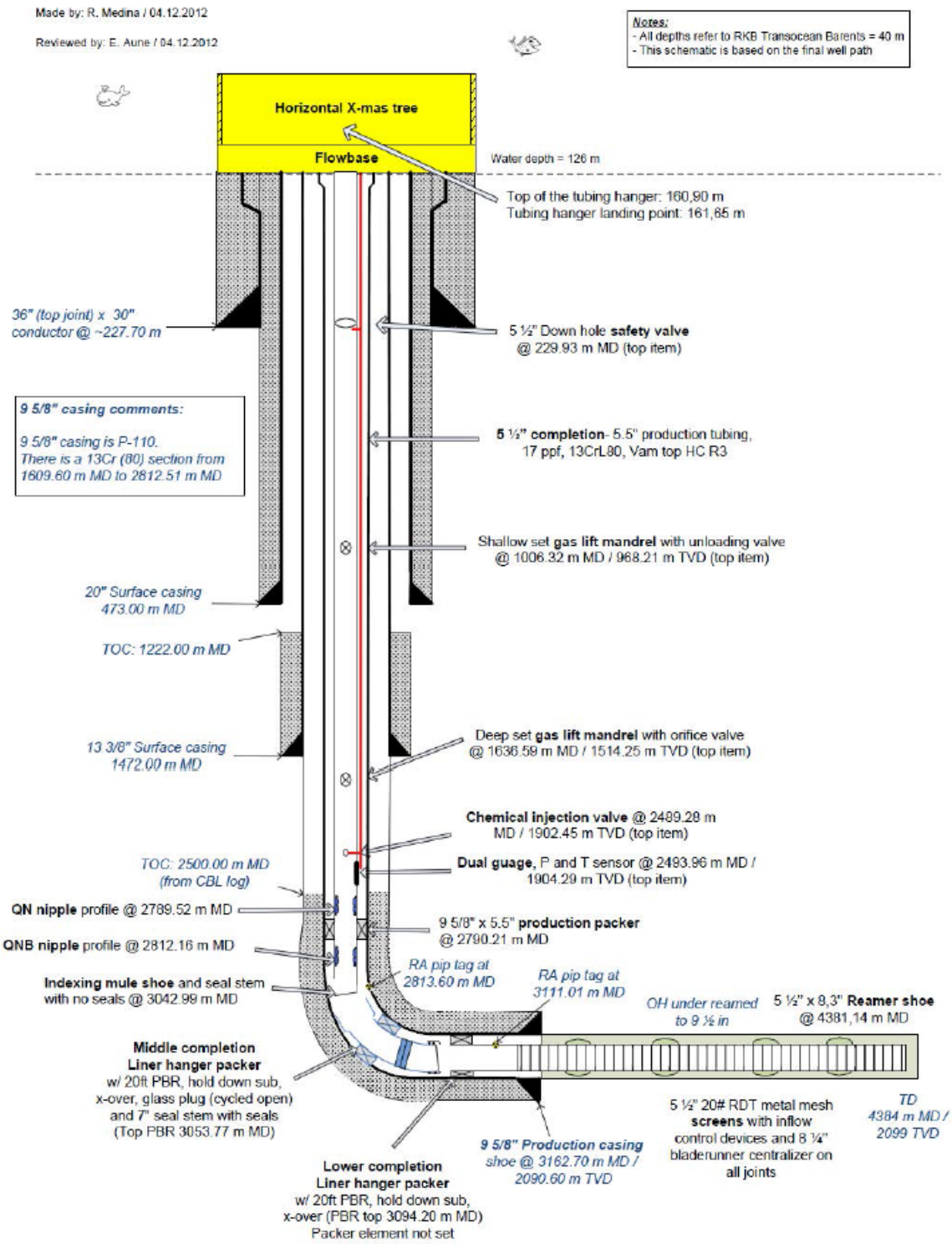

Figure C.3: Completion well schematic for 25/8-E-1 H. From Rodrigues et al. (2013b).

D Dog Leg Severity

Definite Survey Listing, 25/8-D-1 AH T3

Table D.1: Definite Survey Listing, 25/8-D-1 AH T3, from Det Norske Oljeselskap (2013).

Schlumberger

D-1 H T3 8.5in MWD Survey Survey Report

(Non-Def Survey)

Report Date:	august 30, 2012 - 10:58	**Survey / DLS Computation:**	Minimum Curvature / Lubinski
Client:	Det Norske	**Vertical Section Azimuth:**	231.547 ° (Grid North)
Field:	Jette	**Vertical Section Origin:**	0.000 m, 0.000 m
Structure / Slot:	Jette Sor / Jette Sor Respud	**TVD Reference Datum:**	RKB
Well:	Jette Sor	**TVD Reference Elevation:**	40.000 m above MSL
Borehole:	Jette Sor D-1 AH T3	**Seabed / Ground Elevation:**	126.000 m below MSL
UWI / API#:	Unknown / Unknown	**Magnetic Declination:**	-1.222 °
Survey Name:	D-1 H T3 8.5in MWD Survey	**Total Gravity Field Strength:**	1001.9416 mgn (9.8 based)
Survey Date:	august 25, 2012	**Total Magnetic Field**	50690.143 nT
Tort / AHD / DDI / ERD Ratio:	170.951 ° / 1811.868 m / 6.231 / 0.859	**Magnetic Dip Angle:**	72.303 °
Coordinate Reference	UTM Zone 31 on ED50 Datum	**Declination Date:**	august 25, 2012
Location Lat / Long:	N 59° 24' 13.59665", E 2° 22' 10.92149"	**Magnetic Declination Model:**	BGGM 2012
Location Grid N/E Y/X:	N 6585335.100 m, E 464211.250 m	**North Reference:**	Grid North
CRS Grid Convergence	-0.5426 °	**Grid Convergence Used:**	-0.5426 °
Grid Scale Factor:	0.9996157	**Total Corr Mag North->Grid North:**	-0.6791 °
		Local Coord Referenced To:	Structure Reference Point

Comments	MD (m)	Incl (°)	Azim Grid (°)	TVD (m)	VSEC (m)	NS (N/S m)	EW (E/W m)	DLS (°/30m)	Closure (m)	TF (°)
Tie-In	0.00	0.00	257.40	0.00	0.00	N 0.00	E 0.00	N/A	0.00	268.75M
	175.10	0.40	266.75	175.10	0.49	S 0.01	W 0.61	0.07	0.61	80.92M
	181.35	0.33	80.92	181.35	0.49	S 0.01	W 0.62	3.50	0.62	93.39M
	188.77	0.43	93.39	188.77	0.45	S 0.01	W 0.57	0.52	0.57	167.61M
	203.57	0.90	167.61	203.57	0.46	S 0.13	W 0.49	1.80	0.50	180.35M
	214.71	0.87	180.35	214.71	0.55	S 0.30	W 0.47	0.53	0.55	136.34M
	294.61	0.62	136.34	294.60	0.89	S 1.22	W 0.17	0.23	1.23	109.51M
	318.72	0.53	109.51	318.71	0.82	S 1.35	E 0.02	0.35	1.35	112.69M
	346.95	0.40	112.69	346.94	0.70	S 1.43	E 0.24	0.14	1.45	118.23M
	374.82	0.46	118.23	374.81	0.61	S 1.52	E 0.42	0.08	1.58	126.54M
	403.63	0.33	126.54	403.62	0.54	S 1.62	E 0.59	0.15	1.73	144.65M
	430.91	0.29	144.65	430.90	0.53	S 1.73	E 0.70	0.12	1.86	132.89M
	446.41	0.26	132.89	446.40	0.53	S 1.78	E 0.74	0.12	1.93	146.3M
	493.12	0.06	146.30	493.11	0.51	S 1.87	E 0.84	0.13	2.05	190.05M
	521.21	0.11	190.05	521.20	0.53	S 1.91	E 0.84	0.08	2.09	112.01M
	549.72	0.08	112.01	549.71	0.54	S 1.95	E 0.85	0.13	2.13	342.84M
	577.87	0.09	342.84	577.86	0.53	S 1.93	E 0.86	0.16	2.12	300.33M
	606.09	0.06	300.33	606.08	0.52	S 1.91	E 0.85	0.07	2.08	262.42M
	635.04	0.06	262.42	635.03	0.54	S 1.90	E 0.82	0.04	2.07	189.39M
	663.35	0.10	189.39	663.34	0.57	S 1.93	E 0.80	0.11	2.09	220.82M
	691.67	0.08	220.82	691.66	0.61	S 1.97	E 0.78	0.06	2.12	356.35M
	721.20	0.04	356.35	721.19	0.62	S 1.97	E 0.77	0.11	2.11	87.28M
	749.42	0.06	87.28	749.41	0.61	S 1.96	E 0.78	0.08	2.11	222.97M
	777.91	0.09	222.97	777.90	0.62	S 1.98	E 0.78	0.15	2.12	277.63M
	806.33	0.09	277.63	806.32	0.65	S 1.99	E 0.74	0.09	2.12	130.68M
	834.52	0.08	130.68	834.51	0.67	S 2.00	E 0.74	0.17	2.13	166.87M
	862.88	0.08	166.87	862.87	0.67	S 2.03	E 0.76	0.05	2.17	9.05M
	891.28	0.11	9.05	891.27	0.66	S 2.02	E 0.77	0.20	2.16	224.34M
	919.49	0.06	224.34	919.48	0.65	S 2.01	E 0.76	0.17	2.15	95.67M
	947.91	0.09	95.67	947.90	0.65	S 2.02	E 0.77	0.14	2.16	262.02M
	975.79	0.06	262.02	975.78	0.65	S 2.02	E 0.78	0.16	2.17	24.27M
	1003.33	0.12	24.27	1003.32	0.64	S 2.00	E 0.78	0.17	2.15	288.51M
	1031.30	0.09	288.51	1031.29	0.62	S 1.97	E 0.77	0.17	2.11	268.35M
	1059.69	0.11	268.35	1059.68	0.66	S 1.96	E 0.72	0.04	2.09	240.23M
	1088.15	0.55	240.23	1088.13	0.81	S 2.03	E 0.57	0.48	2.11	237.34M
	1116.71	2.33	237.34	1116.68	1.53	S 2.41	W 0.03	1.87	2.41	242.33M
	1145.10	4.48	242.33	1145.02	3.19	S 3.24	W 1.50	2.29	3.57	248.24M
	1173.64	6.79	248.24	1173.42	5.90	S 4.38	W 4.06	2.50	5.97	255.45M
	1203.24	9.07	255.45	1202.74	9.71	S 5.62	W 7.94	2.52	9.73	23.64R
	1231.32	11.20	260.17	1230.38	14.13	S 6.64	W 12.77	2.44	14.39	7.1R
	1259.82	12.22	260.77	1258.29	19.19	S 7.59	W 18.48	1.08	19.98	61.16L
	1288.12	12.70	257.02	1285.92	24.61	S 8.77	W 24.46	1.00	25.99	1.8R
	1316.45	14.82	257.28	1313.44	30.69	S 10.27	W 31.03	2.25	32.69	6.51L
Tie-In	1344.60	16.46	256.62	1340.54	37.55	S 11.99	W 38.43	1.76	40.25	4.91R
	1354.80	16.90	256.75	1350.31	40.20	S 12.66	W 41.27	1.30	43.17	55.97R
	1363.20	17.64	260.22	1358.33	42.42	S 13.16	W 43.72	4.53	45.65	98.63R
	1403.19	17.79	281.13	1396.47	51.70	S 13.01	W 55.69	4.75	57.19	142.75R
	1431.47	16.39	285.00	1423.50	56.88	S 11.14	W 63.79	1.91	64.75	91.14L
	1459.77	16.63	273.72	1450.64	62.26	S 9.84	W 71.69	3.40	72.36	82.47L
	1487.83	17.47	261.65	1477.47	68.88	S 10.19	W 79.86	3.88	80.51	91.92L
	1516.26	17.46	259.86	1504.59	76.33	S 11.56	W 88.29	0.57	89.04	42.15L
	1545.81	17.53	259.65	1532.78	84.16	S 13.14	W 97.03	0.10	97.91	24.93L
	1574.06	18.10	258.80	1559.67	91.81	S 14.76	W 105.52	0.67	106.54	31.15L
	1602.28	18.34	258.34	1586.48	99.67	S 16.51	W 114.17	0.30	115.35	85.09R
	1630.56	18.37	259.35	1613.32	107.59	S 18.23	W 122.90	0.34	124.25	37.02R
	1658.71	18.84	260.44	1640.00	115.49	S 19.81	W 131.74	0.62	133.22	31.53L
	1687.13	20.74	257.20	1666.74	124.04	S 21.68	W 141.18	2.33	142.83	25.51L
	1715.20	23.26	254.19	1692.76	133.64	S 24.30	W 151.36	2.95	153.30	20.94L
	1743.53	25.44	252.26	1718.57	144.50	S 27.67	W 162.54	2.46	164.88	29.44L

Comments	MD (m)	Incl (°)	Azim Grid (°)	TVD (m)	VSEC (m)	NS (N/S m)	EW (E/W m)	DLS (°/30m)	Closure (m)	TF (°)
	1772.01	27.33	249.96	1744.08	156.42	S 31.78	W 174.51	2.26	177.38	45.6L
	1799.91	28.85	246.82	1768.70	168.99	S 36.62	W 186.71	2.28	190.27	35.3L
	1828.09	30.92	244.01	1793.13	182.62	S 42.47	W 199.47	2.66	203.95	31.88L
	1856.53	33.52	241.12	1817.19	197.51	S 49.47	W 212.92	3.19	218.59	31.11L
	1885.25	36.77	237.89	1840.67	213.87	S 57.87	W 227.15	3.91	234.41	19.13L
	1910.96	39.73	236.29	1860.86	229.71	S 66.52	W 240.51	3.64	249.54	7.67L
	1940.66	42.81	235.68	1883.18	249.24	S 77.48	W 256.74	3.14	268.18	2.7L
	1968.91	45.69	235.49	1903.42	268.91	S 88.63	W 273.00	3.06	287.03	6.8L
	1997.12	48.39	235.06	1922.64	289.51	S 100.39	W 289.97	2.89	306.85	1.68L
	2025.44	50.77	234.97	1941.00	311.02	S 112.75	W 307.63	2.52	327.64	3.41L
	2053.74	53.33	234.78	1958.40	333.30	S 125.59	W 325.88	2.72	349.24	13.95L
	2081.96	55.42	234.15	1974.84	356.21	S 138.92	W 344.54	2.29	371.50	34.56R
	2110.49	57.06	235.49	1990.69	379.89	S 152.58	W 363.93	2.08	394.62	39.05R
	2138.82	58.54	236.89	2005.79	403.78	S 165.92	W 383.85	2.01	418.17	2.79R
	2167.07	60.69	237.01	2020.08	428.04	S 179.21	W 404.27	2.29	442.21	3.17R
	2195.59	63.11	237.16	2033.51	453.08	S 192.88	W 425.39	2.55	467.08	10.31L
	2224.02	66.13	236.56	2045.70	478.65	S 206.92	W 446.90	3.24	492.48	20.75L
	2252.58	69.73	235.11	2056.43	505.04	S 221.78	W 468.79	4.04	518.61	8.02L
	2280.65	73.20	234.60	2065.35	531.60	S 237.10	W 490.55	3.74	544.84	21.65L
	2309.16	76.04	233.44	2072.91	559.06	S 253.25	W 512.79	3.21	571.92	27.28L
	2336.10	78.88	231.95	2078.76	585.35	S 269.19	W 533.70	3.55	597.75	11.87L
	2365.47	81.09	231.48	2083.86	614.27	S 287.11	W 556.40	2.31	626.11	37.59L
	2393.56	81.63	231.06	2088.08	642.04	S 304.48	W 578.07	0.73	653.35	9.32L
Tie-In	2404.39	82.96	230.84	2089.54	652.78	S 311.24	W 586.40	3.73	663.88	6.82R
	2437.32	85.63	231.16	2092.81	685.54	S 331.86	W 611.86	2.45	696.07	60L
	2466.27	86.12	230.31	2094.89	714.41	S 350.14	W 634.22	1.01	724.45	99.19L
	2495.14	86.07	230.00	2096.86	743.20	S 368.59	W 656.33	0.33	752.75	53.47L
	2524.09	87.04	228.69	2098.60	772.08	S 387.42	W 678.26	1.69	781.10	13.72R
	2552.74	87.49	228.80	2099.96	800.66	S 406.29	W 699.77	0.49	809.17	82.23L
	2581.69	87.52	228.58	2101.22	829.55	S 425.38	W 721.50	0.23	837.56	79.52R
	2610.43	87.72	229.66	2102.42	858.24	S 444.17	W 743.21	1.15	865.82	131.38L
	2639.43	87.50	229.41	2103.63	887.20	S 462.98	W 765.25	0.34	894.40	94.65L
	2668.26	87.47	229.04	2104.89	915.97	S 481.79	W 787.06	0.39	922.81	87.87L
	2697.32	87.52	227.71	2106.16	944.96	S 501.07	W 808.76	1.37	951.41	153.15R
	2726.28	86.81	228.07	2107.60	973.83	S 520.47	W 830.22	0.82	979.87	25.17L
	2754.97	87.15	227.91	2109.11	1002.42	S 539.64	W 851.51	0.39	1008.11	44.85L
	2783.80	88.87	226.20	2110.11	1031.14	S 559.27	W 872.60	2.52	1036.44	32.39L
	2813.01	90.21	225.35	2110.34	1060.20	S 579.64	W 893.53	1.63	1065.07	9.96R
	2841.79	90.95	225.48	2110.05	1088.82	S 599.84	W 914.03	0.78	1093.28	88.55R
	2870.88	91.01	227.89	2109.55	1117.80	S 619.80	W 935.19	2.49	1121.93	118.46R
	2899.57	90.24	229.31	2109.24	1146.45	S 638.77	W 956.70	1.69	1150.35	89.38R
	2928.72	90.27	232.09	2109.11	1175.59	S 657.23	W 979.26	2.86	1179.36	30.83L
	2957.56	91.61	231.29	2108.64	1204.42	S 675.10	W 1001.89	1.62	1208.11	28.62L
	2986.14	93.33	230.35	2107.41	1232.97	S 693.14	W 1024.02	2.06	1236.55	26.22L
	3015.12	95.13	229.46	2105.27	1261.86	S 711.75	W 1046.13	2.08	1265.30	71.84R
	3043.96	95.42	230.35	2102.62	1290.57	S 730.25	W 1068.09	0.97	1293.87	159.09R
	3072.91	93.04	231.26	2100.48	1319.43	S 748.49	W 1090.47	2.64	1322.64	139.82R
	3102.27	91.18	232.83	2099.40	1348.77	S 766.54	W 1113.60	2.49	1351.92	121.86R
	3130.98	89.98	234.76	2099.11	1377.45	S 783.49	W 1136.76	2.37	1380.61	82.25R
	3159.64	90.15	236.01	2099.08	1406.05	S 799.77	W 1160.35	1.32	1409.27	134.08R
	3188.82	87.75	238.49	2099.61	1435.08	S 815.56	W 1184.88	3.55	1438.43	117.94R
	3217.34	87.21	239.51	2100.87	1463.33	S 830.23	W 1209.31	1.21	1466.87	58.81R
	3246.19	87.67	240.27	2102.16	1491.84	S 844.69	W 1234.24	0.92	1495.61	1.76R
	3275.15	88.32	240.29	2103.17	1520.45	S 859.04	W 1259.37	0.67	1524.46	109.76L
	3304.10	88.18	239.90	2104.05	1549.07	S 873.46	W 1284.46	0.43	1553.31	18.84L
	3334.17	89.47	239.46	2104.67	1578.83	S 888.64	W 1310.41	1.36	1583.30	65.89L
	3363.07	90.24	237.74	2104.74	1607.51	S 903.70	W 1335.07	1.96	1612.17	122.08L
	3390.78	89.30	236.24	2104.85	1635.09	S 918.79	W 1358.31	1.92	1639.87	112.58L
	3420.31	88.15	233.47	2105.51	1664.56	S 935.78	W 1382.45	3.05	1669.39	78.06L
	3448.72	88.61	231.30	2106.31	1692.95	S 953.12	W 1404.94	2.34	1697.73	99.89L
	3477.86	88.24	229.17	2107.11	1722.07	S 971.75	W 1427.33	2.22	1726.72	87.71L
	3499.93	88.29	227.93	2107.78	1744.10	S 986.35	W 1443.87	1.69	1748.61	HS
TD Proj. w/ PDinc	3535.00	90.20	227.93	2108.25	1779.10	S 1009.85	W 1469.90	1.63	1783.36	

E Productivity Evaluation of Jette

E.1 Inflow Performance Relation

The IPR curves describe the inflow performance from the reservoir, based on reservoir pressure, reservoir temperature, water cut, GOR, fluid parameters and the PI. From the inflow performance curve the maximum flow rate, or AOF, performance may be found, which is obtained with maximum drawdown. Maximum drawdown for the two cases are 151 bar and 197 bar.

Figures E.1 and E.2 show the IPR curves with reservoir pressure of 197 bar. As observed in the figures the maximum flow rate is 650-750 m^3/day with maximum drawdown.

Figures E.3 and E.4 show the IPR curves with reservoir pressure of 151 bar. As observed in the figures the maximum flow rate is 900-930 m^3/day with maximum drawdown.

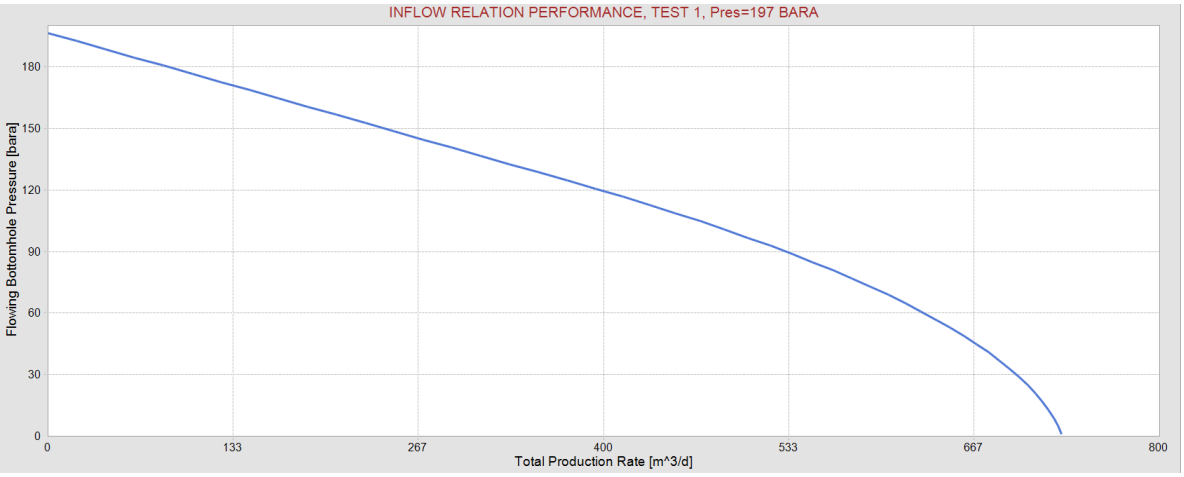

Figure E.1: Inflow performance curve, first multi-rate test. As seen in the figure, the initial reservoir pressure is 197 bar. The absolute open flow rate is 729.9 m^3/day.FromWellFlo(Weatherford 2012b).

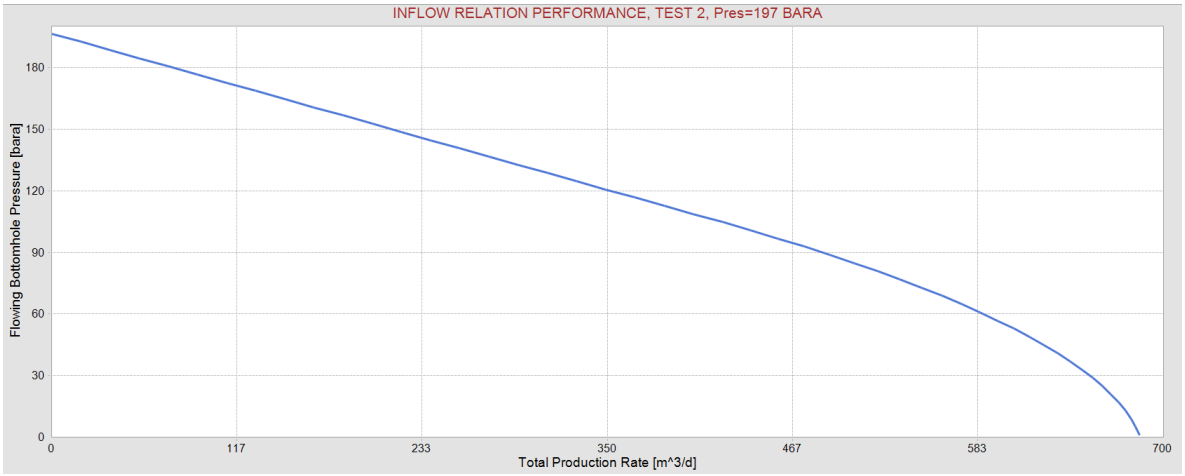

Figure E.2: Inflow performance curve, second multi-rate test. As seen in the figure, the initial reservoir pressure is 197 bar. The absolute open flow rate is 685.3 m^3/day.FromWellFlo(Weatherford 2012b).

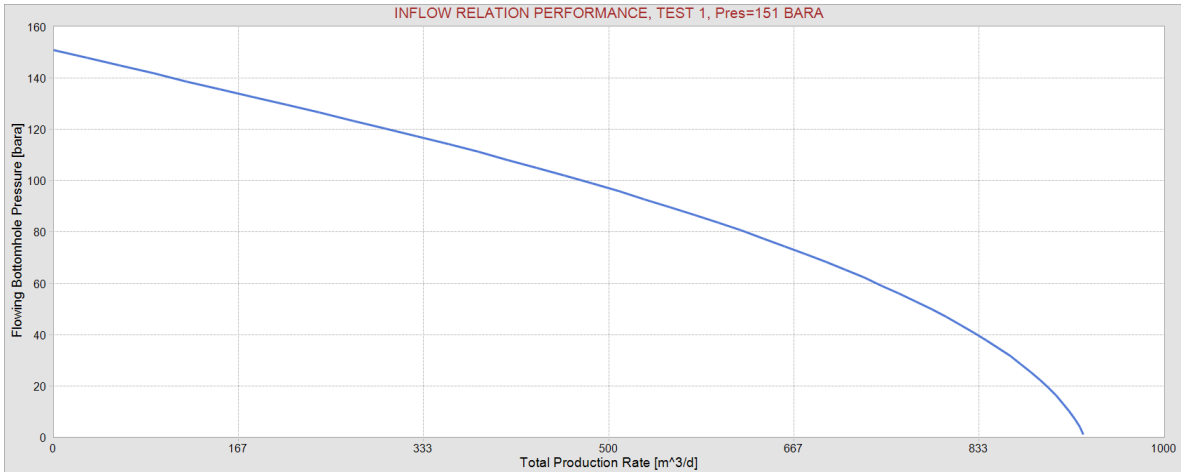

Figure E.3: Inflow performance curve, first multi-rate test. As seen in the figure, the initial reservoir pressure is 151 bar. The absolute open flow rate is 927.7 m^3/day.FromWellFlo(Weatherford 2012b).

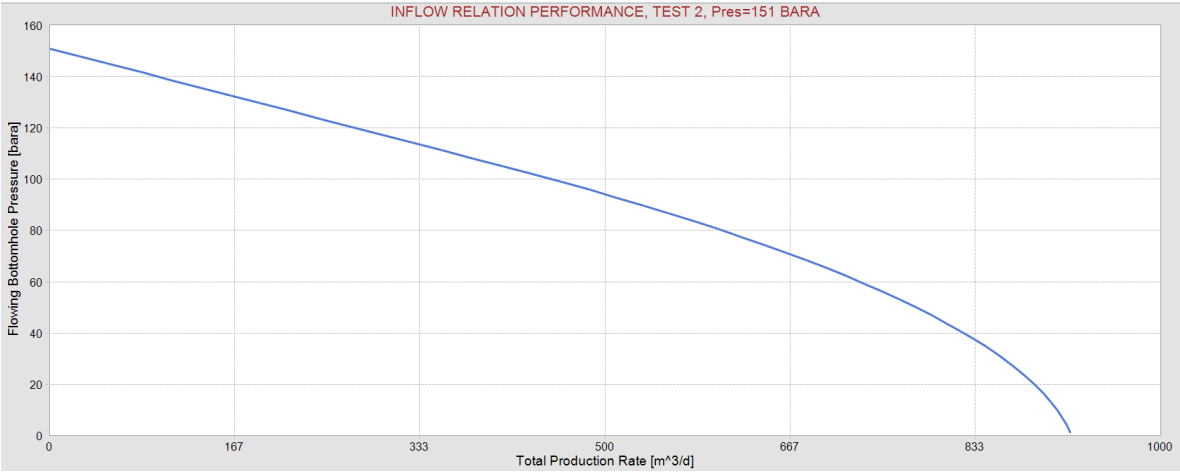

Figure E.4: Inflow performance curve, second multi-rate test. As seen in the figure, the initial reservoir pressure is 151 bar. The absolute open flow rate is 919.2 m^3/day.FromWellFlo(Weatherford 2012b).

E.2 Sensitivity Analysis

E.2.1 Inflow Relation Performance

Gas Lift Rates

A sensitivity analysis with gas lift rates were done at both tests with both reservoir pressures. Different gas lift rates were used in test 1 and test 2 as the tests are based on different input parameters.

Figures E.5 and **E.6** show gas lift rate sensitivity of the tests with reservoir pressure of 197 bar, and **Figures E.7** and **E.8** show gas lift rate sensitivity of the tests with reservoir pressure of 151 bar.

In figure E.5 it is shown that a match in BHP and rates are obtained with a gas lift rate of $150*10^3 Sm^3/day$, 155.1% increase from the measured. In figure E.6 a match obtained with a gas lift of $16*10^3 Sm^3/day$, a decrease of 59.8%. This indicates that the gas lift may be poorly measured, and that there may be great fluctuations in gas lift rate.

The input data in the tests with 151 bar reservoir pressure is almost the same except the reservoir pressure and the respective PI. Hence, it is obvious that the same trend of gas lift rate will be observed. In figure E.7 it is shown that a match in BHP and rates is obtained with a gas lift of $175*10^3 Sm^3/day$, 197.6% increase from the measured. In figure E.6 a match is obtained with a gas lift of $17*10^3 Sm^3/day$, a decrease of 57%. The trend of gas lift rates is the same as seen in figures E.5 and E.6.

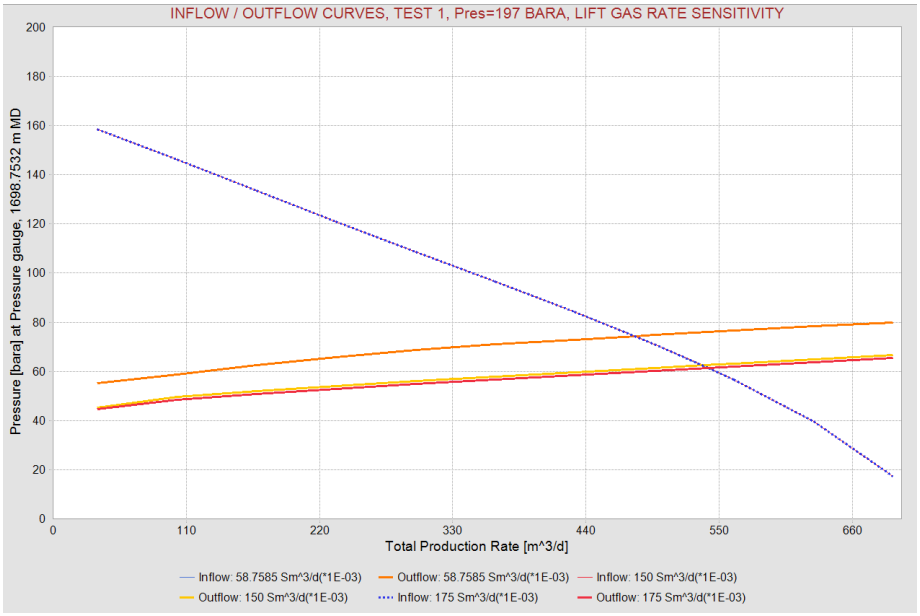

*Figure E.5: Sensitivity of test 1 with reservoir pressure of 197 bara. Gas lift rate sensitivity is 175*10³Sm³/day (red line) and 150*10³Sm³/day (yellow line). The orange line is the original gas lift rate. The dashed blue line is the inflow performance curve. From WellFlo (Weatherford 2012b).*

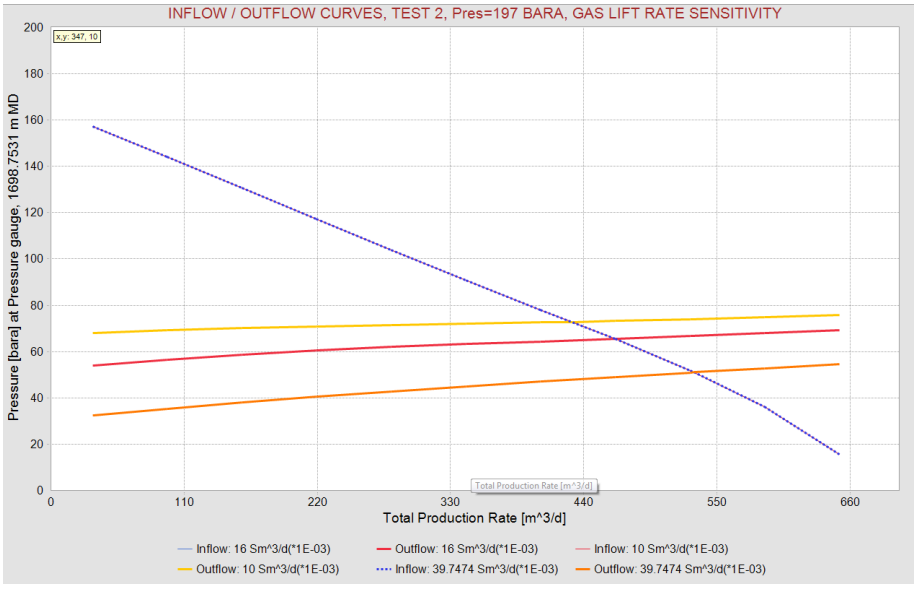

*Figure E.6: Sensitivity of test 2 with reservoir pressure of 197 bara. Gas lift rate sensitivity is 16*10³Sm³/day (red line) and 10*10³Sm³/day (yellow line). The orange line is the original gas lift rate. The dashed blue line is the inflow performance curve. From WellFlo (Weatherford 2012b).*

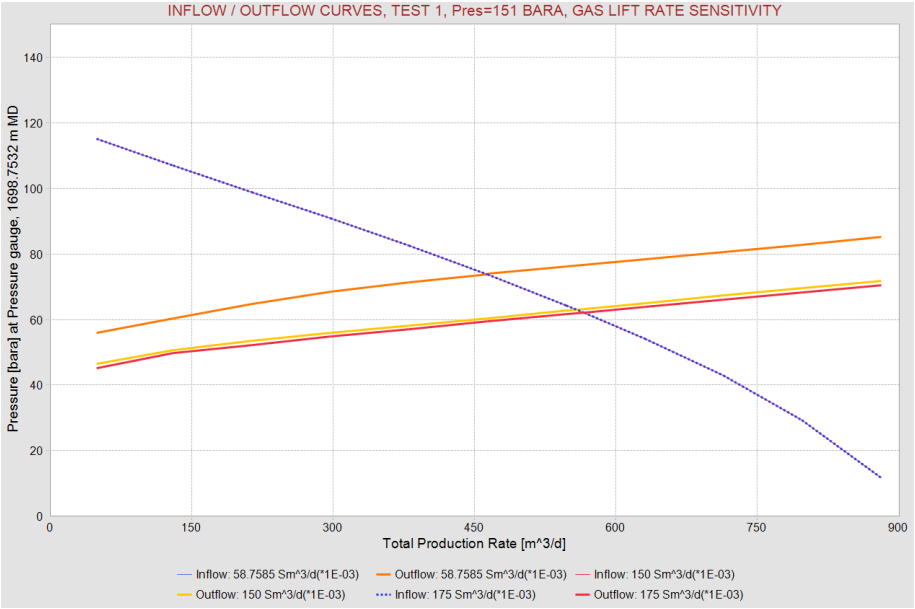

*Figure E.7: Sensitivity of test 1 with reservoir pressure of 151 bara. Gas lift rate sensitivity is 175*10^{3}Sm^3/day (red line) and 150*10^{3}Sm^3/day (yellow line). The orange line is the original gas lift rate. The dashed blue line is the inflow performance curve. From WellFlo (Weatherford 2012b).*

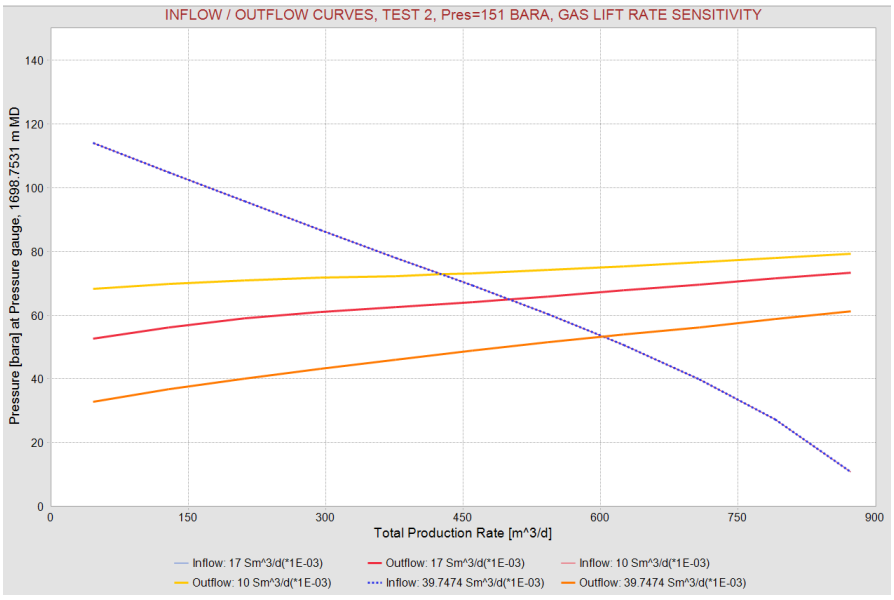

*Figure E.8: Sensitivity of test 2 with reservoir pressure of 151 bara. Gas lift rate sensitivity is 17*10^{3}Sm^3/day (red line) and 10*10^{3}Sm^3/day (yellow line). The orange line is the original gas lift rate. The dashed blue line is the inflow performance curve. From WellFlo (Weatherford 2012b).*

Gas-Oil Ratio

A sensitivity analysis of GOR were done at both tests with both reservoir pressures. Different GOR's were used in test 1 and test 2 as the tests are based on different input parameters.

Figures E.9 and **E.10** show GOR sensitivity of the tests with reservoir pressure of 197 bar, and **Figures E.11** and **E.12** show GOR sensitivity of the tests with reservoir pressure of 151 bar.

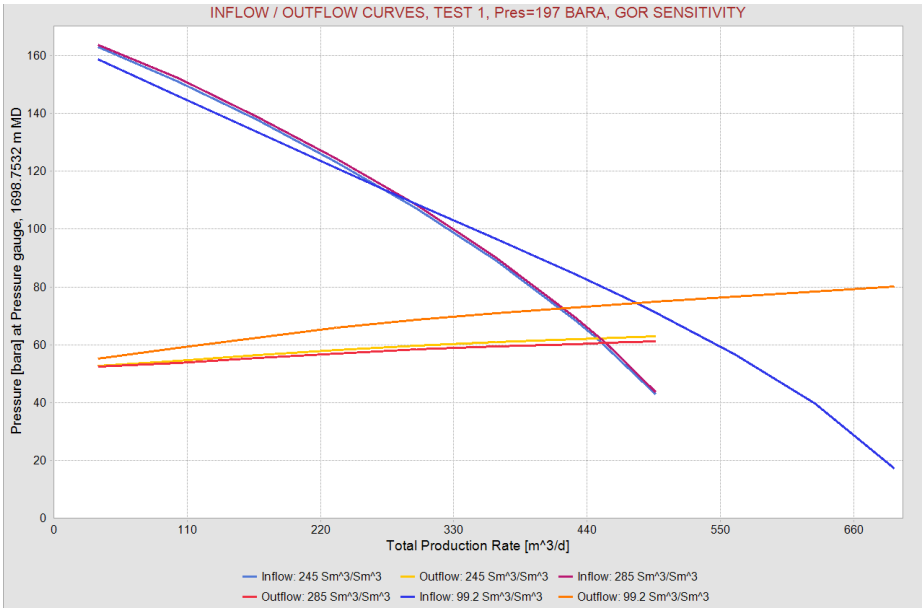

Figure E.9: Sensitivity of test 1 with reservoir pressure of 197 bara. GOR sensitivity is 285 Sm^3/Sm^3 (red line and purple line) and 245 Sm^3/Sm^3 (yellow line and light blue line). The orange line is the original GOR. The dark blue line is the original IPR curve. From WellFlo (Weatherford 2012b).

In figure E.9 it is shown that a match in BHP and rates is obtained with a GOR of 245 Sm^3/Sm^3, an increase of 147 % from the measured. In figure E.10 a match is obtained with a GOR of 20 Sm^3/day, a decrease of 76.5%. This may indicate that the reservoir pressure is lower than initially indicated, or that the measurements at the MPFM are poor.

In figure E.11 it is shown that a match in BHP and rates is obtained with a GOR of 285 Sm^3/Sm^3, an increase of 187.3 % of the measured. In figure E.12 a match is obtained with a GOR of 20 Sm^3/day, a decrease of 76.5%. The results from the sensitivity analysis of GOR indicates the same trend for both reservoir pressures. The measurements of the GOR at the MPFM may be poor, or it may be a combination of both higher GOR and gas lift rates.

Figure E.10: Sensitivity of test 2 with reservoir pressure of 197 bara. GOR sensitivity is 50 Sm^3/Sm^3 (red line and purple line) and 20 Sm^3/Sm^3 (yellow line and light blue line). The orange line is the original GOR. The dark blue line is the original IPR curve. From WellFlo (Weatherford 2012b).

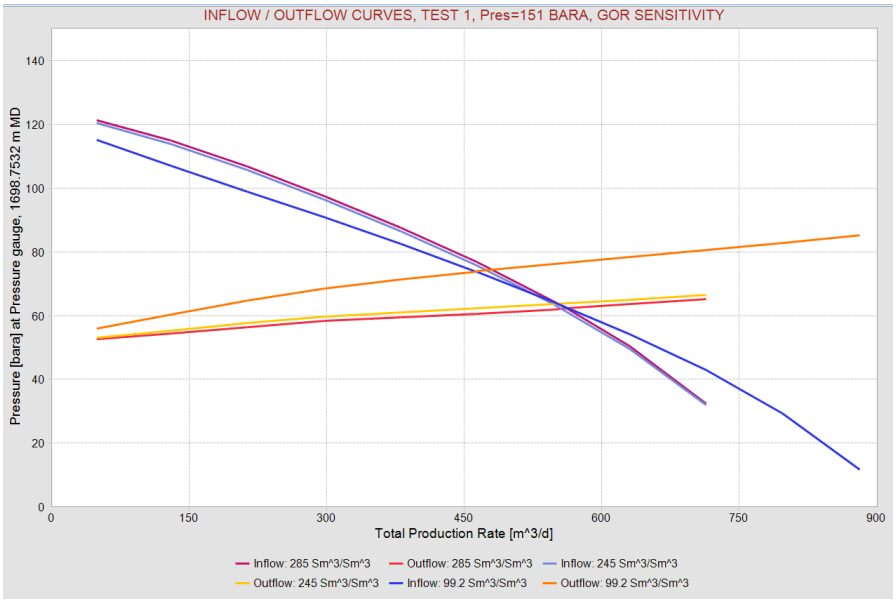

Figure E.11: Sensitivity of test 1 with reservoir pressure of 151 bara. GOR sensitivity is 285 Sm^3/Sm^3 (red line and purple line) and 245 Sm^3/Sm^3 (yellow line and light blue line). The orange line is the original GOR. The dark blue line is the original IPR curve. From WellFlo (Weatherford 2012b).

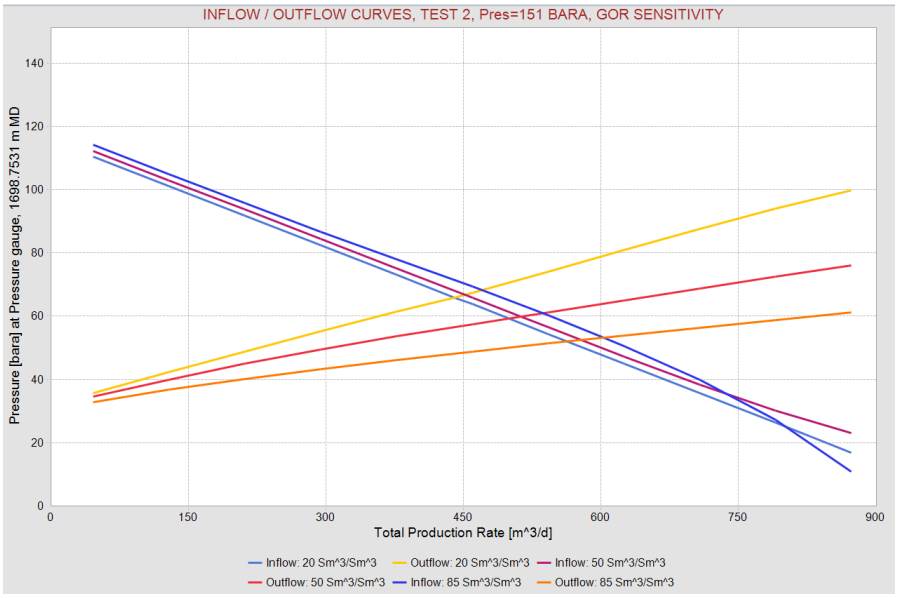

Figure E.12: Sensitivity of test 2 with reservoir pressure of 151 bara. GOR sensitivity is 50 Sm^3/Sm^3 (red line and purple line) and 20 Sm^3/Sm^3 (yellow line and light blue line). The orange line is the original GOR. The dark blue line is the original IPR curve. From WellFlo (Weatherford 2012b).

Inner Diameter Reservoir Section

Section 5.2 describes the process of scale precipitation. As the productivity in Well D is so poor, the estimated producing well length from the build-up test is around 50% of the completed interval, and the well was poorly cleaned up, it may indicate a reduced inner diameter of the reservoir section. Sensitivity analysis is performed for both multi-rate tests with both reservoir pressures, with inner diameters of 50 mm and 400 mm.

Figures E.13 and **E.14** show the sensitivity with reservoir pressure of 197 bar, and **Figures E.15** and **E.16** show the sensitivity with reservoir pressure of 151 bar.

It is observed in the figures that the BHP decreases with decreasing diameter. When increasing the diameter the BHP does not change from the initial BHP. The decrease in BHP may, in test 1 for both reservoir pressures, indicate scale or wax in the well. As the decrease is minor, either/both gas lift or/and GOR is likely to contribute as well. From test 2, it is not indicated a smaller diameter, as the measured BHP is higher than that of the smaller diameter.

The sensitivity analysis with inner diameter is conflicting, as it may indicate two different theories. The scale may reduce the diameter, or it may block/reduce the permeability around the well, leading to reduced PI for both cases. From the sensitivity analysis it is challenging to conclude whether there is a presence of scale or not.

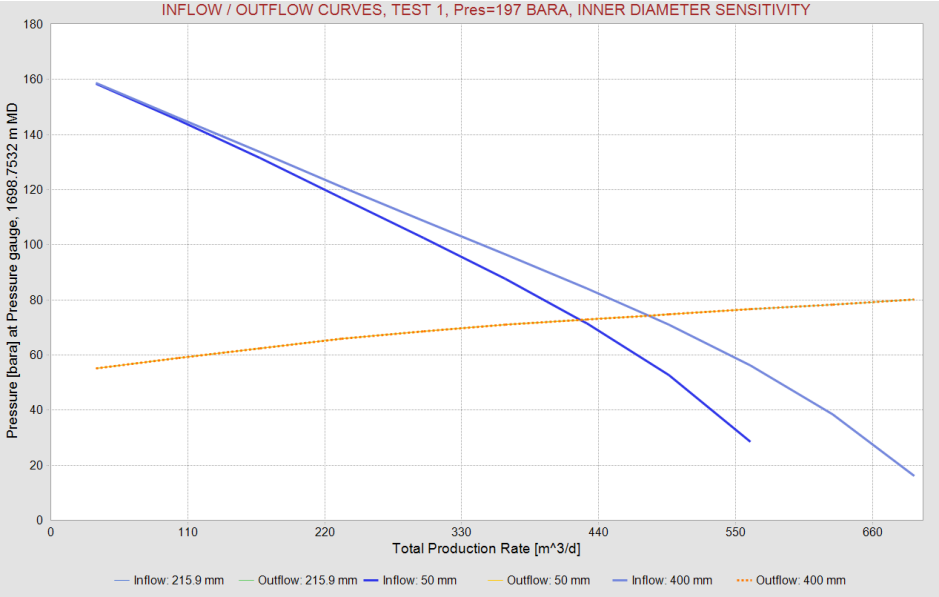

Figure E.13: Sensitivity of test 1 with reservoir pressure of 197 bara. Inner diameter sensitivity is 400 mm (light blue line) and 50 mm (dark blue line). The original inflow curve of the inner diameter follows the light blue line. The dashed line is the outflow curve for all cases. From WellFlo (Weatherford 2012b).

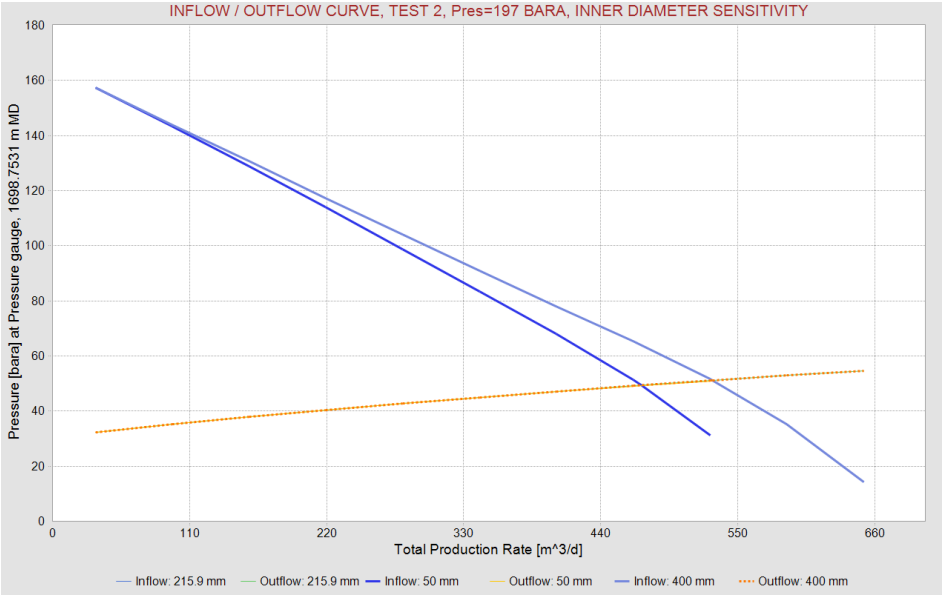

Figure E.14: Sensitivity of test 2 with reservoir pressure of 197 bara. Inner diameter sensitivity is 400 mm (light blue line) and 50 mm (dark blue line). The original inflow curve of the inner diameter follows the light blue line. The dashed line is the outflow curve for all cases. From WellFlo (Weatherford 2012b).

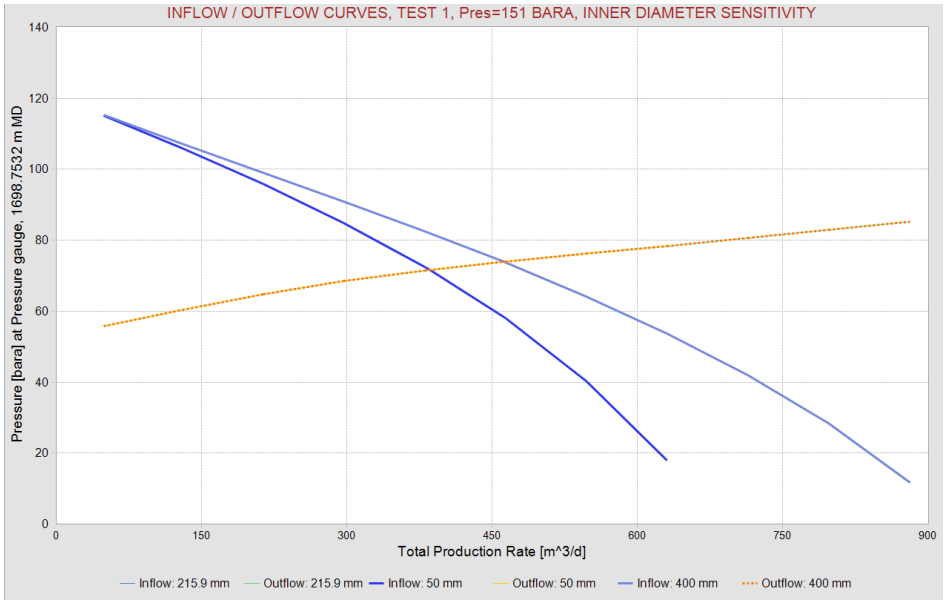

Figure E.15: Sensitivity of test 1 with reservoir pressure of 151 bara. Inner diameter sensitivity is 400 mm (light blue line) and 50 mm (dark blue line). The original inflow curve of the inner diameter follows the light blue line. The dashed line is the outflow curve for all cases. From WellFlo (Weatherford 2012b).

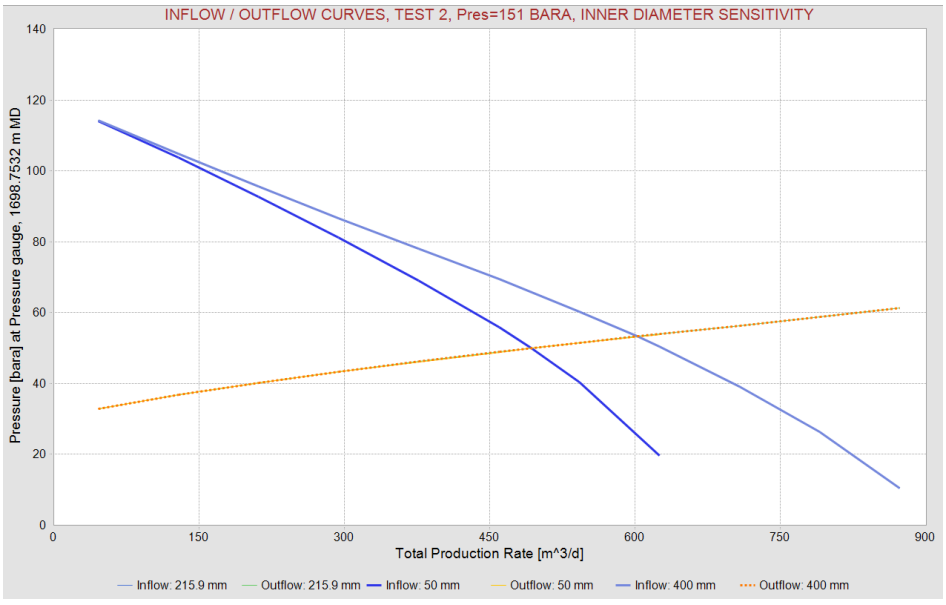

Figure E.16: Sensitivity of test 2 with reservoir pressure of 151 bara. Inner diameter sensitivity is 400 mm (light blue line) and 50 mm (dark blue line). The original inflow curve of the inner diameter follows the light blue line. The dashed line is the outflow curve for all cases. From WellFlo (Weatherford 2012b).

E.2.2 Pseudo-Steady State Model

Drainage Area

As seen in Chapter 7.5 in the pseudo-steady state model there is an uncertainty in the choice of drainage area. The drainage area has a great impact on the respective PI. **Figure E.17** shows the different productivity indices with different drainage areas. The PI deviates with up to 120%.

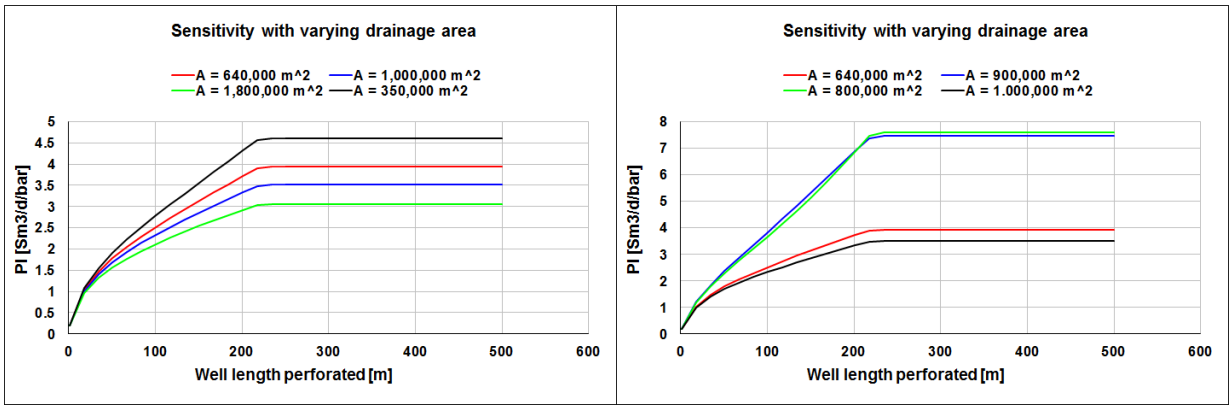

(a) $P_{res} = 197bar$. *(b)* $P_{res} = 151bar$.

Figure E.17: Sensitivity analysis of drainage area.

When altering the drainage area, the shape factors are taken into account. The shape factors, C_A, change when changing the drainage area. This is observed in Table 7.9 and 7.11. Sensitivity performed at the shape factors have a deviation of up to 43%.

Formation Thickness

The formation thickness is one of the three parameters that offers the highest uncertainty, and varies with up to 90%. **Figure E.18** shows the different productivity indices with different formation thicknesses. The thicknesses are 2 m, 5 m and 10 m. 7.7 m is the original thickness used. It is assumed that the well is placed in the middle of the layer.

Well Deviation

Well deviation is another of the parameters that offers highest uncertainty, and varies with up to 120%. **Figure E.19** shows the different productivity indices with different deviation. The deviations are 86°, 87° and 90°. 88° is the original deviation used. As seen in the figures, there is a great deviation in PI from 88° to 90°.

A generally high DLS was pointed out in section 7.1. With the high DLS there will be experienced changes in the productivity index along the wellbore. 88° is used as an average deviation of the well.

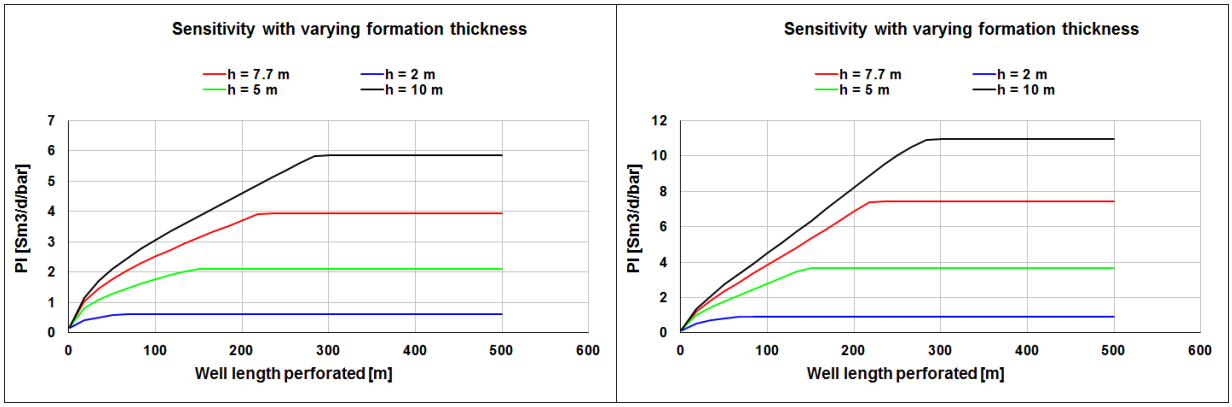

(a) $P_{res} = 197bar$. *(b)* $P_{res} = 151bar$.

Figure E.18: Sensitivity analysis of formation thickness.

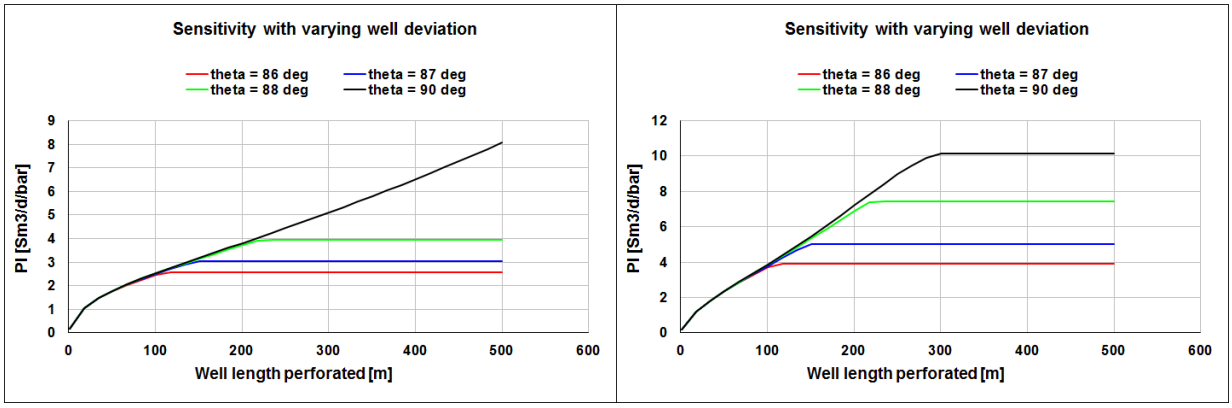

(a) $P_{res} = 197bar$. *(b)* $P_{res} = 151bar$.

Figure E.19: Sensitivity analysis of well deviation.

Vertical Permeability

In Jette, shale barriers and distinct layering may inhibit vertical permeability. Hence, the maximum ratio of k_v/k_h is one (Joshi 1991), that is 13 mD. The maximum deviation found from the sensitivity analysis with vertical permeability is 31%. The vertical permeabilities are 13 mD, 1 mD and 10 mD. 4 mD is the original vertical permeability used. See **Figure E.20**. During the sensitivity analysis of the vertical permeability, the horizontal permeability was kept constant.

Horizontal Permeability

Horizontal permeability is the parameter which offers the greatest uncertainty. In the analysis, it is found to deviate with up to 230%. The sensitivity is done with 4 mD, 20 mD and 50 mD. The original horizontal permeability is 13 mD. See **Figure E.21**. During

the sensitivity analysis of the horizontal permeability, the vertical permeability were kept constant.

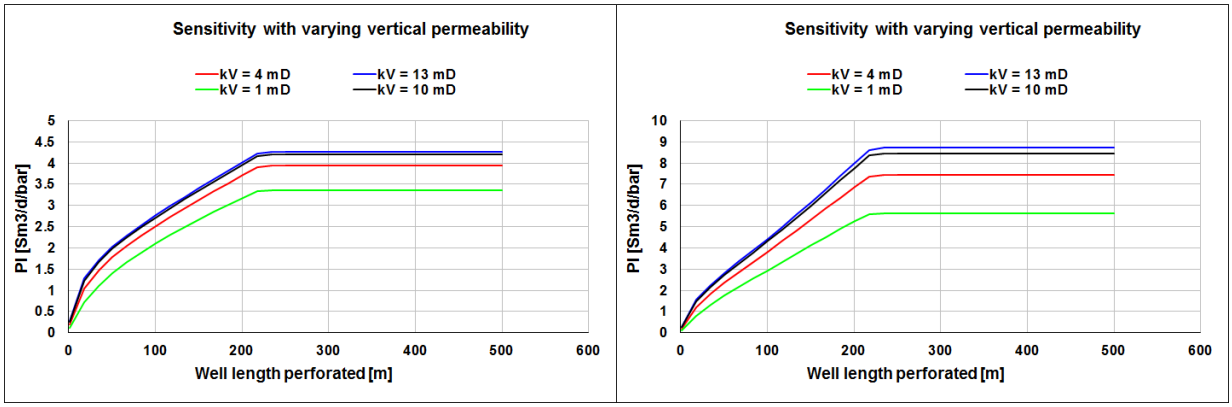

(a) $P_{res} = 197bar$. *(b)* $P_{res} = 151bar$.

Figure E.20: Sensitivity analysis of vertical permeability.

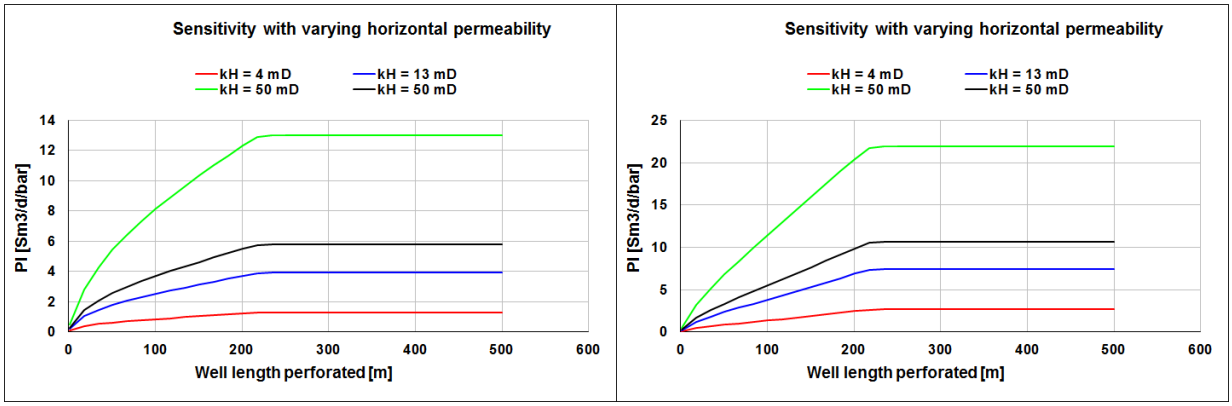

(a) $P_{res} = 197bar$. *(b)* $P_{res} = 151bar$.

Figure E.21: Sensitivity analysis of horizontal permeability.

Well Location

Due to earlier mentioned *snaking* properties of horizontal wells the position of the well will change in the respective layer. It is assumed in the above calculations that the well lies in the middle of layer Z2. The sensitivity analysis done at well location gives a deviation of up to 40%, which is dependent upon the well length. See **Figure E.22**. The well locations are 0 m, 1 m and 2.5 m. 3.85 m is the original well location, that is in the middle of the layer thickness.

Skin Along Well

Changes in skin gives a deviation of PI as given in **Figure E.23**. As seen in the figures, the deviation varies with up to 45% from estimated skin, 1. The different skin values are -1, 6 and -6.

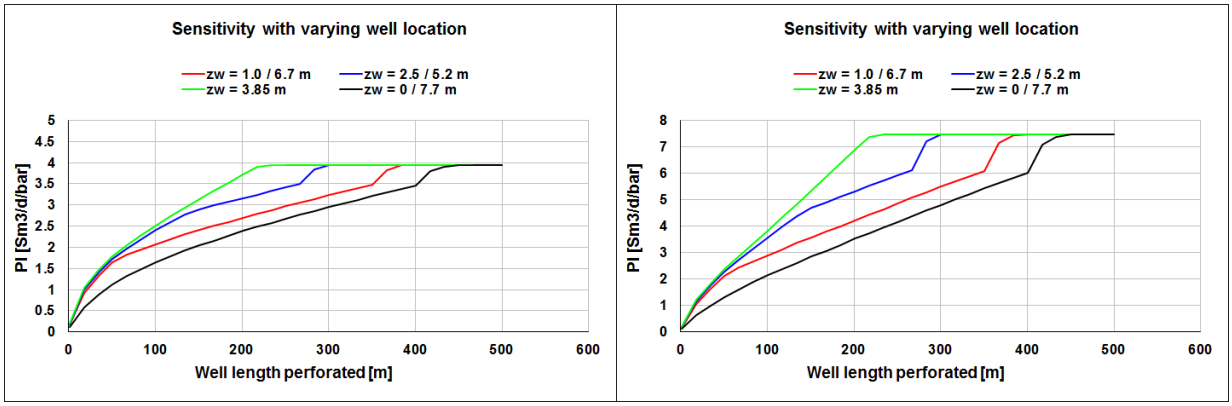

(a) $P_{res} = 197bar$. *(b)* $P_{res} = 151bar$.

Figure E.22: Sensitivity analysis of well location.

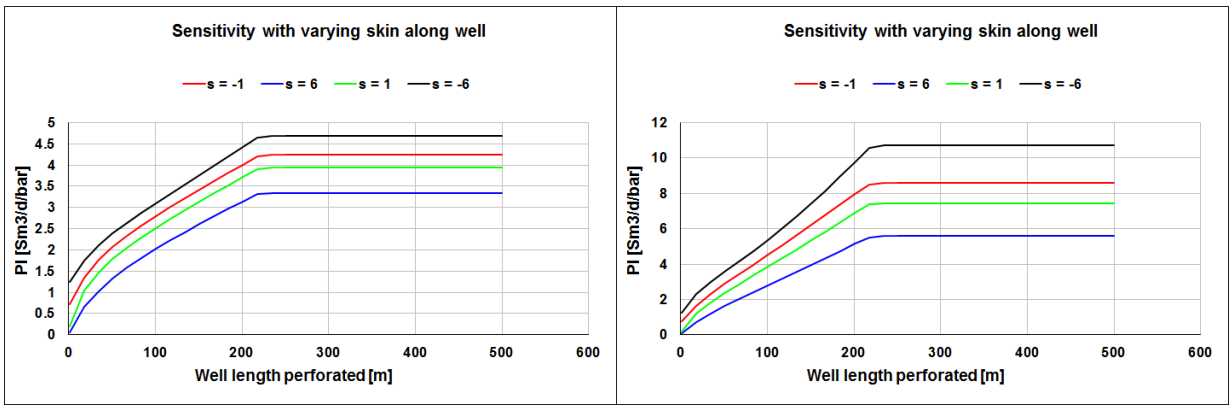

(a) $P_{res} = 197bar$. *(b)* $P_{res} = 151bar$.

Figure E.23: Sensitivity analysis of skin along the well.

F PVT Modeling

F.1 Procedure in PVTsim

A Black Oil PVT model based upon data from sample TS-101404 from well 25/8-17 was made and tuned in PVTsim. From PVTsim the model was exported to the ECLIPSE simulation software.

The fluid was remade in PVTsim, specified with its fluid components, taken from the analysis of the samples. Mol per cent, mol weight and liquid density were some of the input parameters. The plus fraction was set at C36+. See **Figure F.1**.

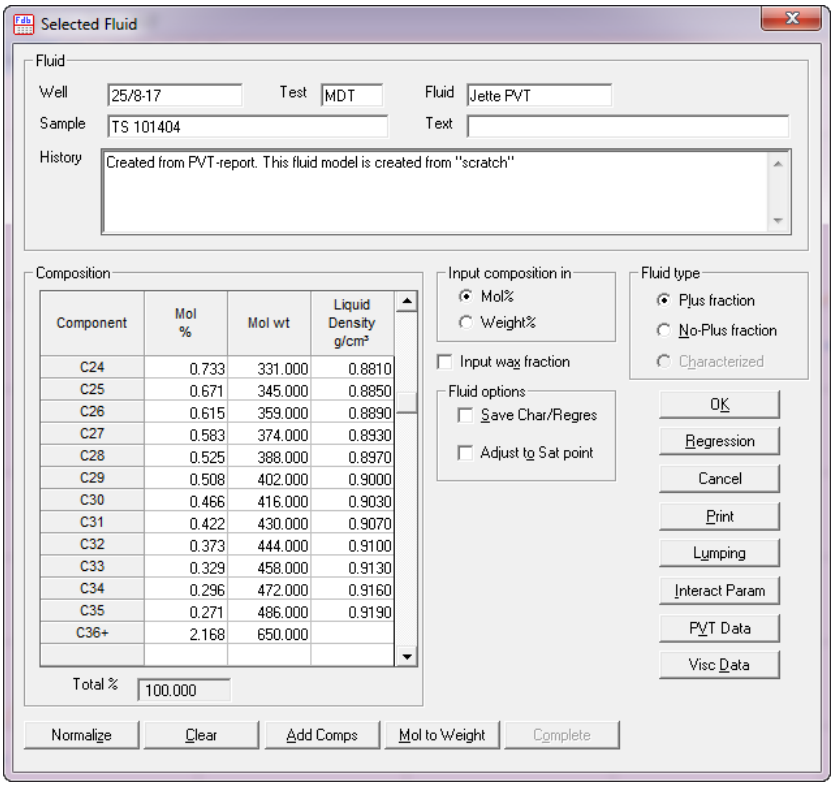

Figure F.1: Initial composition of the fluid. From PVTSim (calsep 2013).

To better define the fluid components and the respective molar composition, the components were lumped in five pseudo components, from C7+. Mol per cent, mol weight, liquid density, critical pressure and temperature were some of the input parameters. See **Figure F.2**.

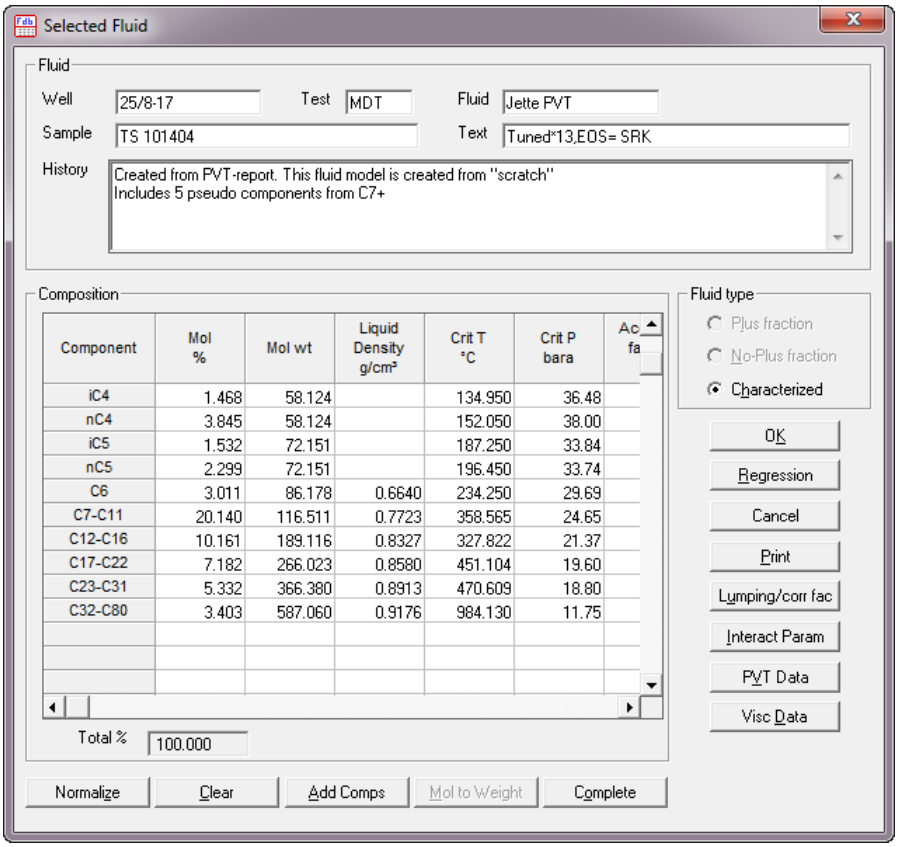

Figure F.2: Lumping from new plus fraction, C7+. From PVTSim (calsep 2013).

When the composition of the fluid was defined, the experimental data from the Weatherford Laboratories A/S report (Sandvik & Ravnås 2010) was added.

Input data from CME are shown in **Figure F.3**, input data from DLE are shown in **Figure F.4**, input data from the three-stage separator test are shown in **Figure F.5**, and input data from viscosity test are shown in **Figure F.6**. The reservoir temperature was set to 83.6 °C, the sampling depth to 2094 m MD RKB, and the system type to bottom hole.

Tuning was done using Soave-Redlich-Kwong with volume shifts (SRK Peneloux), as this Equation of State (EOS) gave the best match. The average deviation after tuning was maximum 2%. The results are shown in **Figures F.7- F.13**. The tuned PVT model was exported to Eclipse.

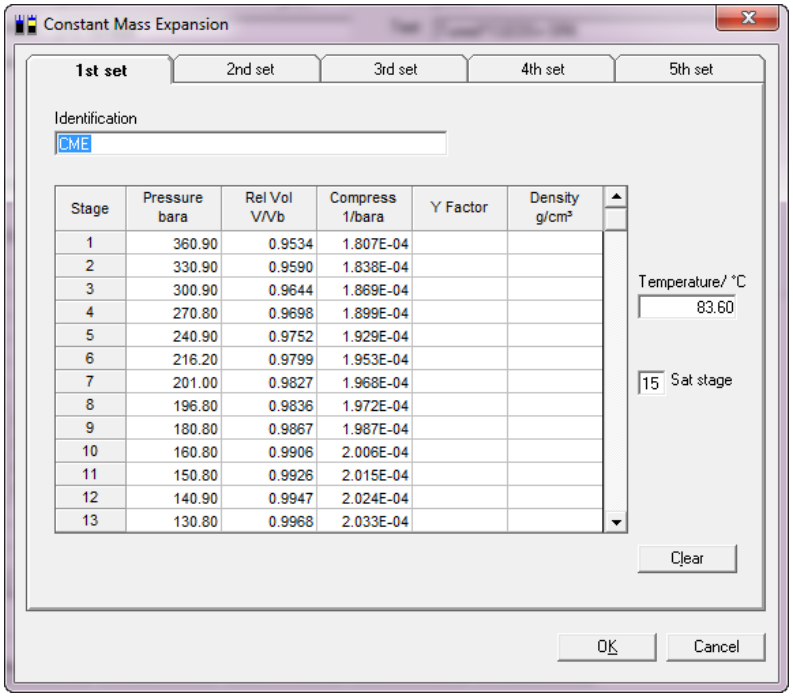

Figure F.3: Experimental input data, Constant Mass Expansion test. From PVTSim (calsep 2013).

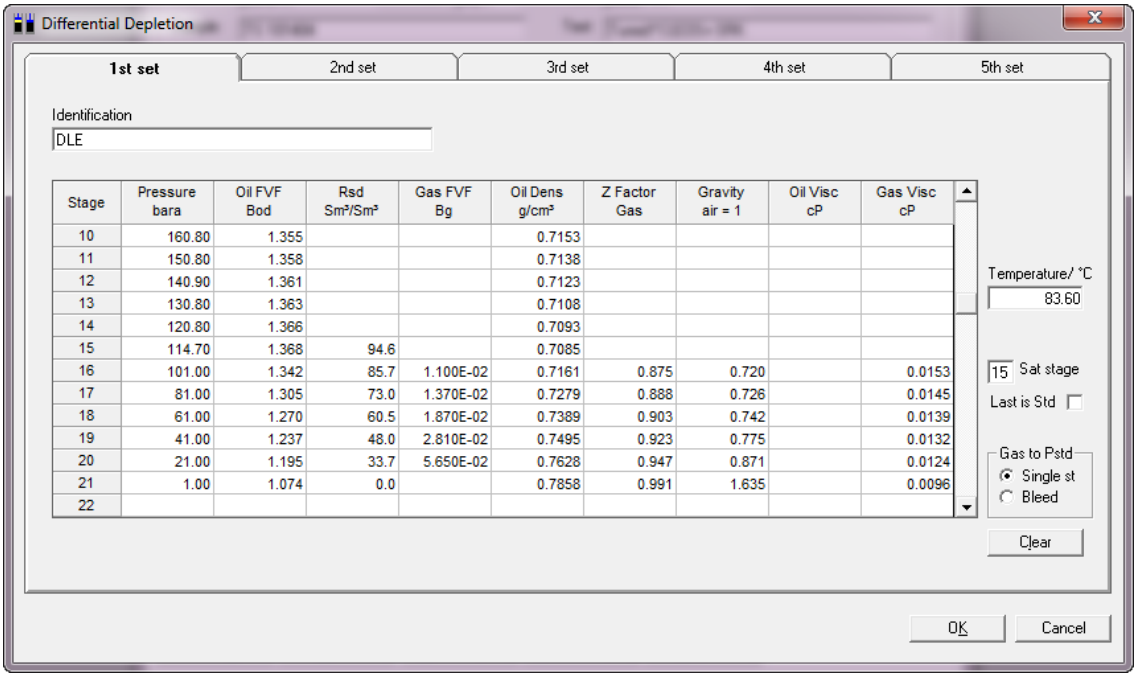

Figure F.4: Experimental input data, Differential Liberation Experiment. From PVTSim (calsep 2013).

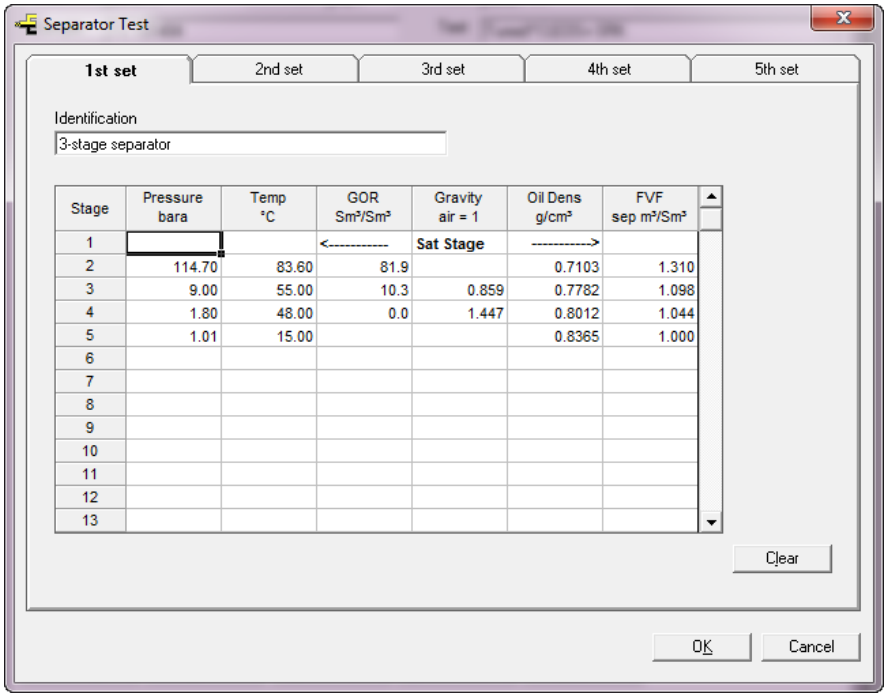

Figure F.5: Experimental input data, Three-stage Separator test. From PVTSim (calsep 2013).

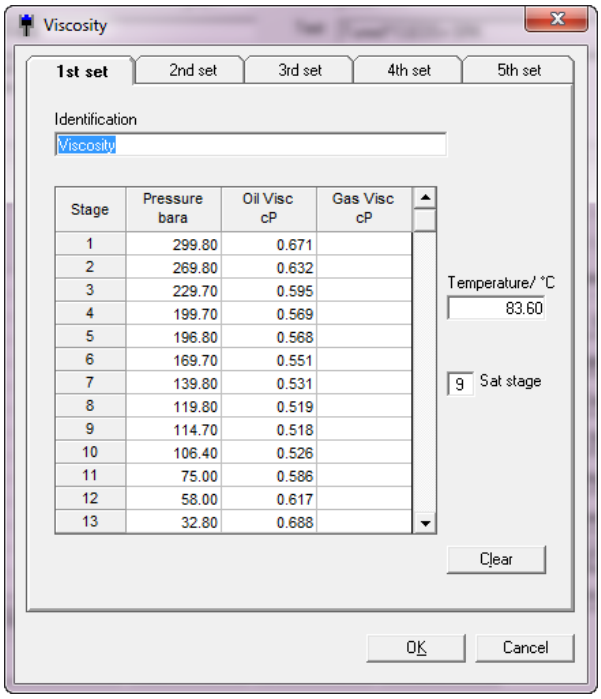

Figure F.6: Experimental input data, Viscosity test. From PVTSim (calsep 2013).

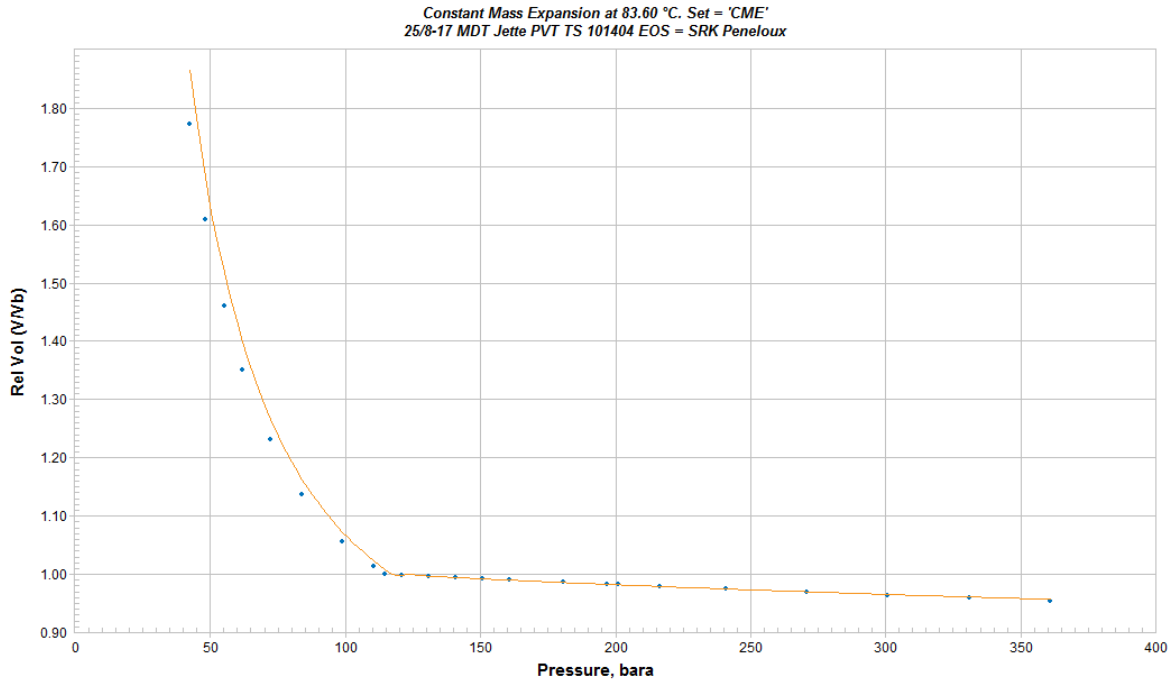

Figure F.7: Results from tuning, showing total relative volume. From PVTSim (calsep 2013).

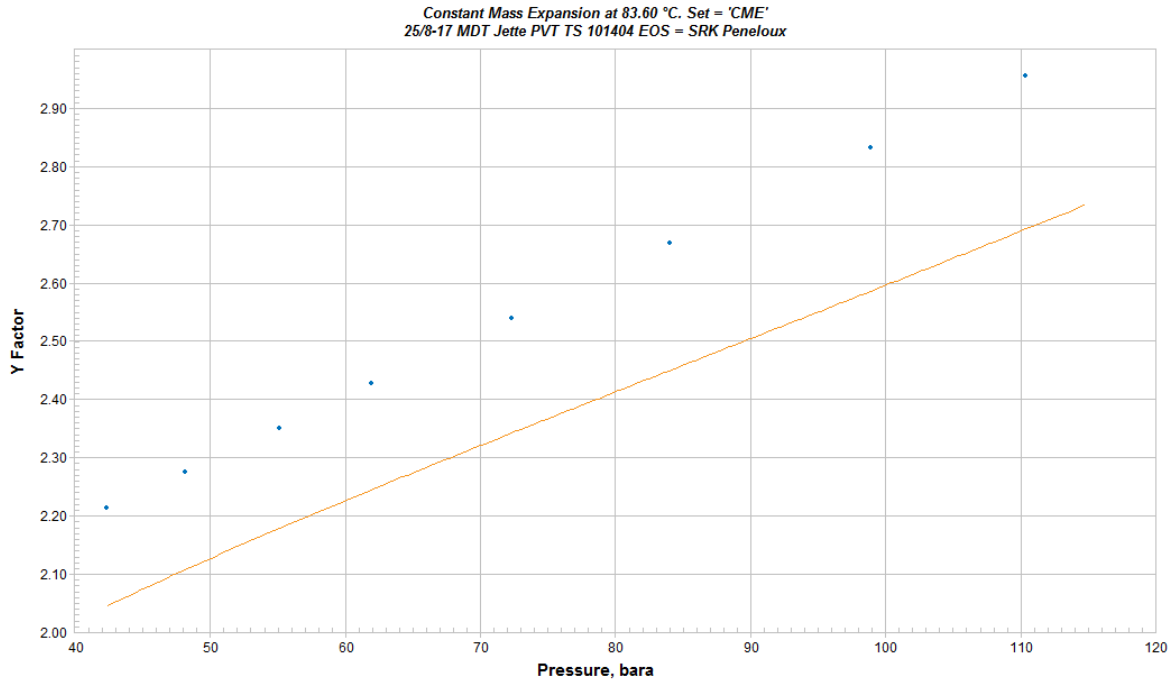

Figure F.8: Results from tuning, showing Y-factor. From PVTSim (calsep 2013).

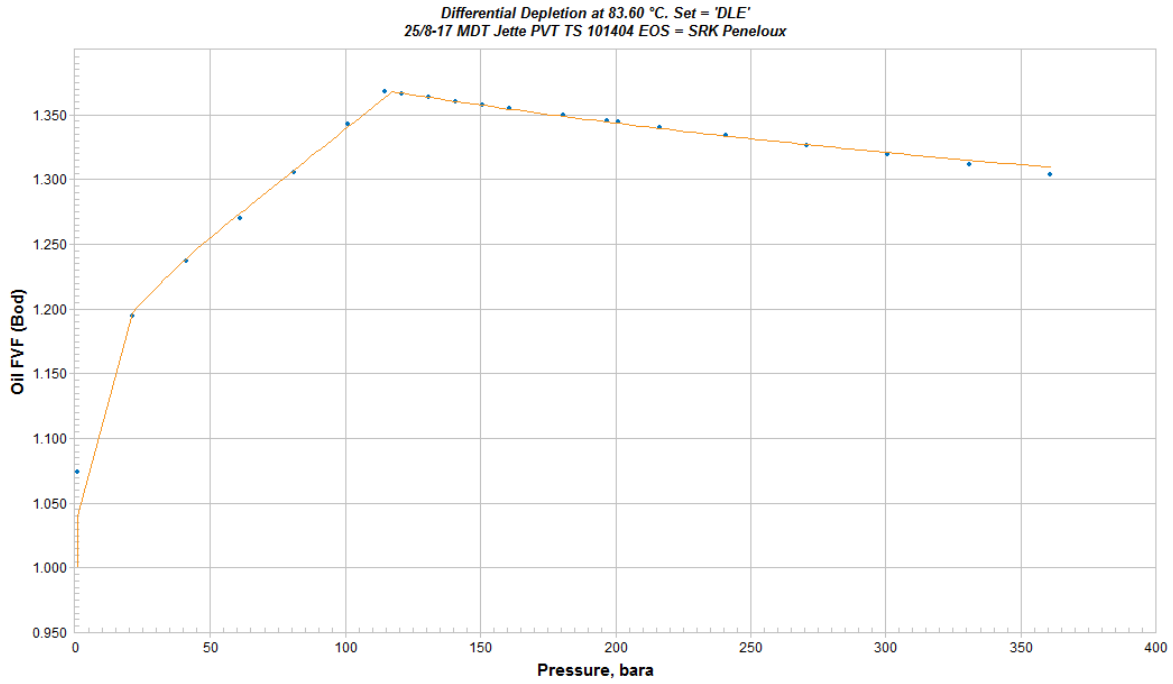

Figure F.9: Results from tuning, showing oil Formation Volume Factor (FVF). From PVTSim (calsep 2013).

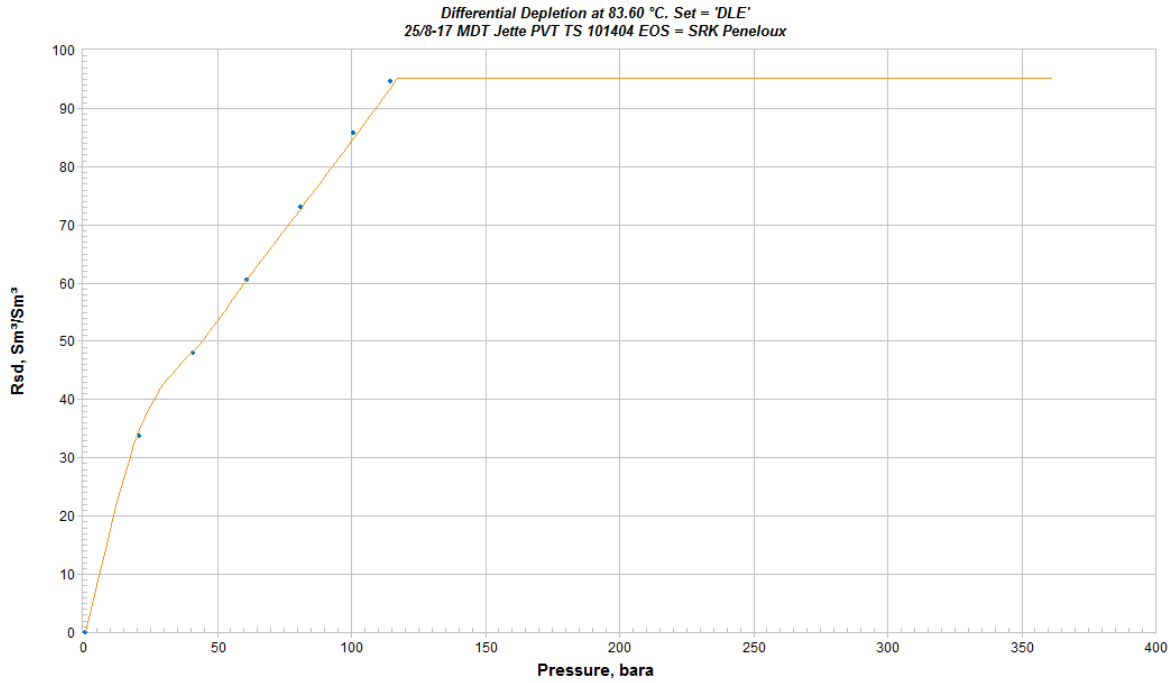

Figure F.10: Results from tuning, showing R_{sd}. From PVTSim (calsep 2013).

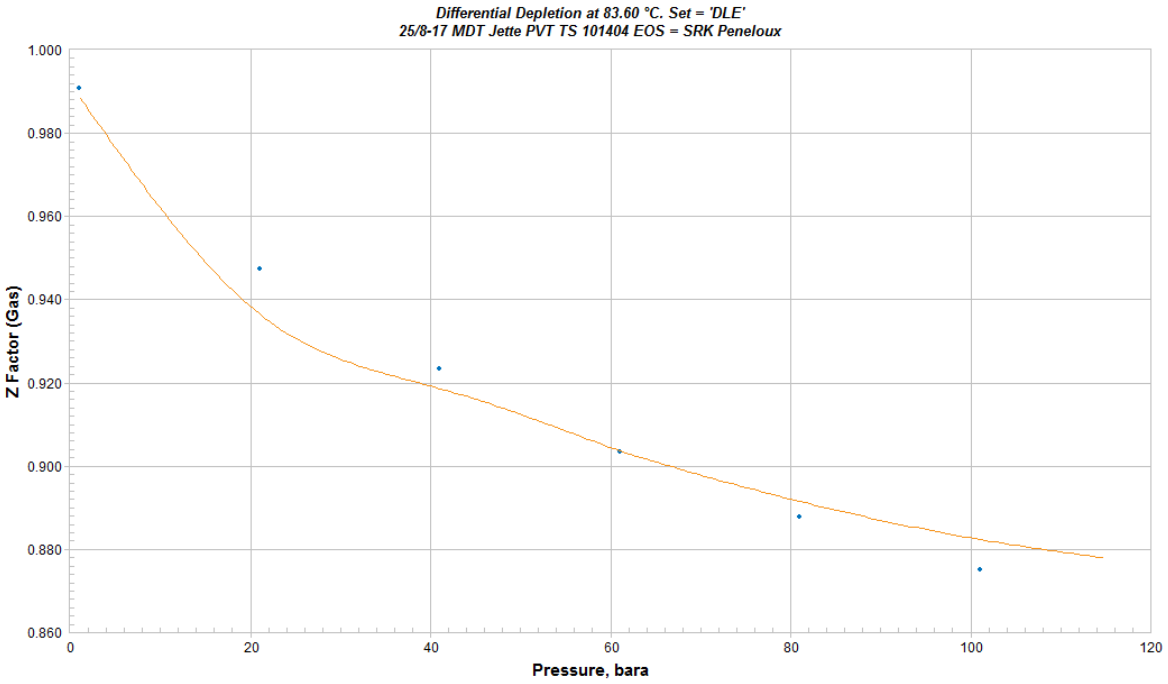

Figure F.11: Results from tuning, showing Z-factor. From PVTSim (calsep 2013).

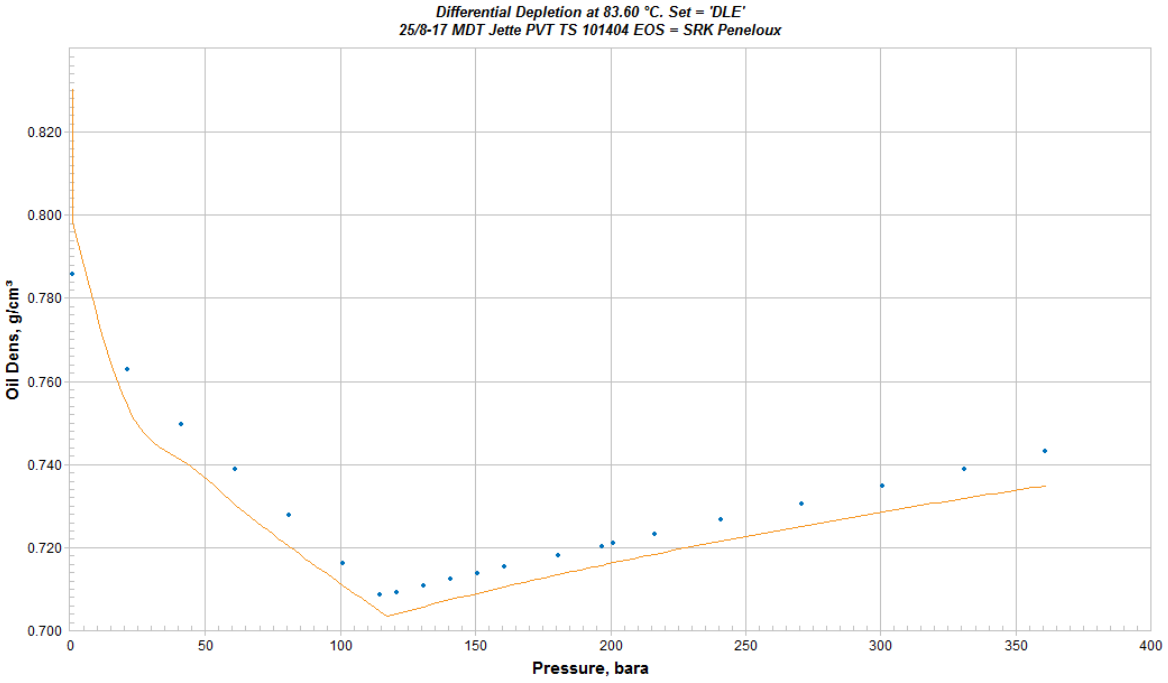

Figure F.12: Results from tuning, showing oil density. From PVTSim (calsep 2013).

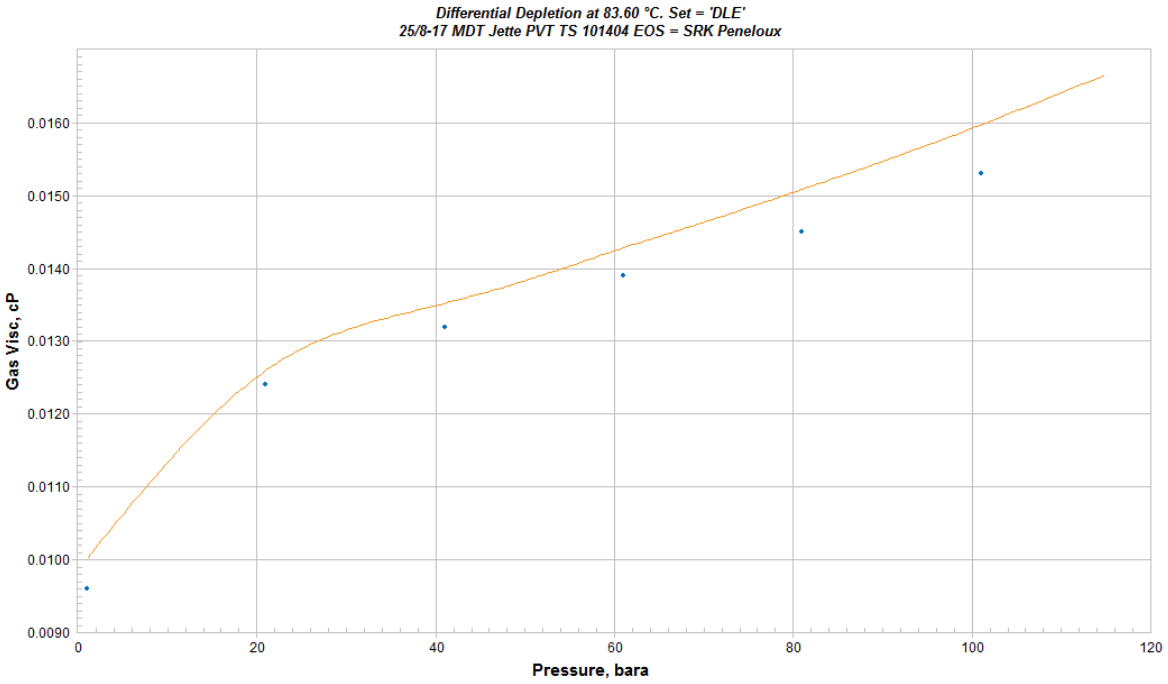

Figure F.13: Results from tuning, showing gas viscosity. From PVTSim (calsep 2013).

F.2 Procedure in PVTflex

A Black Oil PVT fluid model based upon data from sample TS-101404 from well 25/8-17 was made and tuned in PVTflex.

The fluid components and molar composition are used to define the composition in the fluid model. The molecular weight was set to 625 kg/kgmol (maximum molecular weight in PVTflex), gravity at 0.992 and a plus fraction at C36+. See **Figure F.14**.

To better define the fluid components and the respective molar composition, the components were lumped in five pseudo components, from C10+. The following molecular weight was 267.67 kg/kgmol (representative for the components) and a gravity of 0.86, see **Figures F.15** and **F.16**.

When the composition of the fluid was defined, the experimental data from the Weatherford Laboratories A/S report (Sandvik & Ravnås 2010) was added.

Input data from CME are shown in **Figure F.17**, and input data from DLE are shown in **Figure F.18**. The reservoir temperature was set to 83.6 °C, the sampling depth to 2094 m MD RKB, and the system type to bottom hole.

Tuning was done using Soave-Redlich-Kwong with volume shifts (SRK Peneloux), as this EOS gave the best match. Root Mean Square (RMS) after tuning was 3.1045%, which is within 10%, and hence considered as a satisfying match. The results are shown in

Figures F.19- F.21. The tuned PVT model is used as input in WellFlo.

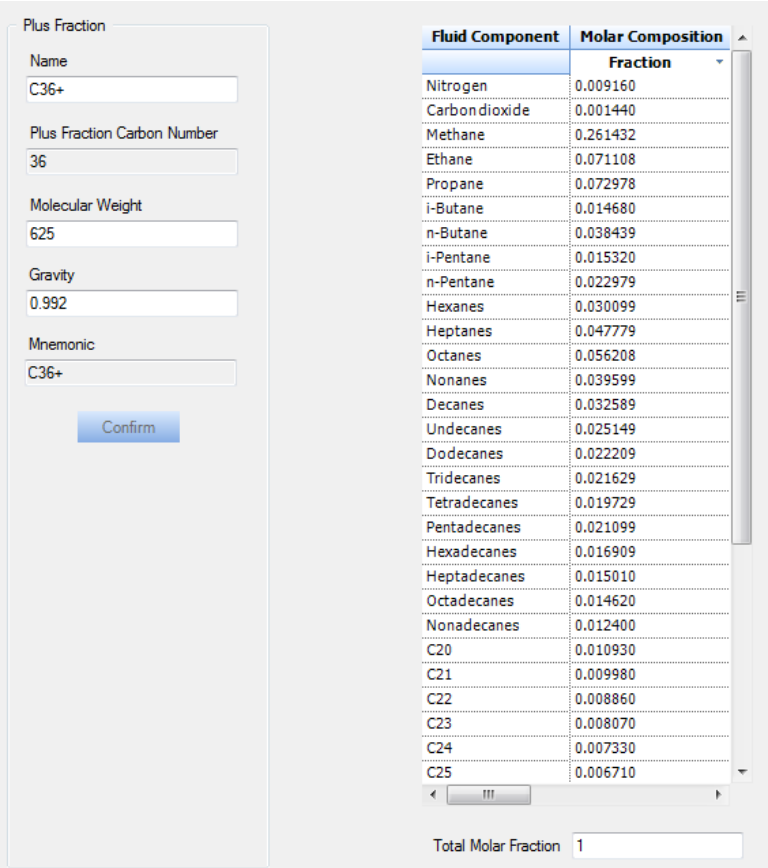

Figure F.14: Fluid composition, input to the PVT model. From PVTflex (Weatherford 2012a).

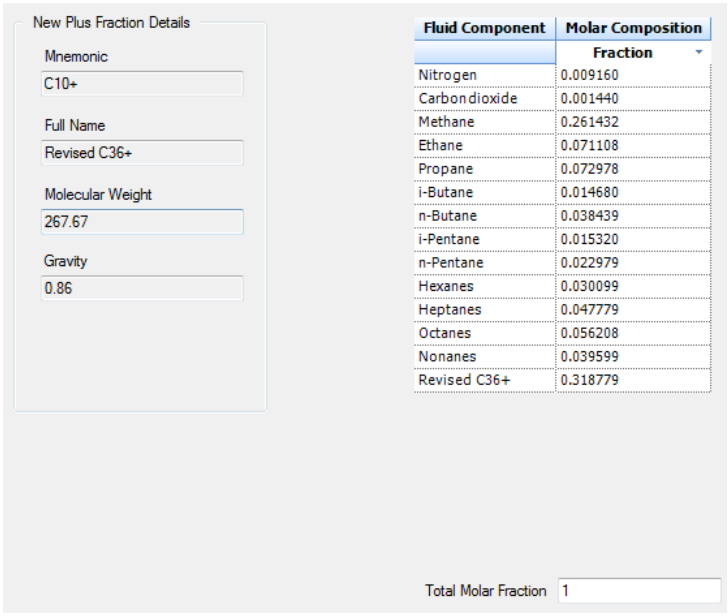

Figure F.15: Revised C36+, plus fraction. From PVTflex (Weatherford 2012a).

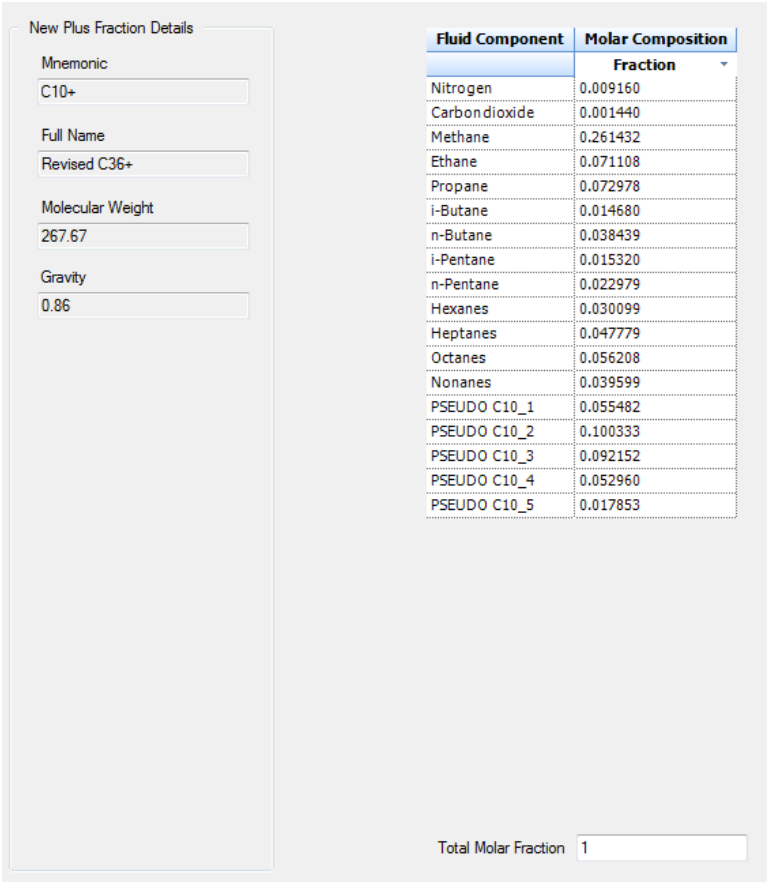

Figure F.16: Lumping from new plus fraction, C10+. From PVTflex (Weatherford 2012a).

Experiment Name: CME

Reservoir Temperature: 182.4800 degF

CME

	Pressure	Liquid Relative Volume	Total Relative Volume	Y Function	Gas Z Factor	Oil Density	Gas Density	Oil Viscosity	Gas Viscosity
	psia	Percent				lb/ft3	lb/ft3	centipoise	centipoise
1	5234.41	0.00	0.9534	0	0	0.000	0.000	0.0000	0.0000
2	4799.30	0.00	0.959	0	0	0.000	0.000	0.0000	0.0000
3	4364.19	0.00	0.9644	0	0	0.000	0.000	0.0000	0.0000
4	3927.62	0.00	0.9698	0	0	0.000	0.000	0.0000	0.0000
5	3493.96	0.00	0.9752	0	0	0.000	0.000	0.0000	0.0000
6	3135.72	0.00	0.9799	0	0	0.000	0.000	0.0000	0.0000
7	2915.26	0.00	0.9827	0	0	0.000	0.000	0.0000	0.0000
8	2854.34	0.00	0.9836	0	0	0.000	0.000	0.0000	0.0000
9	2622.28	0.00	0.9867	0	0	0.000	0.000	0.0000	0.0000
10	2332.21	0.00	0.9906	0	0	0.000	0.000	0.0000	0.0000
11	2187.17	0.00	0.9926	0	0	0.000	0.000	0.0000	0.0000
12	2043.58	0.00	0.9947	0	0	0.000	0.000	0.0000	0.0000
13	1897.09	0.00	0.9968	0	0	0.000	0.000	0.0000	0.0000
14	1752.06	0.00	0.9989	0	0	0.000	0.000	0.0000	0.0000
15	1663.58	0.00	1	0	0	0.000	0.000	0.0000	0.0000
16	1601.22	0.00	1.0132	2.955	0	0.000	0.000	0.0000	0.0000
17	1434.42	0.00	1.0564	2.833	0	0.000	0.000	0.0000	0.0000
18	1218.32	0.00	1.1368	2.669	0	0.000	0.000	0.0000	0.0000
19	1048.62	0.00	1.2308	2.54	0	0.000	0.000	0.0000	0.0000
20	897.78	0.00	1.3513	2.427	0	0.000	0.000	0.0000	0.0000
21	799.16	0.00	1.4598	2.351	0	0.000	0.000	0.0000	0.0000
22	697.63	0.00	1.6083	2.275	0	0.000	0.000	0.0000	0.0000
23	613.51	0.00	1.7732	2.213	0	0.000	0.000	0.0000	0.0000

Figure F.17: Experimental input data, Constant Mass Expansion test. From PVTflex (Weatherford 2012a).

Experiment Name: DLE

Reservoir Temperature: 182.4800 degF

Standard Pressure: 14.6959 psia Standard Temperature: 59.0000 degF

DLE

	Pressure	Oil Formation Volume Factor	Sol. Gas Oil Ratio	Gas Gravity	Gas Z Factor	Oil Density	Gas Density	Oil Viscosity	Gas Viscosity
	psia	bbl/STB	scf/STB			lb/ft3	lb/ft3	centipoise	centipoise
1	5234.41	1.3041	0.0	0	0	46.390	0.000	0.0000	0.0000
2	4799.30	1.3117	0.0	0	0	46.122	0.000	0.0000	0.0000
3	4364.19	1.3190	0.0	0	0	45.866	0.000	0.0000	0.0000
4	3927.62	1.3265	0.0	0	0	45.610	0.000	0.0000	0.0000
5	3493.96	1.3338	0.0	0	0	45.360	0.000	0.0000	0.0000
6	3135.72	1.3403	0.0	0	0	45.142	0.000	0.0000	0.0000
7	2915.26	1.3442	0.0	0	0	45.011	0.000	0.0000	0.0000
8	2854.34	1.3454	0.0	0	0	44.967	0.000	0.0000	0.0000
9	2622.28	1.3495	0.0	0	0	44.830	0.000	0.0000	0.0000
10	2332.21	1.3549	0.0	0	0	44.655	0.000	0.0000	0.0000
11	2187.17	1.3577	0.0	0	0	44.561	0.000	0.0000	0.0000
12	2043.58	1.3605	0.0	0	0	44.467	0.000	0.0000	0.0000
13	1897.09	1.3634	0.0	0	0	44.374	0.000	0.0000	0.0000
14	1752.06	1.3663	0.0	0	0	44.280	0.000	0.0000	0.0000
15	1663.58	1.3678	531.1	0	0	44.230	0.000	0.0000	0.0000
16	1464.88	1.3424	481.2	0	0.875	44.705	0.000	0.0000	0.0153
17	1174.81	1.3052	409.9	0	0.8877	45.441	0.000	0.0000	0.0145
18	884.73	1.2703	339.7	0	0.9033	46.128	0.000	0.0000	0.0139
19	594.65	1.2366	269.5	0	0.9233	46.790	0.000	0.0000	0.0132
20	304.58	1.1948	189.2	0	0.9474	47.620	0.000	0.0000	0.0124
21	14.70	1.0740	0.0	0	0.9907	49.056	0.000	0.0000	0.0096

Figure F.18: Experimental input data, Differential Liberation Experiment. From PVTflex (Weatherford 2012a).

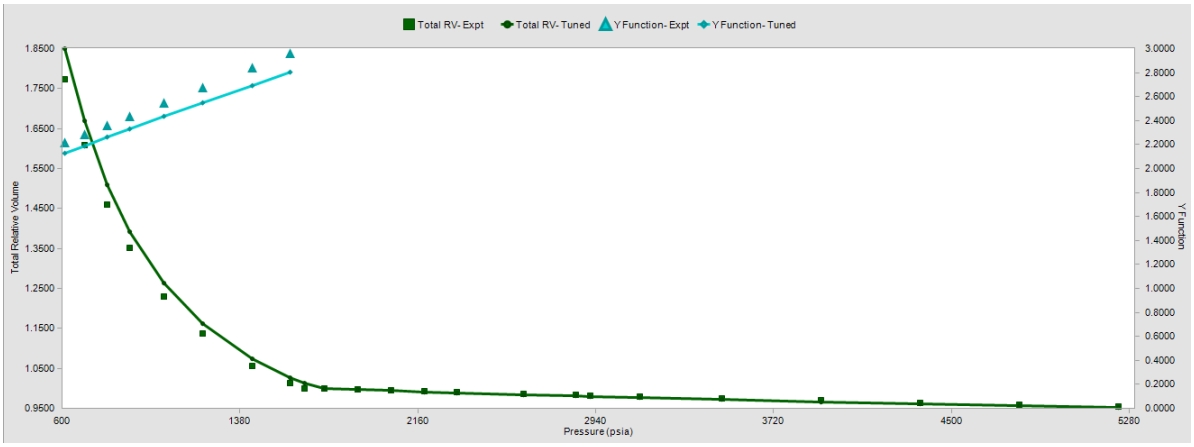

Figure F.19: Results from tuning, showing total relative volume and Y-function. From PVTflex (Weatherford 2012a).

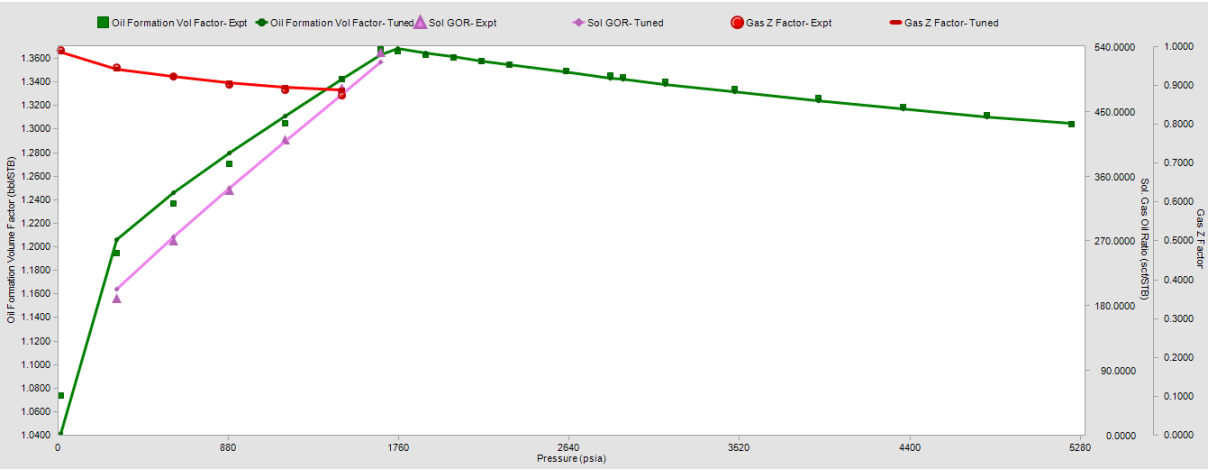

Figure F.20: Results from tuning, showing oil formation volume factor, solution GOR and gas Z-factor. From PVTflex (Weatherford 2012a).

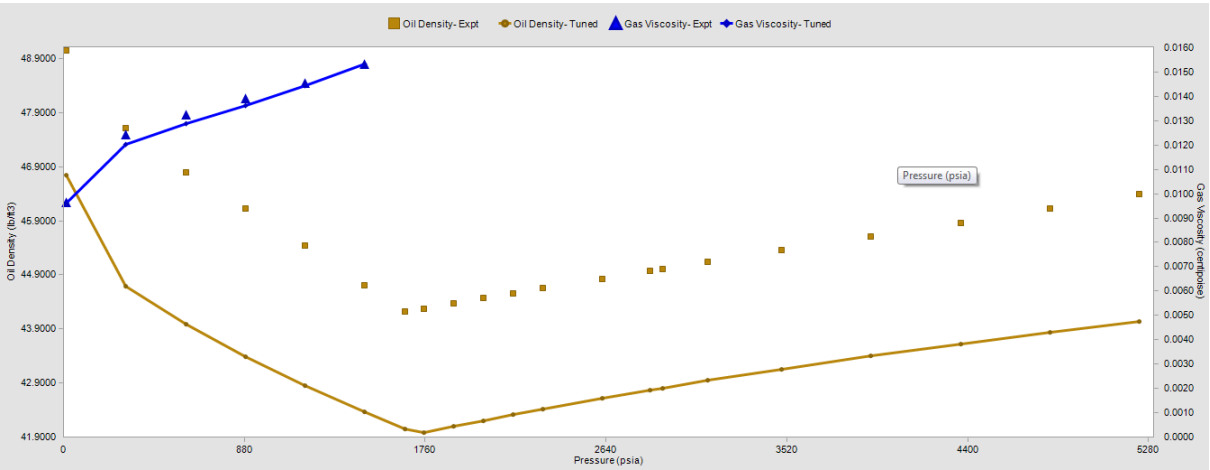

Figure F.21: Results from tuning, showing oil density and gas viscosity. From PVTflex (Weatherford 2012a).

G Well Lift Curves

WellFlo was used for the design of the wells, and their respective lift curves.

The two production wells were initialized with a nodal analysis, continuous gas lift and flow through the tubing, as seen in **Figure G.1**. The models were initialized as black oil models.

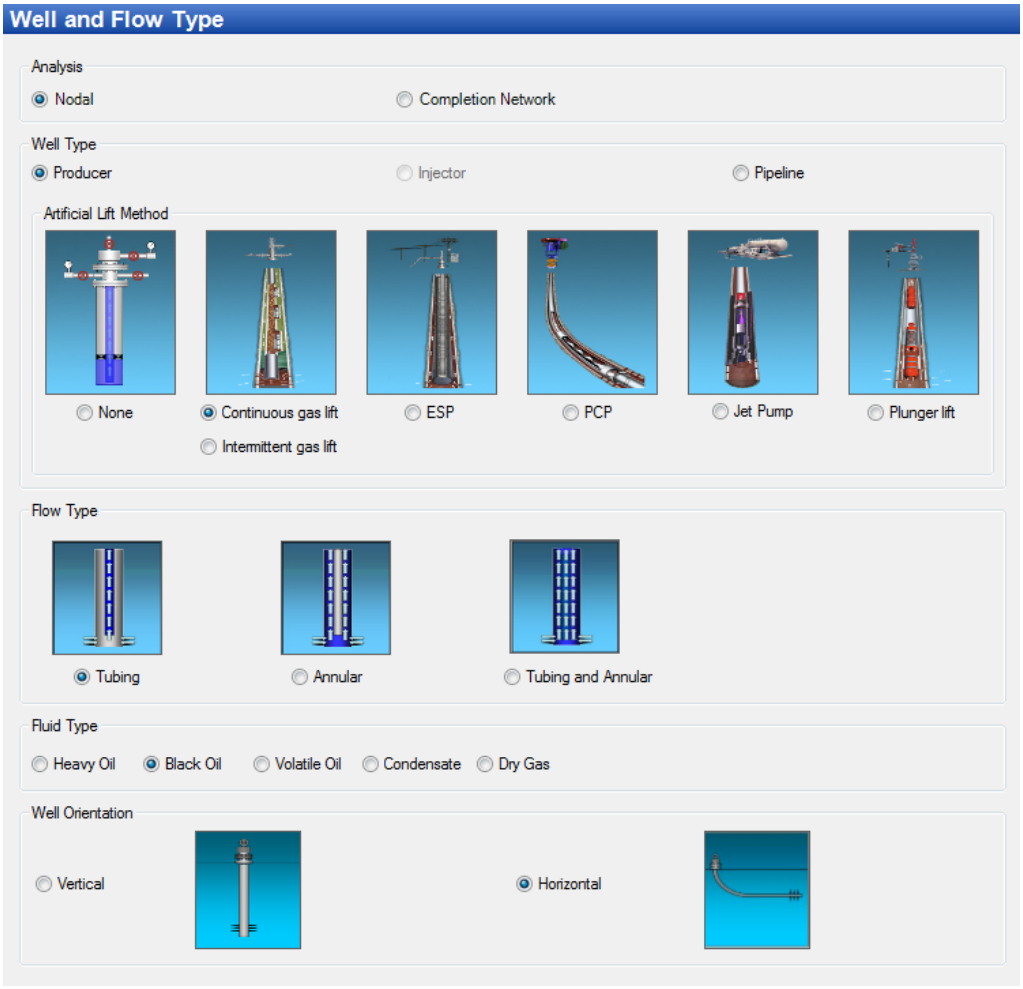

Figure G.1: Initialization of the producers. From WellFlo (Weatherford 2012b).

The OLGA Steady State model has been used as flow correlation for the lower and upper completions of the well. The IPR curves are based on a Vogel model with a coefficient of 0.2.

A reservoir pressure of 196.7 bar (no depletion) is assumed for both wells, and a reference depth of 166 m TVD RKB. See **Figure G.2**. The fluid parameters are shown in **Figure G.3**; The parameters are taken from the latest PVT model, described in Appendix F.

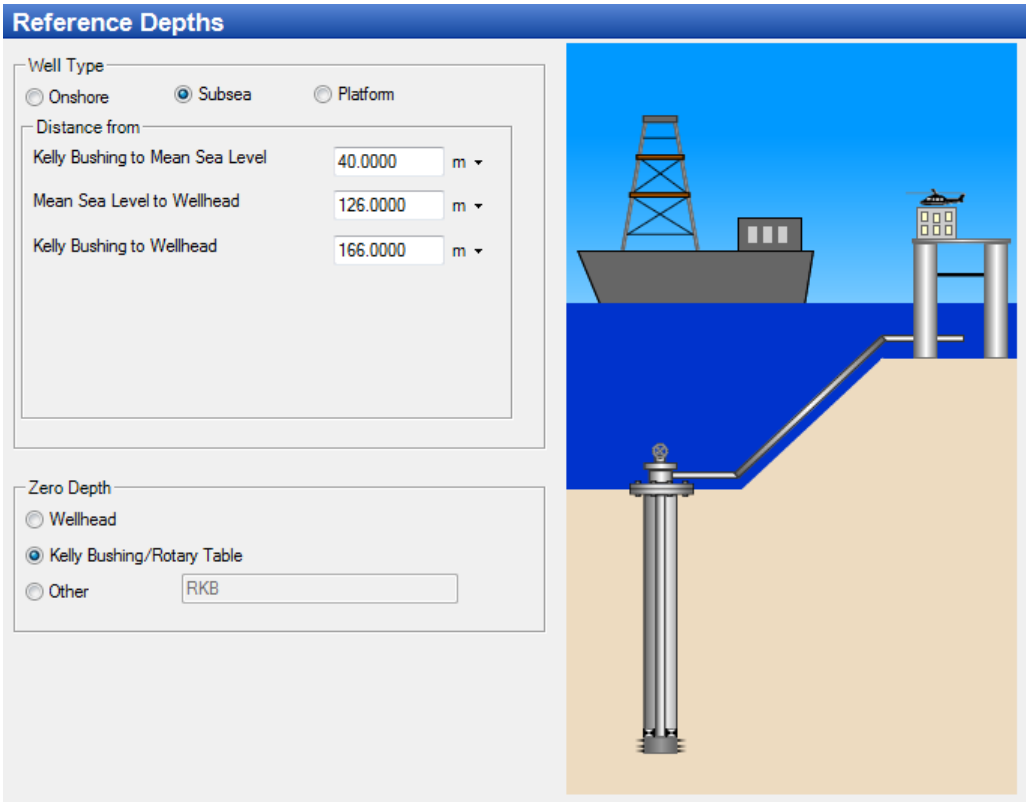

Figure G.2: Reference depths of the producers. From WellFlo (Weatherford 2012b).

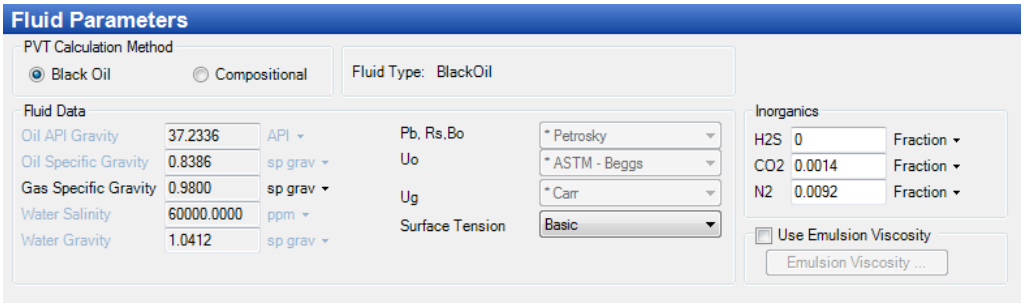

Figure G.3: Fluid parameters of the producers. From WellFlo (Weatherford 2012b).

The input data used in the two well models are taken from well tests in October. The lift curves were exported as ECLIPSE input files.

G.1 Well D

The wellbore is initialized with deviation and equipment, see **Figures G.4**, **G.5** and **G.6**.

The input data for reservoir and surface characteristics are given in **Tables G.1** and **G.2**. The well is initialized as shown in **Figure G.7**.

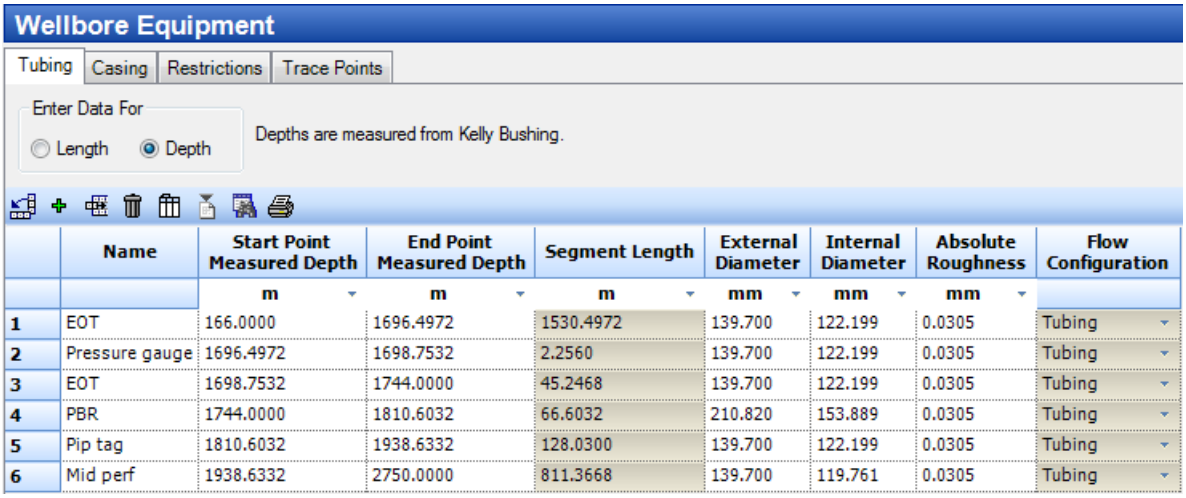

	Name	Start Point Measured Depth	End Point Measured Depth	Segment Length	External Diameter	Internal Diameter	Absolute Roughness	Flow Configuration
		m	m	m	mm	mm	mm	
1	EOT	166.0000	1696.4972	1530.4972	139.700	122.199	0.0305	Tubing
2	Pressure gauge	1696.4972	1698.7532	2.2560	139.700	122.199	0.0305	Tubing
3	EOT	1698.7532	1744.0000	45.2468	139.700	122.199	0.0305	Tubing
4	PBR	1744.0000	1810.6032	66.6032	210.820	153.889	0.0305	Tubing
5	Pip tag	1810.6032	1938.6332	128.0300	139.700	122.199	0.0305	Tubing
6	Mid perf	1938.6332	2750.0000	811.3668	139.700	119.761	0.0305	Tubing

Figure G.4: Wellbore equipment for tubing, Well D. From WellFlo (Weatherford 2012b).

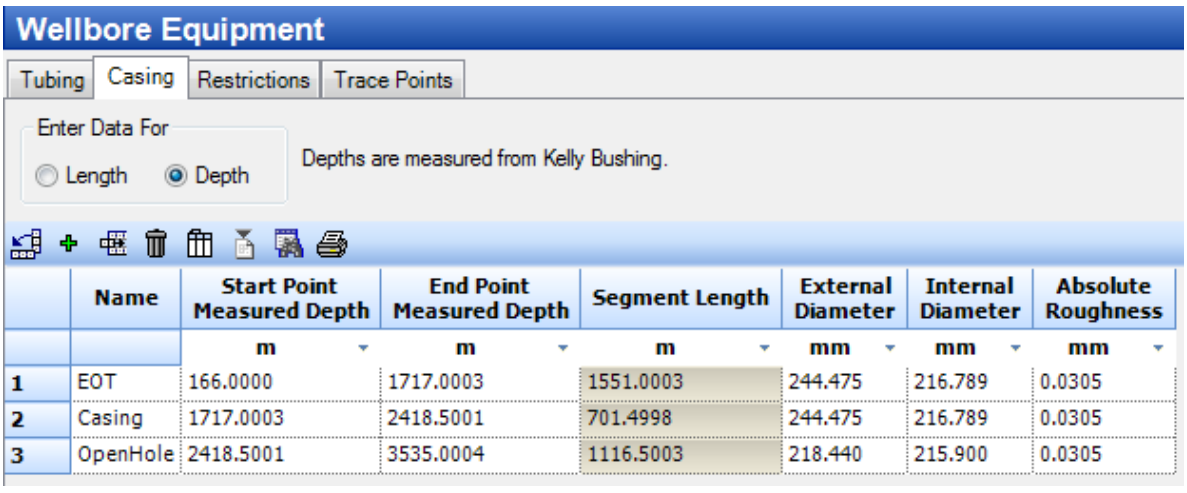

	Name	Start Point Measured Depth	End Point Measured Depth	Segment Length	External Diameter	Internal Diameter	Absolute Roughness
		m	m	m	mm	mm	mm
1	EOT	166.0000	1717.0003	1551.0003	244.475	216.789	0.0305
2	Casing	1717.0003	2418.5001	701.4998	244.475	216.789	0.0305
3	OpenHole	2418.5001	3535.0004	1116.5003	218.440	215.900	0.0305

Figure G.5: Wellbore equipment for casing, Well D. From WellFlo (Weatherford 2012b).

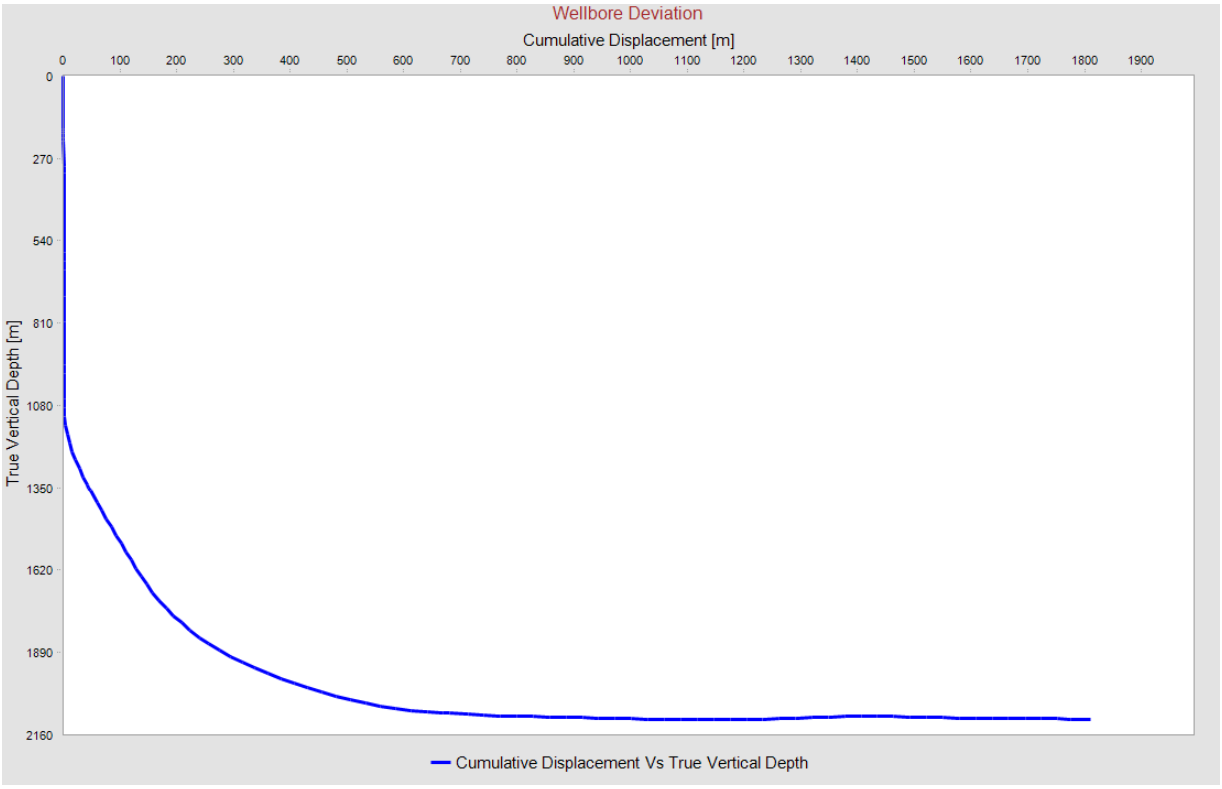

Figure G.6: Wellbore deviation, Well D. From WellFlo (Weatherford 2012b).

Table G.1: Input data used in the model for Well D in WellFlo.

WC	GOR	PI_{liquid}	GOR & GL	Flow rate
Fraction	$[Sm^3/Sm^3]$	$[Sm^3/d/bar]$	$[Sm^3/Sm^3]$	$[m^3/d]$
0.17	99.2	5.2	238.9	507.3

Table G.2: Gas lift input data used in the model for Well D in WellFlo.

Operating pressure	Gas gravity	Gas injection rate
[bara]	[sp grav]	$[Sm^3/d]$
59.4	0.84	58,758.5

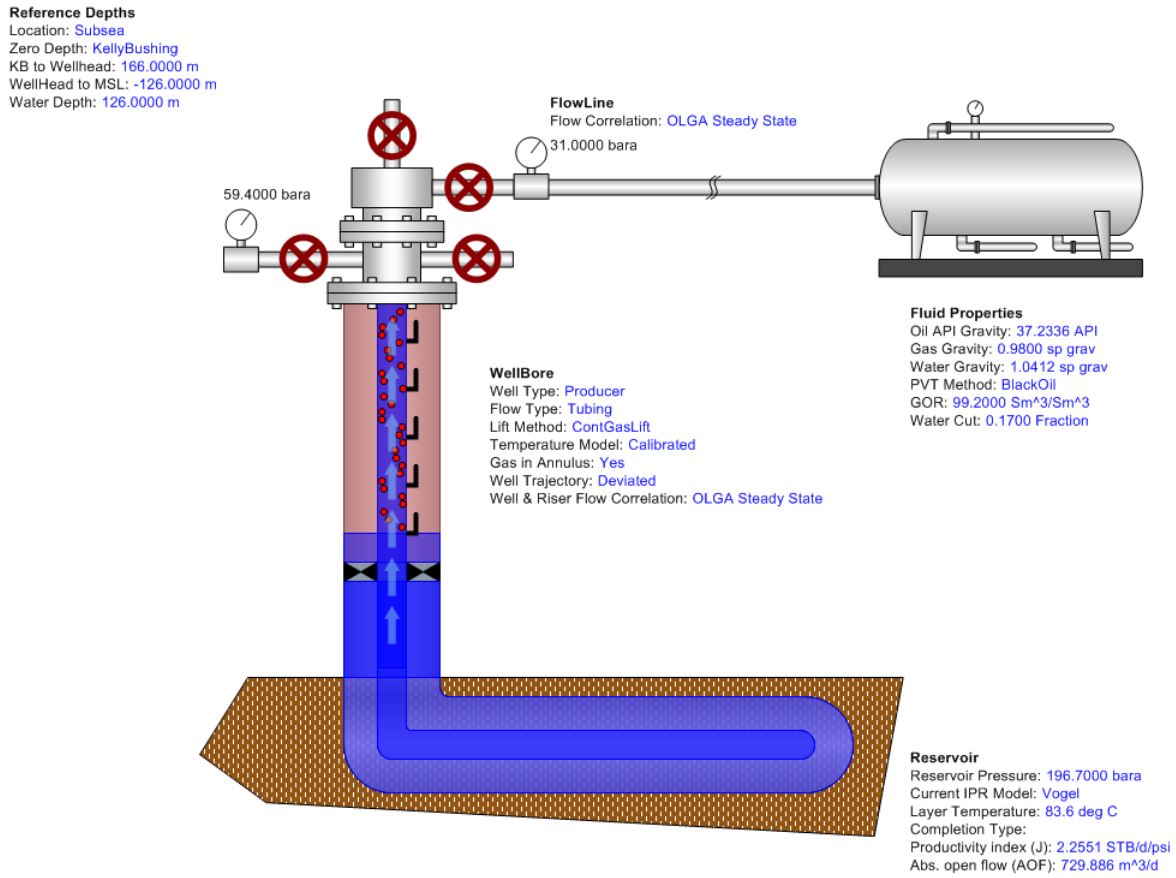

Figure G.7: Initialization of Well D. From WellFlo (Weatherford 2012b).

G.2 Well E

The wellbore is initialized with deviation and equipment, see **Figures G.8**, **G.9** and **G.10**.

The input data for reservoir and surface characteristics are given in **Tables G.3** and **G.4**. The well is initialized as shown in **Figure G.11**.

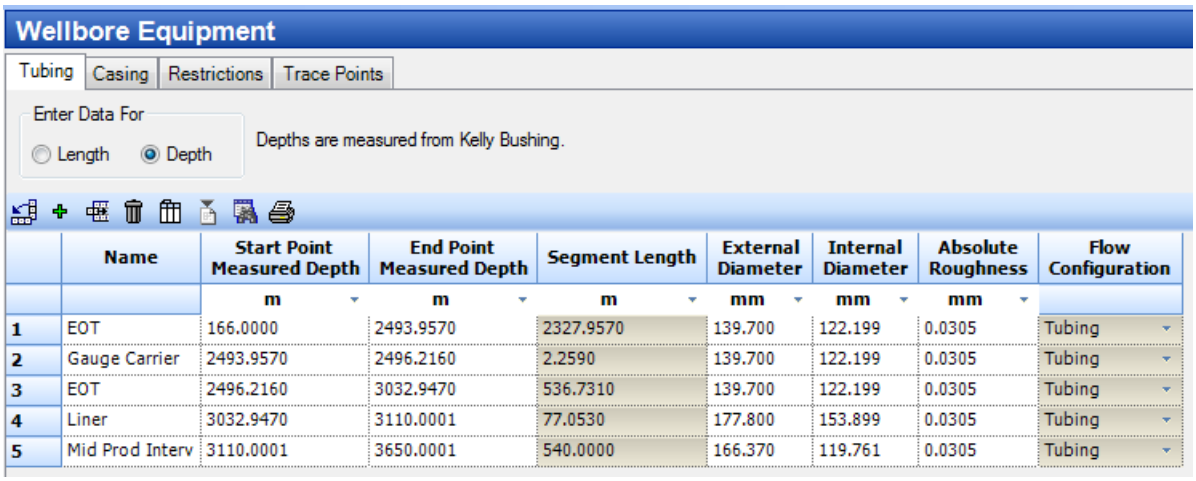

	Name	Start Point Measured Depth	End Point Measured Depth	Segment Length	External Diameter	Internal Diameter	Absolute Roughness	Flow Configuration
		m	m	m	mm	mm	mm	
1	EOT	166.0000	2493.9570	2327.9570	139.700	122.199	0.0305	Tubing
2	Gauge Carrier	2493.9570	2496.2160	2.2590	139.700	122.199	0.0305	Tubing
3	EOT	2496.2160	3032.9470	536.7310	139.700	122.199	0.0305	Tubing
4	Liner	3032.9470	3110.0001	77.0530	177.800	153.899	0.0305	Tubing
5	Mid Prod Interv	3110.0001	3650.0001	540.0000	166.370	119.761	0.0305	Tubing

Figure G.8: Wellbore equipment for tubing, Well E. From WellFlo (Weatherford 2012b).

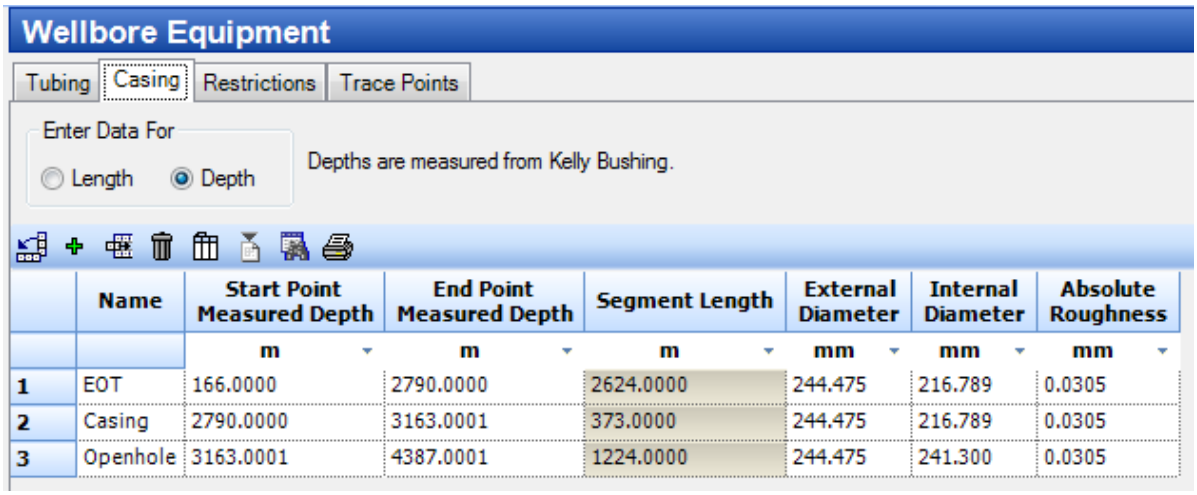

	Name	Start Point Measured Depth	End Point Measured Depth	Segment Length	External Diameter	Internal Diameter	Absolute Roughness
		m	m	m	mm	mm	mm
1	EOT	166.0000	2790.0000	2624.0000	244.475	216.789	0.0305
2	Casing	2790.0000	3163.0001	373.0000	244.475	216.789	0.0305
3	Openhole	3163.0001	4387.0001	1224.0000	244.475	241.300	0.0305

Figure G.9: Wellbore equipment for casing, Well E. From WellFlo (Weatherford 2012b).

Table G.3: Input data used in the model for Well E in WellFlo.

WC	GOR	PI_{liquid}	GOR & GL	Flow rate
Fraction	$[Sm^3/Sm^3]$	$[Sm^3/d/bar]$	$[Sm^3/Sm^3]$	$[m^3/d]$
0.59	86.1	26.17	238	1,355

Table G.4: Gas lift input data used in the model for Well E in WellFlo.

Operating pressure	Gas gravity	Gas injection rate
[bara]	[sp grav]	$[Sm^3/d]$
92	0.84	84,293

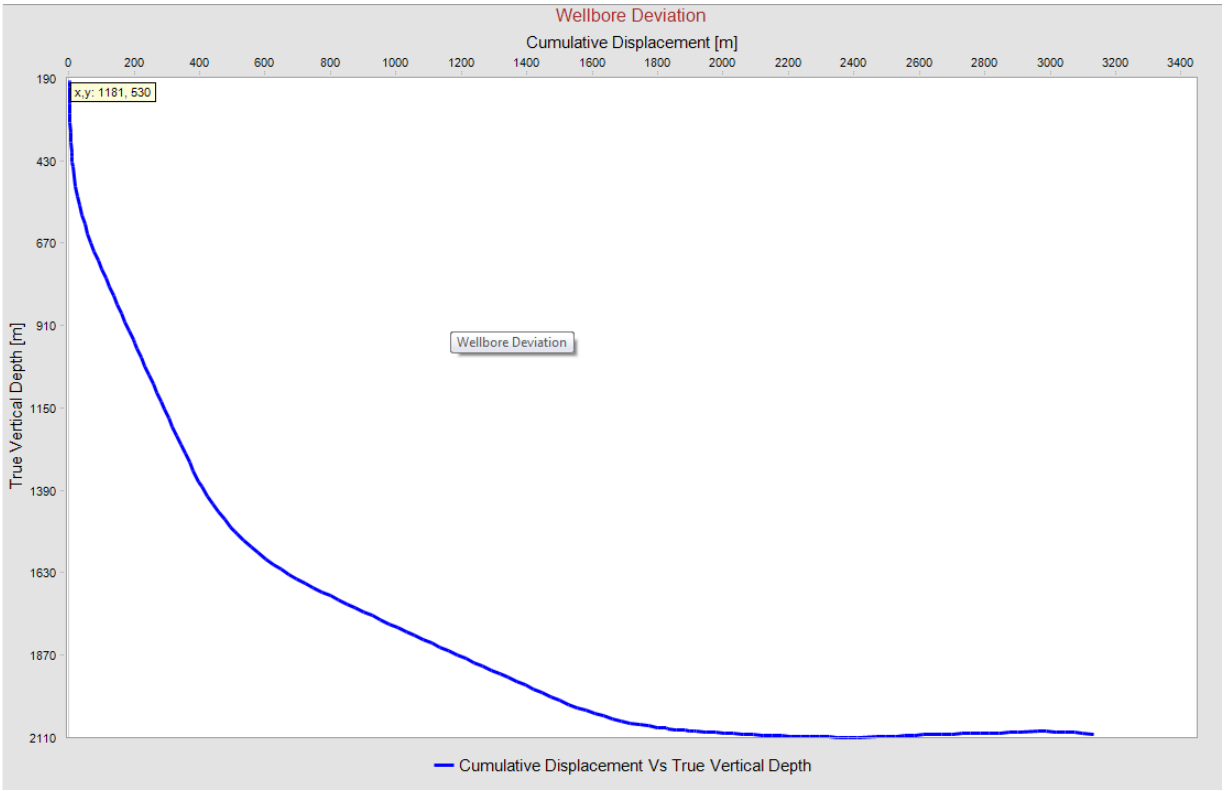

Figure G.10: Wellbore deviation, Well E. From WellFlo (Weatherford 2012b).

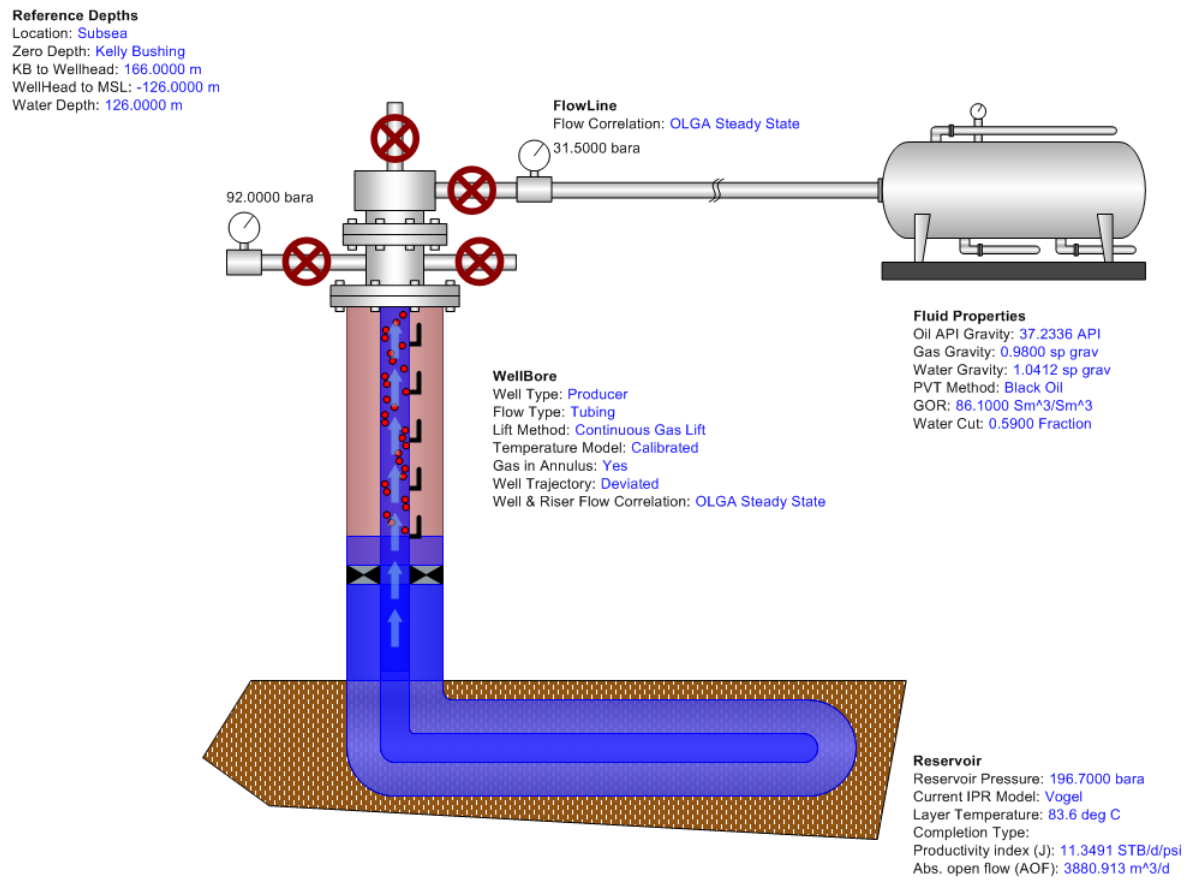

Figure G.11: Initialization of Well E. From WellFlo (Weatherford 2012b).

H Well Path Design in Petrel

New wells may be designed in both ECLIPSE 100 and Petrel. The main difference between these two methods are the output of the "connection factor". The connection factor implies the location of the wellbore within a grid block. In ECLIPSE, if the connection factor is not defaulted or set to zero, the well will be located in the middle of the grid block, as the well is defined to penetrate certain grid blocks. This may be adjusted with the use of WPIMULT, which scale the resulting connection factors. In Petrel, the connection factors will be calculated automatically when drawing the wellbore. Hence, the location of the well within the grid block is taken into account. This gives a smoother wellbore location.

The wells designed as part of the well intervention measures are designed in Petrel. The procedure is described below.

H.1 Procedure

The wells which were designed as part of well intervention measures were all side-tracks of the already existing Well D. The new wells are connected to Well D in the 9 5/8 in casing.

In Petrel, the side-tracks from an already existing well were created by implementing a well intersection in the area of the position of the new well. See **Figure H.1**.

The well intersection has to cross the well in which the side-track is to be connected to, that is Well D. The well intersection can give a better image of the reservoir properties in the chosen area, and help in placing the well path. By implementing an intersection filter wanted properties may be targeted when defining the well path. As seen in **Figure H.2** the intersection is filtered with water saturation, hence only showing the water saturation along the intersection.

The water saturation was chosen as filter in order to avoid water production and/or delay early water break through. From Figure H.2 it is observed that the well should be placed in the top layer of the reservoir to avoid water.

The option of designing a new well is activated by the "Well path design" function in the "Well engineering" menu in the process pane. See framed area in **Figure H.3**.

When the "Well path design" is activated a new well can be designed. When activating

the "Well path design" targeted points for the new well may be chosen. The points are chosen with the framed function seen in **Figure H.4**. With the use of the target point a well path is automatically designed. Petrel designs the best well path according to the points. In order to obtain a smooth well path it is best to choose few points, giving fewer restrictions to Petrel.

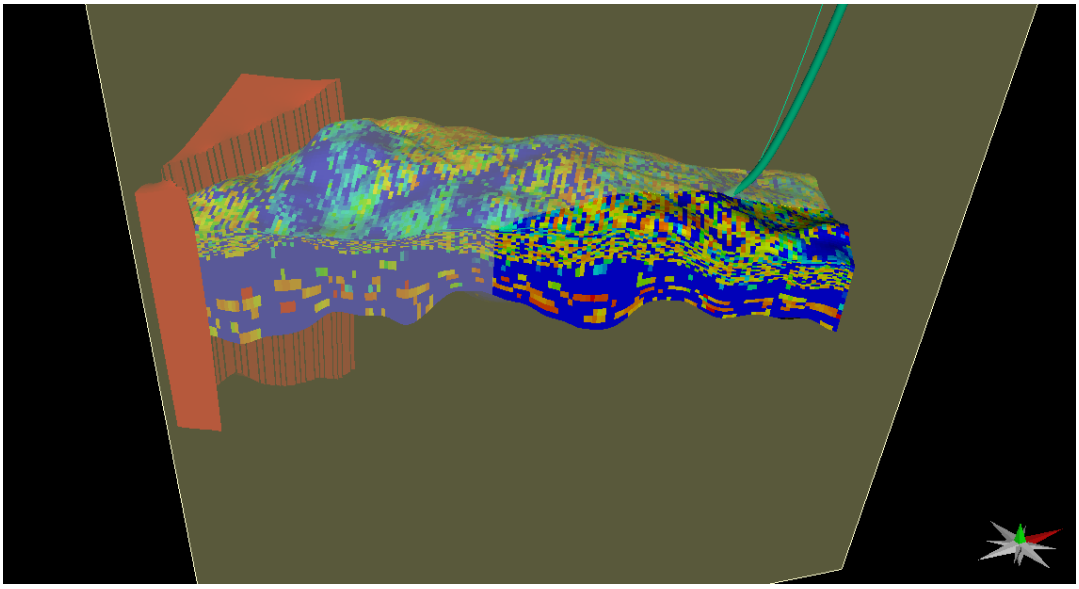

Figure H.1: A well intersection from the original Well D, defining the well path of the new well. From Petrel (Schlumberger 2013c).

The well may be tied in to the main well by targeting the main well. The proposed well is shown in **Figure H.5**.

As seen in Figure H.5 the proposed well is not connected to Well D. Settings for the well may be changed in "Well settings". Main well, kick-off point in main well and DLS may be adjusted in "Well settings". See **Figure H.6**.

The DLS may be checked at the info-pane of the well. An optimal DLS is below 3°/30 m. After the well path and its qualities have been controlled and verified the well path may be exported and further used for simulation.

In the "Process pane" a development strategy is defined. See **Figure H.7**. In the new strategy the main well, in this case Well D, has to be defined in the "Well folder". As the side-track is connected to Well D, the side-track does not have to be defined in the development strategy.

With the use of the new development strategy a simulation case may be defined. The permeability and porosity are defined in the simulations case, see **Figure H.8**. The grid, now with permeability and porosity defined, are exported. The new completion data for the wells may be found below SCHEDULE, at COMPDAT. See **Figure H.9**. The new

completion data may be added to the already existing simulation file in order to simulate the new side-track.

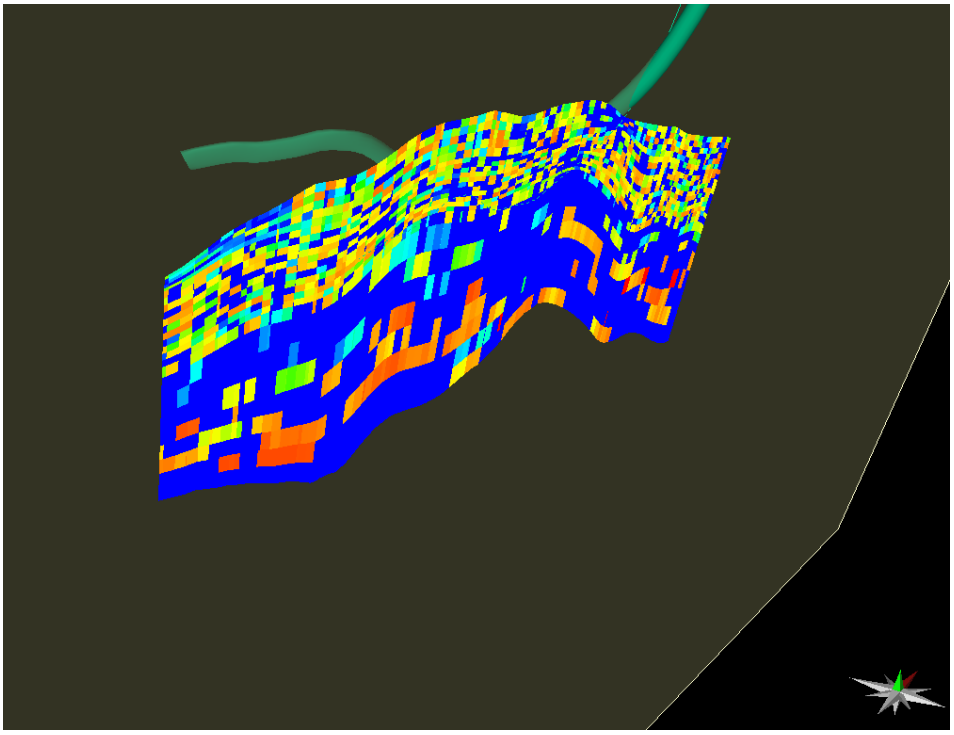

Figure H.2: Cross section of the area of the new well path. The cross section shows the water saturation in the area. From Petrel (Schlumberger 2013c).

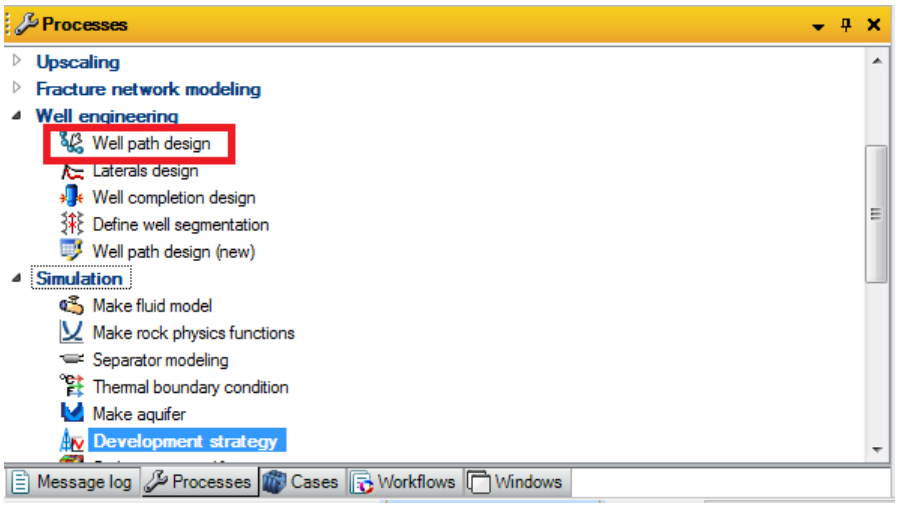

Figure H.3: Activating the "Well path design" in order to design the side-track. From Petrel (Schlumberger 2013c).

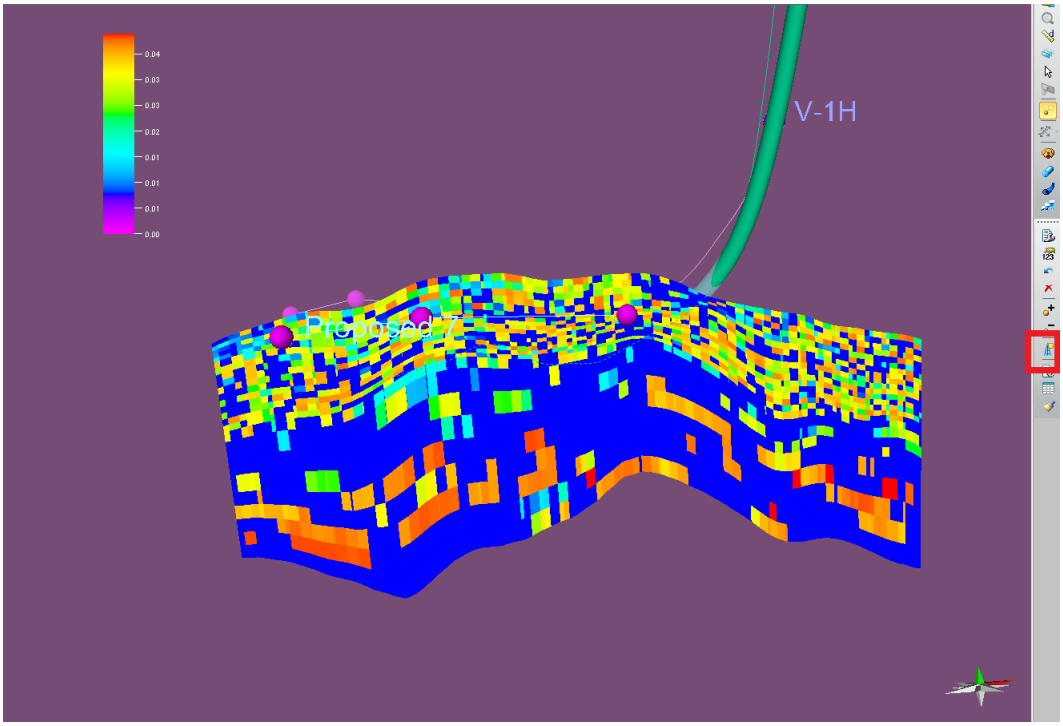

Figure H.4: A well path is designed with the use of target points. The target points are made with the use of the framed function. From Petrel (Schlumberger 2013c).

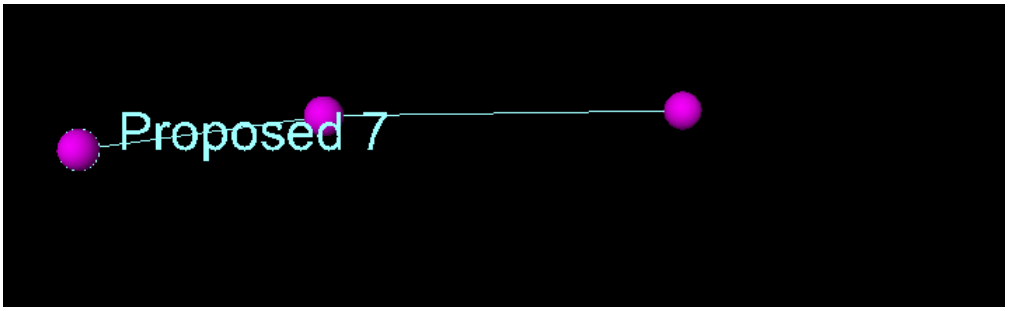

Figure H.5: The proposed well designed from the targeted points. From Petrel (Schlumberger 2013c).

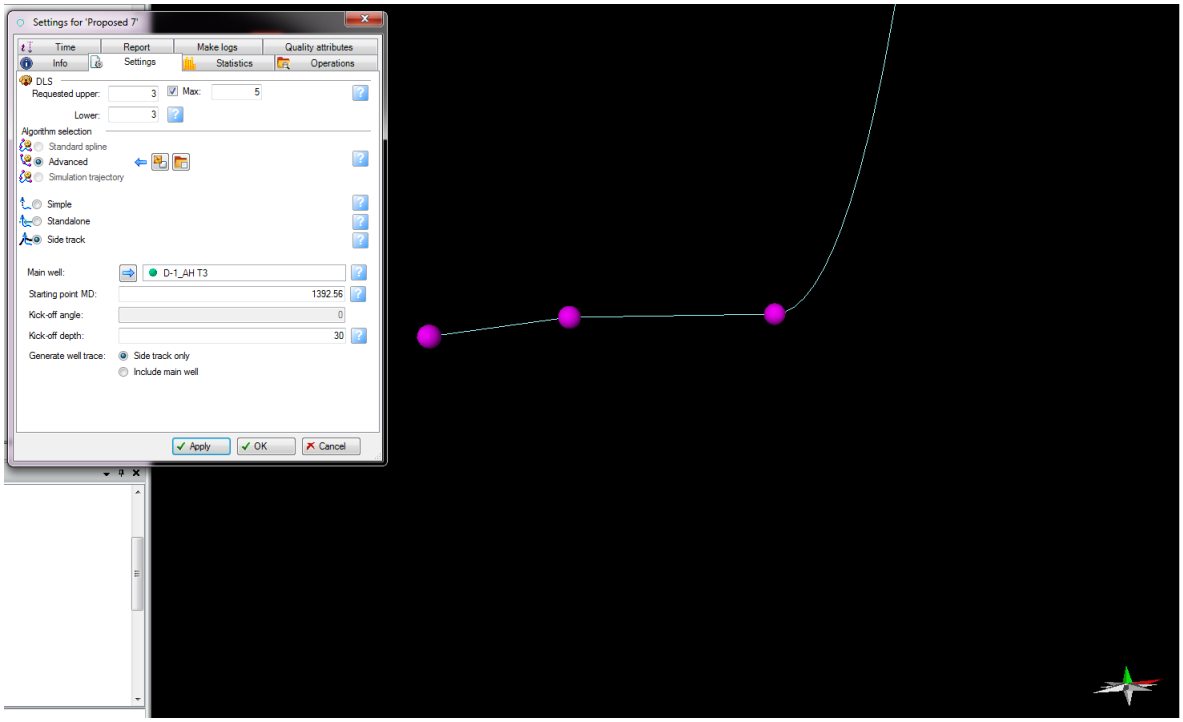

Figure H.6: In "Well settings" the main well may be defined along with the kick-off point from the main well. The DLS may be requested in order to get a smoother well and hence, production. From Petrel (Schlumberger 2013c).

H.2 Software

Petrel

Petrel is a Schlumberger owned Windows PC software application intended to aggregate oil reservoir data from multiple sources. The Petrel EP software platform provides a complete solution from exploration to production, integrating geology, geophysics, geological modeling, drilling, geomechanics, reservoir simulation, and more (Schlumberger 2014*i*). This shared earth approach enables companies to standardize workflows from exploration to production, and make more informed decisions with a clear understanding of both opportunities and risks. Petrel is consistent with Schlumberger's reservoir simulation program ECLIPSE.

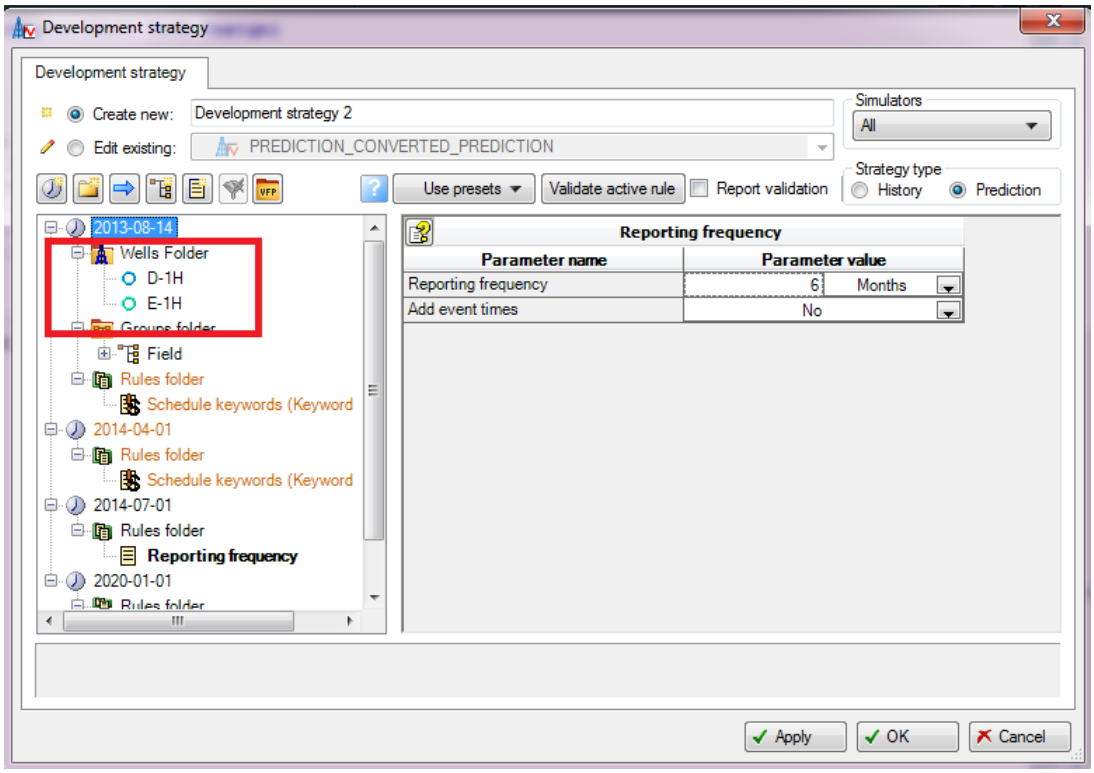

Figure H.7: Defining a new development strategy based on Well D and its new side-track. From Petrel (Schlumberger 2013c).

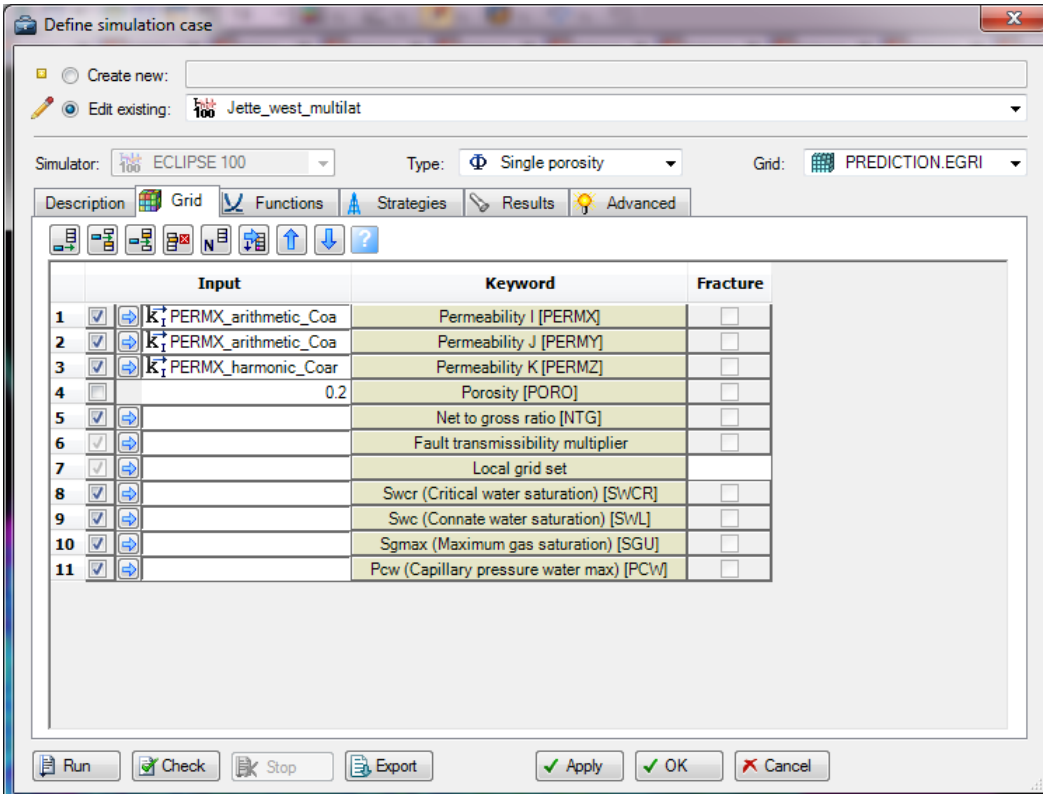

Figure H.8: Defining a new simulation case based on Well D and its new side-track. From Petrel (Schlumberger 2013c).

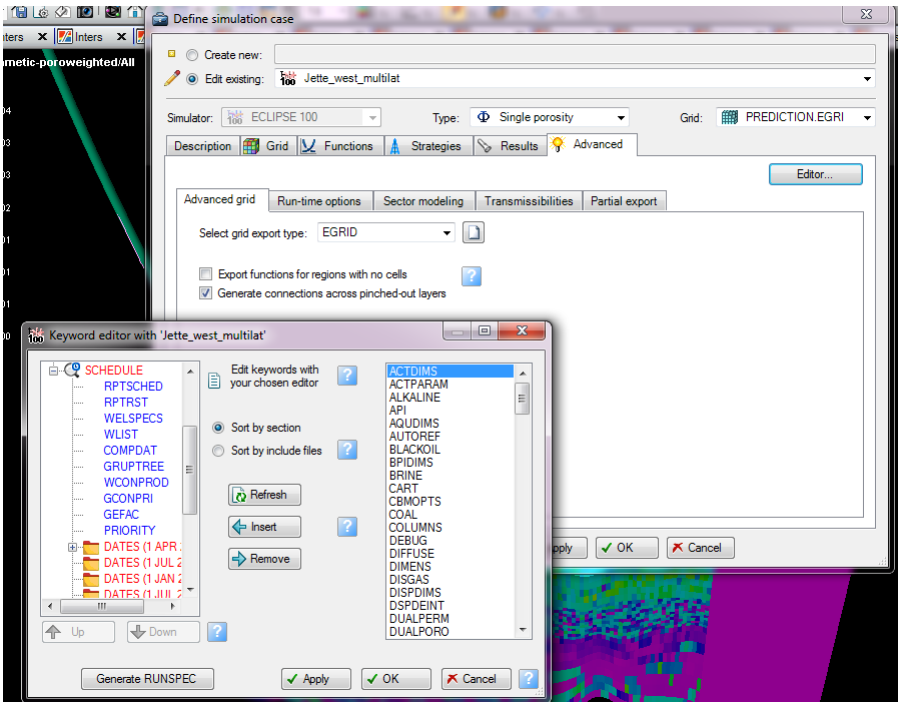

Figure H.9: The new completion data for Well D is found in the COMPDAT file below SCHEDULE. From Petrel (Schlumberger 2013c).

I Well Completions

Single-Lateral Well Completion - Option 1
Single-Lateral Well Completion - Option 2
Multilateral Well Completion - Option 1
Multilateral Well Completion - Option 2
Multilateral Well Completion - Option 3
Multilateral Well Completion - Option 4

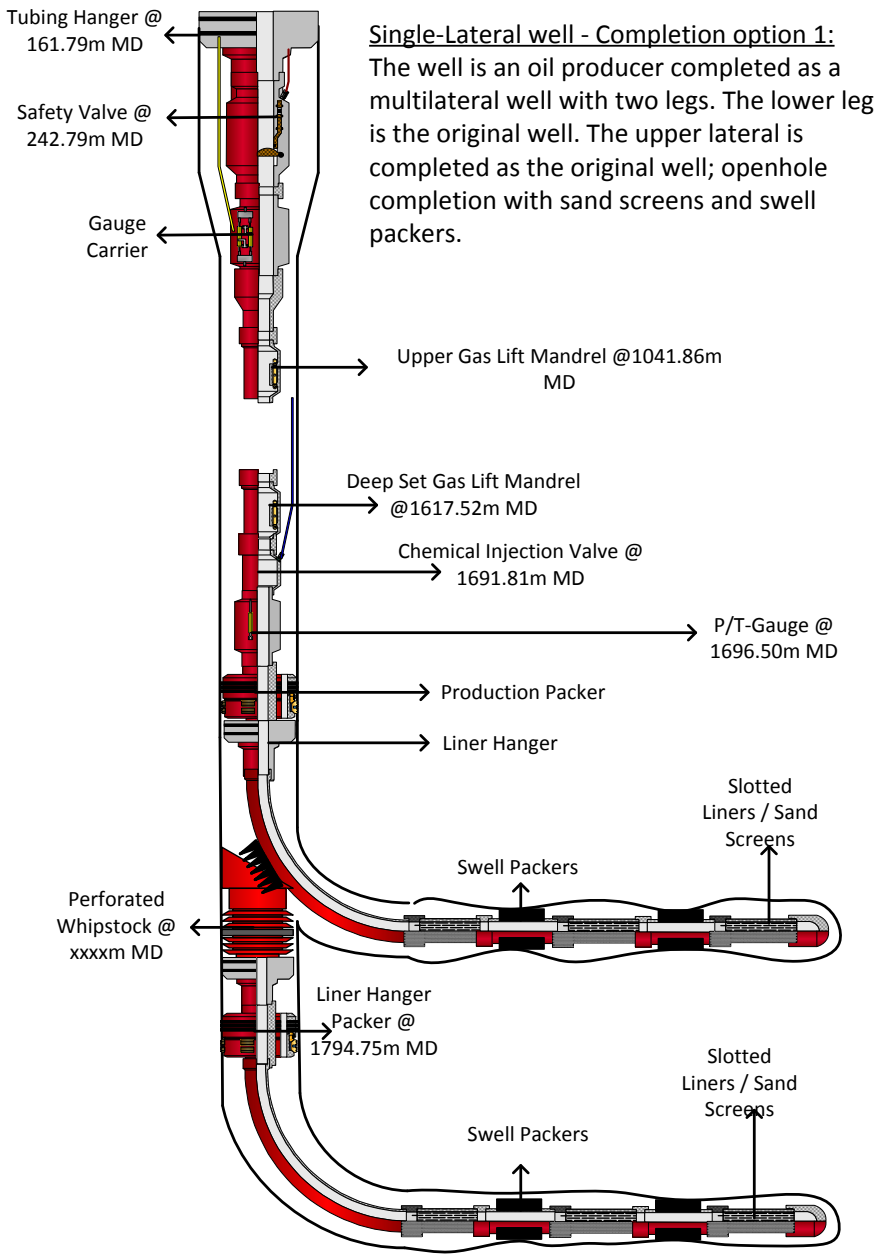

Figure I.1: Single-Lateral Well, Completion option 1, from Microsoft Visio (Microsoft 2010).

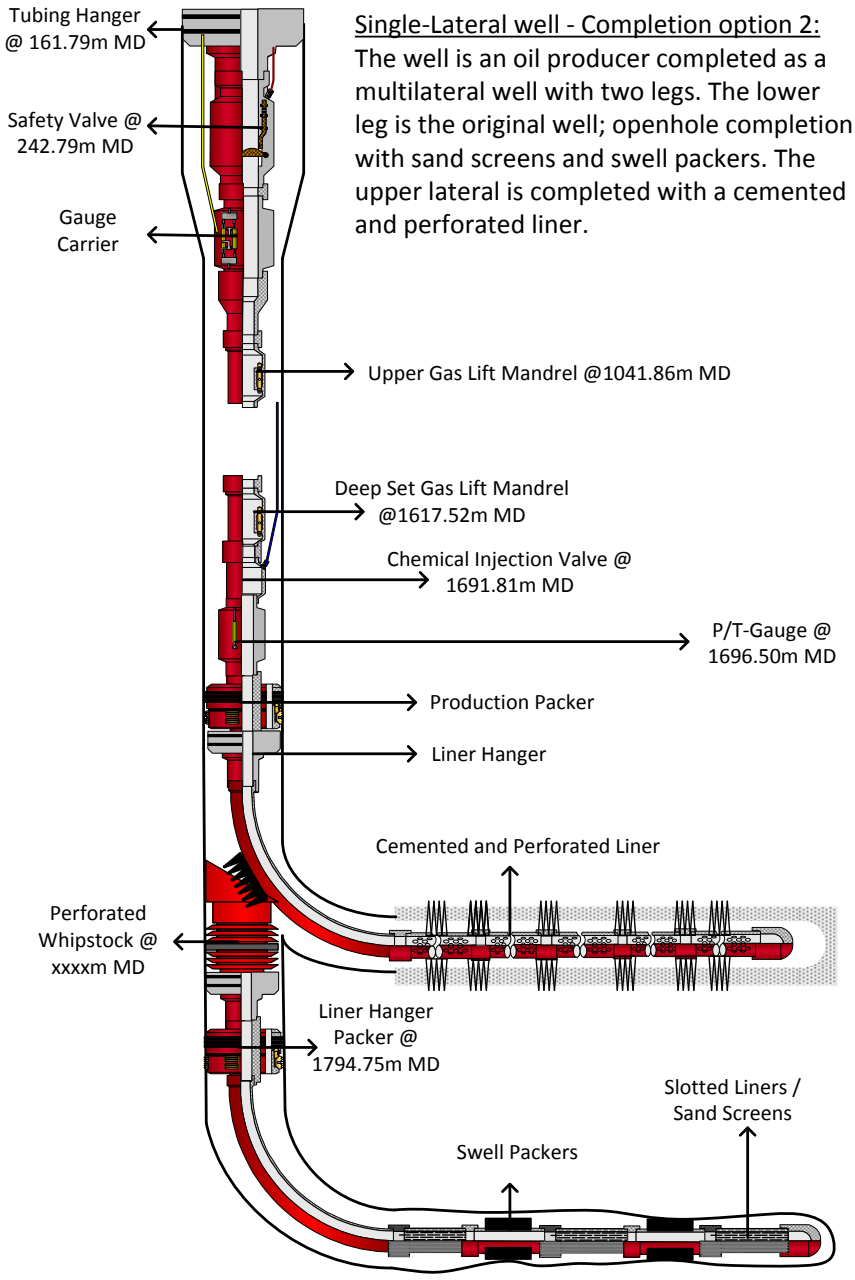

Figure I.2: Single-Lateral Well, Completion option 2, from Microsoft Visio (Microsoft 2010).

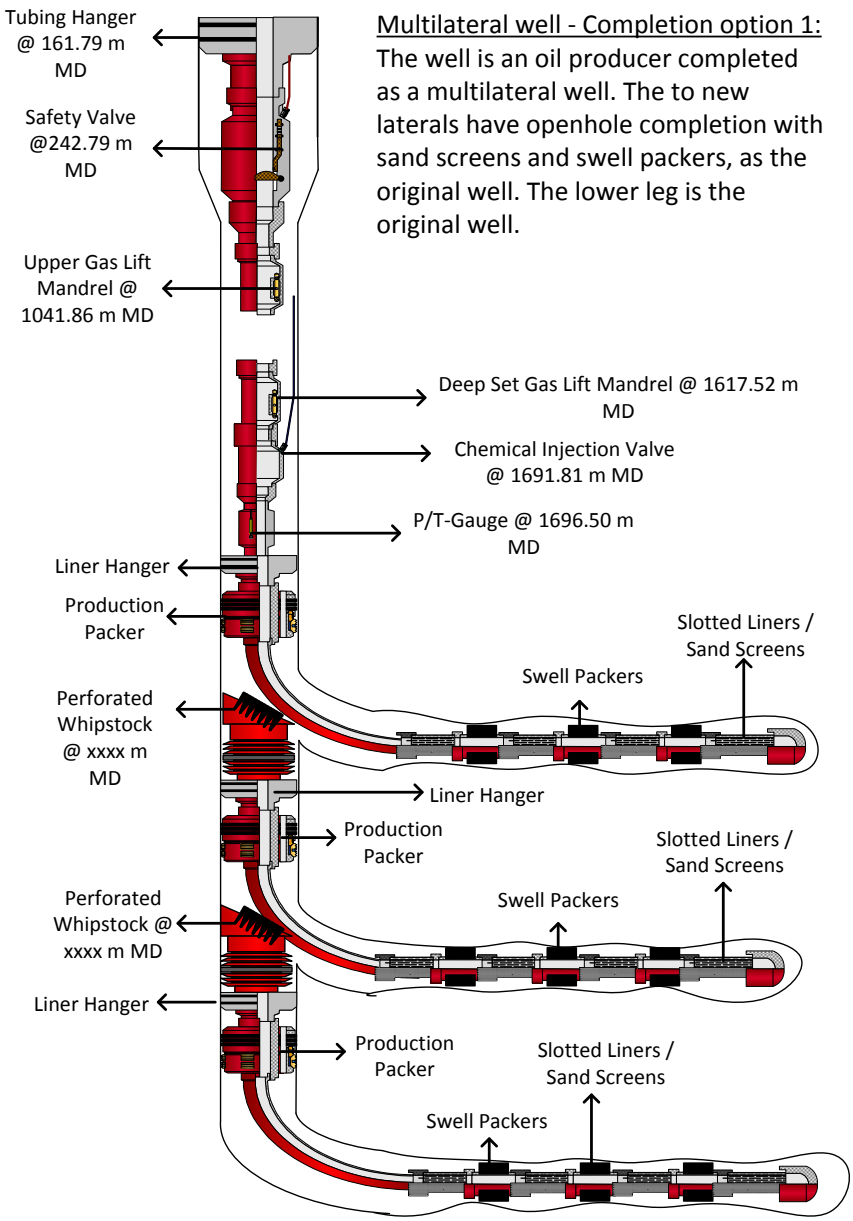

Figure I.3: Multilateral Well, Completion option 1, from Microsoft Visio (Microsoft 2010).

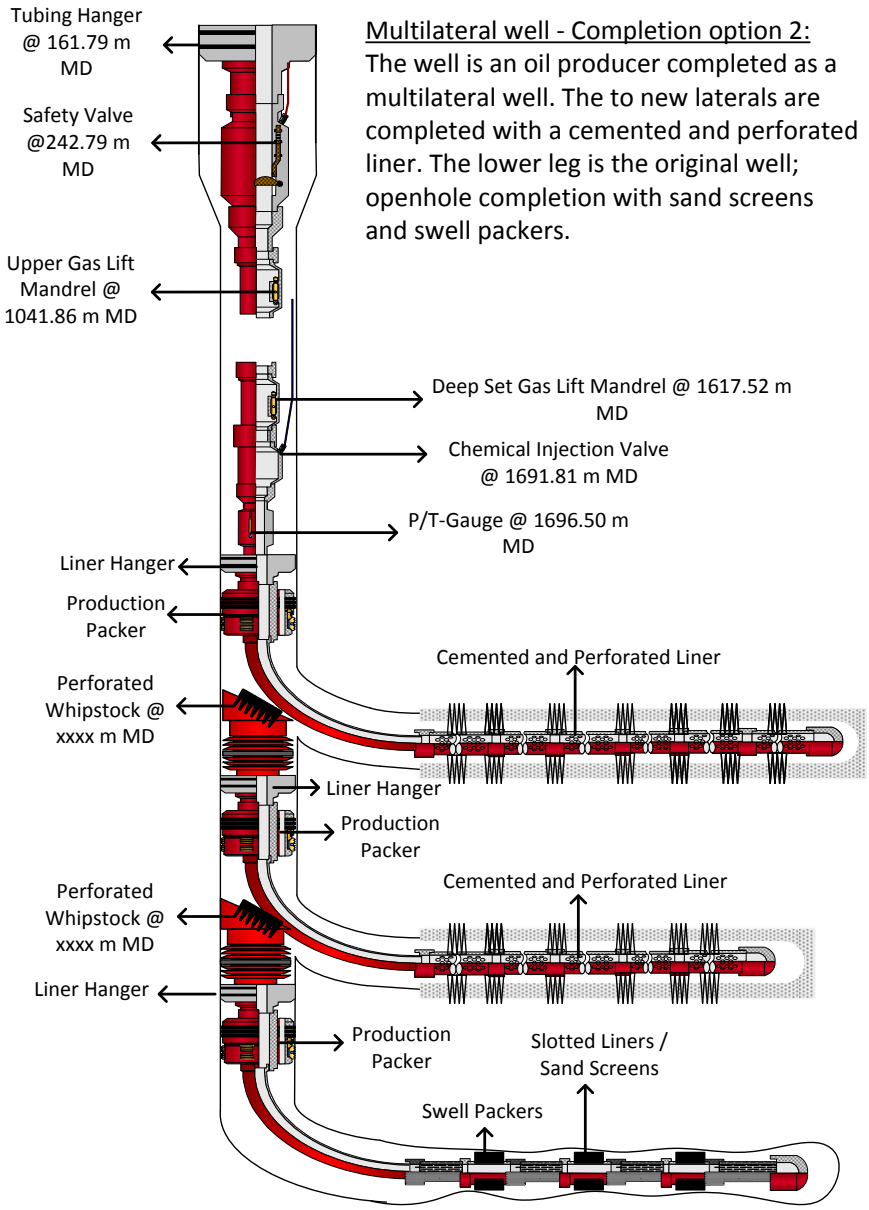

Figure I.4: Multilateral Well, Completion option 2, from Microsoft Visio (Microsoft 2010).

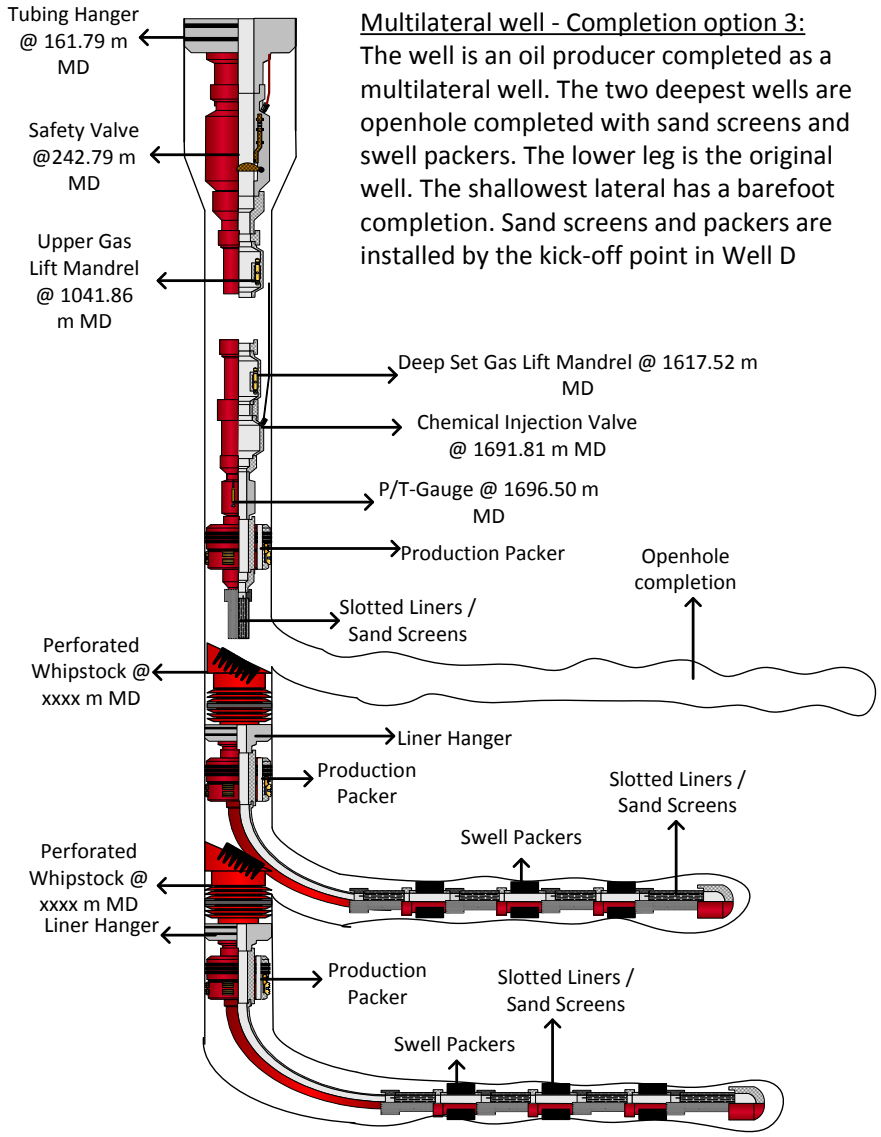

Figure I.5: Multilateral Well, Completion option 3, from Microsoft Visio (Microsoft 2010).

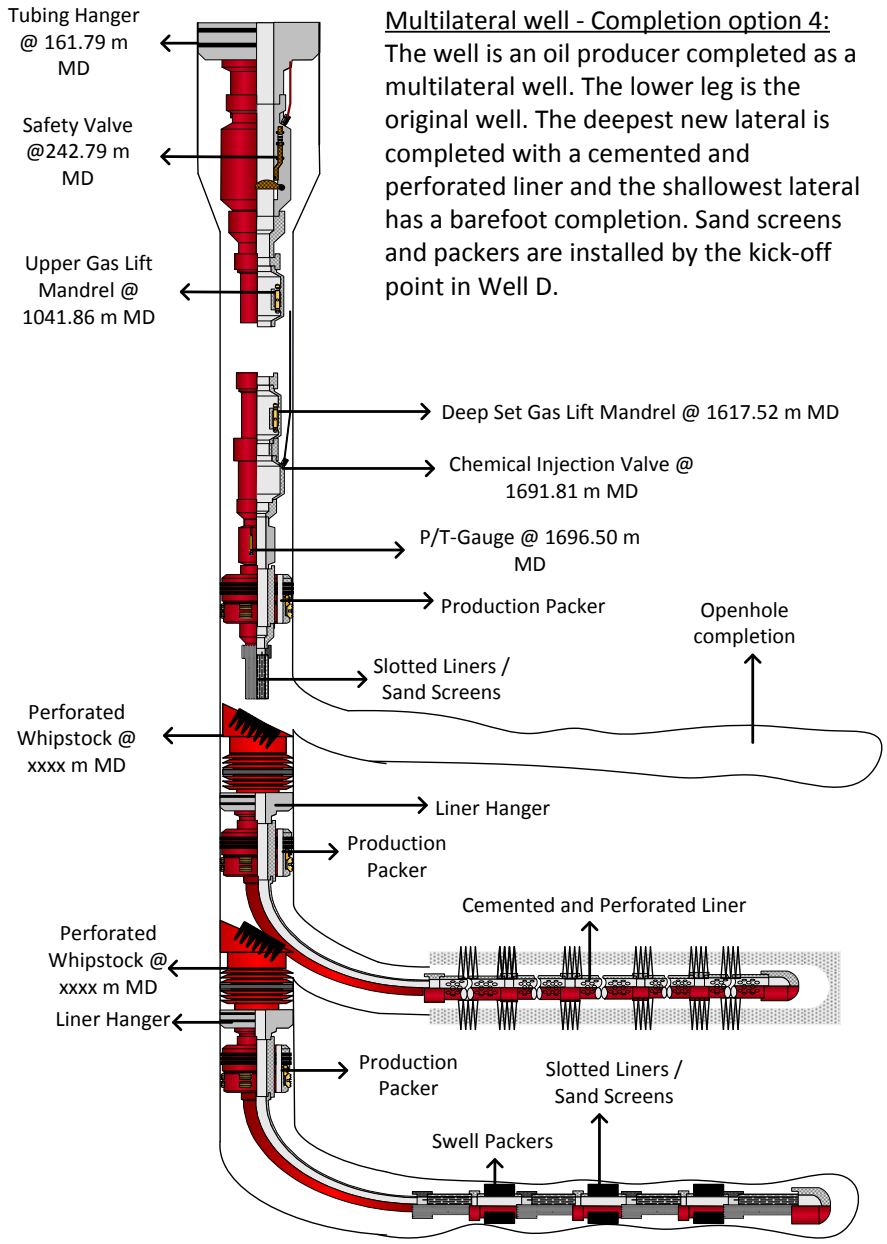

Figure I.6: Multilateral Well, Completion option 4, from Microsoft Visio (Microsoft 2010).

J Probability Distribution Operation Days

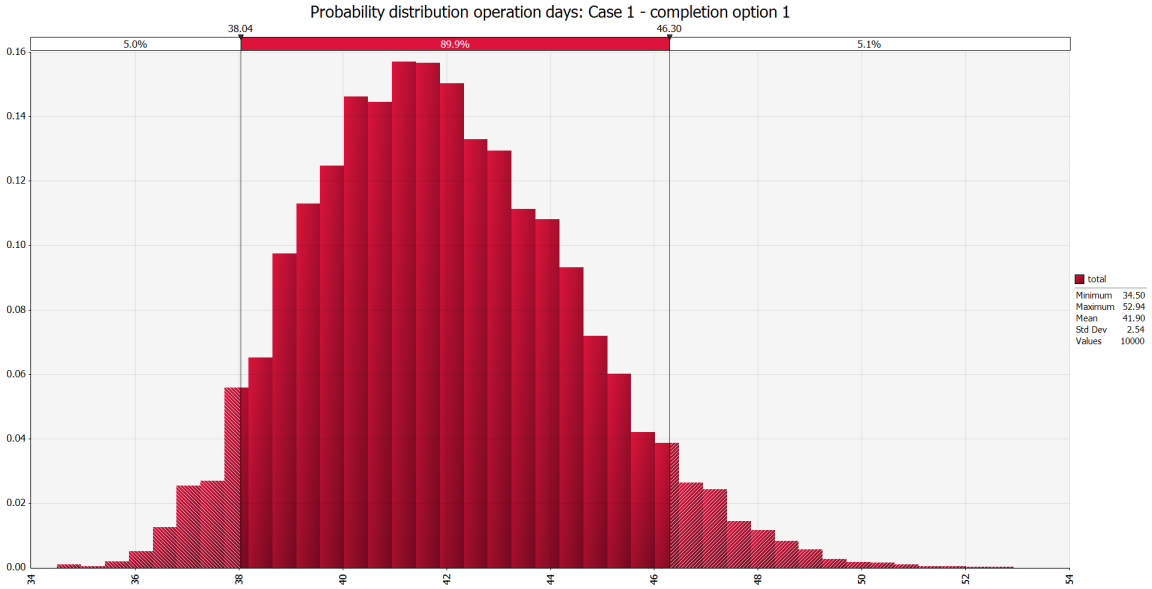

Figure J.1: Probability distribution operation days. Case 1 with completion option 1.

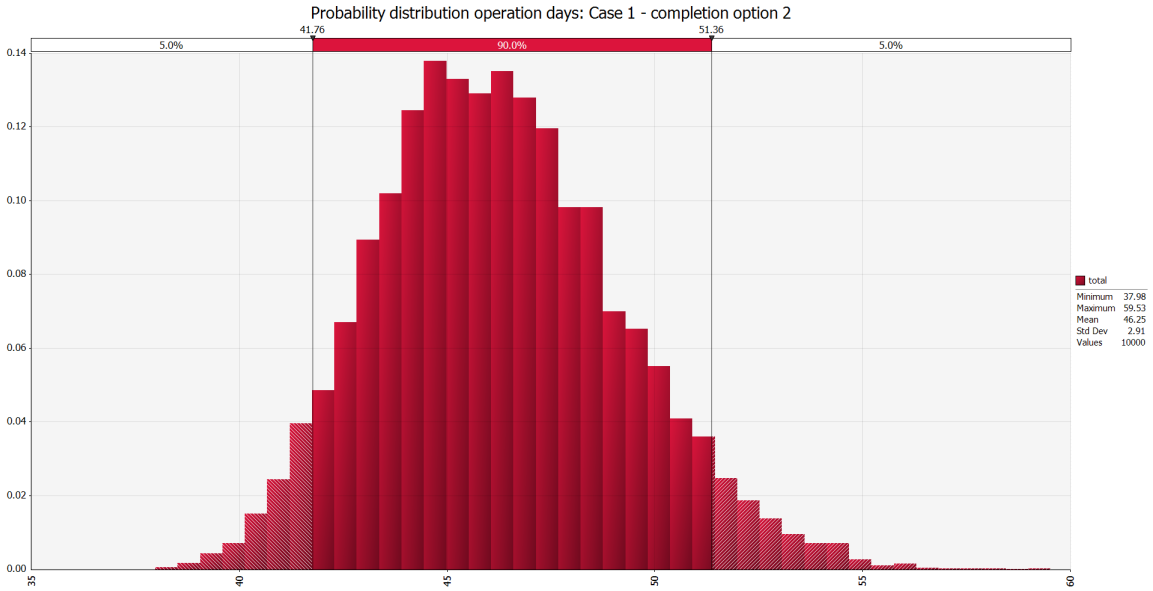

Figure J.2: Probability distribution operation days. Case 1 with completion option 2.

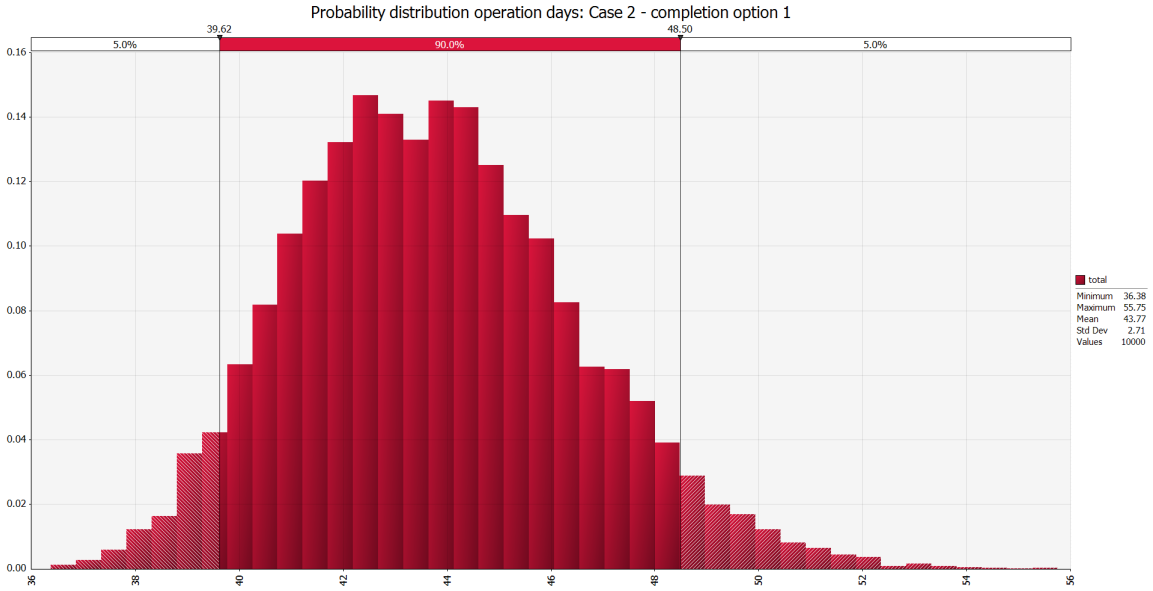

Figure J.3: Probability distribution operation days. Case 2 with completion option 1.

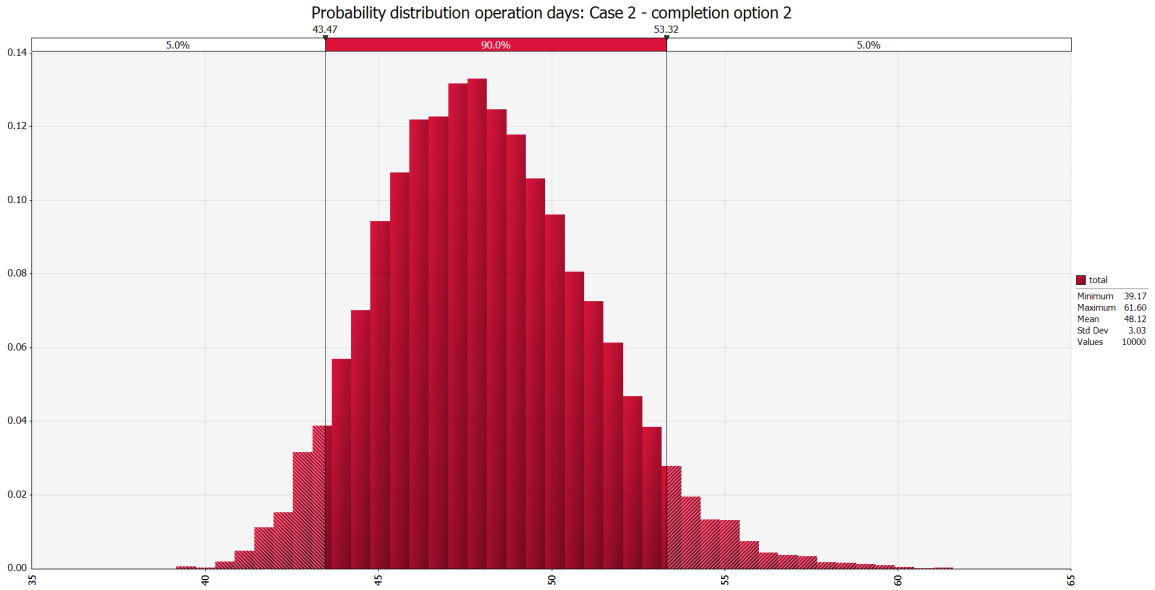

Figure J.4: Probability distribution operation days. Case 2 with completion option 2.

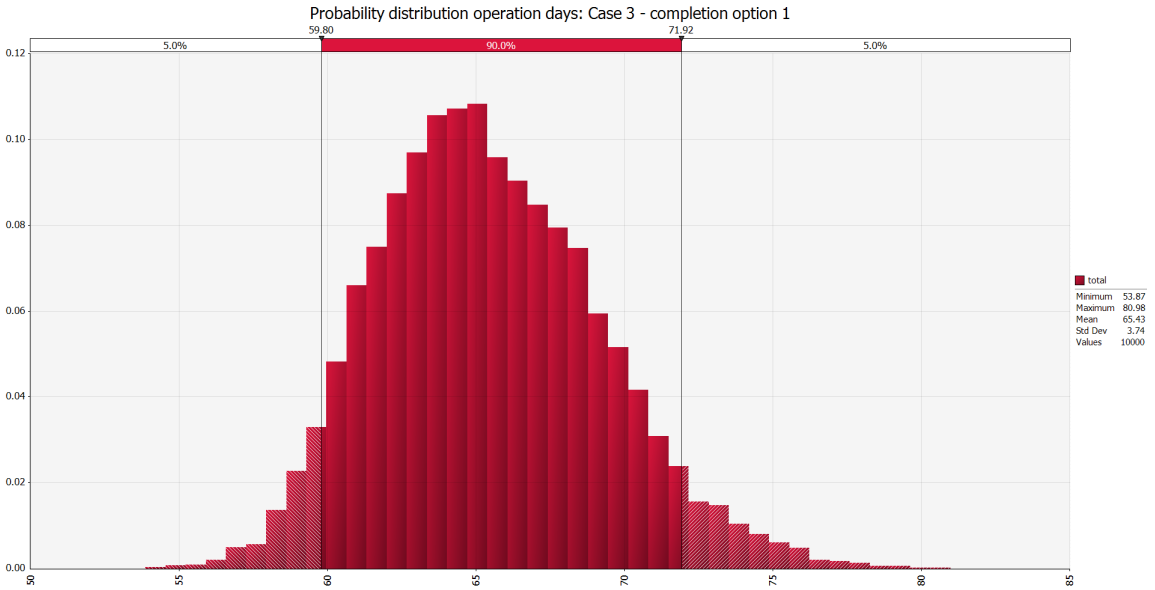

Figure J.5: Probability distribution operation days. Case 3 with completion option 1.

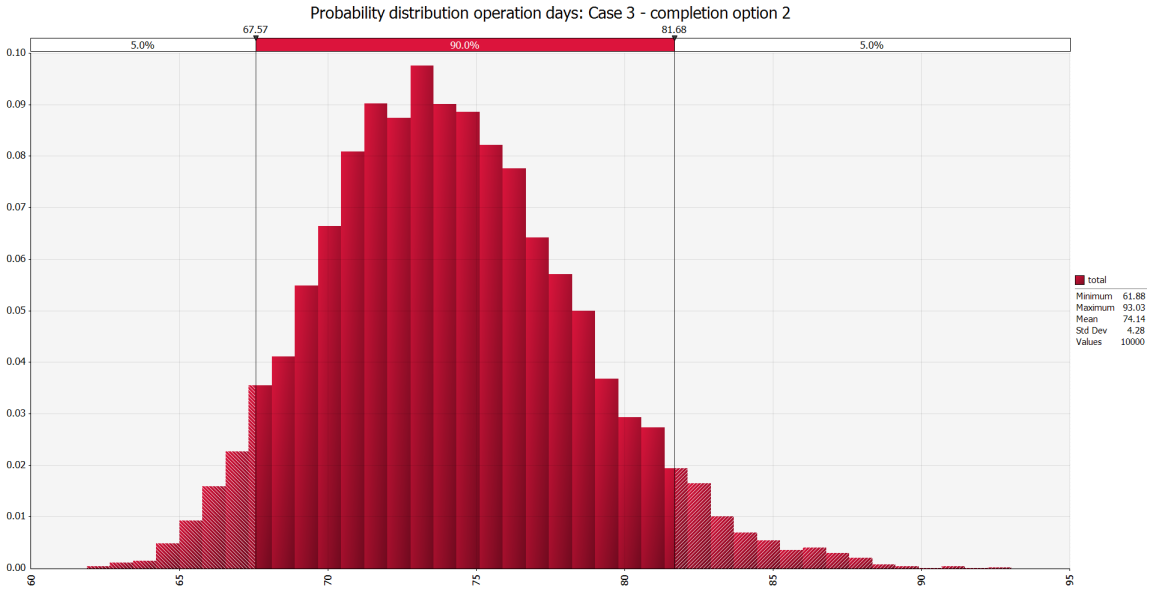

Figure J.6: Probability distribution operation days. Case 3 with completion option 2.

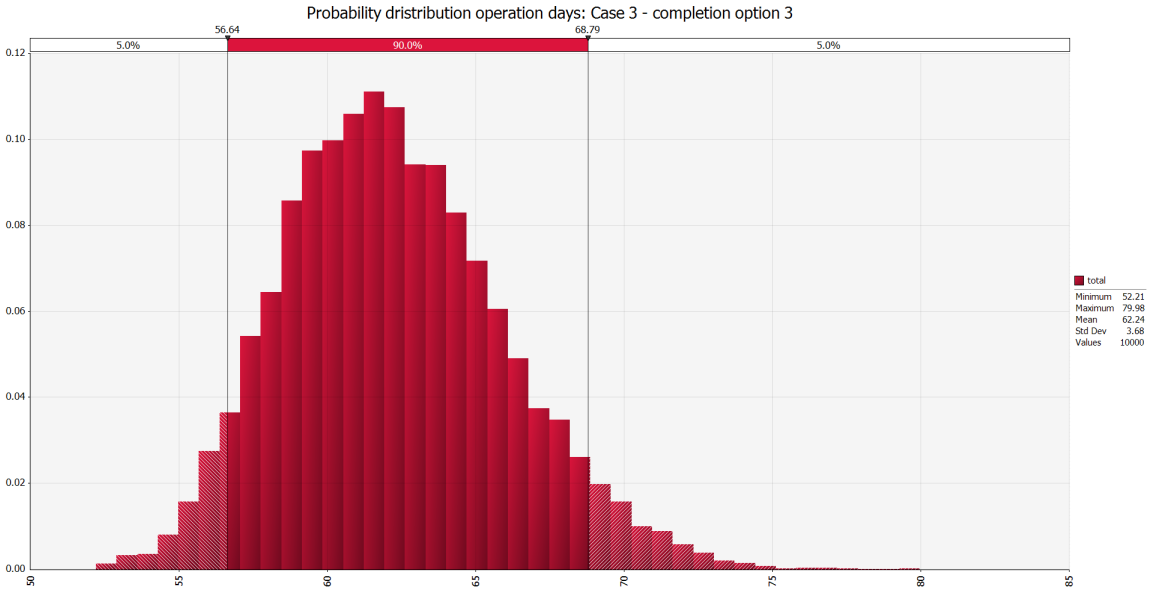

Figure J.7: Probability distribution operation days. Case 3 with completion option 3.

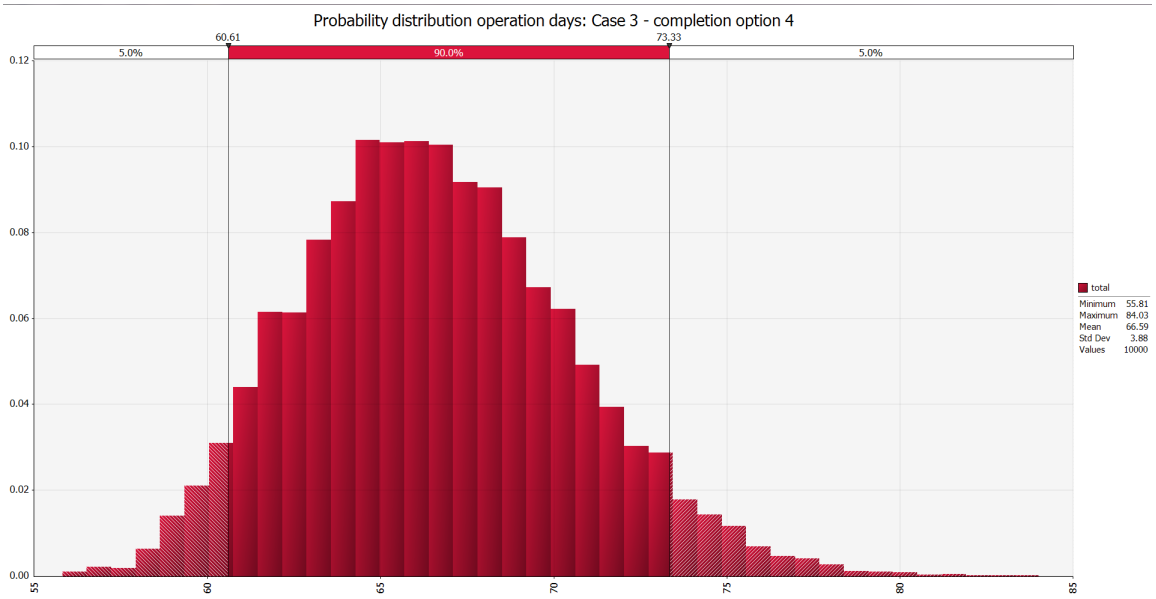

Figure J.8: Probability distribution operation days. Case 3 with completion option 4.

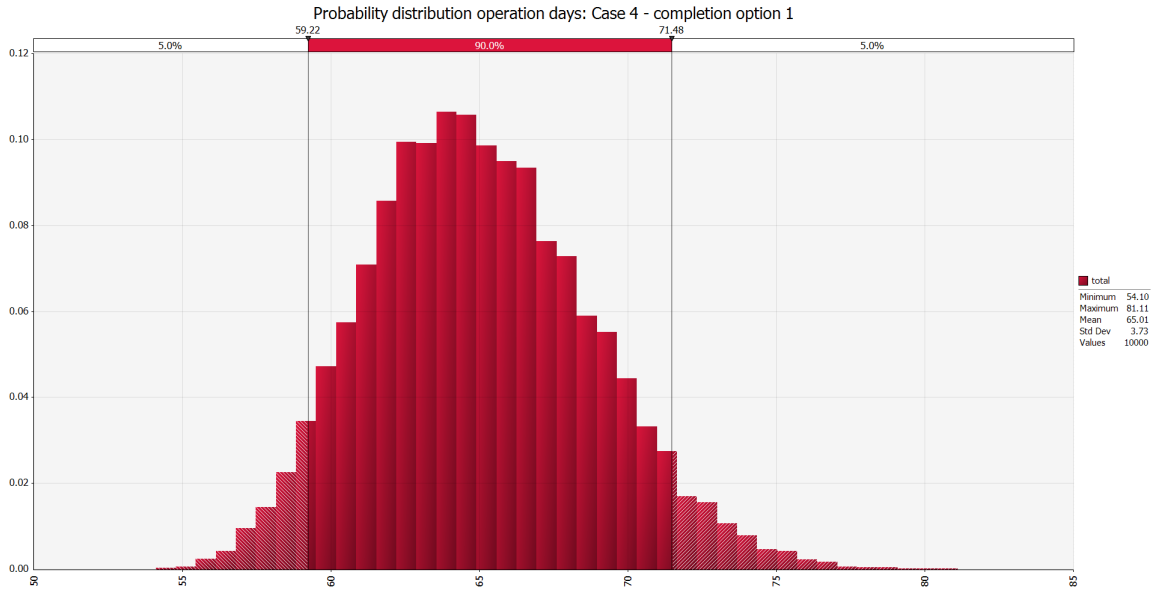

Figure J.9: Probability distribution operation days. Case 4 with completion option 1.

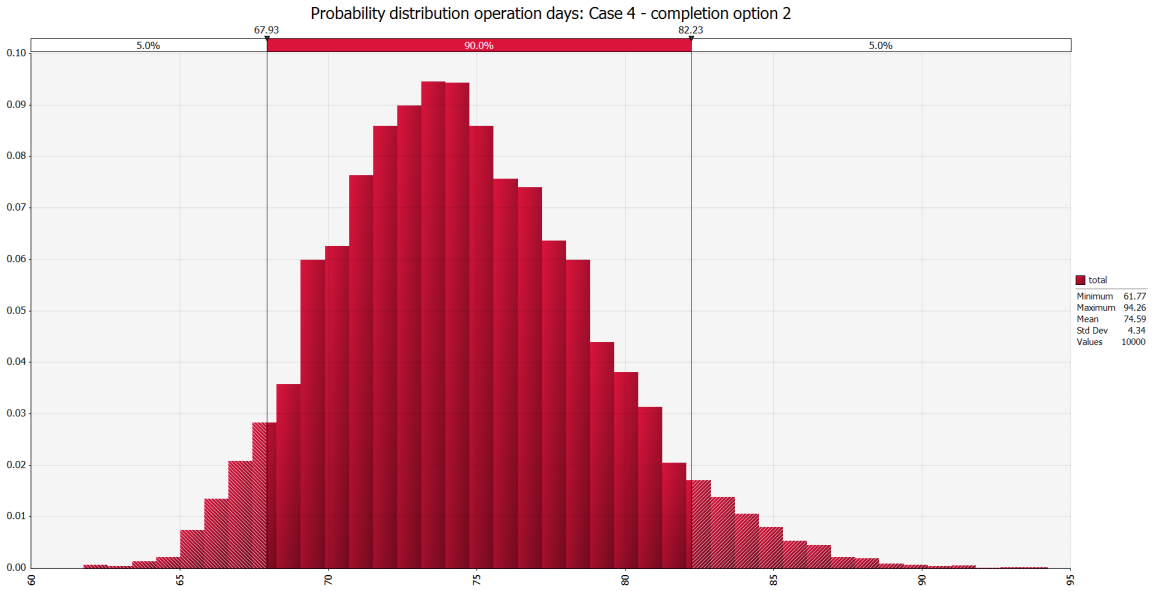

Figure J.10: Probability distribution operation days. Case 4 with completion option 2.

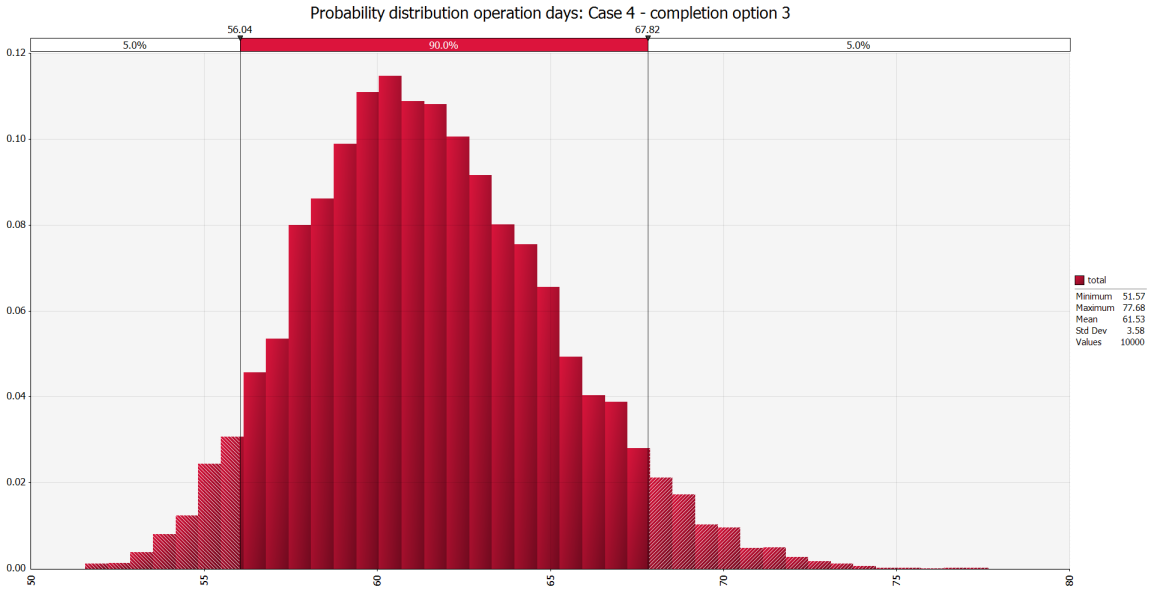

Figure J.11: Probability distribution operation days. Case 4 with completion option 3.

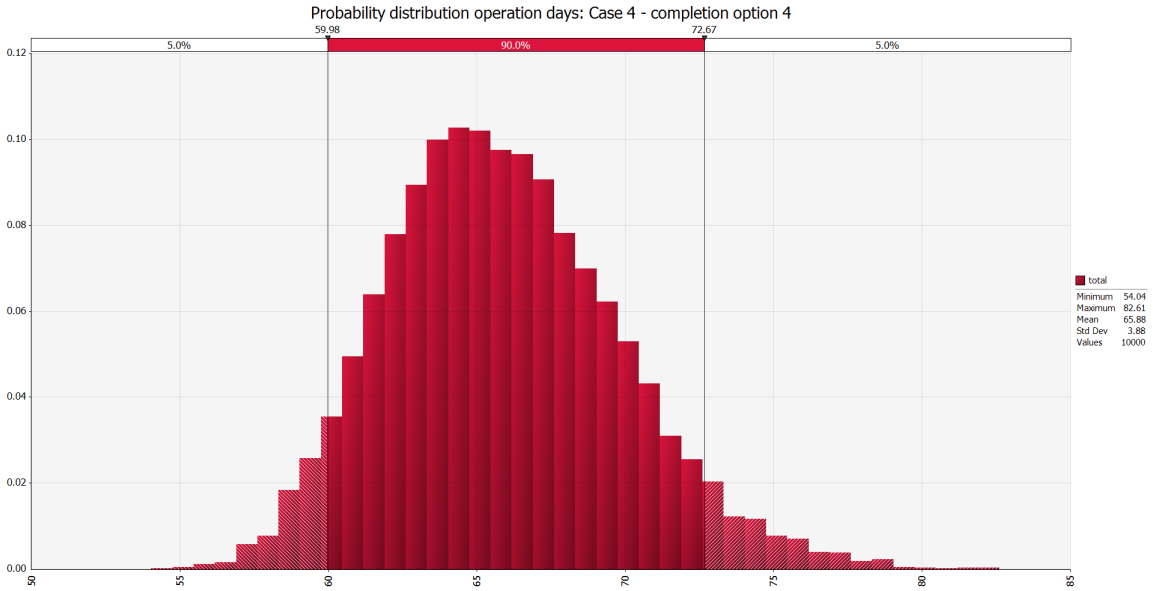

Figure J.12: Probability distribution operation days. Case 4 with completion option 4.

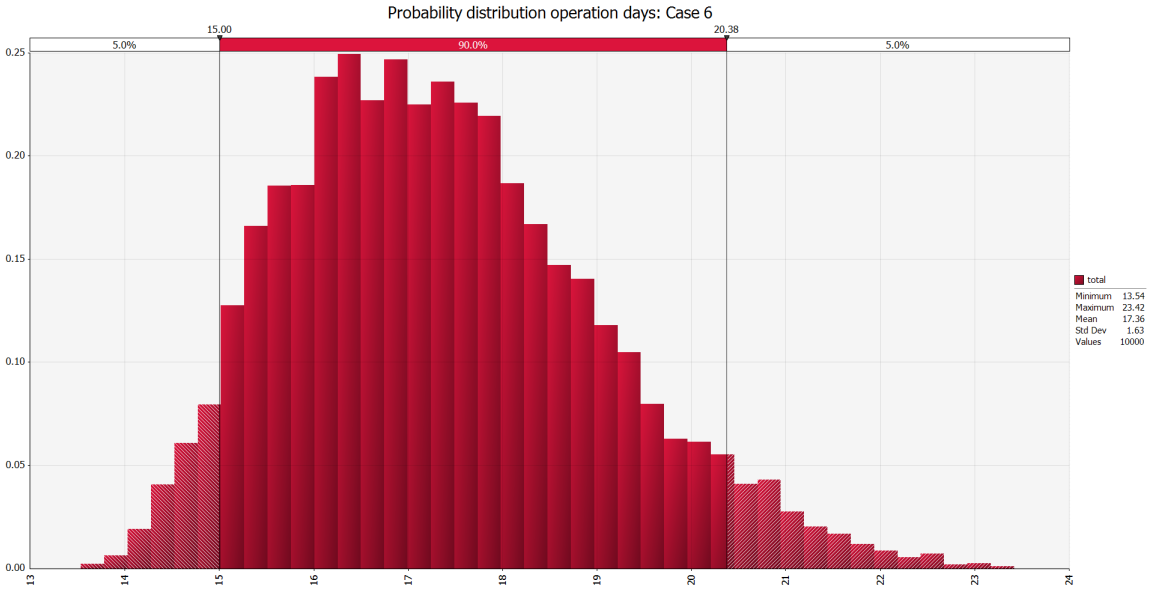

Figure J.13: Probability distribution operation days. Case 6.

K Reservoir Model

DATA file
Schedule file

```
--****************************************************************************************
*************************************************************************
--*********************************************     NEW SECTION
*****************************************************************************************
************
--*****************************************************************************************
*************************************************************************
RUNSPEC

TITLE
History matched Jette IOR model - Tonje

WELLDIMS
  2 189 2 2 /

START
  20 MAY 2013 /

DISGAS

WATER

OIL

GAS

MULTOUT

METRIC

--EDIT TO NEW DIMENSIONS (FROM Z=65 TO Z=25)
DIMENS
  166 69 25 /

TABDIMS
 1 1 50 182 1* 182 182 5* 1 /

UNIFOUT

UNIFIN

VFPPDIMS
 20 10 10 10 10 5 /

WELLDIMS
 20 400 10 20 /

REGDIMS
 35  35 /
-- 12  2 /

EQLDIMS
 1 10 10 /

FAULTDIM
```

```
 1000 /

--AQUIFER DIMENSIONS
AQUDIMS
 7 150  /

--Enables end point scaling
ENDSCALE
/

NSTACK
 150 /

MESSAGES
-- ----------- print limit --------- ---------- stop limit -------------
--  mes  com  war  prb  err  bug     mes  com  war    prb     err  bug
  20000  1* 20000  1*   1*   1*      1*   1*   500000 5400000  1*   100 /

--NOSIM
--************************************************************************************************
**************************************************************************
--*********************************************    NEW SECTION
**************************************************************************************************
************
--************************************************************************************************
**************************************************************************
GRID


NOECHO

--INCLUDE NEW UPSCALED GRID
GDFILE
   '../UPSCALED_PROPS/COARSE_UPSCALED_MODEL.EGRID' /

NOECHO

--INCLUDE NEW UPSCALED PERMEABILITY AND POROSITY VALUES
INCLUDE
  '../UPSCALED_PROPS/PORO_ARITHMETIC.INC' /
INCLUDE
  '../UPSCALED_PROPS/PERM_ARITHMETIC.INC' /
INCLUDE
  '../UPSCALED_PROPS/PERM_HARMONIC.INC' /

MULTIPLY
 'PERMX' 2.0 41 94 39 48 3 20 /
 'PERMZ' 2.0 41 94 39 48 3 20 /
/

MULTIPLY
 'PERMX' 0.5  122 143 41 48 1 15 /
 'PERMZ' 0.5 122 143 41 48 1 15 /
/
```

```
MAXVALUE
'PERMX' 4500 /
/

--COMMENTED FOR USE WITH FLOW BASED PERM UPSCALING
COPY
 PERMX PERMY /
-- PERMX PERMZ /
/

--CHANGED FROM 0 0 TO 0 1 TO INCLUDE GRID PRINT
GRIDFILE
 0 1 /

INIT

PINCH
  0.1 /

MINPV
 10 / -- samt øker akvifer volum


--ADDING NUMERICAL AQUIFER
AQUNUM
--id  i    j   k     A       L        ø     k    Depth  Pi  PVT  SAT
  1   1  1   1  1000000  500000  0.20  1000 2095  /  -- volum/størrelse som antatt i
  PUD/RNB2013 modell (200 GSm³ vs 250 GSm³(PUD))
  2   5  1   1  1000000  500000  0.20  1000 2095  /
/
--AQUIFER CONNECTIONS
--CHANGE INDEX OF LOWER K2 AFTER UPSCALING
AQUCON
--id  i1  i2    j1   j2   k1  k2  face  Tx  Topt
  1   33   99    1    1   1  25  'J-'  1*  1*  YES /
  2  100  166    1    1   1  25  'J-'  1*  1*  YES /
/


ECHO
--********************************************************************************************
**************************************************************************
--*****************************************    NEW SECTION
**************************************************************************************************
************
--*********************************************************************************************
**************************************************************************
EDIT

--EDIT PV TO MATCH OIL IN PLACE
MULTPV
 286350*1.042 /
```

```
--*************************************************************************************
**************************************************************************
--*********************************************    NEW SECTION
**************************************************************************************
************
--*************************************************************************************
**************************************************************************
PROPS

--INCLUDE
-- '../PROPS/PROPS_Jette_D1H_Characterization_Jan2013.txt' / --New characterization
January 2013 from D-1H

-- Includes updated PVT data per 21.01.2014
INCLUDE
'../PROPS/PROPS_new.INC' /

INCLUDE
'../PROPS/TEST_SWOF_SGOF.INC'  /

-- ################################### Fra Draupne
################################################

NOECHO

--NEW UPSCALED CONNATE WATER SATURATION
INCLUDE
  '../UPSCALED_PROPS/SWL_ARITHMETIC-POROWEIGHTED.INC'  /

--INCLUDE
--  '../PROPS/ParalellGrid_Mini_SWATINIT.INC'  /  -- SwJ fra PETREL modell

--NEW UPSCALED CAPILLARY PRESSURE OF WATER
INCLUDE
  '../UPSCALED_PROPS/PCW_ARITHMETIC.INC'  /

NOECHO

-- Apply a maximum limit to SWL (SWL=0.9)
--CHANGE DIMENSIONS AFTER UPSCALING
MAXVALUE
'SWL' 0.6 1 166 1 69 1 25 /
/

-- Equate SWCR and SGU with SWL
COPY
'SWL' 'SWCR' /
'SWL' 'SGU' /
/

-- Make SGU=1-SWL
MULTIPLY
'SGU' -1.0 /
/
ADD
```

```
'SGU' 1.0 /
/

--PPCWMAX
-- 112  NO /

--
##############################################################################################
#############

--**************************************************************************************
**********************************************************************
--*********************************************    NEW SECTION
**************************************************************************************
************
--**************************************************************************************
**********************************************************************
REGIONS

NOECHO

--CHANGE NUMBER OF GRID CELLS AFTER UPSCALING
SATNUM
 286350*1 /

COPY
 SATNUM PVTNUM /
 SATNUM ROCKNUM /
 SATNUM EQLNUM /
/

ECHO
--**************************************************************************************
**********************************************************************
--*********************************************    NEW SECTION
**************************************************************************************
************
--**************************************************************************************
**********************************************************************
SOLUTION

EQUIL
-- DAtum Depth  Pressure@DDepth WOC Pc  GOC
-- No gascap (GOC 1957 - 2057)
        2091         195.9          2091    0     2000       1*   1  / --
        vann/oljekontakt 2090 m
--EDITED DATUM DEPTH TO WOC@2091 FROM 2000
--SHOULD REDUCE THE ENERGY IN THE RESERVOIR AND MAYBE RELEASE MORE GAS IN SIMULATION

--INCLUDE
-- '../PROPS/RSVD_Jette_D1H_Characterization_Jan2013.txt' /

-- Includes updated RSVD data per 21.01.2014
INCLUDE
'../PROPS/RSVD_new.INC' /
```

```
RPTSOL
  RESTART=2 SOIL SWAT SGAS  /


--RPTRST
--  BASIC=3 FREQ=100 / -- FLORES for strømlinjer i Petrel 2012
RPTRST
 BASIC=2 PRESSURE CONV=10 FIP FLORES /
--ADDED FLORES TO GET STREAMLINES
--/////////////////////////////////////////////////////////////////////////////////////
/////////////////////////////////////////////////////////////////////////
--//////////////////////////////////////////////    NEW SECTION
/////////////////////////////////////////////////////////////////////////////////////////
////////////
--/////////////////////////////////////////////////////////////////////////////////////
/////////////////////////////////////////////////////////////////////////
SUMMARY

INCLUDE                                  -- Generated : Petrel
 '../SUMMARY/BASE_11012013_SUM.INC' /

--ADDED EXTRA PRINT

TCPU
FOE
FLPR
WLPR
 /
WBHPH
 /
WTHPH
 /
--HISTORIC PRODUCTION
FOPRH
FLPRH
FWPRH
WLPRH
 /
WOPRH
 /
WWPRH
 /
--LIFT GAS INJECTED
FGLIR
WGLIR
 /
--AQUIFER PRINT
FNQR
ANQR
 /
ANQP
 /

EXCEL
```

```
--*********************************************************************************************
*****************************************************************************
--*******************************************     NEW SECTION
*********************************************************************************************
************
--*********************************************************************************************
*****************************************************************************
SCHEDULE

INCLUDE
 '../SCHEDULE/PREDICTION_FROM_3MONTHS.SCH'   /


END
```

```
--ADDED NEWTON TO SHOW CONVERGENCE REPORT
RPTSCHED
 FIP=2 WELLS=2 NEWTON=1 /

--RPTRST
--  BASIC=2 /


NOECHO

--INCLUDE
--Flowline VFP 1
-- '../VFP/Jette_JotunB_flowline_after_startup.Ecl' / --New PVT April 2013 and match
initial start

INCLUDE
-- Jette Sør VFP 2
 '../VFP/D-well_liftcurves.VFP' /  -- New PVT April 2013 and match initial start


INCLUDE
-- Jette Nord VFP 3
 '../VFP/E-well_liftcurves.VFP' /  -- New PVT April 2013 and match initial start

--LOWERED MINIMUM TIME STEP SIZE AND CHOPPABLE TIME STEP
TUNING
 1*  5 0.001 0.015 /
 1*    /
 2* 150 /                              -- Generated : Petrel

-- Well name, well group, i, j, reference depth, preferred phase
WELSPECS                              -- Generated : Petrel
  'D-1H' 'WELGRUP' 140 45 1622.83 OIL /
  'E-1H' 'WELGRUP' 91 42 1864.29 OIL /
/

--ADD NEW COMPDAT FROM UPSCALED MODEL
INCLUDE
  '../UPSCALED_PROPS/QC_COMPDAT1.INC' /


-- Periodic testing of closed wells
WTEST
 'D-1H'  30   P   /
 'E-1H'  30   P   /
/

WRFTPLT
 '*' TIMESTEP TIMESTEP /
/

COMPORD
 '*'  INPUT /
/
```

```
WPIMULT
 E-1H 3.5 /
 D-1H 0.07 /
/

NUPCOL
4 /

------------------ INSERT NEW HISTORIC DATA ------------------
INCLUDE
 '../SCHEDULE/WCONHIST_MAY13-JAN14.INC' /

--------------------------------------------------------------

--WCONPROD
---- kjører uten network med mottakstrykk på 40 bar
----name      status   Contr.  BHP THP  VFP  G.Lift
--  'D-1H'    OPEN     BHP    5*    65  20   2    50000  1* 1* /
--  'E-1H'    OPEN     BHP    5*    125  20   3    50000  1* 1* /
--/

--GCONPRI
-- Name    Oil-upper  Procedure  Water-upper  Procedure  Gas-upper  Procedure
Liquid-upper  Procedure
-- 'WELGRUP'    1100        PRI         1*           1*       400000       PRI
5500          PR2       /
--/

--GEFAC
-- 'WELGRUP'  0.898 /
--/
--
--GRUPTREE
-- WELGRUP FIELD /
--/
--
--PRIORITY
-- 0  0.0  1.0  0.0  0.0  0.0  0.0  0.0  1.0
--    0.0  1.0  0.0  0.0  0.0  0.0  1.0  0.0
--/

--GRUPNET
-- FIELD    21  /
-- WELGRUP   1*  1 1*  YES FLO /
--/

--WLIMTOL
-- 0.2 /

--GCONTOL
-- 0.01  3  /

--NETBALAN
-- -1  0.01  15  2*  25.0  70.0  /
```

```
-- LIFTOPT
-- -- increment    minimum    optimisation     opt in 1st
-- --   size       gradient     interval       NUPCOL its?
-- 20000  1*  90  YES /

-- WLIFTOPT
-- -- well   optimise   max lift   weighting    min lift
-- -- name     lift?    gas rate    factor     gas rate
-- A-1_AH    'Y'      200000  1* -1    /
-- B-1_H    'Y'      200000  1* -1    /
-- /

-- GLIFTOPT
-- -- group   max liftmax
-- -- name    gas rate   gas rate
-- WELGRUP     200000    400000  /
-- /


-- DATES
-- 3 JAN 2013 /
-- /

--PRIORITY
--90  0.0  1.0  0.0  0.0  0.0  0.0  0.0  1.0
--    0.0  1.0  0.0  0.0  0.0  0.0  1.0  0.0
--/


GEFAC
 'WELGRUP'  0.928 /
/

--DATES
--  1 JUN 2013 /
--  1 JUL 2013 /
--  1 AUG 2013 /
--  1 SEP 2013 /
--  1 OCT 2013 /
--  1 NOV 2013 /
--/

--OOPEN THE WELL DOWN TO PACKER 3

INCLUDE
  '../UPSCALED_PROPS/QC_COMPDAT2.INC' /

-- Periodic testing of closed wells
WTEST
 'D-1H'  30   P   /
 'E-1H'  30   P   /
/

WRFTPLT
```

```
 '*' TIMESTEP TIMESTEP /
/

COMPORD
 '*'  INPUT /
/

WPIMULT
 E-1H 3 /
 D-1H 0.07 /
/

NUPCOL
4 /

------------------ INSERT NEW HISTORIC DATA ------------------
INCLUDE
 '../SCHEDULE/WCONHIST_NOV13-JAN14.INC' /

--------------------------------------------------------------

WCONPROD
-- kjører uten network med mottakstrykk på 40 bar
--name      status   Contr.  BHP THP  VFP  G.Lift
  'D-1H'    OPEN     BHP    5*    65  20   2    100000  1* 1* /
  'E-1H'    OPEN     BHP    5*    125  20   3    100000  1* 1* /
/

--GCONPRI
-- Name    Oil-upper  Procedure  Water-upper  Procedure  Gas-upper  Procedure
Liquid-upper  Procedure
-- 'WELGRUP'    1100        PRI         1*           1*       400000       PRI
5500          PR2       /
--/

GEFAC
 'WELGRUP'  0.898 /
/

GRUPTREE
 WELGRUP FIELD /
/

PRIORITY
 0  0.0  1.0  0.0  0.0  0.0  0.0  0.0  1.0
    0.0  1.0  0.0  0.0  0.0  0.0  1.0  0.0
/



--DATES
--  1 DEC 2013 /
--/
--
DATES
```

```
--  1 JAN 2014 /
  1 FEB 2014 /
  1 MAR 2014 /
  1 APR 2014 /
  1 MAY 2014 /
  1 JUN 2014 /
  1 JUL 2014 /
  1 AUG 2014 /
  1 SEP 2014 /
  1 OCT 2014 /
  1 NOV 2014 /
  1 DEC 2014 /
/

DATES
  1 JAN 2015 /
  1 FEB 2015 /
  1 MAR 2015 /
  1 APR 2015 /
  1 MAY 2015 /
  1 JUN 2015 /
  1 JUL 2015 /
  1 AUG 2015 /
  1 SEP 2015 /
  1 OCT 2015 /
  1 NOV 2015 /
  1 DEC 2015 /
/

DATES
  1 JAN 2016 /
  1 FEB 2016 /
  1 MAR 2016 /
  1 APR 2016 /
  1 MAY 2016 /
  1 JUN 2016 /
  1 JUL 2016 /
  1 AUG 2016 /
  1 SEP 2016 /
  1 OCT 2016 /
  1 NOV 2016 /
  1 DEC 2016 /
/

DATES
  1 JAN 2017 /
  1 FEB 2017 /
  1 MAR 2017 /
  1 APR 2017 /
  1 MAY 2017 /
  1 JUN 2017 /
  1 JUL 2017 /
  1 AUG 2017 /
  1 SEP 2017 /
  1 OCT 2017 /
```

```
  1 NOV 2017 /
  1 DEC 2017 /
/

DATES
  1 JAN 2018 /
  1 FEB 2018 /
  1 MAR 2018 /
  1 APR 2018 /
  1 MAY 2018 /
  1 JUN 2018 /
  1 JUL 2018 /
  1 AUG 2018 /
  1 SEP 2018 /
  1 OCT 2018 /
  1 NOV 2018 /
  1 DEC 2018 /
/

DATES
  1 JAN 2019 /
  1 FEB 2019 /
  1 MAR 2019 /
  1 APR 2019 /
  1 MAY 2019 /
  1 JUN 2019 /
  1 JUL 2019 /
  1 AUG 2019 /
  1 SEP 2019 /
  1 OCT 2019 /
  1 NOV 2019 /
  1 DEC 2019 /
  1 JAN 2020 /
/


END
```